THE UNIVERSITY
of EDINBURGH

Endogenous Mechanisms of Vascular Regeneration Following Myocardial Infarction

Emmanouil Georgios Solomonidis

Thesis submitted for the degree of Doctor of Philosophy in Cardiovascular Science

College of Medicine & Veterinary Medicine

The University of Edinburgh

2022

Στον Ηλία, την Άντα και την Κέλλυ

i Declaration

I declare that this report has been composed solely by myself and that it has not been submitted, in whole or in part, in any previous application for a degree. Except where states otherwise by reference or acknowledgment, the work presented is my own.

Table of Contents

ii Acknowledgements

I have thought about writing the acknowledgements section of my thesis since the first time I saw a completed thesis of a fellow PhD student during my masters in London. Now, years later, amidst a pandemic no-less, it seems strange to me that this time has finally come for my own thesis.

This thesis represents 4 years of scientific work. But it also has another meaning for me. It symbolizes the end of a 9.5-year education journey since I arrived in the UK at the age of 19 years old in September 2012 to start my undergraduate degree at King's College London. It is a surreal feeling.

First and foremost, I need to thank my parents Ilias and Adamantia for giving me the opportunity to study in the UK and supporting me at a time when things were far from certain. I am indefinitely thankful to you for believing in me. Of course, I need to thank my sister Kelly for keeping me sane while chatting on the phone while on those long writing marathons. Σας αγαπώ πολύ.

There have been many people that have helped me and guided me through this scientific journey. The first person I need to thank is my primary PhD supervisor Mairi Brittan. It has been a pleasure to work with Mairi in the team. She has helped me learn a lot on every facet of the job and develop professionally. Mairi was always a great person to discuss science together and I feel we developed a great working relationship throughout the years.

Moreover, I would like to thank my secondary PhD supervisor Paddy Hadoke for always being available for feedback to my progress updates, writing or presentations (with the classic quote "but what is the question?") and generally for being a great person to discuss science (while I am not trying to persuade him to do Movember..). Also, I want to thank members of Paddy's team Junxi Wu and Eileen Miller for providing tips and advice in numerous lab protocols.

Without a doubt, I need to give the strongest of high-fives to Ziwen Cass Li for being a superb colleague all these years in Mairi's group. I enjoyed planning and doing

experiments with Cass immensely and we were always a force to be reckoned with in the lab! (Except when we did an experiment with 80 cell culture plates, then my courage faltered a bit). I would also like to thank Cass for providing me with continuous feedback (still does) in my journey to learn coding using R. This has been a terrific skill I managed to acquire throughout my PhD.

Of course, I couldn't go without thanking the rest of the members of team Brittan-Kate Ross Steward, Bronwyn Berkeley and of course Marlene Magalhaes (during her brief time with us!). It was a great pleasure to discuss progress but also issues that we might have been facing together.

I need to also thank Andy Baker and his team for being great collaborators and for always being available to share their expertise on protocols (and maybe the occasional reagent too..). I also could not omit the contribution of Marco Meloni and Ana-Mishel Spiroski who performed the mouse coronary ligation surgeries that are a core part of this thesis.

I am especially thankful to all my friends at QMRI for building a strong support system for science and tomfoolery alike. It made my experience in Edinburgh awesome.

Additionally, I would like to thank all the staff of the animal housing facility, especially Will and Denisse, who have been instrumental in the experiments presented in this thesis.

Finally, I need to thank the British Heart Foundation for supporting the research, both with regard to consumables but also providing me with a salary throughout all these years.

iii Publications during PhD

- Ziwen Li, **Emmanouil G Solomonidis**, Marco Meloni, Richard S Taylor, Rodger Duffin, Ross Dobie, Marlene S Magalhaes, Beth E P Henderson, Pieter A Louwe, Gabriela D'Amico, Kairbaan M Hodivala-Dilke, Ajay M Shah, Nicholas L Mills, Benjamin D Simons, Gillian A Gray, Neil C Henderson, Andrew H Baker, Mairi Brittan. *Single-cell transcriptome analyses reveal novel targets modulating cardiac neovascularization by resident endothelial cells following myocardial infarction*. European Heart Journal, Volume 40, Issue 30, 7 August 2019, Pages 2507–2520.

- **Emmanouil G Solomonidis,** Andrew H Baker, Mairi Brittan. *Tissue-selective endothelial arousal revealed by vascular endothelial growth factor gene transfer.* Cardiovascular Research, Volume 117, Issue 1, 1 January 2021, Pages 18–20

- Finnius A. Bruton, Aryan Kaveh, Katherine Ross-Stewart, Gianfranco Matrone, Magdalena Oremek, **Emmanouil G. Solomonidis**, Carl Tucker, John Mullins, Mairi Brittan, Jonathan Taylor, Adriano Rossi, Martin Denvir. *Macrophages stimulate epicardial VEGFaa to trigger cardiomyocyte proliferation in larval zebrafish heart regeneration.*BioRxiv2021.06.15.448575;doi:https://doi.org/10.1101/2021.06.15.448575

iv Conferences, Workshops and Awards

- **Public Engagement Hero Award** - **ASCUS Collaboration,** Public Engagement Hero Award, Centre for Cardiovascular Science Annual Symposium, 2018.
- **Scottish Cardiovascular Forum**, 2019, Inverness. Submitted title: *Single Cell RNA-Sequencing Reveals Plasmalemma Vesicle-Associated Protein (PLVAP) as a Novel Target with a Role in New Blood Vessel Formation in the Ischaemic Heart* (poster presentation).
- **British Heart Foundation Student Conference**, Imperial College London, 2019. Submitted title: *Single Cell RNA-Sequencing Reveals Plasmalemma Vesicle-Associated Protein (PLVAP) as a Novel Target with a Role in New Blood Vessel Formation in the Ischaemic Heart* (oral presentation, third place award)
- **3rd Joint Meeting of the European Society for Microcirculation (ESM) and the European Vascular Biology Organization (EVBO),** 2019, Maastricht. Submitted Title: *Single Cell RNA-Sequencing Reveals Plasmalemma Vesicle-Associated Protein (PLVAP) as a Novel Target with a Role in New Blood Vessel Formation in the Ischaemic Heart* (poster presentation).
- **Centre for Cardiovascular Science Annual Symposium**, 2019, Early Career Researcher segment. Submitted Title: *Single Cell RNA-Sequencing Reveals Plasmalemma Vesicle-Associated Protein (PLVAP) as a Novel Target with a Role in New Blood Vessel Formation in the Ischaemic Heart* (oral presentation, first place award).
- **BHF Schools Outreach Programme/STEM ambassador scheme** alongside other CVS PhD students. Nominated for Public Engagement Hero Award Centre for Cardiovascular Science Annual Symposium, 2019.
- **ediRNA Meeting**, The Queen's Medical Research Institute, Title: *Single Cell RNA-Sequencing Reveals Plasmalemma Vesicle-Associated Protein (PLVAP) as a Novel*

Target with a Role in New Blood Vessel Formation in the Ischaemic Heart, October 2019 (poster presentation)

- **Scottish cardiovascular Forum, University of Glasgow, 2020** Title: Single Cell RNA-Sequencing Reveals Novel Targets with a Potential Role in Vascular Regeneration in the Ischaemic Adult Heart (oral presentation)
- **British Heart Foundation Schools Outreach Programme/STEM ambassador scheme** alongside other CVS PhD students. Public Engagement Hero Award, Centre for Cardiovascular Science Annual Symposium, 2020.

v Abbreviations

AAT	serine protease inhibitor alpha-1 antitrypsin
Abcg2	atp binding cassette sub- family g member 2
Akt	protein kinase b
alk1	activin-receptor-like kinase 1
ANOVA	analysis of variance
Apln	apelin
ATP	adenosine triphosphate
BDM	2,3-butanedione monoxime
bFGF	basic fibroblast growth factor
BMMNCs	bone marrow mononuclear cells
BSA	bovine serum albumin
CABG	coronary artery bypass graft
CDCs	cardiosphere-derived cells
Cdh5	cadherin 5
cDNA	complementary dna
CECs	coronary endothelial cells
CNS	central nervous system
Col1a2	collagen i α2
CSCs	cardiac stem cells
CVD	cardiovascular disease
DAPI	4’,6-diamidino-2-phenylindole
Depp	decidual protein induced by progesterone
DLL4	delta like canonical notch ligand 4
DMSO	dimethyl sulfoxide
EBM	endothelial basal media
EC	endothelial cell
ECM	extracellular matrix
ECs	endothelial cells
EDRF	endothelium-derived relaxing factor
EDTA	ethylenediaminetetraacetic acid
EdU	5-ethynyl-2'-deoxyuridine
EGFP	enhanced green fluorescent protein
EGM	endothelial growth media
ELISA	enzyme linked immunosorbent assay

EndMT	endothelial to mesenchymal transition
EPAS1	endothelial pas domain protein 1
EPC	endothelial progenitor cell
ER	oestrogen receptor
ERK	extracellular signal-regulated kinase
ESCs	embryonic stem cells
Fabp4	fatty acid-binding protein 4
FACS	fluorescence activated cell sorting
FAM	fluorescein amidites
FBS	foetal bovine serum
FD	fenestral diaphragms
FFPE	formalin fixed paraffin embedded
FMO	fluorescence minus one
Fsp1	fibroblast-specific protein 1
GAPDH	glyceraldehyde 3-phosphate dehydrogenase
GEMs	gel bead-in-emulsions
GM-CSF	macrophage colony-stimulating factor
H&E	haematoxylin & eosin
HEPES	4-(2-hydroxyethyl)-1-piperazineethanesulfonic acid
HEV	high endothelial venule
HF	heart failure
HGP	human genome project
HIF	hypoxia inducible factor
HMVEC	human dermal microvascular endothelial cells
HSCs	haematopoietic stem cells
HSP90	heat shock protein 90
HUVECS	human umbilical vein endothelial cells
HUVECs	human umbilical vein endothelial cells
HUVECs	human umbilical vein endothelial cells
IFN	interferon
IHD	ischaemic heart disease
iPSCs	induced pluripotent stem cells
IR	ischaemia-reperfusion
IRES	internal ribosomal entry site

Kit	proto-oncogene receptor tyrosine kinase
LAD	left anterior descending
LPS	lipopolysaccharide
LV	left ventricle
mCFP	membranous cyan fluorescent protein
MEM	minimum essential media
MEndoT	mesenchymal-to-endothelial transition
MI	myocardial infarction
MMP	metalloproteinease
mPTP	mitochondrial permeability transition pore
MT	masson's trichrome
nGFP	nuclear green fluorescent protein
NGS	next generation sequencing
NGS	normal goat serum
Npr3	natriuretic peptide receptor 3
NRP1	neuropilin 1
NRP2	neuropilin 2
OCT	optimal cutting temperature
OD	optical density
OHT	4-hydroxytamoxifen
p38MAPK	p38 mitogen-activated protein kinase
PAC	phage artificial chromosome
PAL-E	pathologische anatomie leiden-endothelium
PBMCs	peripheral blood mononuclear cells
PBS	phosphate buffer saline
PBS-T	phosphate buffer saline -triton
PC	principal component
PCA	principal component analysis
PCI	percutaneous coronary intervention
PCR	polymerase chain reaction
Pdgfb	platelet derived growth factor b
Pdgfra	platelet-derived growth factor receptor alpha
Pdln	podoplanin
PFA	parafolmadehyde
PHD2	pronyl hydroxylase domain 2
PI3K	phosphatidylinositol 3-kinase

PLVAP	plasmalemma vesicle associated protein
PMA	phorbol myristate acetate
Postn	periostin
PVDF	polyvinylidene difluoride
qPCR	quantitative polymerase chain reaction
RA	retinoic acid
RFP	red fluorescent protein
ROI	region of interest
RPMI	roswell park memorial institute medium
RT	room temperature
Sca1	stem cell antigen-1
SD	stomatal diaphragms
SM	skeletal myoblasts
Sox9	sry-box transcription factor 9
ST	spatial transcriptomics
TBS	tris-buffered saline
Tcf21	transcription factor 21
TECs	transendothelial channels
tSNE	t-distributed stochastic neighbour embedding
TUNEL	terminal deoxynucleotidyl transferase dutp nick end labeling
UMI	unique molecular identifier
VEGF	vascular endothelial growth factor
VEGF	vascular endothelial growth factor
VWF	von willebrand factor
VW-SC	vascular wall stem cell
WBP	weibel-palade bodies
YFP	yellow fluorescent protein

vi List of Figures

vii List of Tables

viii Abstract

Ischaemic heart disease remains one of the leading causes of death worldwide, responsible for over 8.9 million deaths in 2017 according to the Global Burden of Disease Study. Restoring blood perfusion in the ischaemic border via a functional vascular network may enhance myocardial perfusion, limit infarct expansion and promote cardiac regeneration. However, the pathways driving endogenous vascular regeneration following myocardial infarction (MI) remain poorly understood. The aim of this thesis was twofold; First, to investigate the origin and clonal dynamics of cardiac endothelial cells (EC) post-MI. Secondly, to analyse the transcriptional profiles of pro-angiogenic EC in MI using single cell RNA sequencing in the post-ischaemic adult mouse heart, and investigate potential therapeutic targets in human patient samples. MI was induced in an EC-specific multispectral lineage-tracing mouse, "*Pdgfb-iCreER^{T2}-Brainbow2.1*", by permanent ligation of the left anterior descending coronary artery. Blood vessel formation via clonal proliferation by resident Pdgfb-lineage EC was significantly upregulated in the ischaemic border at 7 days post-MI, compared to the healthy heart. Minimal contribution from the bone marrow was observed. Bioinformatics analyses revealed 10 transcriptionally discrete heterogeneous EC states in the 7 days post-MI heart and revealed molecular pathways through which each cluster was likely to mediate neovasculogenesis following MI. Plasmalemma Vesicle–Associated Protein (*Plvap*) gene expression was upregulated in MI, specifically in clusters of cells from the MI group, indicating its potential relevance to neovasculogenic pathways. I validated increased *Plvap* expression at the protein level, which was EC-specific and was significantly higher in the infarct border of the post-ischaemic mouse heart compared to the healthy heart. PLVAP expression was also significantly increased in EC adjacent to regions of fibrosis and scarring in the ischaemic human heart, compared to healthy human hearts. Moreover, *in vitro* silencing using RNAi in human umbilical vein ECs showed that PLVAP may play a direct functional role in regulating EC proliferation. The single cell gene expression atlas of cardiac resident ECs presented in this thesis can be used to unravel the neovasculogenesis pathways that are activated 7 days post-MI. Cluster

specific PLVAP was identified as a possible target for augmenting endogenous myocardial perfusion following ischaemia and validated in human cardiac ischaemic tissue. Future studies will involve further interrogation of the activated neovasculogenesis pathways from cardiac ECs using the single cell gene expression atlas as well as investigation of the molecular mechanisms of the role of PLVAP in EC proliferation.

ix Lay abstract

Ischaemic heart disease (IHD) is one of the leading causes of death worldwide according to the World Health Organization. Discovering new ways to treat IHD is of paramount importance to reduce death numbers and relieve the global burden from the public health systems of the world. IHD arises when blood circulation that feeds the heart is clogged with fatty substances called plaques, or atheroma. As a result, cardiac muscle cells become starved, injured and can eventually die. An attractive target to save injured cardiac muscle cells in IHD is by regulating the formation of new blood vessels, known as 'angiogenesis'. Generation of new blood vessels can reduce damage caused to the heart in the event of a heart attack. However, the mechanisms under which angiogenesis can be beneficial in IHD are still poorly understood. Using a genetically modified mouse model, I took on the task of investigating the molecular mechanisms by which the cells that line the blood vessels of the heart contribute to the formation of new blood vessels following injury. My results shed further light on the mechanisms by which blood vessels form after heart attack as well as the molecular mechanisms that drive these processes. I identified a gene, Plasmalemma Vesicle Associated Protein or *Plvap*, that might play a role in the formation of new blood vessels. This was studied in human diseased cardiac samples, demonstrating its potential role in disease. These results bring closer the potential for new therapies and improvement of IHD patient outcomes.

Chapter 1 Introduction

1.1 Ischaemic heart disease

Ischaemic heart disease (IHD) is one the leading causes of death worldwide, responsible for 8.9 million deaths in 2017 according to the Global Burden of Disease Study. [1] Statistics show 126 million people currently live with IHD, with 10.6 million new cases occurring in 2017 alone. [1] This indicates that IHD remains a substantial public health challenge in addition to the severe personal, social, and economic burden that it causes.

IHD is the main form of cardiovascular disease (CVD) accounting for 45% of total CVD-related deaths in the UK.[2] Currently, there are 2.29 million people in the UK living with IHD and 650,000 living with heart failure (HF), the main sequela of IHD. There are roughly 200,000 new diagnoses of HF every year in the UK.[2] In addition, myocardial infarction (MI) events, the main complication of IHD, occur more than 100,000 times each year, which translates to someone in the UK having a heart attack approximately every 5 minutes.[2]

Advances in prevention, diagnosis and clinical care have resulted in a dramatic reduction in CVD deaths which have declined by two thirds in developed countries.[3] Specifically, survival following an MI event has also been improved.[4] However, improved survival from MI has contributed to increasing heart failure incidence which remains a significant public health issue.[5]

1.2 Ischaemia and damage to the myocardium

1.2.1 Atherosclerosis

Coronary atherosclerosis can remain asymptomatic and, therefore, unnoticed for the majority of an individual's life. It is the main cause of ischaemic heart disease and includes plaque formation *via* thickening and/or hardening of the inner lining of coronary arteries, which supply the heart with oxygen and nutrients (Figure 1.1, A).[6] This may result in the gradual occlusion of the coronary vessels, limiting blood flow and leading to ischaemia (Figure 1.1, B-C).[7] Additionally, these plaques may rupture or erode resulting in thrombosis that can lead to total occlusion of the coronary vessels thus leading to MI[8] which is defined as myocardial cell death due to ischaemia (Figure 1.1, D).[9] This can lead to massive cardiomyocyte loss. Subsequently, cardiac ischaemia can develop into pathological cardiac remodelling, cardiac dysfunction, and potentially heart failure (Figure 1.1, E-F).[5]

1.2.2 Pathophysiological changes after myocardial ischaemia

Following cessation of blood supply to the myocardium, cardiac cells become starved of oxygen and nutrients, and become ischaemic. [10] Cardiomyocytes have the ability to maintain contraction in the presence of ischaemia due to high energy phosphate reserves.[11] If coronary occlusion is less than 15 minutes in duration, the injury has been shown to be reversible in canine models of reperfusion.[12] However, this has not been confirmed in humans. Myocardial necrosis can be detected as early as 2 to 3 hours in human patients with fatal MI *via* the use of tetrazolium salt solutions, which form a coloured precipitate on fresh heart tissue in the presence of dehydrogenase-mediated activity.[13] Myocardial necrosis can also be seen at a macroscopic level *via* visualisation of the pale colour of the myocardium.[14] In non-reperfused, fatal MI, the infarct area is visible in patients that die at 2 to 3 days post-MI with a central area of yellow discoloration that is surrounded by a rim of highly vascularised hyperaemia.[14] In patients that die 5 to 7 days post-MI the areas are more distinguishable with a central soft area and a depressed hyperemic border region.[14] In patients that die 1 to 2 weeks post-MI, the infarct is depressed, the borders have a white hue and scarring

begins to develop.[14] The process for infarct scar resolution can vary greatly according to the size of the infarct, with small infarcts taking 4-6 weeks and larger ones up to 2-3 months.[14] Resolved infarcts have a white colour from scarring and the ventricular wall is thinned.[14]

In homeostasis, the heart is primarily working under aerobic conditions and derives its energy from fatty acids which supply 60 to 90% of the energy for adenosine triphosphate (ATP) synthesis.[15] The remaining energy originates from oxidation of pyruvate formed from glycolysis and lactate oxidation. Ischaemia due to coronary artery occlusion results in a shift from aerobic or mitochondrial metabolism to anaerobic glycolysis.[15] Reduced aerobic ATP formation activates glycolysis and leads to higher myocardial glucose uptake and glycogen breakdown. [15] Moreover, ischaemia leads to pyruvate not being oxidized in the mitochondria, leading to the production of lactate, a fall in intracellular pH, a reduction in contractile function and an increase in ATP requirement to maintain Ca^{2+} homeostasis. [15] Decreased levels of ATP inhibit Na+/K+ ATPase thus increasing intracellular Na+ and Cl-, leading to cell swelling. [15]

Acidosis occurs from anaerobic metabolism and increased influx of Na^+ via the Na/H^+ exchanger. Levels of intracellular Na^+ are increased as a result of reduced active outward pumping. Moreover, the quick inhibition of the Na^+/K^+ ATPase further enhances the accumulation of Na^+. [16] There is an increase in cytosolic Ca^{2+} due to disruption in transport systems in the sarcolemma and sarcoplasmic reticulum, namely the Na^+/Ca^{2+} exchanger.[15] Calcium overload occurs when Na^+ is exchanged for Ca^{2+} by reverse operation of the sarcolemmal Na^+/Ca^{2+} exchanger.[16] Increased cytosolic Ca^{2+} leads to opening of the mitochondrial permeability transition pore (mPTP) that further increases Ca^{2+} overload and causes hypercontracture.

In addition, cytoplasmic Ca^{2+} overload activates proteases and alters contractile proteins. [15] When reperfusion occurs the quick reactivation of calcium overloaded cells leads to fluctuations in Ca^{2+} cytoplasmic concentration caused by cyclic release

and reuptake of Ca^{2+} into the sarcoplasmic reticulum, thereby causing myofibrillar hypercontraction. [16]

Moreover, acidosis disrupts ionic channels resulting in a decrease in resting potential, increase in the duration of action potential, and early afterdepolarization events.[17] Ischaemia leads to efflux of intracellular K^+ in the extracellular space. This in turn results in a decrease in action potential. [18] Extracellular K^+ reaches a plateau after the first minutes but increases further when cardiomyocytes die and more K^+ is released into the interstitium.[19] The increase of K^+ in the extracellular matrix results in inexcitability and conduction block.

1.2.3 Left ventricular remodelling

Myocardial ischaemia can occur in both the atria and ventricles. [20 21] However, atrial infarction is a rare clinical event.[20] Ventricular infarctions are the most common type of MI.[20] Left ventricle infarction events are, in turn, the predominant form of ventricular MI as the right ventricle is less susceptible due to its thinner walls and reduced energetic demands.[21] Hence, left ventricular infarction will be the focus of this thesis.

Following MI, the left ventricular wall undergoes acute (within 72 hours) and chronic (beyond 72 hours) remodelling.[22] The earlier phase consists of structural changes from cardiomyocyte loss and infarct expansion, and can result in ventricular rupture and death.[23] Late remodelling is associated with ventricular wall dilatation, shape distortion and hypertrophy that can lead to reduction in contractile function and heart failure. [5]

Ventricular ischaemia can result in a transmural or non-transmural infarct, depending the extent of damage in the myocardial wall (Figure 1.1, E-F). [24] A non-transmural infarct will not reach the epicardium, thus sparing epicardial resident cells (Figure 1.1, E).[24]

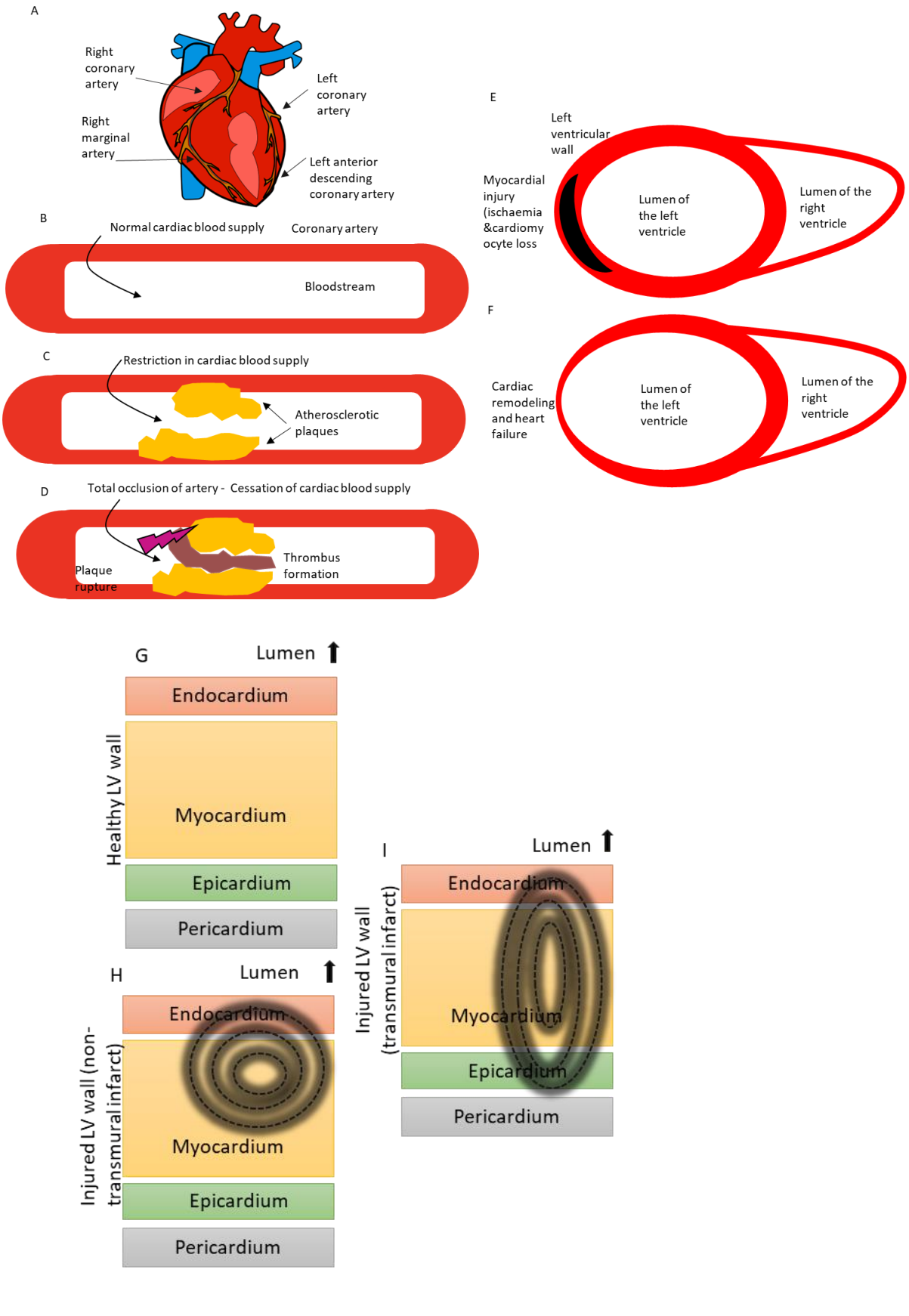
A
Right coronary artery
Left coronary artery
Right marginal artery
Left anterior descending coronary artery
B
Normal cardiac blood supply
Coronary artery
Bloodstream
C
Restriction in cardiac blood supply
Atherosclerotic plaques
D
Total occlusion of artery - Cessation of cardiac blood supply
Thrombus formation
Plaque rupture
E
Left ventricular wall
Myocardial injury (ischaemia &cardiomyocyte loss
Lumen of the left ventricle
Lumen of the right ventricle
F
Cardiac remodeling and heart failure
Lumen of the left ventricle
Lumen of the right ventricle
G
Lumen
Endocardium
Healthy LV wall
Myocardium
Epicardium
Pericardium
H
Lumen
Endocardium
Injured LV wall (non-transmural infarct)
Myocardium
Epicardium
Pericardium
I
Lumen
Endocardium
Injured LV wall (transmural infarct)
Myocardium
Epicardium
Pericardium

Figure 1.1 Pathophysiology of left ventricular myocardial infarction

(A) Schematic of the coronary arteries of the human heart (B) Healthy coronary arteries (C) Coronary artery with atherosclerosis and restriction in myocardial blood supply. (D) Total occlusion of coronary artery blood supply occurs when the atherosclerotic plaques ruptures/erodes, and a thrombus is formed. (E) Upon blockage of the coronary arteries that supply the left ventricle, cardiomyocyte loss occurs due to ischaemia, and an infarct core is formed. (F) Infarction results in left ventricular remodeling with wall dilatation and reduction in contractility. (G) Schematic of the layers of the left ventricle under normal conditions. (H) Example of a non-transmural infarct extending from the myocardium into the endocardium. (I) Example of a transmural infarct extending from the endocardium all the way to the epicardial layer.

1.2.4 Histopathology of myocardial infarction

Histopathological changes in the myocardium can be visible as early as 12 to 24 hours after the onset of myocardial ischaemia.[14] Neutrophils are visible by 24 hours at the border regions of the infarct. [14] After 24 hours, necrosis is occurring with various degrees of nuclear chromatin pyknosis, early karyorrhexis, and karyolysis.[14] There is prominent infiltration of neutrophils by 48 hours. [14] At 3 to 5 days, there is significant loss of myocyte nuclei and striations in the central part of the infarct. [14] Subsequently, the inflammatory influx induces a cascade of chemokines that suppresses inflammation and contributes to scar tissue formation.[25] At this point, around 5 days post-MI, macrophages and fibroblasts appear in the infarct border regions, and by 1 week neutrophil levels fall and granulation tissue is formed next to neocapillaries, lymphocytes and plasma cells. [14] Lymphocytes are not a predominant lineage at any stage in the infarct, but can be present as early as 2 to 3 days. [14] Eosinophils can be detected in the inflammatory infiltration but only in around 24% of infarcts.[26] Finally, after 1 week, necrotic myocytes are removed by macrophages *via* phagocytic removal. [14] After 14 days, fibroblast numbers are significantly elevated but can be seen as early as day 4 at the periphery of the infarct.[14] Fibroblasts produce collagen as more necrotic myocytes are removed by macrophages, and angiogenesis takes place in the region. [14] Depending on the size of the infarct, the scarring process can

take up to 8 weeks or longer to complete and the central area of the infarct may remain unhealed. [14]

1.2.5 Mechanisms of cell death post-MI

1.2.5.1 Apoptosis

Cell death during myocardial ischaemia can occur via a number of different processes. Myocyte oncosis occurs from cell swelling and is independent of cell activity including caspases and ATP consumption. [14] Apoptosis is a type of active cell death that results in cell shrinkage and is energy dependent.[27] This is a complex process that involves various molecular pathways, namely caspases. In the case of myocardial ischaemia, apoptosis is not normally implicated with myocyte death, mostly due to its energy dependent nature. However, apoptosis can be involved in the first hours of ischaemia and possibly during reperfusion injury. [28] Cardiomyocytes can also undergo apoptosis in viable remodeling in the weeks or months after MI.[29] It is worth mentioning that the contribution of apoptosis versus necrosis in cardiomyocyte death remains poorly defined, mainly due to limitations in experimental tools to identify apoptotic and necrotic cells.

1.2.5.2 Necrosis

Necrosis is a faster process compared to apoptosis and is characterised by cell swelling, cell membrane breaking and release of cellular debris that in turn activate inflammation. [28] Necrosis is associated with the opening of the mPTP.[30] In homeostasis, this pore of the inner mitochondrial membrane is impermeable to water, ions and protons. In the ischaemic myocardium, Ca^{2+} entry into the mitochondria can lead into the opening of the mPTP. When open, the influx of water in the mitochondrial matrix results in mitochondrial swelling that leads to cardiomyocyte death. [30]

1.2.5.3 Autophagy

Autophagy is characterised at an ultrastructural level by autophagic vacuoles, cellular degradation and nuclear disruption.[31] Autophagic vacuoles form by ubiquitin attachment to various proteins *via* post-translational modifications which in turn, makes them susceptible to proteasomal degradation.[14]Autophagy is a regulated process with many key players including cathepsin D, cathepsin B, heat shock cognate Hsc73, beclin 1 and microtubule -associated protein 1 light 3.[14] In the context of the myocardium, autophagy has been described in hypertrophied and failing myocardium (reviewed in ref[32]). Autophagy can play an important role in the degradation of damaged proteins or senescent cells for recycling purposes. It can be seen in response to metabolic stress and nutrient starvation. In the context of the heart, autophagy has been shown to occur in homeostasis to remove intracellular protein aggregates as well as failing organelles via the autophagosome (double membrane bound vesicle). The autophagosome delivers its contents to lysosomes for degradation.[33] In cardiac ischaemia, autophagy can be utilized to remove waste and promote cell survival and can occur simultaneously with necrosis and apoptosis.[34,35]

1.2.6 Non-cardiomyocyte cells in ischaemia

The mammalian heart is home to many non-cardiomyocyte cells, including fibroblasts, endothelial cells (ECs), pericytes, vascular smooth muscle cells, adipocytes, neuronal cells, myeloid cells, mesothelial cells and lymphoid cells.[36] Recent studies investigating cellular composition have shown ECs are the most common cardiac cell type, comprising 64% of non-cardiac cell populations.[37] This thesis focuses on the dynamics of proliferation of ECs in the healthy myocardium and after MI.

Following MI, there is a robust angiogenic response in the damaged area [38] but angiogenic mechanisms do not occur rapidly enough to save the ischaemic cardiomyocytes. These new vessels are still important as they can aid supply of oxygen and nutrients to the active mesenchymal cells in the healing infarct thus

promoting healthy scarring. [39] However, the exact mechanisms by which new vessels promote tissue repair are incompletely understood.

Newly formed vessels are hyperpermeable, pro-inflammatory and lack perivascular support by pericytes.[40] Following scarring, the neo-vessels undergo maturation and stabilise the wound as they become less permeable and inflammatory.[40] ECs that do not acquire perivascular support undergo apoptosis. [40] However, the molecular mechanisms underpinning the process of blood vessel formation post-MI are largely unknown and understanding these form the main goal of this thesis.

1.3 Reperfusion and no-reflow

The myocardium is vulnerable to a lack of, or reduction in, blood supply arising from MI. Hence, reperfusion of the tissue is essential for preventing further cardiomyocyte loss. There have been substantial recent developments in acute care leading to a significant decrease in mortality due to the wide adoption of reperfusion therapy via thrombolytic therapy, percutaneous coronary intervention (PCI) [41] and coronary artery bypass grafting (CABG).[42]

1.3.1 Clinical tools for re-establishing perfusion

Thrombolytic therapy has been instrumental at decreasing infarct size, incidence of heart failure and long term-survival (reviewed in Ref[43]). Thrombolytic therapy involves the use of drugs (such as tissue plasminogen activator, streptokinase, and urokinase) to dissolve thrombi arising from the rupture/erosion of atherosclerotic plaques and establishing reperfusion.[43]

PCI was introduced in the 1980s[27] and made a big impact on patient survival outcomes following MI in many parts of the world. This procedure involves the insertion of a catheter and injection of a contrast agent into the coronary arteries. Upon reaching the occluded vessel, the catheter that is equipped with a balloon on its tip, inflates the balloon in order to compress the plaque, thus restoring blood flow. A mesh, or stent, is normally placed in the same area to keep the vessel open following catheter removal.[44]

CABG is a surgical procedure in which autologous arteries or veins are used to bypass coronary vessels that have been partially or totally occluded (reviewed in Ref[42]).

Despite improvements in clinical care, MI patients can be left with substantial ventricular damage[45]. Patients that present with MI have a high likelihood (14-36%).[45] of going on to develop heart failure and be at an increased risk of premature death.[4]

In summary, clinical interventions can improve survival rates but do not initiate cardiac regeneration or prevent scar formation following MI. Hence, developing techniques to improve reperfusion in the post-ischaemic heart has the potential to improve patient outcomes.

1.3.2 Reperfusion injury

There is a balance to be struck between establishing reperfusion to the ischaemic myocardium and reperfusion injury. In early reperfusion (2-3 hours) after the onset of ischaemia, the rescue of myocytes is far more beneficial than any adverse effect (such as free radical damage and Ca^{2+} loading) arising from reperfusion injury.[14]

Early reperfusion following MI remains the most effective way of limiting infarct size and cardiac remodelling. [46] The term "cardiac remodeling" was coined by Hockam and Bulkley in 1982 after they observed regional dilatation and thinning of the infarcted myocardium in rats.[47] Pfeffer *et al*. used the same term to describe the volume increase of the left ventricle (LV) after MI.[48] Nowadays, the term is used to refer to any changes to the heart morphology that arise due to any pathology, not just MI.

Unfortunately, reperfusion injury contributes to irreversible injury to the heart and contributes to final infarct size.[49,50] Final infarct size depends on a variety of factors such as: 1) the size of the ischaemic area; 2) duration of non-perfusion; 3) the magnitude of residual collateral blood flow and severity of microvascular dysfunction.[51] In humans, 30-50 % of the ischaemic area can be salvaged by reperfusion within 4-6 hours from the onset of chest pain symptoms.[14] Viable

myocardium that is salvageable by interventional reperfusion can be seen even after 12 hours post-occlusion[52]. Following 24 hours of occlusion and a subsequent 6 hours of reperfusion in a dog model, myocytes have been shown to be thin, hyper-eosinophilic, devoid of nuclei and showing signs of karyorrhexis.[14] They have ill-defined borders with signs of interstitial haemorrhage.[14] Initially, a mild neutrophil infiltration is visible and macrophages are prominent and are seen to remove necrotic myocytes via phagocytosis.[14] In humans, following reperfusion within 4-6 hours post-onset of pain, myocardial cell salvage takes place and the infarct is restricted to the subendocardial layer.[14] Haemorrhage is present within the infarcted myocardium, as evident by contraction band necrosis. [14] Contraction necrosis bands consist of 3-10 hypercontracted sarcomeres that bring adjacent Z bands close together.[11] Z bands define the boundary of striated muscle between two neighboring sarcomeres. [53] In the case of late reperfusion, contraction bands do not develop.[11] Following a few hours of reperfusion, sparse levels of neutrophils are present within the infarct.[14] Macrophages appear by day 2 to 3 and by day 5 fibroblasts are present and begin the collagen synthesis and scarring process. [14] Interestingly, the scarring process in reperfused infarcts is accelerated compared to non-reperfused infarcts. A reperfused infarct can be fully healed by the 3rd week post-injury but this can depend on the size of the infarct. Early reperfusion has shown clear benefits to reducing infarct size. [14] Preserving viable myocardium has been associated with decreased remodeling and infarct expansion and thus, increased survival. [14]

1.3.3 The no-reflow phenomenon

The success story of PCI and CABG has shown how crucial early reperfusion is at limiting infarct size. However, PCI sometimes fails to fully restore myocardial perfusion, especially at the microvascular level in a phenomenon known as no re-flow. The no-reflow phenomenon is defined as a state of myocardial hypoperfusion in the presence of a patent epicardial coronary artery and has been attributed to microvascular obstruction.[54]

No-reflow is reported in up to 60% of ST-segment elevation myocardial infarction (STEMI) cases.[55] There is still limited information on how the no-reflow phenomenon affects patients with MI that undergo PCI. It is associated with left ventricular remodelling and negatively affects the clinical outcome in patients with acute MI [55]. No reflow is also an independent predictor of adverse clinical outcomes for patients that present with acute MI. [56] Moreover, restoration of coronary blood flow may result in arrhythmias, myocardial stunning as well as microvascular impairment that can lead to myocyte damage and death.[10]

No-reflow can be separated into two categories. Firstly, "reperfusion no reflow" occurs following PCI in a patient presenting with an acute MI.[57] Debris from the thrombus can lead to microvascular obstruction that leads into further ischaemic cell injury. [57] Secondly, "interventional no reflow" takes place in a non-infarct PCI. The key here is that this has the potential to affect myocardium that was not heavily ischaemic before the procedure. [57] Atherosclerotic debris from the initial point of occlusion can travel further down the vessel network and cause microvascular mechanical obstruction and lead to EC inflammation and injury and ultimately ischaemia and cell death. [57] Moreover, endothelial injury can be caused by an acute inflammatory response, generation of reactive oxygen species and rise of intracellular calcium. [57 58] This can further lead to EC swelling and vasospasm that can prolong occlusions of the microvasculature. [57 58]

There is clear evidence that reperfusion of the ischaemic myocardium is extremely beneficial for patients' outcomes which is the reason that it has become standard clinical practice. [41 42] However, as discussed above, not all patients respond well to interventional reperfusion, whether it is an infarct or non-infarct scenario. Moreover, as described in previous sections, the formation of new blood vessels in the damaged myocardium post-MI is essential in driving healthy scarring.[40] There is a need for therapies that drive reperfusion by promoting formation of new blood vessel networks and, thus, increase blood supply to ischaemic tissues and prevent cell death.

1.4 Coronary artery ligation as a model of myocardial infarction

As evident by earlier segments, cardiac injury is a multicellular, dynamic process that is difficult to investigate using traditional models of cell culture, whilst clinical samples from patients are limited for investigative study. As a result, we need robust and reproducible animal models of injury to shed light on the pathological mechanisms involved.

The main model used to simulate acute cardiac injury and progression to heart failure in animals is ligation of the left anterior descending coronary artery (LAD) (reviewed in Ref[53]). This model can be applied to large (e.g. pigs) and small (e.g. mice, rats) animals. Moreover, the LAD ligation model can be used in combination with genetically engineered mouse models such as knock-out models or lineage tracing models. The two predominant variations of this model are permanent LAD ligation (PL) or a temporary ligation resulting in ischaemia-reperfusion (IR). [59]

The procedure of PL involves a left-sided thoracotomy that is carried out on an anaesthetised mouse with a subsequent ligation of the LAD coronary artery which runs along the anterior side of the LV. Consequently, there is an occlusion of blood supply to the LV resulting in ischaemia, cardiomyocyte death and scar formation. The resulting infarct is large, with sizes varying between 30% and 40% of the myocardial area.[60] Survival rate is also variable and is dependent on infarct size, sex and mouse strain.

IR is similar to PL but ligation of the LAD artery is temporary. Following the preferred time of ischaemia (ranging from 15 minutes to 2 hours), blood flow is restored by cutting the fine suture that was used for occlusion. Contrary to the PL model, infarct sizes are more variable and smaller with infarct sizes as low as 4% and up to 30%.[61] Despite IR being more technically challenging and producing a smaller a more variable infarct it is crucial at understanding the mechanisms behind pathology of reperfusion injury.

One of the main differences between the two variations of the LAD ligation model is the infarct size that is generated following the surgical procedure. PL overall produces more significant infarcts but is associated with poor survival compared to IR. When compared to the clinical situation of MI patients, it can be argued that IR is a more representative model than PL as many of the MI patients that present to the clinic will undergo reperfusion therapy via PCI. However, despite the permanent nature of the PL, around 30% of acute MI patients do not receive reperfusion therapy and the PL model is therefore applicable to this group.

Both variations of the cardiac injury ligation model are clinically relevant but depending on the question of the researcher one may be more appropriate than the other. PL is more suitable for studying acute tissue injury as well as the repair responses and progression to heart failure in the absence of reperfusion whereas IR is useful at investigating the secondary damage in the form of reperfusion injury. However, it is worth considering that despite their clinical relevance, IR and PL still have limitations (reviewed in Ref[62]). Importantly they do not simulate the pathogenesis of ischaemic heart disease (coronary atherosclerosis) and rather rely on an acute occlusion of coronary blood supply via ligation. Furthermore, the mice that are involved in experiments modelling MI are often bred from a single background. This is helpful when trying to dissect a molecular mechanism but is in contrast with the heterogeneity in the transcriptomic and epigenetic profile of patients in the clinic. Moreover, these surgical models are used in healthy rodents which is often in contrast to the patients that suffer from cardiac ischaemia. These patients are often older and suffer from a multitude of other risk factors like atherosclerosis and diabetes.[1]

1.5 The circulatory system, endothelial cells, and blood vessel architecture

The vascular system is a closed system that transports oxygen, nutrients, and salts, as well as waste products, between blood and tissues. This is achieved through ejection of blood by the cardiac muscle. Blood is circulated through the pulmonary vasculature, where it becomes oxygenated, and is then delivered to the tissue systems where blood-tissue oxygen transfer occurs.[63]

The vascular network is an incredibly dynamic system that changes radically during growth as well as in response to stimuli such as injury, healing and pathology. The network comprises arteries, veins, capillaries, and lymphatic vessels.[64] The lymphatic system's main role is to take up interstitial fluid, or lymph, that leaks out of the blood vasculature into extracellular spaces and transfer it back to the blood circulation.[65] In the context of this thesis, arteries, veins and capillaries will be discussed. Lymphatic vessel architecture will not be described but is reviewed by Oliver *et al.*[65]

1.5.1 Blood Vessel structure

1.5.1.1 Arteries

Healthy arteries have a tri-laminar structure of tunica intima, tunica media and tunica adventitia (reviewed in Ref [64]). The inner layer, the tunica intima, is in contact with the blood circulation and comprises a layer of ECs that lies on a basement membrane (Figure 1.2, A).[64] ECs are the main component of the vasculature and possess essential and highly regulated mechanisms that are critical in maintaining vascular homeostasis and will be described in more detail in the next section.[64] ECs in the tunica intima are connected by two different types of junctions. These are occluding junctions (*zonulae occludentes*) and communicating junctions (gap junctions). [64] In certain arteries, the tunica intima also contains other types, such as smooth muscle cells, and collagen. [64] The tunica intima is also supported by an internal elastic lamina which functions as a physical barrier between the intima and the subsequent vessel layer, tunica media. [64] Moreover, between the tunica intima and the tunica media there is a network of collagenous bundles and elastic fibers.[66] The tunica media

harbours mainly smooth muscle cells that are responsible for vessel contraction and relaxation. The tunica media can vary in diameter (Figure 1.2, A). This characteristic can be used to differentiate between elastic and muscular arteries.

Large diameter arteries, such as the aorta, are rich in elastic lamellae and are referred as elastic arteries. In contrast, in smaller diameter arteries, the tunica media is less elastic and contains more smooth muscle cells. These are termed as muscular arteries. Smaller arteries less than 100 µm in diameter are termed arterioles or resistance arteries. [67] The tunica media of these vessels contain 1-2 layers of smooth muscle cells.

The tunica intima of elastic arteries is composed of a single layer of ECs that are lined against a layer of fibrous tissue. [66] These ECs are elongated and their long axis is found parallel to the blood flow. [66] Between the tunica intima and the subsequent tunica media there is a network of collagenous bundles and elastic fibers. [66] The tunica media contains concentrically arranged fenestrated elastic laminae alongside smooth muscle cells. [66] The smooth muscle cells are orientated longitudinally and circularly.[66] The adventitia of elastic arteries is thin and contains fibroblasts, inflammatory cells and Schwann cells.[66]

In muscular arteries, the tunica intima is thinner than in elastic arteries. [64] There is a highly fenestrated internal elastic lamina that separates the intima and media. This intermediate layer gradually decreases as the diameter of the muscular artery also decreases. This occurs as the vascular network moves towards the capillary network. The tunica media of muscular arteries is home to concentric layers of spindle-shaped smooth muscle cells that are arranged in a low-pitched helix or spiral. [64] The number of layers of smooth muscle cells can vary according to artery diameter but can range from 1-6 in small arteries and arterioles and 25 to 35 µm in bigger vessels.[66] Interspersed between the smooth muscles of muscular arteries, a distinct external elastic lamina is found between the media and adventitia. However, this lamina may be absent in muscular arteries of small diameter and be replaced by longitudinally

arranged elastic fibrils. In contrast to elastic arteries, the adventitia of muscular arteries is much wider and can take up half the diameter of the vessel wall.[66]

The adventitia contains collagen, elastic fibres, connective tissue cells and some neural cells (Figure 1.2, A). Its role is to connect the vessel to surrounding tissues as well as limiting the extent of its expansion. Recently however, the adventitia has also been shown to harbour cells with stem cell like properties, termed vascular wall-resident stem and progenitor cells (VW-SC) or adventitial cells.[68] In addition, it is home to penetrating blood vessels, termed *vasa vasorum*, that supply nutrients and oxygen to the adventitia and media.[69] [66]

1.5.1.2 Veins

Similar to arteries, veins are classified by their diameter. [64] [69] Veins that range from 10 to 100 µm in diameter are named venules, which are the smallest veins of the circulation. [64] Larger veins can be categorized according to their diameter as small (100 µm-1mm), medium (1mm-10mm) or large (>1cm) as they make their way back towards the heart chambers.[70] Importantly, arteries pulsate whereas veins do not. Furthermore, veins are equipped with valves to prevent retrograde flow. [64] The tunica intima of veins contains pocket-shaped folds that extend into the lumen and form the valves.[70] Moreover, they rely on contraction of surrounding muscle to help movement of blood. [64]

In terms of structure, veins follow the same tri-laminar structure as arteries but with key differences (Figure 1.2, B). [64]Veins have thinner walls than arteries of equivalent position in the circulation but are also larger in size.[64] Moreover, the number of smooth muscle cells is larger in arteries than in veins.[64] The tunica media of small veins is home to only a small number of smooth muscle cells that are separated by collagen. [64] In the media of larger veins, there are a few circularly and longitudinally arranged smooth muscle cells. Furthermore, there are many collagen fibers in the venous wall alongside a network of longitudinal elastic fibers. [64] This is characteristic of venous structure with connective tissue to cell ratio being much different

compared with arteries. The adventitia of veins is also different from that in arteries as it comprises 60 to 70 % of the vessel wall (Figure 1.2, B).[71]

1.5.1.3 Capillaries

Capillaries are the blood vessels with the smallest diameter that can range from 4-9 µm. [64] [66] Their role is crucial as they act as the final delivery system of nutrient and blood exchange in most vascular beds. They consist of a single layer of ECs that rest on a basement membrane. [64] This endothelial layer is often surrounded by supporting cells called pericytes. [64] The vascular system includes three types of capillary beds: continuous, fenestrated, and sinusoidal. [64] Continuous capillaries are defined as an EC layer that is connected by inter-EC junctions that greatly limit molecule exchange between the circulation and extravascular space with only water and ions being able to pass. Some lipid-soluble factors can permeate the EC layer through passive diffusion. Fenestrated capillaries contain pores in their ECs that can range from 50-80nm in diameter, termed fenestrae, that connect the lumen to the extravascular space. Due to their porous nature, fenestrated capillaries are found in vascular beds that undergo continuous fluid and solute exchange such as the kidney and the intestine. Finally, sinusoidal capillaries contain wide gaps of 30-40 µm between the ECs and are characterised by a discontinuous basal lamina. This allows for red and white blood cells as well as serum proteins to pass through and enter the interstitial space. These specialised capillaries are found primarily in the liver, bone marrow, and spleen. [72]

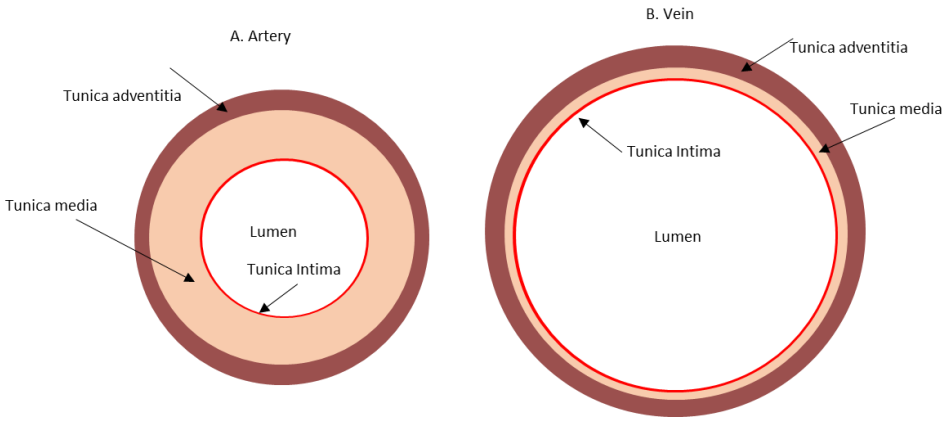

Figure 1.2 Schematic of the typical arterial and venous wall

(A) Schematic of an artery which comprises of an inner tunica intima layer (endothelial cell monolayer), a medial layer (tunica media) comprising of smooth muscle cells and an outer adventitia layer with collagen, elastic fibres, connective tissue cells, neural cells and some progenitor-like cells. (B) Schematic of a vein. Veins are larger in diameter but have a thinner wall. They also contain a tunica intima, a tunica media with smooth muscle cells and collagen fibres and a collagenous adventitial layer.

1.5.2 Endothelial cells

The endothelial cells (collectively the endothelium) are the major regulator of vascular homeostasis.[73] Morphologically, ECs are flat and measure <3µm in thickness along the central axis, which contains the nucleus and cellular organelles.[73] The surface that is in contact with the blood circulation is covered with a thin layer of glycocalyx, a highly-hydrated fibrous mesh of carbohydrates that is critical for modulating interactions between the blood and ECs and for regulating vascular permeability[74]. Furthermore, ECs extend microvilli and filopodia into the vascular lumen. These play a role in blood flow as well as inflammatory cell recruitment. [75,76] The basal side of an EC is characterised by an external lamina that is rich in collagen types III and IV. The endothelial cytoplasmic compartment includes common cellular organelles such as transport vesicles, mitochondria, free ribosomes, rough endoplasmic reticulum, Golgi complex, lysosomes, cytoskeletal filaments and microtubules. A special feature of ECs is the presence of Weibel-Palade bodies (WPBs). These structures are mainly responsible for storing the clotting factor Von

Willebrand Factor (VWF). VWF is also found in α granules in platelets. Upon activation, VWF is released-by α granules due to platelet activation and by WPBs in a basal and regulated manner.[77] However, most reports have shown that VWF is mostly released constitutively from WPBs due to erratic movement inside the granule that results in localization of contents in the periphery and subsequent fusion with the membrane and release.[77] Other functions of the endothelium include roles in haemostasis and thrombosis through the production of procoagulant factors (Factor VIII, plasminogen inhibitor) and anticoagulant factors (prostacyclin).

The roles of ECs include regulation of: vasodilation, vasoconstriction, smooth muscle cell proliferation and migration, and thrombogenesis and fibrinolysis. The importance of the endothelium in vasomotor regulation was first identified in the 1980s when it became apparent that the endothelium is an active paracrine, endocrine and autocrine cell system. [78–82] Nitric oxide was identified as one of the main vasodilatory factors released by the endothelium, originally identified as endothelium-derived relaxing factor (EDRF).[83] Nitric oxide is key to maintaining vascular integrity by preventing inflammation, smooth muscle cell proliferation and thrombosis.[84] Additional vasodilatory factors released by the endothelium include prostacyclin and bradykinin[85]. In addition to vasodilatory factors, the endothelium is capable of releasing several vasoconstrictor factors, such as endothelin-1 and angiotensin II. Angiotensin II also functions as a pro-oxidant and stimulates the production of endothelin-1.[85] Both endothelin-1 and angiotensin II have the ability to promote proliferation of smooth muscle cells and contribute to plaque formation.[86] Furthermore, another component that is critical in maintaining homeostasis in the endothelium is flow mechanics. Specifically, laminar shear stress is essential in maintaining endothelial phenotype.[87]

As described in the previous section, the endothelial types that can be found in capillaries can be either continuous, fenestrated and discontinuous/porous.[73] This can vary greatly across different vascular beds. Fenestrated or discontinuous endothelium occurs across high permeability vascular beds such as the kidney whereas continuous endothelial occurs in low permeability environments. Moreover,

the EC layer can be covered extraluminally by pericytes which stabilize the capillaries and play an important role in signaling via paracrine mechanisms.[88]

EC types display great functional and phenotypic heterogeneity depending on both the tissue system they reside in and their dynamic microenvironment.[73] In addition, the phenotype of ECs can vary greatly depending on their arterial or venous nature. Arterial ECs markers include ephrinB2, delta-like 4 (DLL4), activin-receptor-like kinase 1(alk1), endothelial PAS domain protein 1 (EPAS1), Hey1, Hey2, neuropilin 1 (NRP1) and decidual protein induced by progesterone (Depp).[89] Venous markers include EphB4, neuropilin 2 (NRP2) and COUP-TFII. [89] The phenotype of arterial and venous ECs has been suggested to be epigenetically programmed before blood flow commences. However, studies suggest the phenotype maintains a degree of plasticity and can be reversible.[90] Another example that can provide insights into the plasticity of arterial/venous ECs is coronary artery bypass where saphenous veins are excised and grafted in the coronary vasculature. Venous ECs are, consequently, exposed to arterial pressures and show upregulation of arterial markers.[91] Regarding universal markers, the most commonly used in EC research is platelet/EC adhesion molecule PECAM-1 (also known as CD31). However, CD31 is also expressed in some monocytes.[92] This issue of cross-reactivity with other cell types is an ever-present consideration for even the most robust of EC markers. This is especially the case when pathology or transition is present where cells are in a dynamic state of fluctuating phenotype.[93]

1.6 Mechanisms of blood vessel growth

As described previously in this chapter, the vasculature is fundamental to life. It has evolved into a complex nutrient and oxygen delivery network that reaches every cell. Smaller organisms have no need for this type of network as diffusion is sufficient for nutrient and oxygen exchange between cells, as oxygen is able to travel a distance of 200μm.[94] However, as organisms became increasingly complex, a more sophisticated delivery network was required. Understanding the regulation of the vascular network

requires a deep comprehension of the mechanisms underlying development and regeneration of the vasculature.

1.6.1 Vasculogenesis

Vasculogenesis is the collection of initial events in vascular growth.[95] Blood vessels arise from endothelial precursors called angioblasts that share the same lineage as haematopoietic progenitors. When the mesoderm forms via gastrulation, a subset of mesodermal cells differentiate into angioblasts and haemangioblasts (Figure 1.3).[96] The mesoderm is one of three germ layers (mesoderm, endoderm, ectoderm) that is derived from embryonic epiblast during gastrulation.[96] Subsequent steps involve the formation of early capillary networks from angioblasts. Angioblasts are defined as cellular structures showing positivity for certain markers of ECs but that have not yet formed a lumen.[96] Blood islands are collections of cells that are derived from the mesoderm. The cells in the periphery of blood islands are angioblasts whereas the cells in the centre are haemangioblasts (Figure 1.3). [96] As a result of this close relationship, markers that have been characterised as endothelial have also shown to be expressed by haemopoietic cells, such as CD34.[97]

First signs of vascularisation appear outside the embryo, on the yolk sac, in the form of blood islands. [95] In the mouse, 7.5 days post coitum, a subset of angioblasts migrates to the paraxial mesoderm and proliferates. They subsequently assemble into an early form of an endocardial plexus that gives rise to the dorsal aorta, cardinal veins and embryonic stems of yolk sac arteries and veins. [95] Angioblasts can also mobilise postnatally, circulate, and be recruited for *in situ* vessel growth.[98] The origins of the ability of angioblasts to migrate where needed and initiate vasculogenesis are not well understood. The predominant theory is that, postnatally, a combination of growth factors such as vascular endothelial growth factor (VEGF), granulocyte-macrophage colony-stimulating factor (GM-CSF) and other cytokines are able to recruit bone –marrow-derived angioblasts to sites of neovascularisation. [98]

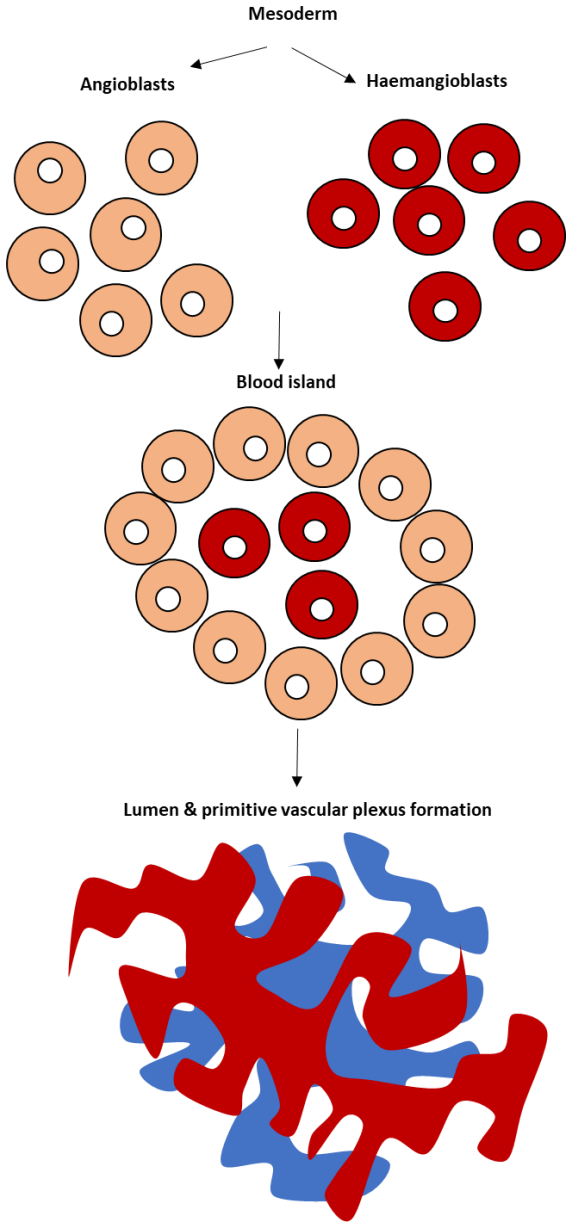

Figure 1.3 Schematic of developmental vasculogenesis

A subset of mesodermal cells forms angioblasts (endothelial cell precursors) and haemangioblasts (haemopoietic cell precursors). Angioblasts and haemangioblasts form blood islands with angioblasts in the periphery and haemangioblasts are in the centre. Blood islands then form the vascular plexus.

1.6.2 Angiogenesis

Angiogenesis refers to vessel sprouting from existing vessels in order to form new vasculature (reviewed in refs[99],[95]**)**. It wasn't until the 1860s that Carl Thiersch demonstrated the formation of new vessels in the tumour stroma from pre-existing vessels.[100] The process of angiogenesis is active throughout growth as per the organism's needs for nutrient supply and is essential for homeostasis. ECs maintain their ability to respond dynamically to changes in their environment such as hypoxia and inflammation.[99]

Angiogenesis is a highly regulated process that follows a step-wise progression.[95] The initial stimulus for angiogenesis is lack of oxygen (hypoxia). Oxygen sensors, such as pronyl hydroxylase domain 2 (PHD2), hydroxylate hypoxia inducible factors (HIFs) and target them for proteasomal degradation when sufficient oxygen is available. Under hypoxic conditions, PHDs are deactivated thus leaving HIFs to freely upregulate pro-angiogenic factors such as VEGF (Figure 1.5). [101] The process of angiogenesis is a complex balance between pro- and anti-angiogenic factors. One of the most prominent pro angiogenic factors is Vascular Endothelial Growth Factor (VEGF). The protagonist of the VEGF protein family is VEGF-A, one of the main regulators of angiogenesis. VEGF-A signalling occurs *via* VEGF receptor-2 (VEGFR-2, also known as FLK1)[102] but is also aided by neuropilins, NRP1 and NRP2 which work as co-receptors.[103] Other members of the VEGF ligand family include VEGF-C, a ligand to VEGFR-2 and VEGFR-3, that is associated with angiogenesis and lymphangiogenesis.[104] VEGFR-3 is essential for developmental angiogenesis but in the adult is mostly associated with lymphangiogenesis.[104]

Activated ECs migrate towards the angiogenic signal. Initially, ECs secrete matrix metalloproteinases (MMPs) with the aim of degrading the basement membrane.[105] The leading EC, termed the tip cell, minimally proliferates and guides the sprout by filopodia and lamellipodia extensions towards the hypoxic environment (Figure 1.4). Tip cells also have the capacity to aid in further degradation of extracellular matrix (ECM). [106–109] The ECs that follow the polarized tip cell, termed stalk cells, proliferate

to elongate the sprout and mediate lumen formation.[110] Tip and stalk cells continuously compete for the leading position in the sprout. This process is mediated by Notch, DLL4 and Jagged1 signalling (Figure 1.6).[106] Following selection of the tip cell, pericytes detach and junctions (VE-cadherin) between ECs become loose through the action of MMPs. Tip cells sprout towards the angiogenic gradient and supporting stalk cells follow the guiding tip cell and proliferate.[111] When two sprouts meet each other, the two tip cells connect via anastomosis to form a new vessel. The new vessel then matures and stabilises by pericyte recruitment and basement membrane deposition.[106] This process is aided by perfusion of the new vessel. [106] The new vessels that are not perfused gradually regress and ECs of those sprouts apoptose.[106] When the ECs return to their quiescent state, they re-establish interconnections through VE-cadherin, claudins and other tight junction proteins.[106]

Another method of angiogenesis is intussusception. This involves splitting of pre-existing vessels that subsequently expand and form an immature capillary plexus.[112] ECs from opposite tunica intimae connect to form a transluminal bridge. Intracellular junctions are reorganised and form an EC bilayer resulting in an interstitial pillar core. Subsequently, myofibroblasts and pericytes invade the interstitial pillar core and cover the interstitial wall. This results in fusion of the pillar with adjacent pillars and a final split into 2 parallel capillaries. [113,114]

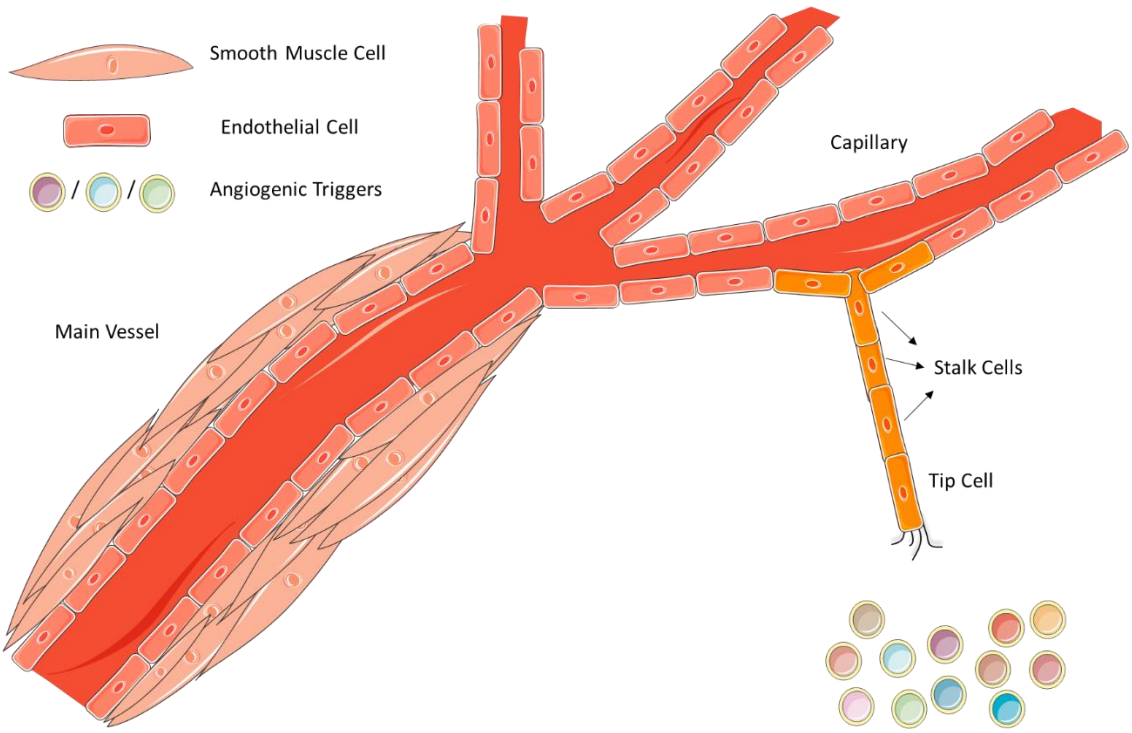

Figure 1.4 Schematic of tip/stalk cell angiogenesis

Upon an angiogenic trigger, endothelial cells of capillaries break the basement membrane then rest upon and arrange themselves as proliferative stalk cells and sprout-leading tip cells in the direction of the stimulus.

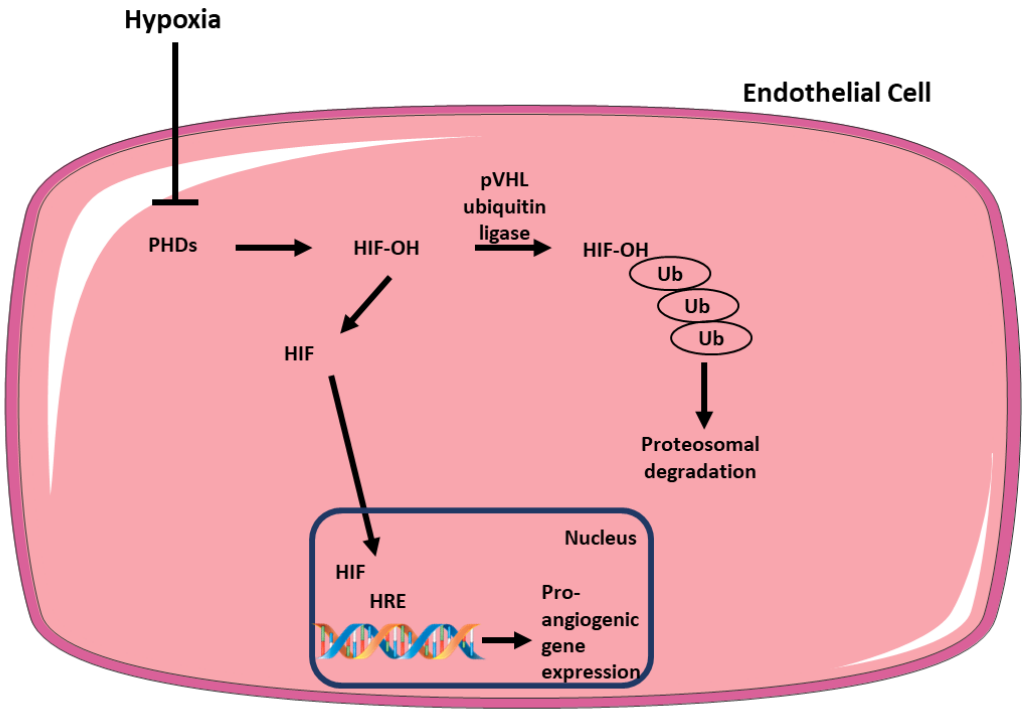

Figure 1.5 Hypoxia activates HIF to initiate transcription of pro-angiogenic genes

Hypoxia inhibits the action of prolyl hydroxylases (PHDs) that, under normoxic conditions, target hypoxia inducible factors (HIFs) by attachment of an -OH group. When attached to a -OH group, HIFs will be targeted for ubiquitination by von Hippel–Lindau protein (pVHL) and HIFs degraded by the proteosome. Upon deactivation of PHDs, HIFs enter the nucleus and bind to hypoxia response elements (HRE) on the DNA and drive expression of pro-angiogenic genes.

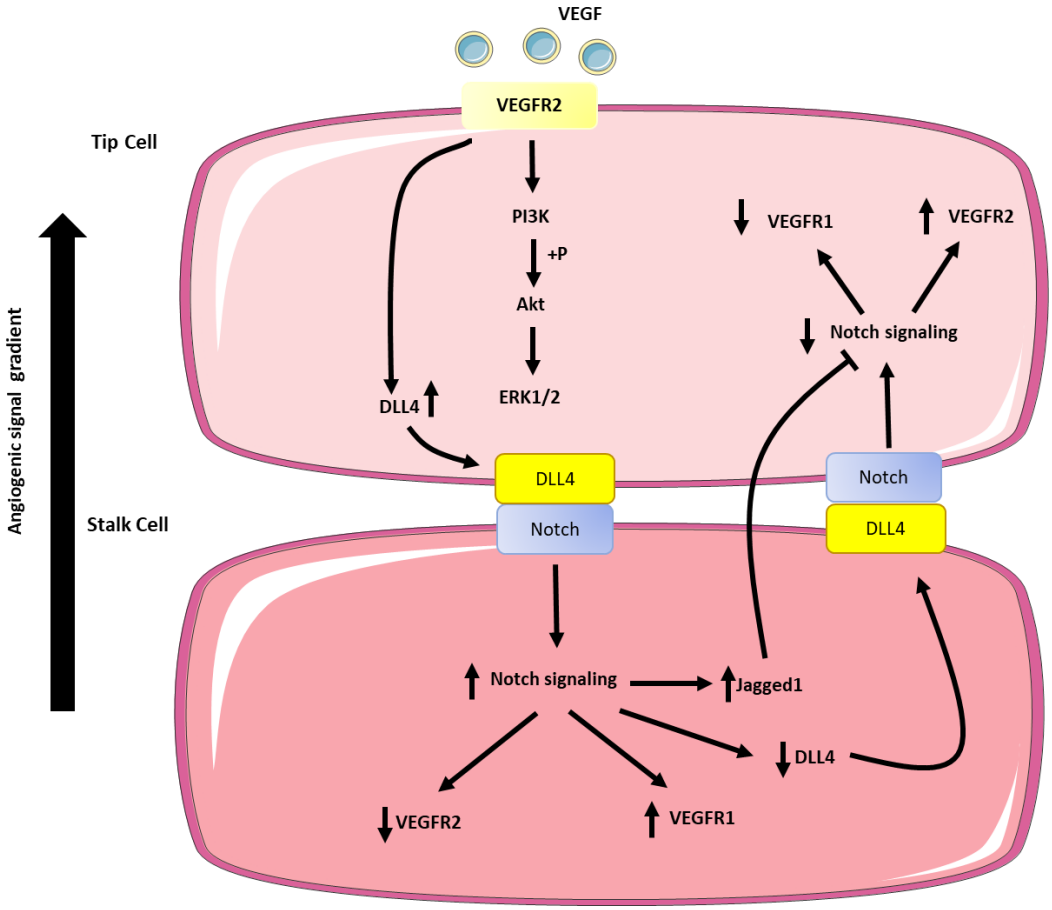

Figure 1.6 VEGF-VEGFR2 mediated tip/stalk cell selection

Vascular growth endothelial factor (VEGF) activates vascular endothelial growth factor receptor 2 (VEGFR2) which, in turn activates extracellular signal-regulated kinase ½ (ERK) *via* a phosphoinositide 3-kinase (PI3K) phosphorylation of protein kinase B (Akt). ERK ½ induces cell proliferation. VEGFR2 also increases expression of Delta Like Canonical Notch Ligand 4 (DLL4) in the tip cells. DLL4 binds to Notch in the neighbouring endothelial cell and takes on a stalk cell phenotype. DLL4/NOTCH crosstalk is a dynamic competitive process between tip and stalk cells that ensures balance in tip selection. Notch in stalk cells downregulates tip cell markers like VEGFR2 and DLL4 and increases expression of stalk cell markers like VEGFR1 and Jagged-1 which inhibit Notch signalling in the adjacent tip cell.

1.6.3 Arteriogenesis

Arteriogenesis is the process of remodelling of an existing artery to increase its luminal diameter in response to increased blood flow. [115] The main trigger of this process is altered shear flow that appears in the collateral arteriole resulting in a large pressure difference. This triggers vascular wall cell proliferation and migration, resulting in structural enlargement of collateral arterioles to arteries (Figure 1.7).[116–118] This phenomenon occurs in the heart often when main arteries are chronically occluded. In response, collateral arteries form to maintain blood flow and can even keep patients asymptomatic of angina. [119]

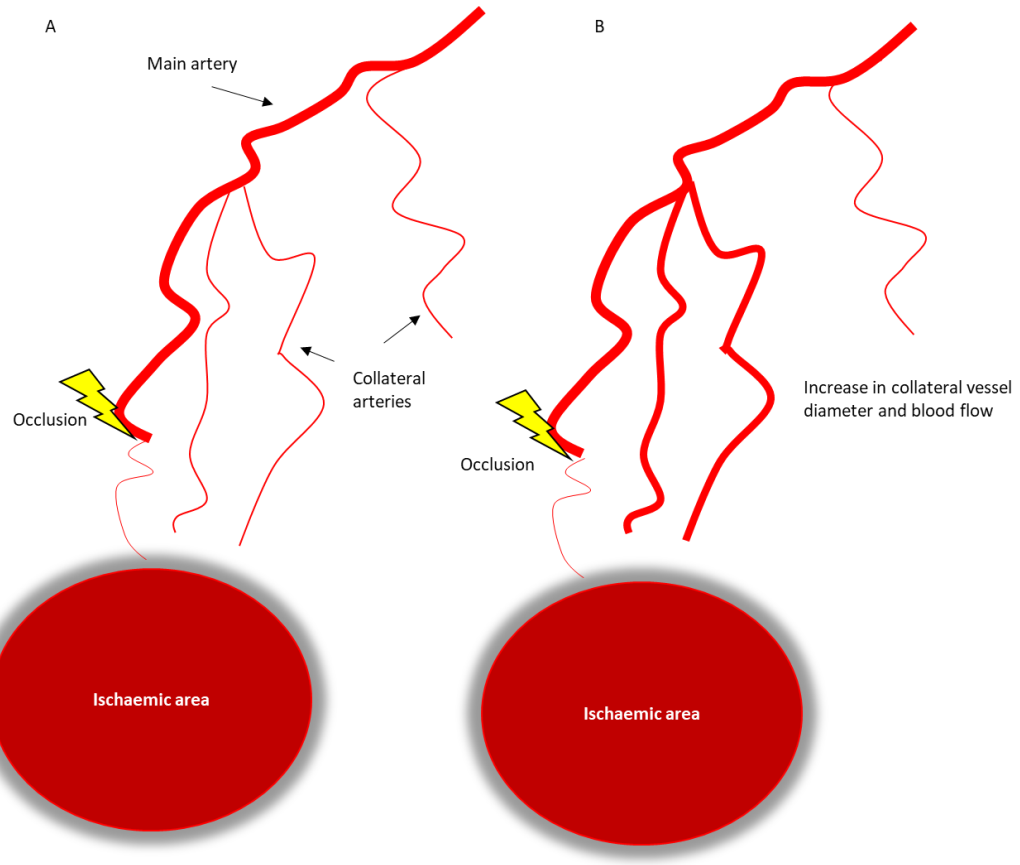

Figure 1.7 Schematic of arteriogenesis

Occlusion of an artery can result in ischaemia in a downstream tissue area. To compensate, collateral arteries increase in diameter *via* vascular wall cell proliferation and migration, thus increasing blood supply into the ischaemic area.

1.7 Development of the coronary vasculature

Coronary vessels are responsible for supplying oxygen and nutrients to cardiac tissue, one of the most metabolically active systems, in which cardiomyocytes are surrounded by a dense network of capillaries.[120]

During mammalian development, once the vascular plexus has been formed, coronary vessels connect to the aorta.[121] The origin of coronary endothelial cells (CECs), a matter of major debate, has been hypothesised to be the proepicardial organ, which contributes progenitor cells during embryonic heart development.[122] More specifically, the epicardium is formed *via* the protrusion of the coelomic mesothelium located close to the septum transversum and the inflow tract. The septum transversum separates the thoracic and abdominal cavities during embryonic development and later gives rise to the diaphragm and ventral mesentery. [123] The case for the proepicardial organ being the origin of CECs was strengthened when experiments conducting ablation or obstruction of the proepicardial organ resulted in failed coronary formation in quail and chick embryos.[124] Interestingly, subsequent studies using lineage tracing in mice show that the proepicardial organ contribution is actually quite low. [125,126]

This debate heightened in 2010 when the sinus venosus, the venous inflow tract in the embryonic heart, was found to be a source of CECs.[127] Later in development, the sinus venosus is incorporated into the right atrium and coronary sinus veins. ECs from the sinus venosus surround and subsequently enter the ventricles. These ECs then differentiate to form arterial and venous ECs.[127] Interestingly, the endocardium, the inner layer of the heart wall, was also found to contribute to CECs during embryonic development[128] as well as postnatally.[129] The contribution from the endocardium to the coronary vasculature begins with a modest effect but increases in the perinatal period, surpassing the contribution of the sinus venosus.[128]

1.8 Neovascularisation in the heart after MI

As discussed in previous sections, atherosclerotic plaque rupture or erosion in the coronary arteries leads to thrombus formation and occlusion of the coronary artery. Subsequent ischaemia leads to progressive cell death.[11] Following tissue damage due to MI, an inflammatory cascade leads to the damaged area being replaced with granulation tissue and a collagen-rich scar. [130] Angiogenesis occurs in the ischaemic border zone of the heart where vessels develop from the endocardium of the left ventricle to perfuse the hypoxic area.[131]

Even though angiogenesis has been observed in post-mortem human samples[132] it has been difficult to establish a reliable timeline of the formation of new cardiac blood vessels following myocardial ischaemia. The most in depth and reproducible results about mammalian heart neovascularisation have come instead from the use of animal models of MI.

In human patients newly formed capillaries are observed in the infarct zone on day 4 and neovascularisation reaches its peak in the second week following MI. [14] [132] Following MI in animal models such as mouse, ECs form capillary-like structures in the border regions.[133,134] Between days 2 and 4 post-injury this capillary network expands within the border zone and branches in the infarct core in an attempt to revascularize the ischaemic tissue.[135] Interestingly, Kobayashi *et al.* reported a subset of cardiomyocytes that expressed apoptotic markers in the murine peri-infarct zone located a distance from newly formed, perfused vessels. This study suggests the importance of new vessels that form post-ischaemia in cardiomyocyte survival.[131] After 7 days, subsets of capillaries 1) mature and obtain a smooth muscle layer 2) continue proliferating or 3) undergo apoptosis in the absence of perfusion. [106] [135]

Cardiomyocytes within the non-perfused area of the infarct core are susceptible to cell death. In mice, however, cardiomyocytes located within 150 μm from the endocardial surface may survive from passive diffusion of oxygen and nutrients from the LV cavity.[131] A capillary network develops within 3 days in this gap between the infarct area and the LV cavity. These vessels are perfused directly from the LV cavity

and are independent of the rest of coronary circulation. [131] The endocardial surface undergoes significant remodelling after MI in mice with cavities and protrusions developing by day 2 and leading to extensive trabeculation by day 7.[135] Interestingly, these trabeculae subsequently merge and become a site of blood vessel regeneration with new arterial conduit vessels being found in the subendocardium. [135]

With regard to the epicardium, it is also susceptible to disruption following ischaemic damage. In mice, following coronary artery ligation, epicardial cells in the infarct border zone proliferate and form a covering layer within 7 days. [135–137] At the same time, a capillary network develops in this epicardium-derived layer. These new vessels form a connection to the coronary vasculature of the underlying myocardium. [135] They initially develop as capillaries but later remodel to form arterioles, thus obtaining a smooth muscle cell layer. [135]

1.8.1 Heterogeneity in endothelial cell contribution to post-MI neovascularisation

The formation of the coronary vasculature has various contributions from the proepicardial organ, the epicardium, the ventricular endocardium, and the sinus venosus. [138–140] The contribution of EC to new vessels following a neovascularisation response after MI has also been a topic of debate. Hypotheses extend from expansion of pre-existing ECs to lineage conversion of non-ECs.[123] Regarding the latter, these hypotheses include EC differentiation from bone marrow-derived cells, vascular progenitor populations and cardiac fibroblasts. Understanding the origin of ECs involved in cardiac neovascularisation post-MI, and what are the mechanisms involved is crucial for realising the prospect of therapeutic angiogenesis.

1.8.1.1 Endocardium contribution to post-MI neovascularisation

As mentioned previously, the endocardial surface undergoes significant remodelling after MI.[135] Following MI, endocardial cells expressing EC markers have been found.[39] Neovessels in the subendocardial region have been shown to share marker profiles with endocardial cells. [39] Furthermore, experiments using *Pdgfb-CreER*^{T2} mice, an EC specific labelling model, showed that a significant percentage of infarct border zone

ECs (26%) were not labelled by the *Pdgfb* lineage. [135] Combined with the lack of *Pdgfb* expression from the endocardium[135], It has, therefore, been hypothesised that the endocardium is a source of ECs following neovascularisation post-MI. This is consistent with reports of endocardial cell plasticity in myocardial injury.[139] The *Pdgfb*-lineage negative vasculature has been suggested to form via injury-induced remodelling of the endocardium, in a process that resembles embryonic trabeculation and compaction. [135]

Miquerol *et al*. [141] strengthened this claim by describing distinguishable vascular structures resembling "flowers" in the endocardium alongside the infarct zone in the adult mouse heart. The exact mechanism of this process is still unclear but the same study suggested that formation occurred due to VEGFA-VEGFR2 signalling and subsequent connection, via stalk-like structures, to the subendocardial coronary vasculature. [141] However, this has been challenged. Tang *et al*. utilized a natriuretic peptide receptor 3 (*Npr3)-CreER* to label the endocardium but not the remaining coronary ECs in the adult mouse heart. [134] Findings showed minimal contribution of the endocardium to the infarct or border zone neovascularisation. [134] This aligns with the study by He *et al*. that showed neovascularisation post-MI was achieved solely by pre-existing ECs. [133] Interestingly, when endocardial cells were injected and "trapped", as the Tang *et al*. put it, in the subendocardial regions this did indeed result in endocardium-derived neovascularisation. This finding suggests that endocardial cells retain the potential to contribute to neovascularisation, if appropriately stimulated. [134]

1.8.1.2 Epicardium contribution to post-MI neovascularisation

The epicardium has been explored for its regenerative potential in the adult myocardium due to its pluripotency during embryonic development. [122] The epicardium has also been explored for its potential to coronary EC contribution to post-MI neovascularisation. Studies using epicardial Wilms Tumour 1 homolog *Wt1-CreER* showed that epicardium-derived cells did not give rise to ECs or smooth muscle cells forming neovessels post-MI. Interestingly, they were shown to contribute to

pericytes that provide extramural support to vessels in the infarct border zone.[134,135] These epicardium-derived cells have been suggested to promote neovascularisation in the infarct region by secreting paracrine factors such as VEGFA, FGF2, Wnt family member 1 and thymosin beta 4. [142] Moreover, epicardial KIT proto-oncogene receptor tyrosine kinase (KIT+) cells have been found to have proliferative capacity as well as expressing EC markers post-MI. [143] Initially, these KIT+ cells were hypothesised to be vascular precursor cells. [143] Lineage tracing studies, however, showed that epicardial KIT+ cells are a subpopulation of ECs that retain their endothelial identity following myocardial injury. [144]

1.8.1.3 Cardiac fibroblasts contribution to post-MI neovascularisation

Cardiac fibroblasts have been considered for their contribution to neovascularisation post-MI due to mesenchymal-to-endothelial transition (MendoT).[145] To address this hypothesis, lineage tracing experiments following the dynamics of fibroblasts in the heart post-MI were conducted. Lineage tracing using fibroblast-specific protein 1 (Fsp1)-Cre mice by Ubil and colleagues showed that fibroblasts do indeed transition from a fibroblast to an endothelial phenotype, therefore undergoing MendoT and support the vasculature post-MI. [146] However, *Fsp1* is also expressed in ECs, making lineage tracing with this promoter inaccurate in the search of fibroblast-derived ECs.[133] [147] The same study by Ubil and colleagues used collagen I α2 (*Col1a2*)-*CreER* lineage tracing in mice and showed that a significant number of fibroblasts undergo MendoT following myocardial injury. [146] However, these results were not reproduced by He *et al*. using the same *Col1a2-CreER* transgenic lineage tracing model.[133] He *et al*. also utilised a *Col1a2-2A-CreER* knock-in mouse model and again found no evidence of MendoT after MI. [133] Additional lineage tracing models were used to address the MendoT hypothesis namely: i) platelet-derived growth factor receptor alpha (*Pdgfra)-DreER* ii) SRY-box transcription factor 9 (*Sox9)-CreER* iii) transcription factor 21 (*Tcf21)-MerCreMer*, and iv) periostin (*Postn)-MerCreMer*.[133] These studies all indicated that neither fibroblasts nor myofibroblasts contribute to new ECs post-MI. [133] Instead, all evidence points to only pre-existing cardiac ECs taking part in neovascularisation post-MI. [133] [134] Specifically labelling coronary ECs with lineage

tracing mouse models Apelin (*Apln*)-*CreER*, cadherin 5 (*Cdh5)-CreER* and fatty acid-binding protein 4 (*Fabp4)-CreER* showed no dilution of vascular labelling post-MI; therefore, strengthening the claim that contribution of non-EC sources is minimal.[133] [134]

1.9 Neovascularisation as a therapeutic strategy for MI

Reperfusion of the myocardium is critical to cardiomyocyte survival and is associated with improved LV function and long-term survival in MI patients as well as experimental animal models.[148] [149] It is believed that the formation of new blood vessels or remodeling of existing collateral vessels can help mitigate damage originating from the occlusion of a coronary artery.[150]

The necessity of a neovascularisation response in the injured heart is supported by experiments using zebrafish, an animal model that retains its cardiac regenerative capacity into adulthood.[151] Poss and colleagues in 2002 demonstrated the regenerative ability of zebrafish following ventricular amputation[152]. In contrast to mammalian hearts, in zebrafish hearts the fibrotic tissue generated in response to injury is degraded and replaced by a fully functional and vascularised myocardium.[153] Hindering the process of neovascularisation in zebrafish show that it is essential for cardiomyocyte proliferation and subsequent heart regeneration (reviewed in Ref[151]). More specifically, Marín-Juez *et al.* showed that zebrafish with mutant forms of dominant negative Vegfaa showed minimal neovascularisation post-injury and that subsequently attenuated replacement of damaged cardiac tissue by proliferating cardiomyocytes.[154]

Compared to organisms such as zebrafish, the adult mammalian heart is unable to regenerate the lost myocardium following MI and is thus susceptible to cardiac contractility issues arising. The same cannot be said for the mammalian neonatal heart. Porrelo *et al.* used a model of neonatal mouse myocardial injury to show that until 7 days post birth, murine hearts fully regenerate following partial apical surgical resection.[155] This response was characterised by cardiomyocyte proliferation and minimal fibrosis.[155] Moreover, through a cardiomyocyte specific lineage tracing

(*αMHC-MerCreMer)* mouse model, Porrelo *et al.* showed that the regenerated tissue originated from pre-existing cardiomyocytes.[155] Interestingly, this method of repair is similar to adult zebrafish where pre-existing cardiomyocytes, and not a special cell population, is responsible for cardiomyocyte replacement.[156] Moreover, similar to zebrafish[153], ECs are also crucial in the transient regenerative ability of the mammalian heart.[157] Ingason *et al*. showed that cardiac angiogenesis precedes cardiomyocyte migration in regenerating mammalian mouse hearts.[157] This may suggest that there are some developmental mechanisms, in which ECs are important players, that can be potentially manipulated and reactivated to restore this regenerative ability.[135] Since the original findings by Porrelo *et al.* there has been a considerable interest in mammalian neonatal regeneration with many independent research groups validating these findings (Reviewed in Ref[158]).

With regard to human neonatal heart regeneration, to my knowledge, there is only a single published case study showing that the human neonate (under 18 months of age) can recover LV function following myocardial injury.[159,160] However, this study did not include serial histological analyses accompanied with functional analyses, thus making it difficult to reach a conclusion regarding human neonatal heart regenerative capacity.

Despite poor regenerative capacity in the adult mammalian heart, our view of the heart being a terminally differentiated organ with minimal cell turnover has been challenged in the last 10 years. Bergmann *et al* showed, *via* carbon dating, that ECs have the highest turnover rate in the heart with the whole population being exchanged every 6 years in human adulthood at a rate of 16.7% per year in adult life. Cardiomyocytes were shown to have a 0.8% turnover per year at the age of 20 and 0.3% per year by the age of 75. [161]

There is extensive literature describing research aiming to stimulate heart regeneration by different methods (reviewed in Cambria *et al*. [162]). Potential therapies can be exogenous in nature, in which a biological product (such as cells or tissue) is implanted in the damaged myocardium, or endogenous, where products

like growth factors are introduced to the heart with the aim of stimulating endogenous regenerative responses. Heart regeneration therapies vary with regard to their attempted target of regeneration. The first and most studied approach has been to replace, or to stimulate repair of, cardiomyocytes in the injured heart. Studies using this approach have used a variety of different products, such as: skeletal myoblasts (SM), embryonic stem cells (ESCs), induced pluripotent stem cells (iPSC), cardiac stem cells (CMCs), cardiosphere-derived cells (CDCs), as well as tissue engineering approaches in which cells can be grown on a scaffold that is later planted on the damaged myocardium. [163] Another approach that has been thoroughly studied is the indirect 61timulateon of regeneration, or salvaging of injured cardiomyocytes, via enhancement of the neovascularisation response post-MI. As mentioned in previous sections, the revascularisation response is critical post-MI for stimulating regeneration. [154] For the purposes of this introduction, the therapeutic approaches that have aimed to indirectly stimulate regeneration via enhancing the neovascularisation process post-MI will be discussed.

1.9.1 Cell-based therapies

1.9.1.1 Bone marrow mononuclear cells (BMMNCs)

Bone marrow mononuclear cells (BMMNC) are one of the most studied cell populations for heart regeneration. Despite this, their mechanism of action is still unclear. The capacity of BMMNCs to differentiate into other cell lineages has been controversial thus far. BMMNCs have been shown to differentiate into cardiomyocytes in rodents[164,165] but this has been refuted in later studies.[166] BMMNCs are a heterogenous population that contains subpopulations including haematopoietic stem cells (HSCs) and blood-circulating EPCs.[162] HSCs can be isolated via the use of markers such as CD34 and CD133. [162] Few preclinical studies have investigated HSCs in the context of myocardial injury. Existing studies, however, showed no evidence of CD34+ HSC differentiation into cardiomyocytes but have shown increased angiogenesis/vasculogenesis that was mostly attributed to paracrine effects.[167]

Endothelial progenitor cells

Initially, postnatal blood vessel growth was thought to take place via migration and proliferation of mature ECs. In the 1970's the seminal discovery was made that vessel wall ECs retained the capacity to undergo self-replication, possibly through clonal expansion. [168,169] This property did not appear to be exhibited by all ECs, but by cells in specific focal clusters in the aortic intima. [168] This challenged traditional dogma that postnatal blood vessel growth occurs exclusively through angiogenesis *via* sprouting of existing mature vasculature. Furthermore, recent evidence supports the vascular wall as a site of origin for EPC [170]. More specifically, studies have identified EC-like, non-haematopoietic populations in the adventitial layer of vessels, with self-replication potential. However, the precise phenotype of these cells is still unclear.[170]

Asahara *et al*. purified CD34 positive haematopoietic progenitor cells, termed EPCs, from adult circulation and showed that they can differentiate into an EC phenotype *ex vivo*. EPCs showed endothelial marker expression and migrated into newly formed vessels in models of hindlimb ischaemia. [171] The precise phenotypic characterisation of EPCs is difficult as they share many common markers with ECs as well as haematopoietic stem cells. [172] EPCs are currently defined by expression of haematopoietic stem cell markers (e.g. CD34, CD133) and an EC marker (e.g. VEGFR2).[173]

EPCs have been plagued by unresolved questions such as their definitive origin and identity. Much debate persists in this area, with other sources indicating that EPCs are also found outside the vessel wall; for example, in the bone marrow or the circulation. [174] However, this has been challenged by a recent study with male patients receiving bone marrow from female donors suggesting that EPCs did not originate from this source.[175]

Data from cell culture studies indicate that highly clonogenic EPC may reside in a niche in the intimal layer of the adult human vessel wall [176]. However, whether the *in situ* endothelium is composed of clonal units generated following expansion of a single ancestral EPC, whose origin remains unknown, or whether it is a polyclonal

tissue maintained by turnover of adjacent mature ECs is unresolved. Historically, in animal injury studies, cell expansion has not been observed to be evenly distributed throughout the endothelial monolayer but rather in a hierarchical fashion from clusters of cells in the aortic intima. [177,178]

Clinical administration of BMMNCs for the stimulation of cardiac repair

In the clinic, BMMNCs (predominantly administered by intracoronary infusion[179,179–182]) have been used extensively in the context of myocardial injury, with mostly inconsistent results. Trials have reported significant improvement of cardiac function [183–185] but also a number of studies did not find evidence of beneficial effects from BMMNC cell therapy.[186–189]

A number of clinical trials (TOPCARE-AMI[185], REPAIR-AMI[190–192],BOOST[193,194] and FINCELL[183)] showed functional improvement in the heart by measure of LV ejection fraction, following administration of BMMNCs. In contrast, there are also several trials (ASTAMI[195], BONAMI[196], Leuven-AMI[197], HEBE [198] [199] and SWISS-AMI[200]) that showed no change between cell-treated groups and controls.

One critical issue in cell therapy is timing of cell administration. Randomised, double-blind, placebo-control clinical trials TIME and LateTIME used autologous BMMNCs and were conducted at 3/7 days and 2-3 weeks post-PCI, respectively.[201,202] Overall, no significant effect was detected in LV ejection fraction when comparing the placebo treated group to the BMMNC treated group in both clinical trials.

The heterogenous results from these clinical trials emphasise the gap in our knowledge about the mechanism of action of these cells. A large-scale meta-analysis conducted in 2014 pooled data from 43 randomised trials of 2635 patients to evaluate efficacy of BMMNCs for MI patients [203]. This study revealed that, despite the large number of trials conducted, results are inconsistent and modest at best. This may be explained, in part, by *in vivo* studies showing that fewer than 1% of injected cells are retained in the myocardium after 24 hours indicating very poor engraftment [204].

The BAMI clinical trial aimed to eliminate ongoing controversies relating to the clinical value of BMMNC therapy.[205] Since 2017, this study investigated the effects of intracoronary infusion of BMMNCs on all-cause mortality in acute MI. [206] It has been hypothesised that BMMNCs may act indirectly to stimulate the release of pro-angiogenic paracrine factors such as VEGF and monocyte chemotactic protein-1 (MCP-1) from ECs [207] and prevent cardiac cell apoptosis .[208] Disappointingly however, despite being the largest trial of autologous BMMNC-based therapy in the treatment of AMI, low recruitment prevented any meaningful group comparisons and interpretations to be made by the authors.[205]

1.9.1.2 Mesenchymal stem cells

Mesenchymal stem cells (MSCs) are multipotent stromal cells that have the capacity to differentiate into different cell types, including adipocytes, chondrocytes, and osteocytes.[209] MSCs have been mostly isolated from the bone marrow but have also been observed in adipose tissue, synovial tissue, umbilical tissue, peripheral blood, and the heart. [210–212]The main subtypes of MSC are bone marrow-derived MSCs (BMMSCs), adipose-derived MSCs (AMSCs) and umbilical cord-derived MSCs (UMMSCs).[213] Differentiation into cardiomyocytes by BMMSCs has been reported experimentally[212], but is controversial as others studies have failed to show BMMSCs adopt a cardiomyocyte phenotype.[214] Instead, BMMSCs have been shown to differentiate into ECs, pericytes and smooth muscle cells when introduced in the ischaemic myocardium.[215–218]

With regard to MSC differentiation into ECs, this has been debated. Some studies have refuted the claim[219], whereas others reported increased neovascularisation in ischaemic heart models attributed to MSC differentiation into ECs.[220] Preclinically, MSCs have shown promising results.[221–224] The POSEIDON trial compared the safety and efficacy between transendocardial delivery of autologous versus allogeneic BMMSCs using three different doses in patients with LV dysfunction due to ischaemic cardiomyopathy. Interestingly, the lowest dose showed the greatest efficacy in the LV ejection fraction endpoint. The authors suggested that this inverse dose response

may reflect the concentration of cells and not total cell number, as the injection volume was constant for the different doses. Moreover, both therapies showed good safety profiles.[225,226] Due to the debatable differentiation ability of MSCs to an EC phenotype in cell therapy it has been hypothesised that MSC therapy promotes angiogenesis via paracrine mechanisms by secreting VEGF, basic fibroblast growth factor (bFGF), and PDGF.[227,228]

1.9.1.3 Cardiopoietic MSCs (cpMSCs)

BMMSCs can be used to specifically target cardiogenic growth. This is achieved by priming autologous BMMSCs using cardiogenic growth factors. Cardiogenic growth factors are induced by activation of TGF-β, BMP-4, Activin-A, retinoic acid, IGF-1, IL-6, and IL-6.[229] When used in preclinical mouse models of MI, cpMSCs have been shown to be beneficial.[230] In larger animal models of MI, there have been reports of beneficial effects including higher ejection fraction and reduced infarct size. Mechanisms of action of this effect were not thoroughly investigated but authors suggested involvement of paracrine mechanisms due to low cell retention.[230]

cpMSCs have been used in the C-CURE trial which investigated their benefit in ameliorating LV ejection fraction via transendocardial injection.[231] Results showed no significant differences between treatment and control groups. Despite that, the trial did show safety of treatment. Other trials include the CHART-1 and CHART-2 trials. CHART-1 is an ongoing study studying cpMSCs in ischaemic heart failure, which has not managed to meet the primary efficacy endpoints (all-cause mortality, worsening heart failure, 6-min walk distance, left ventricular end-systolic volume, and ejection fraction) at 39 weeks.[232] The CHART-2 trial is investigating a subgroup of the CHART-1 study that was identified as a potential responsive target group. Similar to other cell types, cpMSCs have had a complicated history. Hints of efficacy are there but the literature has not reached a definitive consensus on the mechanism of action or most suitable clinical target group.

1.9.1.4 Cardiac stem cells and cardiosphere-derived cells

Cardiac stem cell studies have a complicated and controversial past. The primary issue is that the existence of cardiac stem cells (CSC) has not been established in a convincing manner. The idea is that by stimulating endogenous CSCs, there is the potential to generate new cardiomyocytes to restore the damaged myocardium. However, studies in regenerative organisms have shown that pre-existing cardiomyocytes, rather than a subpopulation of stem-cell-like cells, are responsible for heart regeneration. [233]

Work by Dr Piero Anversa's team who initially described CSCs has sparked controversy. Studies from the group have suggested that there is a resident stem cell population in the adult heart termed ckit+ CSCs with differentiation ability into cardiomyocytes, ECs, and smooth muscle cells.[234] Moreover, they showed that when delivered to the coronary arteries of rats these cells can enhance functional recovery via cardiomyocyte differentiation.[235] Controversy arose however, when independent groups failed to replicate these results and showed no evidence of cardiomyocyte differentiation.[236,237] Studies suggested these were in fact mast cells, generating even more confusion on the topic. [236,237] Further studies pursuing the existence of these ckit+ CSCs used advanced Cre knock-in lineage tracing mouse models and showed minimal, if any, contribution of CSCs to cardiomyocytes during homeostasis and after injury. [238–240] Overall, there is no evidence to suggest the existence of ckit+ CSCs.

A number of clinical trials have been conducted using CSCs. The SCIPIO trial was conducted to prove safety and efficacy of intracoronary ckit+ CSCs in heart function. Results showed a significant increase in LV ejection franction.[241] However, this trial has been deemed controversial and *the Lancet* has raised concerns against the integrity of the data generated. [242]

Another population of cells thought to represent CSCs are Sca1+ (stem cell antigen-1) cells. Initial experiments found that Sca1 stem cells can differentiate into cardiomyocytes *in vitro*.[243] However, further studies showed that Sca1 cells can differentiate into cardiomyocytes, osteocytes and adipocytes.[244–248] With regard to

cardiac function, transplantation of sheets (applied onto the surface of the infarcted anterior-lateral region) of clonally-expanded Sca1+ cells were shown to improve cardiac function following myocardial injury.[249] The mechanism of action was suggested to be via cardiomyocyte differentiation as well as paracrine activity.[249] Other studies have shown myogenic potential of Sca1+ cardiac cells[250,251] but several studies have since challenged these results by showing that Sca1 cells do not generate new cardiomyocytes.[252–256] Sca-1 genetic lineage tracing showed that Sca-1+ cells mainly adopt an endothelial, and not a cardiomyocyte, cell fate in homeostasis and also in injury.[256] This suggests that any benefit from Sca-1+ cell therapy may be due to indirect/direct angiogenic effects rather than cardiomyocyte differentiation.

Another population that has generated a lot of interest in the heart regeneration community is the ATP binding cassette sub- family G member 2+ (Abcg2+) cell. These cells have been observed in the adult heart with potential to differentiate into cardiomyocytes *in vitro*. [257] Moreover, when injected into the infarcted mouse heart, these cells have been reported to give rise to cardiomyocytes, ECs, and smooth muscle cells.[258] However, genetic lineage tracing of Abcg2+ cells showed that this population can differentiate into other lineages only during the embryonic stage.[259,260] and proposed that Abcg2+ cells may fuse with pre-existing cardiomyocytes to stimulate cardiomyocyte cell cycle re-entry and proliferation.[261]

Another population proposed as an endogenous cardiac progenitor is the Bmi1+ cardiac stem cell population.[262,263] This relatively recent discovery has not been verified independently but initial reports showed that Bmi1+ cells can differentiate into vascular ECs, smooth muscle cells, and cardiomyocytes when cocultured with neonatal rat cardiomyocyte.[262,263] Moreover, Bmi1+ cells were shown to contribute to new cardiomyocytes after MI in mice.[278] The high level of cardiomyocyte generation reported contradicts existing studies that show much lower cardiomyocyte turnover of 1% a year in human adulthood.[264–266] A contradictory finding is that Bmi1+ cells show Sca1+ positivity.[262] However, as mentioned previously, cardiac Sca1+ cells have been found to be endothelial and not

cardiomyocyte in nature.[256] Clearly, more work needs to be conducted on Bmi1+ cells to verify their identity and potential.

Another approach of cell therapy is cardiospheres which are defined as self-assembling multicellular clusters from the cellular outgrowth from cardiac explants cultured in non-adhesive substrates.[267] Cardiospheres can be dissociated from cells derived from cardiac explants yielding cardiosphere-derived cells (CDCs). They were first isolated from cells of cardiac explants growing as self-adherent clusters. These clusters had originated from postnatal atrial or ventricular heart tissues.[268] When injected in the infarcted myocardium of animal models of MI they generated cardiomyocytes and vascular ECs.[269–273] However, it was postulated that the mechanism of action of CDCs may be stimulation of endogenous cardiac cells via paracrine means.[274,275] The CADUCEUS trial, investigated the safety and efficacy of intracoronary autologous CDC application in patients with MI-induced LV dysfunction.[276] Results showed no changed in LV ejection fraction but showed some beneficial structural changes compared to controls such as reduced scar mass, increased regional contractility, and systolic wall thickening. However, the CADUCEUS trial has a small sample size (n=17) and any findings would need further validation.

1.9.1.5 Embryonic stem cells and induced pluripotent stem cells

Embryonic stem cells (ESC) have the potential to differentiate into any cell type. Studies have aimed to program ESCs into a cardiomyocyte phenotype *in vitro* using a transcription factor cocktail.[277] These cardiomyocyte-like cells expressed cardiac transcription factors and showed beating activity. However, the use of ESCs has been controversial due to ethical concerns and safety issues, namely the potential for teratoma formation. [278]

Embryonic stem cells (ESC) have the potential to differentiate into any cell type. Studies have aimed to program ESCs into a cardiomyocyte phenotype *in vitro* using a transcription factor cocktail.[277] These cardiomyocyte-like cells expressed cardiac transcription factors and showed beating activity. However, the use of ESCs has been

controversial due to ethical concerns and safety issues, namely the potential for teratoma formation.[278]

In contrast, induced pluripotent stems cells (iPSCs) can be obtained from adult somatic cells via expression of reprogramming genes. [279] iPSCs can differentiate in multiple lineages and overcome some of the ethical limitations of ESCs. [279]

Preclinical results using ESCs/iPSCs have been mixed. The clinical study ESCORT utilised ESC-derived CPCs embedded into a fibrin scaffold delivered via a patch on the LV lateral wall (peri-infarct border) of a patient with advanced HF.[280] Preliminary results were promising but the full analysis has yet to be published. Interestingly, iPSC-derived cells have improved outcomes in ischaemia via angiogenesis.[281] ESCs and iPSCs can be terminally differentiated into an EC lineage prior to transplantation.[282–285] This can be achieved by differentiation protocols that utilize VEGF, bone morphogenetic protein-4, bFGF and Wnt signalling pathways.[282–285] Injection of syngenic VE-cadherin+ ESC ECs into the peri-infarct zone of mice increased capillary density and improved LV functional recovery.[286] iPSC CD31+ ECs derived from pigs were transplanted into a mouse model of MI. [287] This resulted in improved LV ejection fraction by 3.5% compared to controls. Interestingly, several proangiogenic and antiapoptotic factors were released from the transplanted cells and were hypothesised to be responsible for the observed neovascularisation and increased cardiomyocyte survival in the infarct region.[287]

In summary, cell therapy approaches for the treatment of MI appear safe and feasible. However, there are still many questions regarding efficacy and mechanism of action. Cell engraftment levels are extremely low, so any perceived beneficial effect is normally attributed to paracrine effects, without concrete evidence. More recently, a hypothesis has been developed to ascribe beneficial effects of cell therapies to exosomes, a family member of extracellular vesicles.[288] Extracellular vesicles are a variety of small-membrane-enclosed vesicles that include exosomes, microvesicles, ectosomes, budding vesicles, shedding vesicles, and apoptotic bodies.[289] Exosomes are double-membraned nanovesicles that are 30 to 100 nm in

diameter and have the capacity to transfer lipids, proteins, mRNA, and microRNAs.[290–292] Furthermore, most beneficial effects from cell therapies that are shown from clinical or preclinical trials are modest at best. Moreover, the identity of the cells chosen for therapy is often disputed and debated amongst the scientific community with some populations being argued to not even exist. In an interesting turn of events, a recent study by Vagnozzi *et al*. suggested that the beneficial effects of cell therapy are in fact driven by an endogenous, acute, inflammatory-based wound-healing response, spearheaded by macrophages. [293] This further reinforces the idea that we are still lacking an in-depth understanding of the endogenous mechanisms in the heart post-MI.

1.9.2 Therapies using pro-angiogenic factors

The rationale of protein therapy is to deliver growth factors that promote neovascularisation post-ischaemia. This can be delivered by intravenous, intra-arterial, intramuscular, or intramyocardial injection.[288] An important limitation of using recombinant protein for therapy is the short half-life (e.g. 30 minutes for VEGF[294]) once introduced into the patient. A way to combat this issue is to introduce sustained expression of the protein via gene therapy. Initial attempts of inducing therapeutic angiogenesis in the 1990s were performed using intramyocardial injections of naked plasmid DNA that coded for angiogenic factors. However, results of this approach have been largely disappointing, mainly due to low efficiency of cell uptake. [295]

The main target in this field has been VEGF-A 165. Initially, delivery strategies involved intramyocardial injections of plasmids encoding VEGF-A 165.[295] However, when done in a randomised, double-blinded, placebo-controlled manner this approach failed to show an improvement in perfusion (studies; EUROINJECT[296], NORTHERN[297], KAT[298]). This was also the case when a plasmid coding for VEGF-A 165 was co-injected with FGF2[299] and G-CSF. [300]

Inefficient delivery is one of the reasons behind current gene therapy limitations. Improvements were made by using adenovirus as a vector for cDNA delivery for

cardiac gene therapy. These have the benefit of transducing postmitotic cells resulting in sustained protein expression. One of the first adenoviral vectors designed for clinical application was Ad_{GV} VEGF121.10N, also known as BIOBYPASS.[301] This vector expressed VEGF-A 121 under the control of the CMV promoter.[301] BIOBYPASS was delivered in patients with coronary artery disease during coronary bypass artery grafting (REVASC trial[302]) as well as by transendocardial delivery (NOVA trial[301]). The REVASC trial reported improvements in angina symptoms and exercise induced ischaemia.[302] However, these results need to be validated in a randomised, double-blind, placebo-controlled trial. Unfortunately, the NOVA trial had to be terminated before completion as no difference was observed between treatment groups.[301] This was also the case for the AGENT clinical trial which involved intracoronary delivery of an adenoviral vector that coded for FGF4.[303] Following recruitment of over 500 patients, results showed no improvement in the primary endpoint (change in stress-related reversible perfusion defect size) and further enrolment was stopped. A follow up to the AGENT trial was performed using the same FGF4 coding vector in patients with myocardial ischaemia and stable angina (ASPIRE trial[304]). This study ran between 2012 and 2016 but results have not been reported yet. The same vector was used in women with refractory angina who were not candidates for revascularisation (AWARE trial) but enrolment has also been discontinued, most probably due to low recruitment.[305] More positive results were reported by the KAT study[298] which showed improvement in myocardial perfusion, assessed by SPECT imaging, when using a catheter-based intracoronary-delivered adenovirus expressing VEGF-A 165. However, no significant difference were observed in mortality or incidents of major cardiovascular events. [298] A different adenoviral vector that was recently used induced expression of VEGF-D which also possesses angiogenic activity.[306] The vector was delivered via transendocardial injections to ischaemic myocardium and after a one year follow up myocardial perfusion was increased.[307] Recent clinical studies include a Phase I/II trial using adenoviral vectors that expressed 3 VEGF-A isoforms [308] but the study has stopped recruitment due to lack of funding (trial NCT01757223).

As demonstrated in the clinical trial reports discussed above, improvements in cardiac function post-MI using pro angiogenic factor therapies have been reported but results are inconsistent. Moreover, the choice of the therapeutic gene is a matter of debate. The vascularisation process is extremely complex and requires the interplay of many different factors and cell types. An argument can be made that many pro-angiogenic factors need to be combined in a single therapeutic strategy for there to be a robust beneficial effect. On the other hand, the design of "gene cocktails" raises questions about gene delivery and clinical safety despite being a rational alternative to single gene strategies.

1.10 Lineage tracing technology

Lineage tracing analysis is a tool where a group of cells is labelled with a specific label resulting in the progeny of the labelled cells maintaining the marker. This tool is powerful when investigating tissue development and stem cell properties in adult tissues.[309] This is especially the case when investigating the behaviour of cells in the context of disease states such as ischaemic heart disease, as opposed to studying these cells *in vitro*. The key feature of a good lineage tracing label is the ability of the label to be passed in all the progeny of the founder cell and that it shouldn't change the properties of the founder cell. Moreover, the label should be stable and be retained over time.

Lineage tracing *via* genetic recombination is currently the preferred approach in murine models (reviewed in ref[310]). This involves the expression of a recombinase enzyme in specific manner (tissue or cell specific) to activate the expression of a constitutive or conditional reporter gene. This leads to a permanent label of the marked cells. The main recombinase enzyme that is used in this context is adapted from bacteriophage P1 and is called *Cre-loxP*.[311] The Cre recombinase is expressed under the control of a specific (cell or tissue) promoter in a mouse line. Subsequently, a second line with a label that is flanked with a "floxed" STOP sequence (loxP-STOP-loxP) is bred with the Cre mouse line. In the mice resulting from the breeding pair and express both constructs, the Cre recombinase removes the STOP sequence

flanked by loxP resulting in expression of the label. Initially, labels included β-galactosidase on the ROSA-26 locus which can be visualized using brightfield microscopy. However, fluorescent reporters can also be used. The most commonly used one is green fluorescent protein (GFP) [312] but markers such as tdTomato also can be used. [313]

Temporal control of activation of the Cre-recombinase can be induced with inducible recombination. This can be achieved by fusing the Cre-recombinase with the human oestrogen receptor (ER).[314] When ER ligands such as 4-hydroxy-tamoxifen are not present then the Cre-recombinase is kept in the cytoplasm and does not induce label expression. When ER ligands are present, the Cre-recombinase is free to enter the nucleus and recombine the loxP sites, resulting in the expression of the label.[314]

1.10.1 The *Brainbow* mouse model

One of the most exciting additions in lineage tracing technology *via* genetic recombination of the last 20 years is the development of the Brainbow cassettes by Livet *et al*. which were initially used to visualise and trace connectivity of neurons in the brain (Figure 1.8.). [315] Previous lineage tracing labelling mouse models had managed to combine two fluorophores in one animal.[316] However, these are not appropriate to investigate diverse clonal populations due to the limited number of labels. Challenges of this nature were circumvented by the Brainbow lineage tracing models which allow for multicolour labelling of a cell population that can then be traced in order to investigate clonality as labels are inherited. [315]

There has a number of iterations of the Brainbow lineage tracing model (described in more detail below). The basis of the model is the use of a Cre-mediated activation gene by DNA excision, inversion or intrachromosomal re-arrangement of transgenic elements[317] resulting in stochastic expression of multiple fluorescent proteins from a single transgene.[315]

The initial version of the model (*Brainbow 1.0*) used Cre-mediated excision of pairs of incompatible *lox* sites to result in mutually exclusive recombination events.[318] The

transgene cassete contains canonical prokaryotic *loxP* elements as well as *lox* variants (*lox2272)* that are incompatible with canonical *loxP.* Due to the alternation in *lox* sites the Cre recombinase can choose between recombination only one of the two *lox* combinations (Figure 1.8, A). [318] The *Brainbow 1.0* model produced two recombination outcomes, switching fluorophore expression from the default red to yellow or cyan (Figure 1.8.,A). [315] Importantly, following validation experiments in HEK 293 cells that were transfected with the construct, neither recombination event was strongly favoured over the other, suggesting the stochastic nature of the Cre-recombinase activity.[315] Importantly, no co-expression of yellow or cyan was observed.[315] The next iteration of the Brainbow cassette, called *Brainbow-1.1*, included an additional *lox* variant (*loxN)* that upon Cre mediated excision resulted in a choice of three recombination events, yellow, red or cyan with orange being expressed in the absence of recombination (Figure 1.8., B).[315] In *Brainbow 2.0,* the ability of the Cre-recombinase to invert DNA segments flanked by *lox* sites facing each other was utilized. [315] Importantly, Cre can continuously invert DNA segments that are flanked by *loxP* sites that face each other. When Cre activity is stopped then the transgene stabilises and the cell expresses the fluorophore in the final orientation that took place, in a stochastic manner. [315] In the *Brainbow 2.0* cassette there is a Cre-invertible construct that contains RFP and CFP in head-to-head orientation. Upon expression of the construct, HEK cells express red colour. Upon Cre activation, inversion results in expression of either RFP or CFP (Figure 1.8., C). [315] Finally, the Brainbow2.1 cassette (Figure 1.8., D) consists of adjacent loxP flanked head-to-tail tandem dimers: the first contains nuclear tagged Green Fluorescent Protein (nGFP) in forward orientation and Yellow Fluorescent Protein (YFP) in reverse orientation. The second contains Red Fluorescent Protein (RFP) in forward orientation and membrane bound Cyan Fluorescent Protein (mCFP) in reverse orientation. In *Brainbow2.1*, Cre activation can result in three different inversions of the aforementioned transgene elements ((i), (ii) and (iii) in Figure 1.8, D). Moreover, Cre mediated excision can result in either of two DNA excision events ((iv) and (v) in Figure 1.8, D) that can shorten the construct to single elements (nGFP-YFP element

vs RFP-mCFP) that can be inverted by the Cre. When crossed with mice that express a cell promoter driven by tamoxifen-inducible Cre recombinase, selected lineages are stochastically labelled with an inheritable green, yellow, red, or cyan fluorescent protein tag. [315]

This system has been used for progenitor cell tracing in several systems to date. In 2016, a study by Mondor *et al*. utilized the Brainbow multicoloured fluorescent fate-mapping model to study clonal proliferation of high endothelial venule (HEV) cells in lymph node expansion during an immune response. They showed that the expansion of the lymph node vasculature relies on the sequential assembly of EC proliferative units. [319] Other recent studies showed the power of this lineage system by investigating clonality of blood progenitor cells [320] and tumour cell subpopulations in colon cancer. [321]

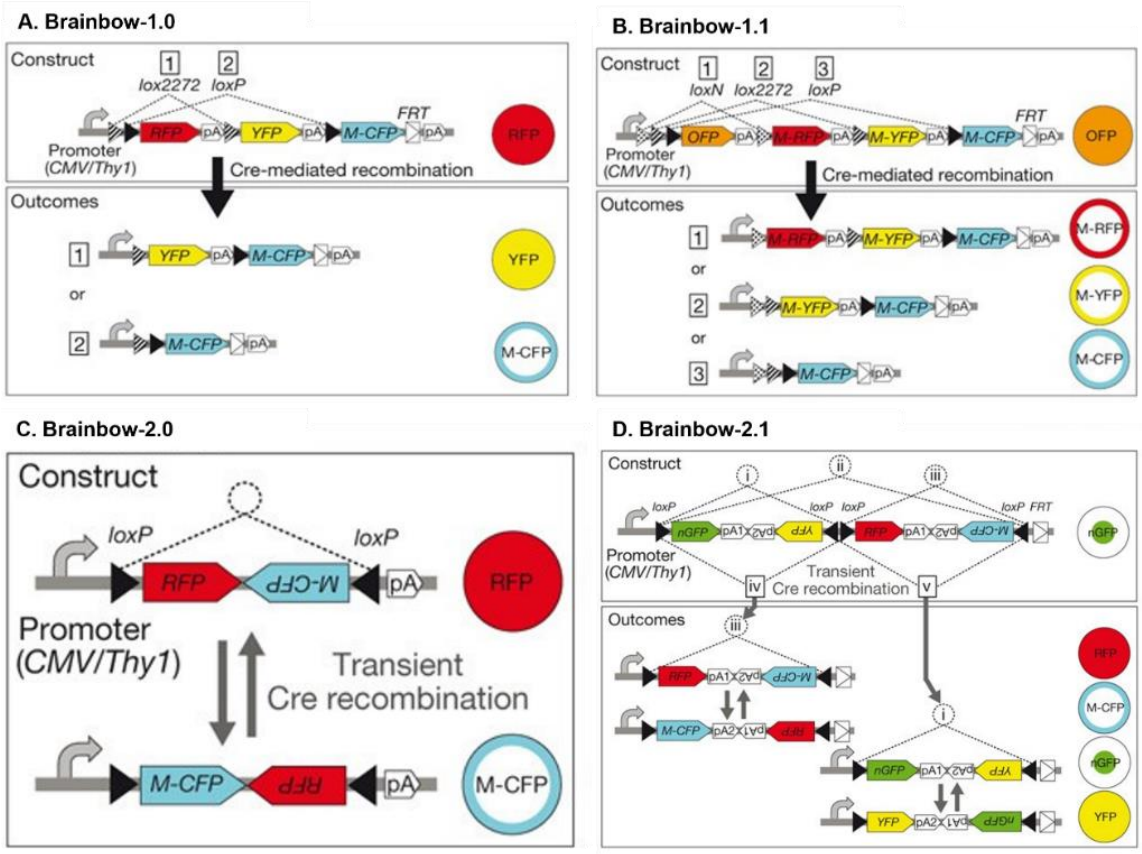

Figure 1.8 Cassettes of Brainbow transgenes versions 1 and 2

(A) The *Brainbow 1.0* cassette used Cre-mediated excision of pairs of incompatible *lox* sites to produce two mutually exclusive recombination outcomes and switch fluorophore

expression from the default red to yellow or cyan.(B) The *Brainbow 1.1* cassette produces three recombination events: yellow, red or cyan with orange being the default fluorophore in the absence of recombination. (C) The *Brainbow 2.0* cassette harbours a Cre-invertible construct that contains regions coding for red fluorescent protein (RFP) and cyan fluorescent protein (CFP) in head-to-head orientation. Upon recombination this results in expression of either red or cyan. (D) The *Brainbow 2.1* cassette contains adjacent loxP flanked head-to-tail tandem dimers. The first dimer includes nuclear tagged Green Fluorescent Protein (nGFP) in forward orientation and Yellow Fluorescent Protein (YFP) in reverse orientation. The second dimer contains RFP in forward orientation and membrane bound CFP (mCFP) in reverse orientation. Upon recombination this results in stochastic expression of either green, yellow, red or cyan. Adapted from Livet *et al*., 2007.[315]

1.10.2 Chasing endothelial cells - The *Pdgfb* lineage inducible mouse model

The choice of a promoter for a cell lineage tracing experiment is crucial and ECs are no different (reviewed in Ref[322]). The promoter must be specific enough to the population of interest to efficiently label the cells of interest and study their dynamics. This is especially the case when investigating multicellular processes such as in the case of myocardial injury. If a promoter is chosen that is not cell-specific, then wrong conclusions can be drawn for origin and dynamics of the labelled population.

In the case of EC lineage tracing, a variety of promoters have been used. The most commonly used EC lineage mouse model is the *Tie2-Cre*.[322] Tie2 expresses an angiopoietin receptor that is shared by all ECs both in development and adulthood.[323–325]. However, in the case of Tie-2, 85% of circulating adult blood cells and 82% of embryonic yolk sac derived blood cells have been shown to exhibit Tie-2 driven Cre activity which suggests that Tie2 is expressed in progenitors that give rise to blood cell and EC lineages.[326] Moreover, Tie-2 driven Cre-lox models have been shown to exhibit non-specific Cre recombinase activity with reports of 13% of mice in later generations showing non-EC specific Cre activity.[327] In addition, in certain Tie-2 drive Cre lineage tracing mouse lines, Cre activity has been shown to vary from animal to animal, ranging from ubiquitous to EC specific.[328]

The Cdh5 driven Cre-lox model is another very popular model of EC specific targeting. Cdh5 (or VE-cadherin) is an EC junction protein that is essential for vascular homeostasis.[329] In the adult, Cdh5 driven lineage tracing labels all ECs. However, Cdh5-Cre models label also haematopoietic cells.[330] More specifically, it has been shown that up to 96% of CD45+ adult bone marrow derived cells were expressing Cdh5 driven Cre.[330]

Another EC lineage tracing mouse model that is used to target ECs is the Kdr-Cre (or VEGFR2-Cre) model. As described in section 1.6.2 VEGFR2 is essential for EC functions such as angiogenesis but is also required for EC migration and proliferation. [331] The Kdr-Cre is a pan-EC target model. [322] However, similar to Cdh5 and Tie2, Kdr is also expressed by haematopoietic cells in the bone marrow.[322]

Finally, more EC lineage tracing mouse models have been developed to target EC subtypes rather than a pan-EC targeting. These are reviewed by Payne *et al.* [322] For instance, Sox17-Cre and Bmx-Cre/ERT2 mouse lines can be used to target arterial specific ECs. [332,333] However, the specificity of these subtype models makes them difficult to use when the phenotype of the studied EC population is not well known, such as in the case of ECs participating in neovascularisation post-MI.

As discussed previously (*1.8.1 Heterogeneity in endothelial cell contribution to post-MI neovascularisation*), the sources of ECs contributing to neovascularisation post-MI are greatly debated. One of the hypothesised sources is the bone marrow. [334] Lineage tracing studies of ECs in the heart have predominantly used Cdh5-driven expression. However, this is problematic as Cdh5 is not only expressed by ECs but also by cells of haematopoietic origin. [335,336] Therefore, if the expression driver of choice is also expressed in cells of haematopoietic origin, then the origin of ECs taking part in neovascularisation post-MI remains inconclusive.

Another promoter that has been used to label ECs is *Pdgfb*. *Pdgfb* is expressed by ECs and is responsible for recruitment of pericytes and smooth muscle cells. [337] In 2007, Claxton *et al*. developed a Cre-inducible *Pdgfb*-driven mouse model to efficiently and

specifically label ECs.[337] The inducible Cre, iCreER^{T2}, was created by fusing an improved version of Cre recombinase [338] with a mutant form of the human oestrogen receptor (ER^{T2}) that is insensitive to naturally occurring oestrogen but activated in the presence of the artificial ligand 4-hydroxytamoxifen (OHT). [339] In the absence of OHT, the iCreER^{T2} protein remains in the cytoplasm, isolated by heat shock protein 90 (HSP90). When OHT is introduced, iCreER^{T2} translocates to the nucleus to mediate recombination.[337] The construct contains an internal ribosomal entry site (IRES) element downstream of iCreER^{T2} as well as a sequence coding for enhanced green fluorescent protein (EGFP). The construct was recombined into the mouse *Pdgfb* gene in a phage artificial chromosome (PAC). The PAC was introduced to mice using pronuclear injection. [337]

Validation of the construct using a ROSA-lacZ reporter strain[340] in 3-day-old mouse pups showed labelling of ECs in the vasculature of striated muscle, skin, kidney, pancreas, lung, and central nervous system (CNS).[337] In the same pups, non-endothelial recombination was observed solely in some keratinocytes[337] which can be explained by *Pdgfb* expression seen before in keratinocytes.[341] Recombination was not observed in the liver or in large vessels, such as the dorsal aorta. In adult animals, administration of tamoxifen showed labelling in vessels of skeletal muscle, heart, skin, and gut with minimal labelling in brain and liver. Moreover, *Pdgfb* labelling was found in the retinal vasculature. More specifically, in the adult, labelling was found in ECs of capillaries and certain arterioles located in branches from arteries of the retinal vasculature. Importantly, labelling was not found in pericytes or smooth muscle cells, strengthening the claim that *Pdgfb* expression is EC specific. *Pdgfb* labelling was also not found in macrophages even though there have been some reports that macrophages may express *Pdgfb*.[342] As far as the expression of *Pdgfb* in the heart is concerned, Cre-activation via tamoxifen administration has been shown to drive recombination in 99% of adult coronary ECs (albeit absent from the endocardium) which makes it an attractive lineage tracing model for coronary vasculature studies.[135]

1.11 Single Cell RNA Sequencing

As described in earlier segments of this introduction, MI-induced neovascularisation is a multicellular and dynamic process. Novel methodologies investigating the transcriptome of the ECs involved are critical to effectively decipher the molecular pathways involved, with aim of exploiting these to ameliorate MI patient outcomes. This section will discuss the development of methods characterising transcriptomics and specifically the use of single cell RNA sequencing as a tool to investigate MI-induced neovascularisation.

The Human Genome Project (HGP)[343] was an essential first step to commence deciphering our genome. It revealed how little we understood about our genetic identities, with only 25% of the predicted 100,000 coding genes receiving protein-coding gene status. Moreover, new variants and isoforms of genes have been discovered, whilst non-coding genes previously thought to be "junk" DNA have been shown to be crucial in regulating key biological processes.[344] The HGP was achieved using the high fidelity but slow and costly Sanger Sequencing[345]. Initially, DNA sequencing was only possible using Sanger sequencing and the Maxam-Gilbert chemical cleavage method [346]. This was revolutionary at the time but laborious due to manual gel type electrophoresis where DNA fragments that differed in a single base pair could be read.[345] Due to its fidelity, Sanger sequencing is still used today for short length sequencing where high throughout is not necessary, such as in the case of validation of a PCR product.

Following development of sequencing strategies, next generation sequencing (NGS) was the next step in revolutionising genomic research. With the use of NGS a human genome can be sequenced within a single day whereas the HGP took over a decade. NGS involves sequencing millions of small DNA fragments in parallel. This information is later bioinformatically aligned to the corresponding genome. One of the more popular NGS strategies is characterisation of the transcriptome via RNA sequencing. This involves reverse transcription of total RNA to cDNA followed by cDNA amplification, fragmentation, and parallel sequencing and finally bioinformatic

analysis. Despite RNA sequencing being excellent at helping us increase our understanding of the transcriptome of various species, it comes with some disadvantages. When conducted, bulk RNA sequencing is averaging gene expression of all cells in a sample. As a result, when looking for gene expression genes that arise from a subset cell population this can lead to a dilution of results and misinterpretation due to potential false negatives. A workaround of this issue is selection of a certain cell population via Fluorescence-Activated Cell Sorting (FACS). However, the prerequisite in this case is known cell markers that can be used to isolate cell populations. Consequently, unknown or poorly studied cell populations cannot be investigated. Moreover, FACS relies on good and reproducible antibody batches for robust selection of cell populations, and these are not always available. A different method of isolating cells for downstream molecular analyses is *via* laser capture microdissection.[347] This technique involves microscopy-aided removal of a cell or region of interest *via* a laser. However, similar to FACS, this relies on visualisation of the target cell via a known marker.

Our idea of a cell signature has been challenged over the last 10 years as sequencing studies give insights on the heterogeneity of cells within the same tissue system as well as across organs. Moreover, the drawbacks of existing technologies have stimulated the development technologies which gives us the ability to interrogate the transcriptome of each individual cell. One such technique is single cell RNA sequencing. Single cell RNA sequencing provides an unbiased approach of investigating the gene expression signature of thousands of cells of a cell-by-cell basis. Initially, single cell RNA sequencing was carried out in tissues for which starting material was limited. The first published study of single cell sequencing was in 2009[348] only 2 years after the first applications of RNA sequencing to bulk samples. Tang *et al*. implemented single cell RNA sequencing technology on a single mouse blastomere and detected 5,270 more genes than established microarray strategies as well as 1,753 previously unknown splice junctions. Overall, single cell RNA sequencing datasets have been critical at providing a high-resolution view of the identity of a cell at a given time as well as the intermediary stages of cellular transition. Furthermore,

it has documented that cells are hardly static but exist in a dynamic environment with the potential for varying degrees of plasticity.[349–351]

Single cell sequencing can provide powerful information when assessing differences in cells that would otherwise go undetected in techniques that use pooled cells. As an example, this can be applied in immune cell profiling. Shalek *et al.* utilized this technique to characterise peripheral mononuclear cells from healthy patients as well as COVID-19 and influenza patients.[352] This study revealed that distinct signaling pathways are activated in COVID-19 patients (STAT1 and IRF3) versus influenza patients (STAT3 and NFkB).[352] Examples also include single cell RNA sequencing of diverse T-cell populations[353], neurons in the brain[354] as well as cells during embryonic development.[355] In addition to defining transcriptomic signatures of cell populations, single cell RNA sequencing provides useful formation on splicing patterns[356] and RNA velocity dynamics.[357]

A popular strategy of single cell sequencing is droplet-based sequencing or Dropseq. Following attaining viable cells in a single cell suspension, cells are encapsulated in a barcoded nanoliter-scale droplet. Subsequently, polyadenylated RNA is transcribed to cDNA via oligoT priming and then amplified by PCR. Naturally, the total cDNA material of a single cell is small and thus requires further amplification and library preparation. Libraries refer to DNA fragments of defined length with barcoded oligomer adapters at the 5' and 3' end.[358] Following library preparation, libraries are sequenced using next generation sequencing instruments such as Illumina instruments (reviewed in Ref.[359]). The data are then aligned in the reference genome using tools similar to those used for build RNA sequencing (reviewed in Ref[360]). Subsequently, the data undergoes quality control where single cells that produce inadequate quality data are excluded. The most common quality control checks include relative library size, number of detected genes, number of detected unique molecular identifiers, and fraction of reads mapping to mitochondria-encoded genes.[361] Following quality control, the data can be analysed using existing bioinformatic tools (reviewed in Ref [362,363]). The main approach involves the reduction in the dimensionality (i.e. complexity) of the data to make visualisations and

interpretations easier. This can be achieved through principal component analysis (PCA) and subsequent machine learning, cluster building algorithms to reveal the transcriptomic profile similarities between cells and cluster them into subpopulations followed by data interpretation.[361]

1.12 Hypothesis and aims

This thesis addressed the following hypotheses:

1) *Clonal proliferation is a key cellular mechanism through which resident ECs contribute to neovasculogenesis in the peri-infarct border region of the post-ischaemic adult mouse heart.*
2) *Resident cardiac EC and not bone marrow cells are the primary contributors to new blood vessel formation in the infarct border after MI.*
3) *Proliferative cardiac ECs in the post-ischaemic adult mouse heart express markers that can be identified using single cell RNA-sequencing and bioinformatics analyses.*
4) *Vascular regeneration can be promoted in adult ECs via manipulation of candidate markers.*

These hypotheses will be addressed, respectively, by the following aims:

1) Assessment of neovascularisation by clonal expansion of *Pdgfb* lineage cardiac ECs in the adult mouse heart during homeostasis and at 7 days post-MI in *Pdgfb-iCreER^{T2}-Brainbow2.1* mice.
2) Investigation of contribution of bone marrow derived *Pdgfb* lineage ECs in cardiac neovascularisation at 7 days post-MI in *Pdgfb-iCreER^{T2}-Brainbow2.1* mice.
3) Investigation of the transcriptome of *Pdgfb* lineage cardiac ECs from healthy and 7-day post-ischaemic adult *Pdgfb-iCreER^{T2}-Brainbow2.1* mice to identify key markers specific to pro-angiogenic cardiac ECs.
4) Investigation of candidate markers, identified in Aim 3, in human patient samples of ischaemic heart disease, in human primary ECs lines and mouse cardiac tissue *in vitro.*

Chapter 2 Materials & Methods

2.1 Mouse models

2.1.1 Approval of animal work

Experiments with mice were performed in accordance with the *Guide for the Care and Use of* Laboratory Animals by the Institute of Laboratory Animal Resources and approved by the UK Home Office and the University of Edinburgh Animal Welfare and Ethical Review Committee.

2.1.2 Mouse models for endothelial cell lineage tracing

EC-specific, tamoxifen-inducible *Pdfdb-iCreER^{T2}-R26R-Brainbow2.1* mice were generated by crossing C57Bl/6J mice expressing tamoxifen-inducible CreER^{T2} recombinase under the control of the *Pdgfb* promoter[337] (described in section *1.10.2. Chasing Endothelial Cells)* and R26R-Brainbow2.1 mice containing the Brainbow2.1 cassette (Described in section *1.10.1 The Brainbow mouse model*) (donated from Professor Kairbaan Hodivala-Dilke, Bart's Cancer Institute, London) (Figure 2.1). [315] When tamoxifen is present, the resulting mouse line of *Pdgfb-iCreERT2-R26R-Brainbow2.1* will induce Cre-mediated excision inversion in *loxP* sites that are facing each other in the transgene cassete in cells expressing *Pdgfb*, resulting in expression of one of four fluorophores, green, yellow, red or cyan (explained in section *1.10.1* (Figure 2.1). In the case of the *Pdgfb-iCreERT2-R26R-Brainbow2.1 the Brainbow2.1* transgene is inserted in the commonly used Rosa26 locus (exons 1 and 2).[364] The benefit of the Rosa26 locus is that its chromosomal location is known, and it has been shown to not affect the function of other genes.[365] Moreover, it contains a STOP element (Figure 2.1) that prevents expression of the Brainbow2.1 in the absence of Cre activity. Furthermore, it contains a CAG promoter (cytomegalovirus (CMV) major immediate-early enhancer combined with the chicken beta-actin promoter (CAG) to drive expression of the Brainbow2.1 transgene (Figure 2.1).

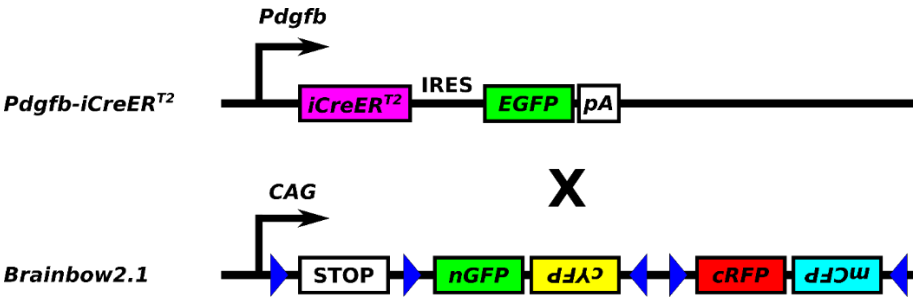

Figure 2.1 The *Pdgfb-iCreERT2-R26R-Brainbow2.1* mouse model

The *Pdgfb-iCreER^{T2}-R26R-Brainbow2.1* mouse houses an endothelial cell (EC)-specific Brainbow2.1 cassette, driven by the *Pdgfb* gene. Exposure to tamoxifen induces stochastic expression of a cytoplasmic red fluorescent protein (RFP), nuclear green fluorescent protein (nGFP), cytoplasmic yellow fluorescent protein (YFP) or membranous cyan fluorescent protein (mCFP), specifically in promoter-expressing EC. Fluorophore expression is inherited by daughter progeny following cell division, permitting visualisation of clones formed by EC proliferation, and lineage tracing of EC fate.

2.1.3 Genotyping

Genotyping of *Pdgfb-iCreER^{T2}-R26R-Brainbow2.1* was outsourced to TransnetYX (USA) using the probes displayed in Table 2.1 .

Table 2.1 Probes designed for genotyping Pdgfb-iCreER^{T2}-R26R-Brainbow2.1 mice

Pdgfb-iCreERT2-R26R-Brainbow2.1	ROSA WT	hrGFP Tg	Cre
Forward	TTCCCTCGTGATCTGCAACTC	CGAGGACATCAGCGACTTCTT	TTAATCCATATTGGCAGAACGAAAACG
Reverse	CTTTAAGCCTGCCCAGAAGACT	GGTGCGCTCGTACACGAA	CAGGCTAAGTGCCTTCTCTACA

2.1.4 Tamoxifen injection for iCreER^{T2} recombination

Pdgfb-iCreER^{T2}-R26R-Brainbow2.1 mice were injected with tamoxifen (Sigma, UK) intraperitoneally at a concentration of 150 mg/kg or the equivalent volume of peanut oil (Sigma, UK) for *Pdgfb-iCreER^{T2}-R26R-Brainbow2.1* littermate controls. Injections were carried out 14 days prior to surgery in 8-12-week-old mice. For healthy control mice, tamoxifen was administered 21 days or 42 days before collection of tissues.

2.1.5 EdU and isolectin B4 injections

Mice were administered 50 mg/ kg 5-ethynyl-2'-deoxyuridine (EdU) (Invitrogen™, UK) via a single intraperitoneal injection 1 – 2 hours prior to cull to label newly synthesised DNA. EdU-expressing cells were detected in mouse cardiac tissues (ventricles) using the Click-iT™ EdU Alexa Fluor™ 647 Imaging Kit (Invitrogen™, UK) as *per* manufacturers' instructions. To label perfused vessels in the healthy and 7-day post-MI murine hearts, biotin-labelled Lycopersicon esculentum lectin (isolectin B4) was injected (2 mg/mL, 100 µL, Sigma-Aldrich, UK) *via* the tail vein 15 minutes prior to cull.

2.1.6 Injections with recombinant human VEGFC

Mice aged 8-12 weeks were injected intraperitoneally with recombinant human VEGF-C (Biotechne, UK) at a dose of 0.1 µg/g or phosphate buffer saline (PBS) for controls (100 µL injection volume). Injections took place at days -1, -3, -5 and -7 before heart tissue collection.

2.1.7 Left anterior descending coronary artery ligation surgery.

Myocardial infarction (MI) was induced by permanent LAD coronary artery ligation, as described previously.[366] Animals were anaesthetised with 2% isoflurane/98% oxygen and ventilated *via* endotracheal intubation at 120 strokes per minute with a 200 µL stroke volume. Under a surgical microscope (Zeiss, Germany) an incision was made at the left fifth intercostal space level and MI was induced by permanent ligation of the left anterior descending coronary artery by using a 7.0 Mersilene

suture (Ethicon, UK). After closure of the thorax, mice were allowed to recover with aseptic precautions and received post-operative Buprenorphine analgesic (0.05 mg/ kg subcutaneous, Ceva, UK). Mice were killed by cervical dislocation or by perfusion fixation (described in 2.2.1) and hearts were collected 7/28 days post-surgery (21/42 days post-tamoxifen) (Figure 2.2)

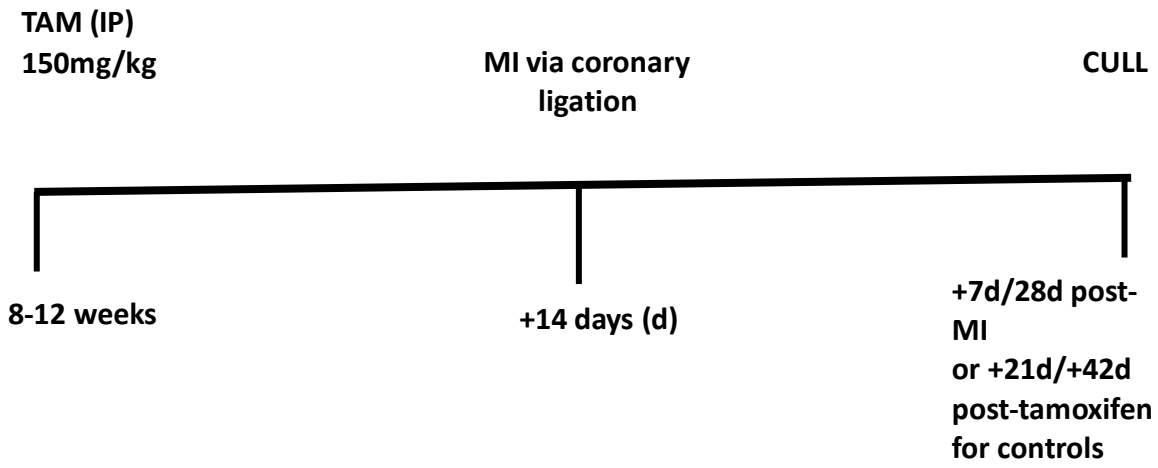

Figure 2.2 Timescale of MI surgeries

Mice 8-12 weeks were administered tamoxifen as per section 2.1.4. Subsequently, myocardial infarction (MI) was induced by permanent ligation of the left anterior descending coronary artery (LAD) in mice aged 8-12 weeks and hearts were collected at 7- or 28-days post-surgery, along with healthy control hearts at the equivalent day post-tamoxifen (21d or 42d post-tamoxifen).

Figure 2.3 Cardiac injury induced via left anterior descending coronary artery ligation

The model of cardiac ischaemia by permanent ligation of the left anterior descending coronary artery. The arrow points at the infarct (image adapted from Gray *et al.*, 2013[366]).

2.2 Animal Tissue handling and preparation

2.2.1 Tissue collection and storage

Mice were killed *via* cervical dislocation or perfusion fixation. Perfusion fixation involved mice terminally anaesthetised with a 40 mg intraperitoneal injection of sodium pentobarbital Euthatal© (Dopharma Research B.V, UK) in 200 µL excipient (propylene Glycol, ethanol, patent Blue V E131, water) and perfused with 10 mL sterile PBS and 10 mL 4% PFA. Tissues were collected and post-fixed overnight in 4% paraformaldehyde (PFA) at 4°C. Tissues were stored in sterile PBS (short term, <2 months) or in 0.025 % sodium azide (long term > 2 months) at 4°C. For work relating to gene expression analysis, hearts were fresh frozen using liquid nitrogen and stored in -80 ^{o}C following dissection.

2.2.2 Tissue processing and sectioning

For vibratome sectioning, fixed hearts were mounted in 4% low melting point agarose and serial transverse sections (100-200 µm) were cut with a Compresstome® VF-300 Vibrating Microtome (Precisionary Instruments, US). Free-floating sections were stored in 0.025% sodium azide in PBS at 4°C.

For cryosectioning at a thickness of 10 µm, fixed hearts were incubated in 30% sucrose in PBS overnight at 4°C and subsequently embedded in optimal cutting temperature compound Tissue-Tek® (O.C.T. Compound, Sakura® Finetek, UK) on dry ice for storage at -80°C. Cryopreserved hearts were sectioned (10 µm) coronally along the apex-base axis using a cryostat (Leica, Germany) and collected on VWR® Superfrost® Plus Micro slides (UK) and stored at -80 °C.

2.3 Tissue staining

2.3.1 Haematoxylin and Eosin Staining (H&E)

Formalin fixed paraffin embedded (FFPE) sections were deparaffinized in two changes of xylene solution (2 x 5 minutes). Rehydration of FFPE sections was performed using decreasing concentrations of ethanol (100%, 90%, 80%, 70%, 20 seconds each). FFPE sections and cryosections were submerged in Mayer's haematoxylin (Dako, UK) for 5 minutes followed by acid ethanol (1% HCl in 70% ethanol, 20 seconds), Scott's tap water (30 seconds) and Eosin Y solution (Abcam, UK) for 20 seconds. Slides were then dehydrated through increasing concentrations of ethanol (70%, 80%, 90%, 100% ethanol, 20 seconds each). Slides were then cleared in xylene (2 x 5 minutes). Coverslips were mounted on the slides using pertex mounting medium (CellPath, UK).

2.3.2 Masson's Trichrome Staining

FFPE sections from hearts of patients of acute and chronic ischaemic heart disease (ventricles) and cryosections from 7day post-MI mouse hearts (ventricles) were stained using Masson's trichrome (Abcam, ab150686, UK) as per manufacturer's instructions to detect levels of fibrosis.

2.3.3 Immunofluorescent staining

Mouse heart wholemounts and cryosections for immunohistochemical analyses were permeabilised in 0.5% Triton-X in PBS (PBS-T) for 1 hour (for wholemounts) or 30 minutes (for cryosections), adapted from abcam[367], followed by blocking in 10%

normal goat serum (NGS) (Thermo Fisher Scientific, UK), 1% bovine serum albumin (BSA) (Sigma Aldrich, UK), 0.5% PBS-T for 1 hour at room temperature on a mechanical SSL1 orbital shaker (VWR, UK). Primary antibodies (Table 2.2) were diluted in 10% NGS, 1% BSA in PBS-T and sections were incubated at 4°C overnight. After further washes in PBS-T (2 x 15 minutes), sections and wholemounts were incubated with species-specific fluorescence-conjugated secondary antibodies (Table 2.2) diluted at 1:400 in 10% NGS in PBS-T for 2 hours (for wholemounts) or 1 hour (for cryosections) at room temperature and washed in PBS. Cryosections were mounted in Fluoromount-G with 4',6-diamidino-2-phenylindole (DAPI) (Invitrogen, UK). Wholemount sections were counterstained with DAPI (Sigma-Aldrich) and mounted in RapiClear 1.47 (SunJin Lab, China).

Human paraffin-embedded sections were requested from the MRC Edinburgh Brain & Tissue Bank with ethical approval (Table 2.8). The sections were dewaxed, rehydrated and antigen retrieval performed using 10 mM sodium citrate buffer (pH 6.0) followed by permeabilisation in PBS-T and blocking of non-specific binding in 1 % BSA/ 10 % NGS in PBS-T for 30 minutes. Primary antibodies (Table 2.2) were diluted in 10% NGS, 1% BSA in PBS-T and sections were incubated at 4°C overnight. After further washes in PBS-T (2 x 15 minutes), sections were incubated with appropriate fluorescence-conjugated secondary antibodies (Table 2.2) diluted at 1:400 in 10% NGS in PBS-T for 1 hour at room temperature and washed in PBS. Sections were mounted in Fluoromount-G with DAPI (Invitrogen). All immunohistochemical analyses were performed with appropriate isotype controls.

Table 2.2 List of antibodies

Primary Antibodies	**Source**
Isolectin GS-IB4 From Griffonia simplicifolia, biotin-XX Conjugate	Thermo Fisher 121414
Rabbit Anti-CD31 (1:50 dilution)	ab23864
Rat Anti-CD31 (1:50 dilution)	CD Pharmingen 550274
Anti-PLVAP (1:200 dilution)	ATLAS ANTIBODIES HPA002279
pan ECA (MECA-32) (1:400 dilution)	SANTA CRUZ sc-19603
Secondary antibodies (used in 1:400 dilutions)	**Resource**
Streptavidin, Alexa Fluor™ 647 conjugate	Thermo Fisher S21374
Goat Anti-Rat IgG H&L (Alexa Fluor 647)	abcam ab150159
Goat Anti-Rabbit IgG (H+L) Cross-Adsorbed Secondary Antibody, Alexa Fluor 488	Thermo Fisher # A-11008
Goat Anti-Rabbit IgG (H+L) Cross-Adsorbed Secondary Antibody, Alexa Fluor 546	Thermo Fisher # A-11010

Goat Anti-Rabbit IgG (H+L) Cross-Adsorbed Secondary Antibody, Alexa Fluor 647	Thermo Fisher # A-21244
Isotype Controls	**Resource**
Rabbit IgG [EPR25A]	abcam ab172730
Rat IgG2a, kappa [RTK2758]	abcam ab18450

2.3.4 Terminal deoxynucleotidyl transferase dUTP nick end labeling (TUNEL)

Cardiac cell apoptosis was detected in cultured murine myocardial slice sections (prepared and cultured according to section 2.7.2) using the Click-iT TUNEL Alexa Flour imaging assay (Invitrogen, UK) according to the manufacturer's instructions.

2.4 Flow cytometry and FACS

2.4.1 Flow cytometry of bone marrow cells

Mouse femurs were isolated, surrounding muscle removed, and collected into sterile PBS. Both ends of the bone were removed using a scalpel (Fisher Scientific, UK). Using a 23g needle (Fisher Scientific, UK) and 15mL syringe (VWR, UK), 1 mL sterile PBS was used to flush cells into a 15mL Falcon tube. The cells were resuspended in the same solution to prevent formation of clumps and was then centrifuged at 500g for 5 minutes and the supernatant was discarded. The cells were subsequently resuspended in 400 µL FACS lyse solution (BD Biosciences, UK) in FACS tubes (VWR, UK) before proceeding to flow cytometry analysis to investigate Brainbow2.1 fluorophore expression.

2.4.2 FACS of mouse cardiac endothelial cells and single cell sequencing sample preparation

Mouse hearts were collected in tissue collection solution (Table 2.3). Atrias were removed and the ventricles were minced using scalpels and transferred to a pre-warmed (37°C) digestion buffer (Table 2.4). Tissues were incubated for 20 minutes at 37°C and vortexed every 5 minutes. The digest was transferred to GentleMACS tubes (Miltenyi Biotec, UK) and homogenised using a gentleMACS tissue dissociator (Miltenyi Biotec, UK). Immediately afterwards, 6 mL of ice-cold wash buffer (1x DPBS, 2% FBS, 0.5 M EDTA) was added to the digest. The digest was collected through a 40 µm strainer and centrifuged (Eppendorf, UK) at 500 g for 5 minutes at 4°C. The supernatant was removed and red blood cells were lysed using 1 mL Red Blood Cell Lysing Buffer Hybri-Max™ (Sigma-Aldrich) for 1 minute. Subsequently, 30 mL of ice-cold wash buffer was added to neutralise the reaction. The cells were centrifuged at 500 g for 5 minutes and then resuspended in 500 µL ice-cold wash buffer. Samples were stained with conjugated antibodies AlexaFluor® 647 anti-mouse CD31 antibody (5 µg/mL, BioLegend) and APC/Cy7 anti-mouse Podoplanin antibody (2 µg/mL, BioLegend) for 30 minutes in the dark at 4 °C. Unstained and single stained controls were included for analysis. Following this, a further 500 µL wash buffer was added and samples were centrifuged at 500 g for 5 minutes. The cells were resuspended in 500 µL using FACS buffer (1x DPBS + 5% w/v BSA) and transferred into FACS sorting tubes (BD Biosciences, UK) that had been coated previously with neat FBS for 30 minutes. Cells were sorted using a FACS Aria II (BD Biosciences, UK) with a 100 µm nozzle.

Using BD FACSDiva software (BD Biosciences, UK), a gate was set to exclude debris and doublets. Fluorescence minus one (FMO) controls were used to determine the gates for CD31 and Podoplanin expression. Cardiac ECs from age-matched wild type mice on the same genetic background as *Pdgfb-iCreERT2-R26R-Brainbow2.1* mice (C57Bl6) were used as controls to determine the threshold for detection of Confetti reporter fluorophore expression. Unstained cells and single antibody-stained cells were used as controls to detect CD31 and podoplanin expression. DAPI solution (BD

Biosciences, UK) was used as viability marker. 100,000 viable Confetti+ CD31+ Podoplanin- cells were collected per sample into ice-cold sterile PBS with 0.5 % UltraPure BSA (Thermo Fisher Scientific, UK) and immediately processed for single cell RNA sequencing as per section 2.8)

Table 2.3 Heart tissue collection buffer for flow cytometry

Abbreviations; RPMI (Roswell Park Memorial Institute Medium), FBS (Foetal Bovine Serum)

Reagent	1x HEART
RPMI1640	3.56mL
FBS (working concentration 10%)	0.4mL
Glutamax (100x dilute to 1x)	40µL
Total volume	4 mL

Table 2.4 Heart digestion solution buffer for flow cytometry

Abbreviations; RPMI (Roswell Park Memorial Institute Medium), FBS (Foetal Bovine Serum)

Reagent	1x HEART
Collagenase V	4.25 mg
Collagenase D	6.25 mg
Dispase	10 mg
DNAase	300 µg
FBS	500 µL
GlutaMAX	50 µL
RPMI1640	4450 µL
Total volume	5 mL

2.4.3 Flow data analysis

Flow cytometry data were analysed using Flowjo v10 (FlowJo LLC, USA).

2.5 Gene expression analysis

2.5.1 RNA extraction

RNA from mouse heart tissue (as *per* 2.2.1),FACS isolated ECs (as *per* 2.4.2) or cultured HUVECs (as *per* 2.7.1) was extracted using a phenol-chloroform based miRNeasy Mini RNA extraction kit (Qiagen, UK) as *per* manufacturer's instructions.

2.5.2 RNA assessment

RNA quality and concentration from RNA samples as *per* section 2.5.1 were assessed using the Qubit™ RNA HS Assay Kit (Thermofisher, UK) and a Qubit 4 Fluorometer (Thermofisher, UK) or with a Nanodrop 1000 (Thermofisher, UK) as per manufacturer's instructions.

2.5.3 cDNA synthesis

cDNA was synthesized from 200 ng of total RNA (extracted as *per 2.5.1*) in 40 µL reactions using TaqManTM Reverse Transcription Reagents (ThermoFisher Scientific, UK) as *per* manufacturer's instructions (Table 2.5). Cycling conditions consisted of 25°C (10 minutes), 48°C (30 minutes), 95°C (5 minutes).

Table 2.5 Reagents for cDNA synthesis

Reagent	40µL reaction
10x buffer	4 µL
25mM MgSO4	8.8 µL
dNTPs	8 µL
Random Hexamers	2 µL
RNAse Inhibitor	0.8 µL
Multiscribe	1 µL
Total volume	24.6 µL
RNA+H20 (100ng)	15.4 µL

2.5.4 Quantitative Polymerase Chain Reaction (qPCR)

Quantitative PCR was performed using Taqman chemistry using cDNA synthesised as above. Individual 10 µl Taqman real-time PCR reactions consisted of 1.5 µl of cDNA, 5 µl of 2x Taqman mastermix and 0.5 µl of Fluorescein amidites (FAM) labelled probe (ThermoFisher Scientific, UK) in 3 µl RNase-free water. All probes' codes can be found in Table 2.6. All probes were selected to be exon spanning using the Thermofisher predesigned and pre-optimised "Taqman Assays" library with an amplicon length of 69-187bp size and a Fluorescein amidites-minor groove fluorescent dye. [368]The PCR was carried out in triplicate on a QuantStudio 5 Real-Time PCR system using the following cycling conditions: 10 minutes at 95 °C and 40 cycles of 15 seconds at 95 °C, 60 seconds at 60 °C. For normalisation purposes housekeeping genes UBC[369] and 18S[370] were used. UBC and 18s were selected as a reference genes for qPCR analysis of *in vitro* cultured ECs according to existing studies. [371,372] 18s was selected as a reference gene for qPCR analysis of *in vivo* derived adult mouse cardiac ECs according to existing studies.[373–376]

Table 2.6 Taqman probes for qPCR

Gene	Species	Probe code
PLVAP	Human	Hs00229941_m1
Plvap	Mouse	Mm00453379_m1
18S	Human	Hs99999901_s1
18S	Mouse	Mm03928990_g1
UBC	Human	Hs00824723_m1

2.5.5 qPCR data analysis

For analysis, the ΔCt values were calculated as the differences between the Ct values of the target gene and housekeeping genes UBC or 18S. The mean of the ΔCt values from the 'no treatment' groups was subsequently used to calculate the ΔΔCt values and RQ (2^- ΔΔCt) values. Statistical analyses were conducted using ΔCt values. Gene expression levels are presented using RQ values.

2.6 Protein analysis

2.6.1 Protein extraction

Protein was extracted from human umbilical vein endothelial cells (HUVECS) 48 hours after transfection by trypsinising them using 0.05% Trypsin-Ethylenediaminetetraacetic acid (EDTA) (Gibco, UK), centrifuging at 600 g at 4 °C twice for 10 minutes and transferring to 100 µl lysis buffer containing 1.5x RIPA buffer (Cell Signaling Technology, UK) and 1x protease inhibitor mixture (complete ULTRA Mini EDTA-free Protease Inhibitor Cocktail, Sigma-Aldrich, UK). Cells were re-suspended by vortexing and incubated on ice for 30 minutes. The crude cell extracts were centrifuged at 600g at 4 °C for 10 minutes.

2.6.2 Protein measurement

Protein concentrations of cultured HUVECs (prepared as *per* 2.7.1) were measured using a Pierce™ BCA Protein Assay Kit (Thermo Scientific, UK) *per* manufacturer's instructions and the plates were read on a VICTOR X3 multimode plate reader (PerkinElmer, UK). Protein standards were plated in triplicate and a 2nd-order polynomial curve was fitted through the standard points. The sample measurements were interpolated on the fitted curve and the protein concentration for each sample was then calculated.

2.6.3 Western blotting of PLVAP

Protein samples were denatured at 95 °C for 10 minutes in Bolt LDS Sample buffer (ThermoFisher Scientific, UK) and separated using NuPAGE™ Novex 4-12% Bis-Tris Gel (Invitrogen, UK) electrophoresis followed by transfer to Amersham™ Hybond™ 0.2 µm polyvinylidene difluoride (PVDF) membranes (GE Healthcare, UK). After blocking in Sea block buffer (Thermo Fisher Scientific, UK) for 1 hour at room temperature, the membrane was incubated in primary Anti-PLVAP antibody (Atlas Antibodies HPA002279) diluted 1:200 or Glyceraldehyde 3-phosphate dehydrogenase (GAPDH) (14C10, Cell Signalling, UK**)** in blocking buffer on a mechanical SSL1 orbital shaker at 4°C overnight (VWR, UK). After three washes with Tris-buffered saline (TBS) containing 0.1% Tween-20, the membrane was incubated with IRDye 800CW Donkey anti Rabbit IgG (LI-COR, UK) diluted 1:10000 in blocking buffer for 1 hour at room temperature. After a further 3 washes with TBS containing 0.1% Tween-20, the membrane was detected and imaged using the LI-COR Odyssey CLx imaging system (UK).

2.7 Tissue culture

2.7.1 Human umbilical vein endothelial cells (HUVECs)

Human umbilical vein endothelial cells (HUVECs; n=3 individual lines/biological replicates, passage 3 to 5; Lonza, UK) were maintained in collagen-1-coated cell culture flasks (Corning, UK). HUVECs were seeded in collagen-coated 6-well plates

(Biocoat Collagen I Cell ware, Corning, UK) in triplicate at 3-5 x 10^5 cells per well in EC basal medium-2 (CC-3156, Lonza) supplemented with 10% fetal bovine serum (Hyclone SH30071.03) and Endothelial Growth Medium (EGM-2) SingleQuots BulletKit (CC-4176, Lonza, UK). The transfection mix was dispensed at 500 µL/well and cells were incubated for 6 hours before being transferred back to Endothelial Basal Medium-2 (EBM-2) media for 48 hours before RNA extraction.

Transfection mix was made in Opti- Minimal Essential Medium (MEM) Reduced Serum Media (Thermofisher, UK) at a 1:1 ratio of transfection reagent mix to OPTI-MEM. Transfection reagent mix consisted of Lipofectamine RNAiMAX transfection reagent (ThermoFisher Scientific, UK) in OPTI-MEM (3µL RNAiMAX per 500 µL OPTI-MEM). The transfection mix was incubated for 20 minutes at RT. Transfection mix consisted of 10 nM of control (Silencer Select Negative Control No.1 siRNA 4390843, ThermoFisher Scientific, UK) or 10 nM PLVAP siRNA oligonucleotides (Silencer Select PLVAP s37973, ThermoFisher Scientific, Sense GGUCAUCUACACGAACAAUTT and Antisense AUUGUUCGUGUAGAUGACCCG) were used.

2.7.1.1 HUVEC proliferation assay

HUVECs were seeded onto collagen-coated coverslips in 48-well plates (Collagen, Type I solution from rat tail, SIGMA C3867-1VL) and cultured as described in section 2.7.1. Cells were starved of FBS for 24 hours after transfection followed by treatment with 10 µM EdU, reconstituted in Dimethyl sulfoxide (DMSO) (ThermoFisher Scientific, UK) and 15% fetal bovine serum (HyClone, USA) for 24 hours. Coverslips were collected and subsequently fixed in 4% PFA in PBS for 15 min at RT, permeabilised using 0.5% Triton X-100 in PBS for 20 min at room temperature and incubated in Click-iT™ reaction cocktail (prepared *per* manufacturer's instructions, Invitrogen™, UK) for 30 min at RT, protected from light. The coverslips were then washed in 3% BSA (KPL 10% BSA Diluent/Blocking Solution Kit, Seracare, USA) in PBS and mounted on slides with Fluoromount-G™ with DAPI (ThermoFisher Scientific, UK).

2.7.2 Myocardial slices

This protocol is an adapted version from Watson *et al*., 2017.[377] Mice were killed by cervical dislocation. Following dissection, the heart was collected in pre-warmed (37ºC) heparinized slicing solution (100 IU of heparin sodium (1,000 IU/mL) into 50 mL Tyrode's solution, prepared as per Table 2.7). The heart was placed in a petri dish with Tyrode's solution. Lungs and other surrounding tissues were removed. The atria were removed along with the right ventricle by making an incision along the right ventricular-septal junction toward the apex. The septum was located, and an incision was made towards the apex to allow the left ventricle to open. The left ventricle was flattened by making small incisions in the papillary muscles of the surface of the left ventricle. The tissue block was encased in 4% agarose (Sigma Aldrich) in the compresstome specimen holder (Precisionary, USA) and placed in the compresstome and the bath filled with cold Tyrode's solution. Slice thickness was set at 200 µm and slicing speed was 1.4 mm/s at a frequency of 20 Hz. Slices were collected and washed with PBS + 3% penicillin–streptomycin at room temperature. Myocardial slices were cultured on an air–liquid interface using Transwell membrane cell culture inserts and 1 mL of medium (Medium-199 + 3% penicillin–streptomycin + 0.001% ITS liquid media supplement). The slices were incubated in humidified air at 37 °C with 5% CO_2 or at 37 °C with 1% O_2 and cultured for 24 hours. Slices were then fixed using a 4 %PFA solution for 15 minutes at RT and stored in PBS for further processing.

Table 2.7 Tyrode's solution

Abbreviations; BDM (2,3-Butanedione monoxime), HEPES (4-(2-hydroxyethyl)-1-piperazineethanesulfonic acid)

Reagents for a 500mL solution	To Add
BDM	1.5 g
Glucose	0.93 g
HEPES	1.19 g
KCl	0.225 g
NaCl	4.09 g
1M $MgCl_2$	500 µL
1M $CaCl_2$	900 µL

2.8 Single cell RNA sequencing and analysis

Pdgfb lineage cardiac ECs were isolated for single cell RNA sequencing as per section 2.4.2. Samples were then processed according to the 10X Chromium™ Single Cell 3' Reagent Kit v2 user guide. Cells were partitioned into Gel Bead-In-Emulsions (GEMs) and incubated with primers containing an Illumina R1 primer sequence, a 16 bp 10X barcode, a 10 bp Unique Molecular Identifier (UMI) and a poly-dT primer sequence to generate full-length barcoded cDNAs from poly-adenylated mRNAs. cDNAs were amplified by PCR followed by enzymatic fragmentation and size selection for optimised amplicons, prior to library construction. P5, P7, i7 sample index and R2 primer sequence were added during library construction *via* end-repair, A-tailing, adaptor ligation and PCR. Quality control and quantification were performed using a DNA high sensitivity kit (PerkinElmer) on a LabChip GX Touch 24 Nuclei Acid Analyzer (PerkinElmer). Sequencing was performed by Edinburgh Genomics using an Illumina HiSeq 4000 (75bp paired-end sequencing). This resulted in an average read depth of 71,000 reads/cell for the healthy group (N=4) and 83,000 reads/cell for the MI group (N=4).

Raw reads were aligned to the mouse reference genome mm10 (Ensembl 84) using the 10X Genomics Cell Ranger Single Cell 2.1.0 pipeline and the output gene expression matrices were further analysed using the Seurat (v2.3) R package. Low quality cells (<400 genes/ cell and >20 % mitochondrial transcript presence/ cell) were excluded from downstream analyses. The average percentage of cells with high mitochondrial transcript levels were 8.7% (range 3 % - 13 %) for healthy mice and 0.6% (range 0.1 % - 2.3 %) for mice post-MI. Gene expression data was log normalised to a scale factor of 10,000 and then regressed on the number of molecules detected per cell (nUMI). The mean nUMI was 2232 (range 2035 - 2398) for cells from healthy mouse hearts and 5041 (range 4165 – 5604) from mouse hearts post-MI. Cell number post filtering was 2637, 3423, 3535, 3176 cells in the healthy mouse heart sample (N=4) and 4069, 4744, 3679, 3326 cells in the samples of post-MI mouse hearts. Highly variable genes were identified and used for principal component analysis (PCA). Significant principal components (PCs) were determined using the JackStraw analysis and 32 PCs were used for graph-based clustering at a resolution of 0.6 to identify distinct clusters of cells. Cluster resolution was chosen according to Seurat instructions which dictated satisfactory clustering with a clustering parameter of 0.4 to 1.2.[335]The same PCs were used to project the clusters onto t-distributed stochastic neighbour embedding (tSNE) plots for visualisation. Highly differentially-expressed genes in each cluster compared to the remaining population were used for GO term searching using PANTHER (http://pantherdb.org), Gorilla (http://cbl-gorilla.cs.technion.ac.il) and GENEMANIA (https://genemania.org) to annotate the functional identity of each cluster. Dot plots and violin plots showing gene expression were generated using R packages Seurat and Plotly (Dr Cass Li).

2.9 Trajectory analysis

Pseudotime trajectory analysis of *Pdgfb* lineage ECs belonging to clusters 6, 7, 8 was conducted using Monocle[378,379] (Dr Richard Taylor) to order cells along a calculated trajectory. Trajectories were visualised in pseudotime with values scaled from 0 to 1.

The value assigned to each cell was visualised by mapping on Monocle trajectory plots. These plots were generated using the function plot_cell_trajectory.

2.10 Enzyme linked immunosorbent assay (ELISA) for PLVAP

Plasma was obtained from venous blood taken into EDTA from patients with or without Type I myocardial infarction (MI) (n=15 *per* group). All subjects had normal haemoglobin and renal function and provided written informed consent. Ethical approval was obtained from the Lothian Research Ethics Committee (Edinburgh; UK), and this study was conducted in accordance with the declaration of Helsinki and institutional guidelines. Enzyme Linked Immunosorbent Assay (ELISA) was performed using a human PLVAP ELISA kit (Assay Genie, Ireland) as *per* manufacturer's instructions (Range 0.156-10ng/mL, Sensitivity< 0.094ng/mL). Concentration of standard human PLVAP stock solution was 10ng/mL. Standard concentrations that were used were 5ng/mL, 2.5 ng/mL, 1.25 ng/mL, 0.625 ng/mL, 0.313 ng/mL, 0.156 ng/mL and 0.078 ng/mL. Volume of sample/standard used per well was 100 µL and all measurements were taken in duplicate. Samples were used non-diluted. Optical density (OD) absorbance values were measured at 450 nm in a microplate reader (Tecan Sunrise) and PLVAP concentrations were calculated using a second order polynomial (quadratic) equation.

2.11 Human cardiac tissue information

Formalin-fixed, paraffin-embedded sections of human cardiac tissue from patients with acute MI or ischaemic heart disease, and from healthy subjects, were obtained from the Edinburgh Tissue and Brain Bank as in Table 2.8.

Table 2.8 Human cardiac patient and controls information

	BBN	Age	Sex	Cause of death
Control	BBN_3771	25	M	Suspension by ligature
	001.29731	53	M	Suspension by ligature
	001.34150	63	M	Ruptured atherosclerotic abdominal aortic aneurysm
	BBN_4175	52	M	1a Chest injuries, 1b Road traffic collision (cyclist)
	001.34215	50	M	Pulmonary thromboembolism
Diseased	001.26797	49	M	1a Ischaemic heart disease, 1b coronary artery atherosclerosis
	BBN_24479	46	F	1a complications of ischaemic heart disease and hepatic steatosis, 2 obesity
	001.26308	69	M	1a Ischaemic and hypertensive heart disease
	BBN_22629	59	F	1a coronary artery atherosclerosis and hypertensive heart disease
	001.26313	44	M	1a Ischaemic heart disease, 1b coronary artery atherosclerosis

	BBN_9508	76	M	1a myocardial infarction,1b coronary artery atherosclerosis, 2 Hypertensive heart disease
	BBN_14397	45	F	1a coronary artery atherosclerosis
	001.26124	40	F	1a haemopericardium, 1b rupture acute myocardial infarction, 1c coronary artery thrombosis, 1d coronary artery atherosclerosis
	001.30178	72	M	1a haemopericardium, 1b rupture acute myocardial infarction, 1c coronary artery thrombosis, 1d coronary artery atherosclerosis
	001.30916	71	M	1a haemopericardium, 1b rupture acute myocardial infarction, 1c coronary artery thrombosis, 1d coronary artery atherosclerosis
	001.29525	52	M	1a haemopericardium, 1b rupture acute myocardial infarction, 1c coronary artery thrombosis, 1d coronary artery atherosclerosis

2.12 Confocal microscopy

Images were obtained using an LSM780 confocal microscope (Zeiss, Germany) using a 20x air objective. Tiled (2 x 1) Z-stacks (5-60 µm thickness with a slice interval of 3 µm) and an optical resolution of 1024 x 1024 pixels were collected, and images were stitched using Zen (Zeiss, Germany) software. Fluorophores were detected using the following excitation wavelengths (nm): DAPI 405 laser, 454/515), YFP 514 laser, 517/562), RFP (561 lasers, 563-649), membranous CFP (458 laser, 454-515), nuclear GFP (488 laser, 490-535) and AlexaFluor 647 (633 nm, 650-700 nm).

Myocardial slice imaging was done using the Leica Confocal SP8 (5 Detectors) using a 25x water lens was used to capture an image of the total myocardial section and 3 region of interest stacks, with laser lines and detectors as follows: DAPI (405 nm, 417-508 nm), CFP (458 nm, 454-502 nm), GFP (488 nm, 498-506 nm), YFP (514 nm, 525-560 nm), RFP (561 nm, 565-650 nm) and AlexaFluor 647 (633 nm, 650-700 nm).

2.13 Image analysis

Images were processed and analysed using Fiji v2.0 (ImageJ, USA) and Imaris v9.0 (Bitplane, USA).

2.13.1 Image analysis of clonal data

To determine whether *Pdgfb*-lineage cardiac EC responded to ischaemic injury by undergoing clonal expansion, Brainbow2.1 lineage tracing was used to stochastically mark ECs with one of 4 hereditary fluorescent labels. Clones were quantified in 3D using IMARIS from thick (100-200 µm) wholemount sections of the healthy and injured left mouse ventricle. Two or more neighbouring cells labelled by the same Brainbow2.1 fluorophore were considered to be part of the same clone as the Brainbow2.1 expression is inherited and would thus be expressed by a daughter cell. However, The possibility of merger events where two independent, neighbouring ECs are labelled by the same Brainbow2.1 fluorophore was likely. Hence, quantitative clonal analysis was undertaken in control and MI samples independently to consider

such events (Benjamin Simons, Cambridge, UK).[380]As far as control samples as concerned, Brainbow2.1 recombination frequency ranged from 39.3 % - 57.1 % with an average of 46.6%. The degree of mosaicism was assessed based on the proportion of EC number: YFP: 45 % (n = 19 clones); RFP: 24% (n = 15); nGFP: 15% (n = 9); and mCFP: 16% (n = 9) (raw data presented in section 3.4.1). A stochastic stimulation was used to estimate the baseline (control) level of merger events. Labelled and unlabelled ECs were randomly assigned to the sites of a cubic lattice in proportion to the observed levels of mosaicism. Subsequently, the score of size distribution of cell clusters was defined as groups of neighbouring cells that were labelled by the same Brainbow2.1 fluorophore. Cluster distribution analysis from a randomly seeded 100 x 100 x 100 lattice, focusing on clusters of 2 or more cells, an average cluster size of YFP: 4.8 cells; RFP: 2.9 cells; nGFP: 2.4 cells; and mCFP: 2.5 cells was found. This result was in agreement with the average cluster sizes of YFP: 4.9 cells; RFP: 3.3 cells; nGFP: 3.4 cells; and mCFP: 3.8 cells obtained from the stochastic simulation (model prediction without fitting parameters). Analysis of the cumulative cluster size distribution showed the hallmark tail of large cluster sizes that characterise the percolation problem (Figure 2.4).

Subsequently, the clonal results from the injured heart were analysed. Here, the degree of mosaicism based on the proportion of cell numbers was found to be: YFP: 42 % (n = 61 clones); RFP: 26 % (n = 40); nGFP: 21 % (n = 43); and mCFP: 11 % (n = 25) (raw data presented in section 3.4.1).However, the average size of labelled cell clusters, was larger than the control, with YFP: 12.6 cells; RFP: 12.1 cells; nGFP: 9 cells; and mCFP: 7.9 cells, suggesting that clonal expansion is taking place. To assess this interpretation the stochastic simulation was modified as follows. The cubic lattice was seeded with ECs labelled in proportion to the degree of mosaicism observed in the injured tissue. Cell division was mimicked by allowing rounds of neighbouring cell loss and replacement at randomly selected sites, thus maintaining the overall size of tissue. Cells of these sites were replaced by a neighbouring cell labelled with the same Brainbow2.1 fluorophore, evidence of symmetric cell division. The model was resumed until individual cells would have gone through D rounds of

loss/replacement, where D was defined as an adjustable parameter. Statistical analysis showed a best fit to the average cluster sizes for the Brainbow2.1 fluorophores with D=5.4, and averages YFP: 12.8 cells; RFP: 8.9 cells; nGFP: 8.4 cells; and CFP: 7.5 cells. Assessment of the cumulative cluster size distribution also displayed favourable agreement with the stochastic model (Figure 2.5). From these results, a conclusion can be drawn that following myocardial injury, cardiac ECs undergo cell division.

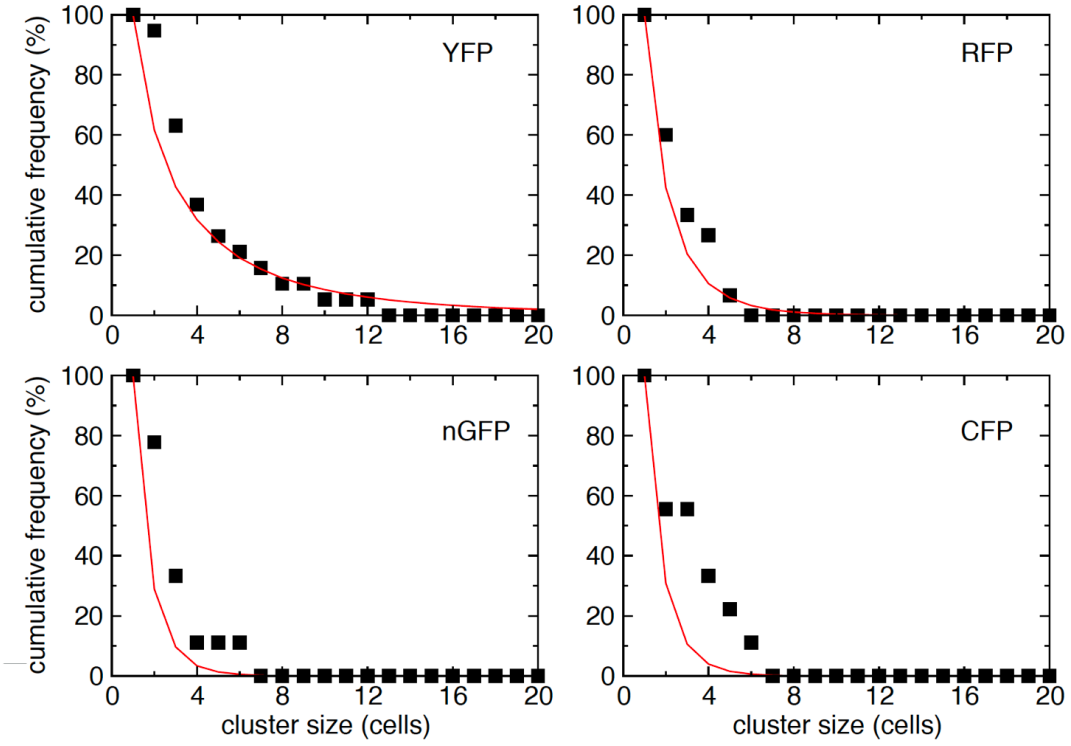

Figure 2.4 Cumulative cluster size distributions of endothelial cells for Brainbow2.1 fluorophore obtained from control hearts

Graphic representation of clusters of 2 or more cells labelled with the same Brainbow2.1 fluorophore. The points data and the red lines show results from stochastic simulation based on the observed levels of mosaicism (adapted from Li *et al.*[205]).

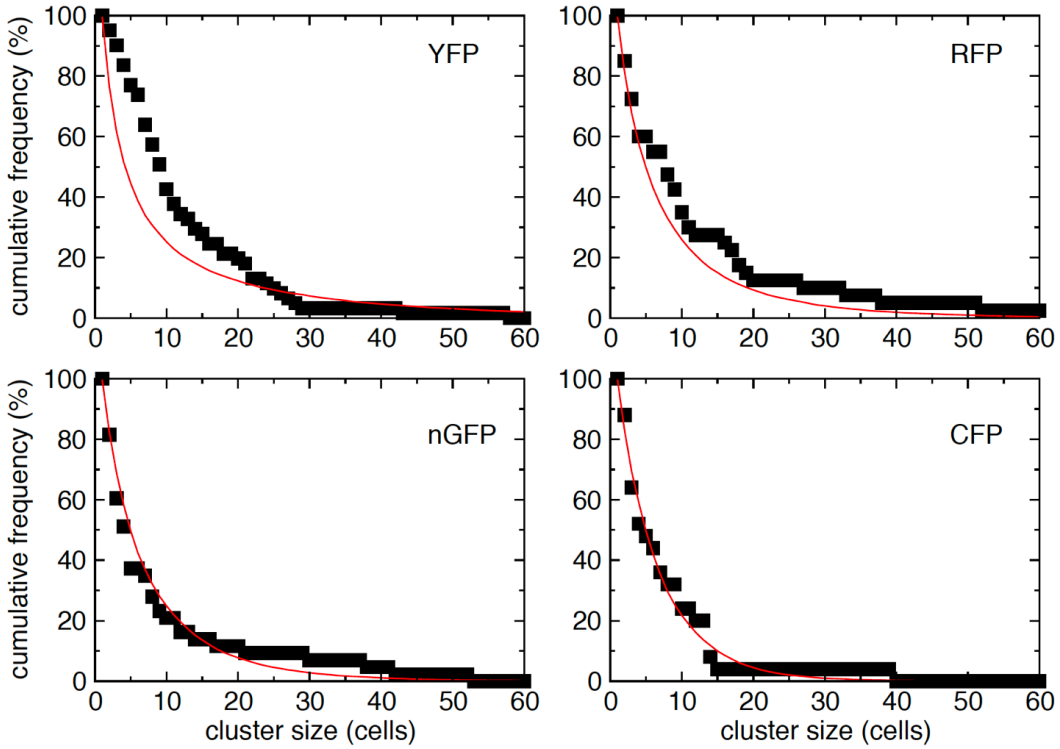

Figure 2.5 Cumulative cluster size distributions of endothelial cells for different Brainbow2.1 fluorophores obtained from injured hearts

Graphic representation of clusters of 2 or more cells labelled with the same Brainbow2.1 fluorophore. The points data and the red lines show results from stochastic simulation based on the observed levels of mosaicism (adapted from Li *et al.*[205]).

2.13.2 Image analysis of myocardial slices

IMARIS (Bitplane, USA), a tool for 3D visualisation and rendering for microscopy, was utilised to generate 3D rendering of nuclei and blood vessels in the myocardial slice culture images. Nuclei were rendered from DAPI immunofluorescent signal (Figure 2.6). The expected diameter for the nuclei was set to 6 µm. Total nuclei number for each ROI was recorded. Blood vessels were rendered based on CD31 immunofluorescence signal. The area and volume of blood vessels for each region of interest (ROI) was recorded. The average total nuclei number, area and volume were determined across the 3 ROI per mouse (n=3 mice/ group).

The IMARIS “spots close to surface” function was used to quantify ECs (Figure 2.6). As the expected nucleus diameter was 6 µm, the expected radius was therefore 3 µm. The distance from the centre of a nucleus to the surface to the nearest blood vessel was set at 0-1µm. This subset of nuclei were a proxy for ECs.

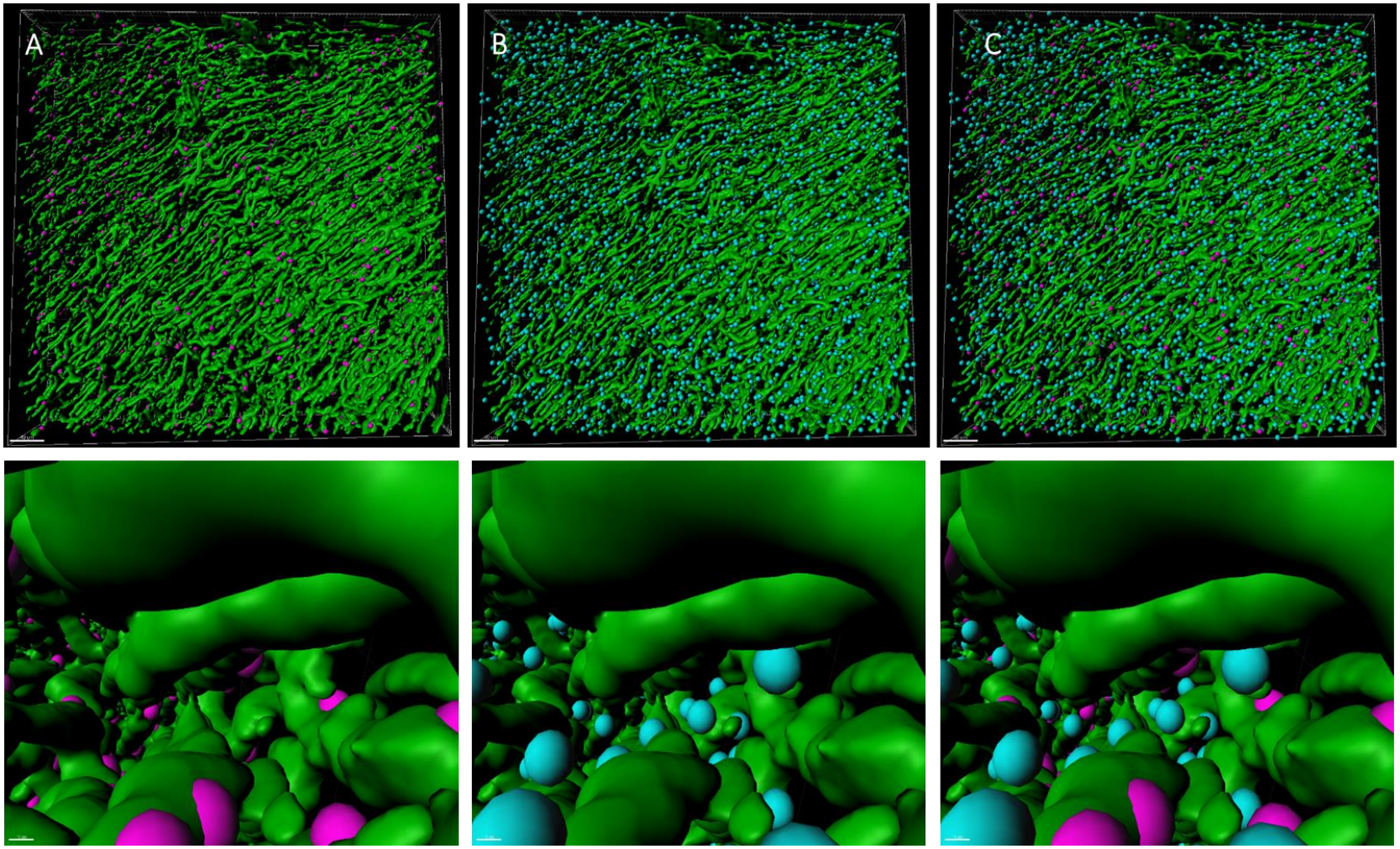

Figure 2.6 Thresholding the distance from nuclei to the vessel surface

(A) Distance from centre of nuclei to vessel surface set at 0-1µm (pink) as a proxy for EC nuclei. (B) Distance from centre of nuclei to vessel surface >1µm (blue). (C) Composite image of nuclei included in (pink) and outside (blue) the threshold set for the distance from the centre of nuclei to the vessel surface. Scale bar for total view = 40 µm. Scale bar for zoomed region = 10 µm. Images are representative of a mouse injected with PBS, where myocardial slices were cultured in normoxia and not treated with VEGF-C.

2.14 Statistical analysis

Statistical analyses were conducted using GraphPad Prism 9. Results are expressed as mean ± SEM. Normality was assessed using D'Agostino-Pearson test, following which data were analysed using a parametric unpaired t-test or non-parametric Mann Whitney test, as appropriate. Comparison of multiple groups was achieved using one-way analysis of variance (ANOVA). $P < 0.05$ was considered statistically significant.

Chapter 3 Clonal Expansion of Endothelial Cells in the Adult Mouse Heart

3.1 Chapter acknowledgements

I would like to thank Professor Ben Simons for performing the quantitative clonal analysis. Moreover, I would like to thank Dr Cass Li for part of the bioinformatic analyses as well as teaching me the principles of bioinformatics using R. Also, I would like to thank Dr Ross Dobie, Dr Beth Henderson and Professor Neil Henderson for their help in designing and performing the single cell experiment that is presented in this chapter. Moreover, I would like to thank the flow cytometry core facility in their help in designing and performing the flow cytometry and FACS experiments in this chapter. Finally, I would like to thank Dr Marco Meloni and Dr Ana-Mishel Spiroski for performing the LAD coronary ligation surgeries.

3.2 Introduction

Following myocardial infarction (MI), the border region of the ischaemic area of the adult heart has been shown to be an active site of blood vessel regeneration.[38,39,381,382] Importantly, the endogenous neovascularisation response is critical post-MI for stimulating regeneration of the myocardium.[154] Consequently, a substantial amount of work has been dedicated to investigating regenerative therapies, with the aim of inducing vascular regeneration following MI (reviewed in Cambria *et al.*[162]). However, most results have been mixed with many of the studies having inconclusive results, resulting in a lack of consensus in the efficacy and mechanism of action of neovascularisation therapies post-MI (described in more detail in *1.8 Neovascularisation as a therapeutic strategy*).

The origin of ECs that participate in the neovascularisation response after MI has been a topic of debate. Suggested origins have been explored in-depth earlier in this thesis (section *1.7.1 Heterogeneity in endothelial cell contribution in post-MI neovascularisation)*. In brief, hypotheses extend from expansion of pre-existing ECs to lineage conversion of non-ECs.[123] The predominant view is that pre-existing cardiac ECs form new vessels after cardiac ischaemia.[133] Moreover, our knowledge of the turnover dynamics of the cardiac EC population has increased over the last 15 years and recent reports show that the EC population of the heart is the population with the highest turnover in the human heart in homeostasis (16.7% per year in adulthood).[161] This high turnover rate signifies the dynamic nature of the cardiac endothelium, even in homeostasis, and shows that is capable of proliferation that can be potentially augmented in post-MI. However, the cellular and molecular mechanisms underlying cardiac EC turnover are currently unknown. Additionally, the proliferative dynamics and transcriptomic profile of cardiac ECs following MI have not been investigated. [133]

In 1997 the seminal discovery of an EPC population in the adult circulation was made by Asahara *et al.*[171] (described in more detail in section *1.9.1 Cell-based therapies*). However, EPCs have remained poorly defined and plagued by unresolved questions

such as their definitive origin and identity. Despite this, evidence from *in vitro* studies indicates that highly clonogenic EPC may reside in a niche in the intimal layer of the adult human vessel wall. [176] However, whether *in situ* endothelium is composed of clonal units generated following expansion of a single ancestral EPC, whose origin remains unknown, or whether it is a polyclonal tissue maintained by turnover of adjacent mature ECs, is unresolved. This is important as it would guide future therapeutic directions.

I hypothesise that a transcriptionally unique EPC population resides within a niche in the cardiac vessel wall and undergoes clonal expansion as a mechanism to maintain endothelial integrity in homeostasis and after injury.

Transcriptomic heterogeneity between cells of the same population has been documented in cells such as embryonic and immune cells and applying this to the EC population post-MI has the potential of unravelling key heterogenic differences. [383,384] Furthermore, the endothelium has been shown to be an extremely heterogenous cell population.[73,89] New technologies such as single cell RNA sequencing can help expand knowledge of EC cell diversity and transcriptome profile. It allows for the understanding of complex biological systems such as the heart *via* unbiased identification of novel cell phenotypes as well as cellular plasticity in dynamic processes.

The aim of this chapter was to investigate the spatiotemporal dynamics and transcriptomic profile of ECs in the heart both in physiological conditions and following MI. In this study, the *iCreER^{T2}/lox*-driven lineage-tracing *Brainbow2.1* technology[315] was used to drive expression of the EC-specific *Pdgfb* promoter (described in more depth in *1.10.2 Chasing endothelial cells - The Pdgfb lineage inducible mouse model* and *2.1.2 Mouse models for endothelial cell lineage tracing*) to map EC fate and investigate clonal proliferation by endogenous ECs in the healthy adult mouse heart as well as in response to ischaemia, in a tamoxifen-inducible manner (*Pdgfb-iCreET^{t2}-R26R-Brainbow2.1*) (Figure 3.1, A-B).

This study also aimed to investigate the origin of ECs that participate in neovascularisation post-MI. In the case of ECs, a variety of expression drivers for lineage-tracing experiments have been used. As described in more detail in section *1.10.2 Chasing endothelial cells – The Pdgfb lineage tracing system*, lineage tracing studies have predominantly used Tie-2 or Cdh5 driven expression. This is problematic, as these markers are not only expressed by ECs but also by cells of haematopoietic origin.[335,336]

In summary, ECs are the main drivers of neovascularisation in the heart following MI.[30,121] However, the cellular and molecular mechanisms that govern EC turnover in homeostasis are unknown. Moreover, the cellular and molecular mechanisms of the neovascularisation responses following MI are still largely unknown. Identifying the molecular mechanisms and cell signatures of the ECs that participate in neovascularisation post-MI is critical for increasing our understanding on how we can potentially manipulate these mechanisms for therapeutic angiogenesis post-MI.

3.3 Experimental plan, hypothesis and aims

The following hypotheses were formed:

1. *Clonal proliferation is a key cellular mechanism through which resident ECs contribute to neovasculogenesis in the peri-infarct border region of the post-ischaemic adult mouse heart.*
2. *Resident cardiac EC and not bone marrow cells are the primary contributors to new blood vessel formation in the infarct border after MI.*
3. *Proliferative cardiac ECs in the post-ischaemic adult mouse heart express markers that can be identified using single cell RNA-sequencing and bioinformatics analyses.*

The 1st hypothesis will be addressed by the following aim:

- Assessment of clonal proliferation and neovascularisation by cardiac ECs in the adult mouse heart during homeostasis and following induction of MI in *Pdgfb-iCreER^{T2}-Brainbow2.1* mice (Figure 3.1, C-D).

The 2nd hypothesis will be addressed by the following aim:

- Investigation of contribution of bone marrow cells in cardiac neovascularisation post-MI in *Pdgfb-iCreER^{T2}-Brainbow2.1* mice (Figure 3.1,D)

The 3rd hypothesis will be addressed by the following aim

- Cardiac CD31+, but not lymphatic (Podoplanin-), ECs that expressed Brainbow2.1 fluorophores (Brainbow2.1+) will be isolated from healthy and post-ischaemic adult *Pdgfb-iCreER^{T2}-Brainbow2.1* mice for single cell RNA-sequencing and bioinformatics to identify key markers specific to pro-angiogenic cardiac ECs. (Figure 3.1, D)

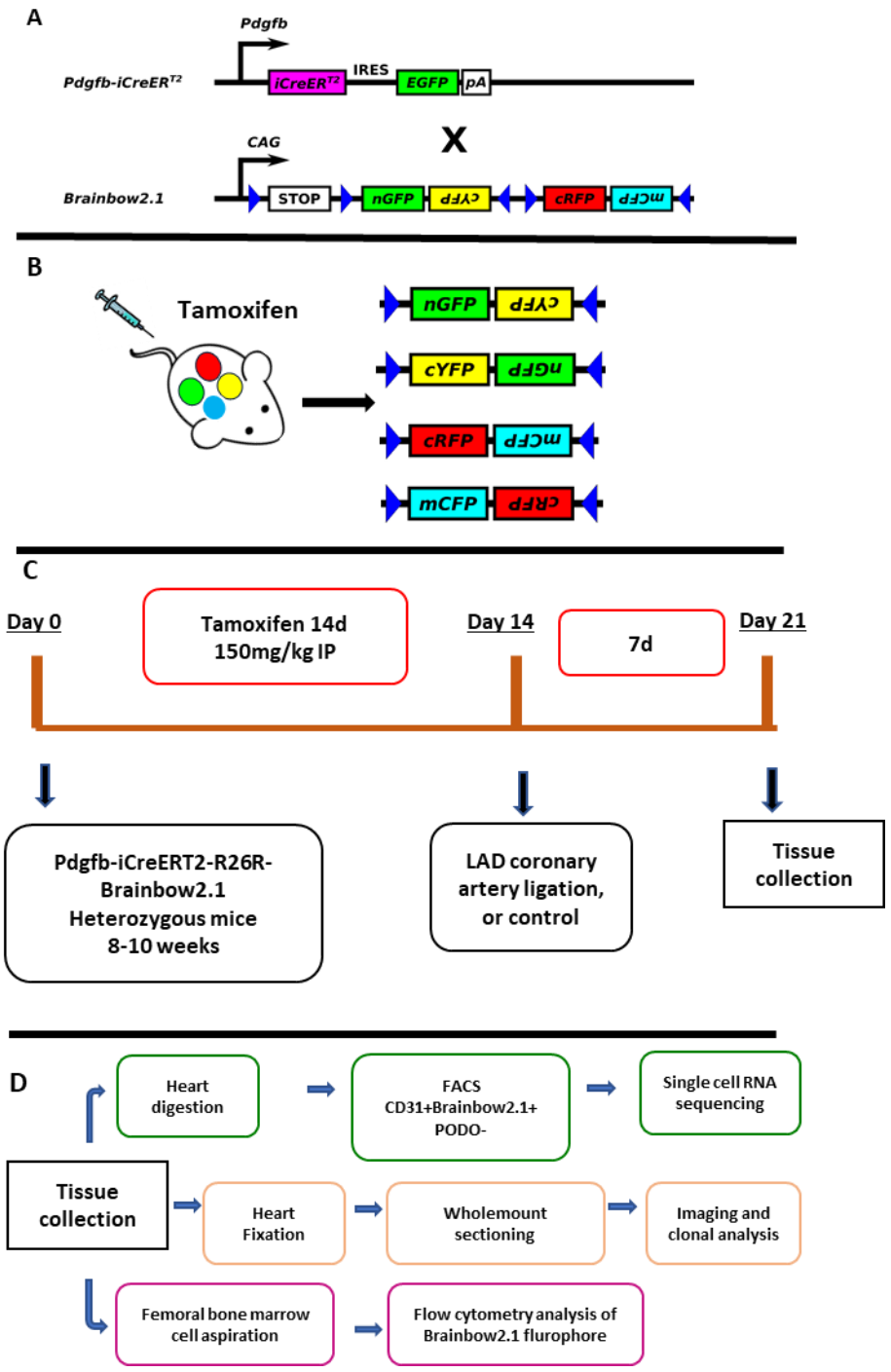

Figure 3.1 Experimental plan

(A) The Cre-inducible *Pdgfb* mouse model developed by Claxton *et al.*[337] to efficiently and specifically label endothelial cells. In the presence of hydroxytamoxifen OHT the iCreER^{T2} translocates to the nucleus to mediate recombination. The construct contains an internal ribosomal entry site (IRES) element downstream of iCreER^{T2} as well as a sequence coding for

enhanced green fluorescent protein (EGFP). The Brainbow2.1 cassette consists of adjacent loxP (blue arrow) flanked head-to-tail tandem dimers: the first contains nuclear tagged Green Fluorescent Protein (nGFP) in forward orientation and Yellow Fluorescent Protein (YFP) in reverse orientation. The second contains Red Fluorescent Protein (RFP) in forward orientation and membrane bound Cyan Fluorescent Protein (mCFP) in reverse orientation. When crossed with mice that express a cell promoter driven by tamoxifen-inducible Cre recombinase, selected lineages are stochastically labelled with an inheritable green, yellow, red, or cyan fluorescent protein tag. (B) The possible four recombination outcomes of Brainbow2.1 that result in expression of either GFP, YFP, RFP or mCFP. (C) Experimental timeline of the study. (D) Plan of tissue analysis following tissue collection.

3.4 Results

3.4.1 The adult mouse heart endothelium undergoes clonal expansion under physiological conditions and the process is significantly upregulated post-MI.

Initially, the recombination efficiency of the *Pdgfb-iCreER^{T2}-R26R-Brainbow2.1* mouse model with tamoxifen (single IP injection, 150mg/kg) was investigated. Due to this project's interest in clonal proliferation of cardiac *Pdgfb* lineage ECs, a high recombination efficiency would not be optimal as it would result in an inability to track formed clones due to Brainbow2.1 reporter overexpression. The proportion of Brainbow 2.1 reporter fluorophore expressing cells that co-localised with *Pdgfb*-endogenous green fluorescent protein (EGFP) was quantified *via* confocal microscopy. It was calculated that Cre recombination efficiency was 46.6 (± 9.3) % of total cardiac *Pdgfb*-EGFP+ cells (Figure 3.2, A, B). Finally, as seen in Figure 3.2 (C, D), no reporter expression was observed in mice administered peanut oil as a vehicle control for tamoxifen or in Cre-negative mice that were administered tamoxifen, showing that *Pdgfb-iCreER^{T2}* is not susceptible to activation in the absence of tamoxifen and that the *R26R-Brainbow2.1* cassette is not susceptible to spontaneous recombination in the absence of Cre activity (issues described in Ref [385]).

Subsequently, the *Pdgfb-iCreER^{T2}-R26R-Brainbow2.1* mouse model was utilised to investigate the role of the adult endothelium in the neovascularisation process following MI. The expression of the Brainbow2.1 transgene was induced by tamoxifen injection and, following a wash-out period of 14 days, the left anterior descending coronary artery was permanently ligated (according to section *2.1.7 Left anterior descending coronary artery ligation surgery*. Tissues were collected 7 days post-surgery for analysis. Ischaemic damage of the heart leading to an infarct was validated using Masson's trichrome staining (Figure 3.3 A, B). RFP, CFP, YFP and GFP fluorophores were visible in ECs in the healthy and ischaemic heart vasculature (Figure 3.3 C, F). The *Pdgfb* lineage adult ECs in the heart underwent clonal proliferation under physiological conditions and the response was significantly upregulated in MI (Figure 3.3, E). The size of clones was quantified where a clone was

defined as 2 or more adjacent cells expressing an identical fluorophore. A significant increase in cell number per clone in regions of neovascularisation was observed in the peri-infarct region at 7 days post-MI, compared to the healthy heart (mean ± SEMs cells per clone = 4.0 ± 2.1 versus 10.3 ± 10.6, P <0.0001, Figure 3.3, G). Visualisation of the Brainbow2.1 fluorophores showed a bias in fluorophore distribution in both healthy and MI. YFP, RFP, nGFP and mCFP expression in healthy mouse heart *Pdgfb*-lineage EC was 51.9 ± 13.5, 25.7 ± 8.7, 11.3 ± 6.2 and 11.8 ± 5.8 % of total reporter expressing cells, respectively ($P < 0.001$) (Figure 3.3, K). YFP, RFP, nGFP and mCFP expression in infarcted mouse heart *Pdgfb*-lineage EC was 52.9 ± 26.5, 18.8 ± 15.0, 26.5 ± 29.8 and 8.8 ± 7.8 % of total reporter expressing cells, respectively ($P < 0.001$) (Figure 3.3, I). However, mean clonal size did not differ between each fluorophore in healthy samples (Cells/Clone; YFP: 7.91±1.5, RFP: 5.06±1.03, GFP: 3.44±0.5, CFP: 3.78±0.64, P=0.1, Figure 3.3, H) or MI samples (Cells/clone: YFP 12.6 ± 10.2, RFP 12.1 ± 13.4, nGFP 7.0 ± 10.4, mCFP 8.1 ± 8.1, $P = 0.07$, Figure 3.3, J).

The possibility of merger events, where two independent, neighbouring ECs are labelled by the same Brainbow2.1 fluorophore was assessed using quantitative clonal analysis in control and MI samples (described in section 2.13.1)

Finally, perfusion of newly formed clonal vessels was tested using Isolectin-B4 staining (according to section 2.1.5). Co-localisation of the isolectin-B4 signal and Brainbow2.1 fluorophores confirmed perfusion (Figure 3.3, L).

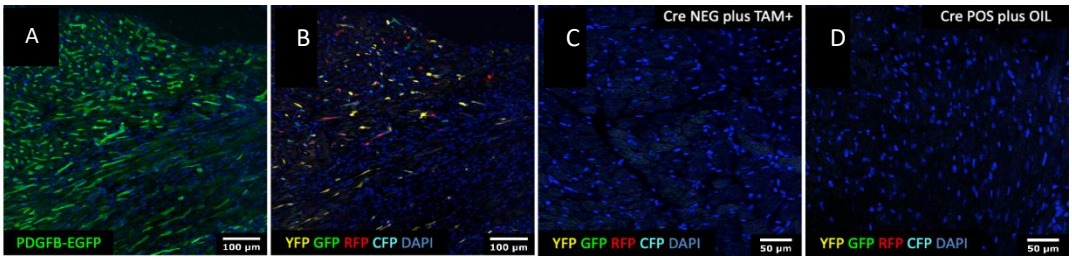

Figure 3.2 Validation of the *Pdgfb-iCreER^{T2}-R26R-Brainbow2.1* mouse model

(A) A single IP injection of 150 mg/kg tamoxifen induced CreER^{T2} and subsequent *Pdgfb*-endogenous green fluorescent protein (EGFP) expression. (B) Recombination efficiency of the Brainbow2.1 fluorophore expression was calculated by measuring cells expressing

Brainbow2.1 fluorophores as a percentage of cells expressing EGFP (calculated at 46.6 ± 9.3 % Brainbow2.1+ cells of total EGFP+ *Pdgfb*-lineage endothelial cells in the adult heart left ventricle (data from N = 3 mice in both healthy and MI groups). (C) No fluorophore expression was observed in Cre-negative mice administered tamoxifen (TAM) or (D) in Cre-positive mice administered peanut oil vehicle control (N = 6 per group).

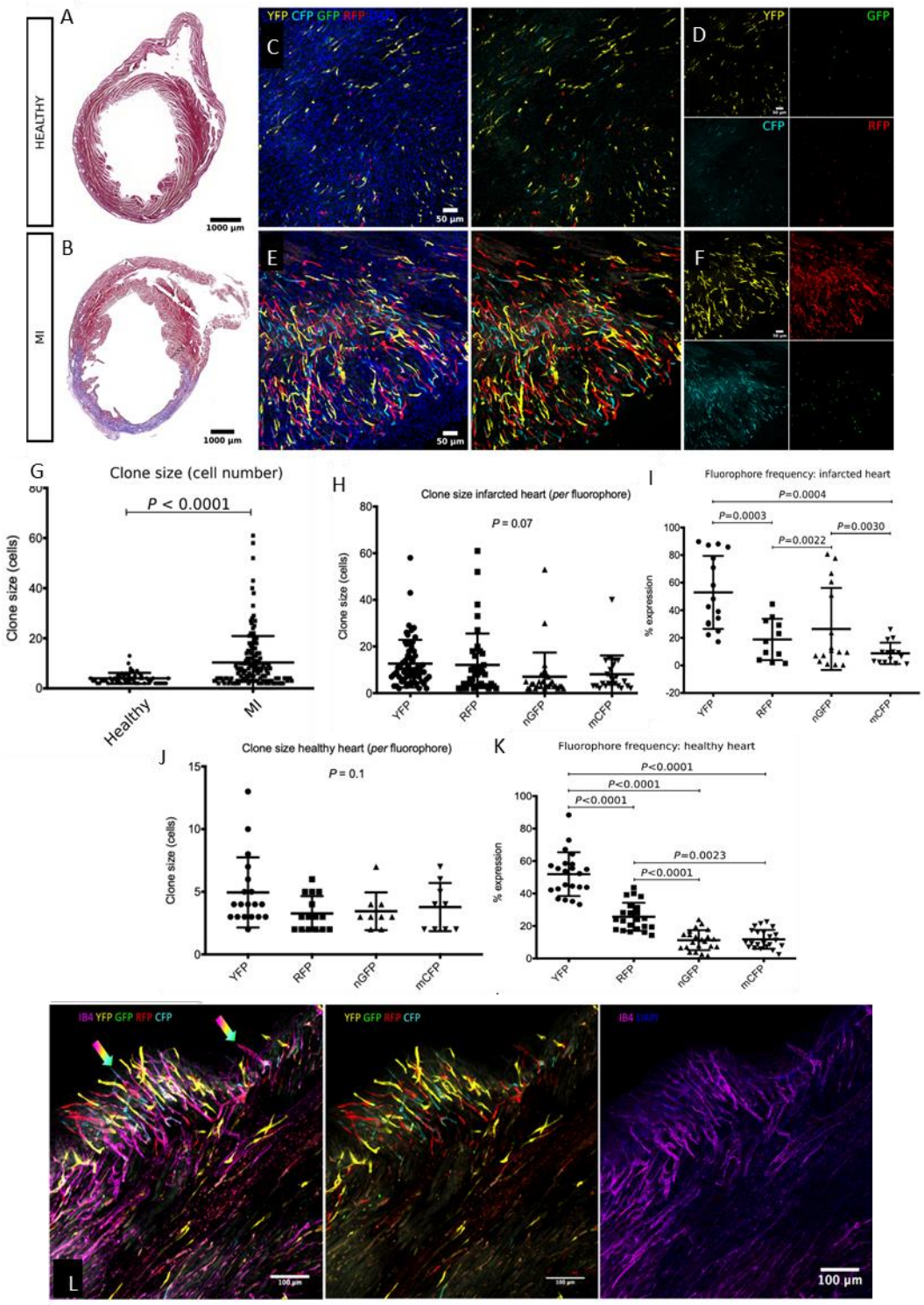

Figure 3.3 The heart undergoes endothelial clonal expansion under physiological conditions and the process is significantly upregulated 7 days post-MI

Ischaemic damage of the heart leading to an infarct was validated using Masson's trichrome staining in (A) healthy and (B) post-ischaemic adult mouse heart tissue. (C) Brainbow2.1 fluorophore expression in healthy adult mouse heart tissue and (D) individual fluorophores

YFP, nGFP, mCFP, RFP. (E) Brainbow2.1 fluorophore expression was increased in 7day post-ischaemic adult mouse heart tissue. (F) individual fluorophores YFP, nGFP, mCFP, RFP in ischaemic tissue. (G) A significant increase was seen in cell number per clone in regions of neovasculogenesis in the peri-infarct region at 7 days post-MI, compared to the healthy heart (mean ± SEMs cells per clone = 4.0 ± 2.1 versus 10.3 ± 10.6, P <0.0001, Mann-Whitney test). (I) & (K) A bias in fluorophore distribution in both healthy and MI groups was observed. YFP, RFP, nGFP and mCFP expression in healthy mouse heart Pdgfb-lineage EC was 51.9 ± 13.5, 25.7 ± 8.7, 11.3 ± 6.2 and 11.8 ± 5.8 % of total reporter expressing cells, respectively. YFP, RFP, nGFP and mCFP expression in infarcted mouse heart Pdgfb-lineage EC was 52.9 ± 26.5, 18.8 ± 15.0, 26.5 ± 29.8 and 8.8 ± 7.8 % of total reporter expressing cells, respectively (P < 0.001 for both, one-way ANOVA). (H) & (J) Clone size did not differ between each fluorophore in the healthy (mean cells *per* clone: YFP 4.9 ± 2.8, RFP 3.3 ± 1.4, nGFP 3.4 ± 1.5, mCFP 3.8 ± 1.9, P = 0.1, One-way ANOVA) or MI group (mean cells *per* clone: YFP 12.6 ± 10.2, RFP 12.1 ± 13.4, nGFP 7.0 ± 10.4, mCFP 8.1 ± 8.1, P = 0.07, one way ANOVA). (L) Qualitative analysis of co-localisation of the isolectin-B4 (IB4) signal and Brainbow2.1 fluorophores confirmed showed that Brainbow2.1+ vessel clones were perfused. N=7 for healthy. N=6 for MI.

3.4.2 Brainbow2.1 reporter fluorophore expression is minimal in bone marrow cells in *Pdgfb-iCreER^{T2}-R26R-Brainbow2.1* mice

The contribution of bone marrow derived ECs following MI was investigated. Flow cytometry was performed and minimal Brainbow2.1 reporter expression was observed in femoral bone marrow cells in both healthy and MI groups (0.04 ± 0.02 % versus 0.03 ± 0.009 %, P = 0.79).

Subsequently, the possibility of migration of Brainbow2.1+ ECs from other regions of the heart or different vascular beds was explored *via* analysis of founding number of recombined events, where a Brainbow2.1+ cell or clone was counted as 1 event. The founding number of recombined events did not differ between groups (72.3 ± 9.0 *versus* 67.3 ± 6.6 events *per* section, *P* = 0.46), thus supporting the fact that migration of *Pdgfb*-lineage Brainbow2.1 fluorophore expressing EC was unlikely (Figure 3.4).

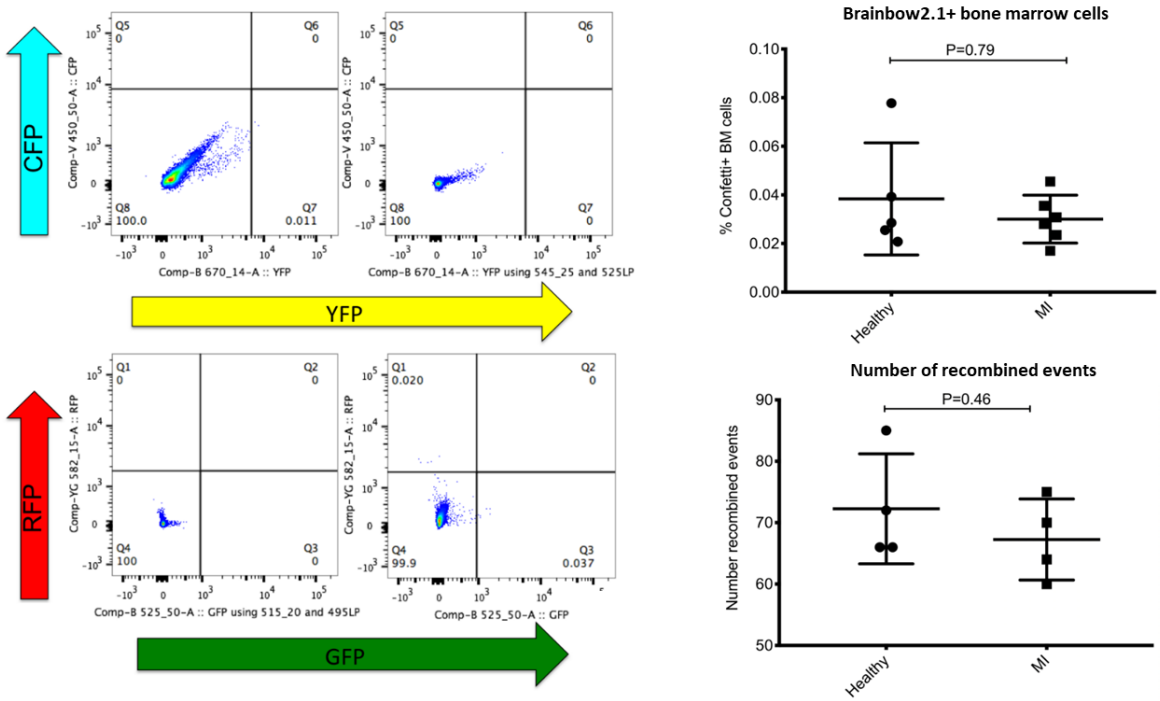

Figure 3.4. Contribution from bone marrow ECs in MI is minimal

Flow cytometry plots showing very low reporter fluorophore expression in femoral bone marrow cells from adult Pdgfb-iCreER^{T2}-R26R-Brainbow2.1 mice. Threshold gates were set for each fluorophore using C57Bl6 wild type mice bone marrow cells as a negative control.

No difference in fluorophore expression by bone marrow cells was observed between healthy and MI groups (0.04 ± 0.02 % *versus* 0.03 ± 0.009 %, *P* = 0.79, N=5 for healthy, N=6 for MI). The founding number of recombined events (a Confetti^{+} cell or clone was counted as 1 event) was unchanged between healthy and MI groups (72.3 ± 9.0 *versus* 67.3 ± 6.6 events *per* section, *P* = 0.46, N=4/group). Mann-Whitney test.

3.4.3 Single cell RNA sequencing of cardiac ECs reveals 10 heterogeneous transcriptional cell states

Following the observation that clonal proliferation of *Pdgfb* lineage cardiac ECs is a cellular mechanism for neovascularisation 7days post-MI, the transcriptome of these proliferative ECs was investigated using single cell RNA sequencing. Healthy and 7-day post ischaemic cardiac ECs were isolated using flow cytometry using a CD31+PODO-Brainbow2.1+ panel (Figure 3.5) and were subsequently processed for single cell RNA sequencing (according to section *2.8 Single cell RNA sequencing and analysis*). The likelihood of a spectral overlap between the EGFP expression (from the *Pdgfb-iCre^{T2}* cassete) and the nGFP (of the *Brainbow2.1* cassete) was addressed due to difference in brightness levels between the two fluorophores and is described in Li *et al.*[205]

Initially, bioinformatics analyses confirmed the endothelial nature of the cells as shown by widespread expression of EC markers such as *Cd31/Pecam1* and *Vegfr2/Kdr* (Figure 3.6, D). Furthermore, a lack of lymphatic (*Pdpn*) and haematopoietic (*Ptprc*) marker expression were observed in the dataset (Figure 3.6, D). Following clustering of ECs according to their similarities in transcriptomic profile, 10 unique clusters were identified (Figure 3.6, A).

The ratio of cardiac ECs from the healthy and MI groups was different according to the cluster they belonged to. Some of the clusters, such as cluster 1, appeared to have an equal distribution whereas others, such as cluster 6, 7 and 10, were composed mostly or solely from cells from the MI dataset. (cluster 1; healthy 13.10 ± 0.01 % vs MI 11.90 ± 0.25%, P=0.3429 – cluster 2; healthy 5.619 ± 0.9766% vs MI 19.38 ± 3.305%, P=0.0212 – cluster 3; healthy 3.921± 0.5949% vs MI 9.340± 0.3659%,

P=0.0006, Cluster 4 healthy 18.54 ± 3.091% vs MI 7.881 ± 2.168%, P=0.0729 - Cluster 5; healthy 11.39 ± 2.695% Vs MI 13.61± 0.3567%, P=0.5057- cluster 6; healthy 1.66 ± 0.33 % vs MI 23.34 ± 1.71 %, P=0.0057 - cluster 7; healthy 0 ± 0 % vs MI 25.00± 14.03%, cluster 8; healthy 2.68 ± 0.60% vs MI 22.36 ± 7.11%, P=0.069 - Cluster 9; Healthy 13.61 ± 3.293% Vs MI 11.39± 2.006%, P=0.6857- Cluster 10; Healthy 3.006 ± 0.1251% Vs MI 21.99± 3.945%, P=0.0170, Mann-Whitney test).

Gene Ontology (GO) enrichment analysis was conducted to show significant biological terms associated with the top differentially expressed genes in each cluster. The top differentially genes and associated GO terms per cluster are found in Table 3.1**.** For instance, cluster 10 was associated with cell cycle and proliferation markers (*Hmgb2, Stmn1, Top2a, Cenpf, Cks2, Birc5, Cenpa, Ube2c, Cdc20, Prc1*[386]), cluster 2 was associated with interferon signalling (*Ifit3, Cxcl10, Ifit1, Rsad2, Ifit3b, Isg15, Ifit2, Usp18, Cmpk2, Cxcl9*[387,388]), cluster 5 showed EC regulation via Notch signalling (*Fbln5, Gja4, Stmn2, Clu, Glul, Nebl, Hey1, Vegfc, Alpl, Mgp* [389]), cluster 7 showed high expression of stalk cell markers (*Lrg1, Plvap, Ackr1, Clu, Tmem176a, Ehd4, Tmem176b, Tmem176b, Tmem252, Selp, Tagln*[390,391]*).*

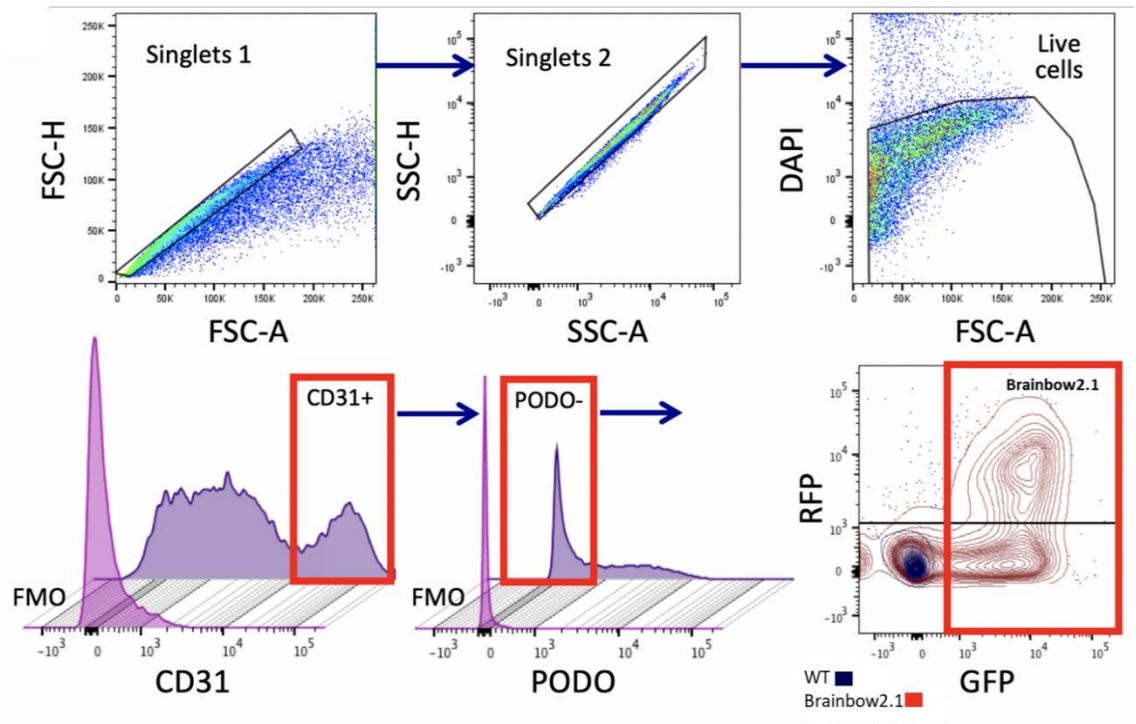

Figure 3.5 Selection of CD31+Brainbow2.1+Podoplanin- cardiac endothelial cells for single cell RNA sequencing

Gating strategy for Fluorescence-Activated Cell Sorting (FACS) isolation of CD31+Brainbow2.1+Podoplanin- endothelial cells from *Pdgfb-iCreER^{T2}-R26R-Brainbow2.1* mice for single cell RNA-sequencing. Doublets and non-viable (DAPI^{+}) cells were removed before selection of cells expressing CD31. Lymphatic endothelial cells were then excluded by negative selection for Podoplanin (PODO^{-}) and *Pdgfb*-lineage EC selected by Brainbow2.1 fluorophore expression. Fluorescence minus one (FMO) controls were used to determine the gates for CD31 and PODO expression. Cardiac endothelial cells from age-matched wild type mice on the same genetic background as *Pdgfb-iCreER^{T2}-R26R-Brainbow2.1* mice (C57Bl6) were used as controls to determine the threshold for detection of Confetti reporter fluorophore expression. FSC=Forward scatter, SSC= side scatter.

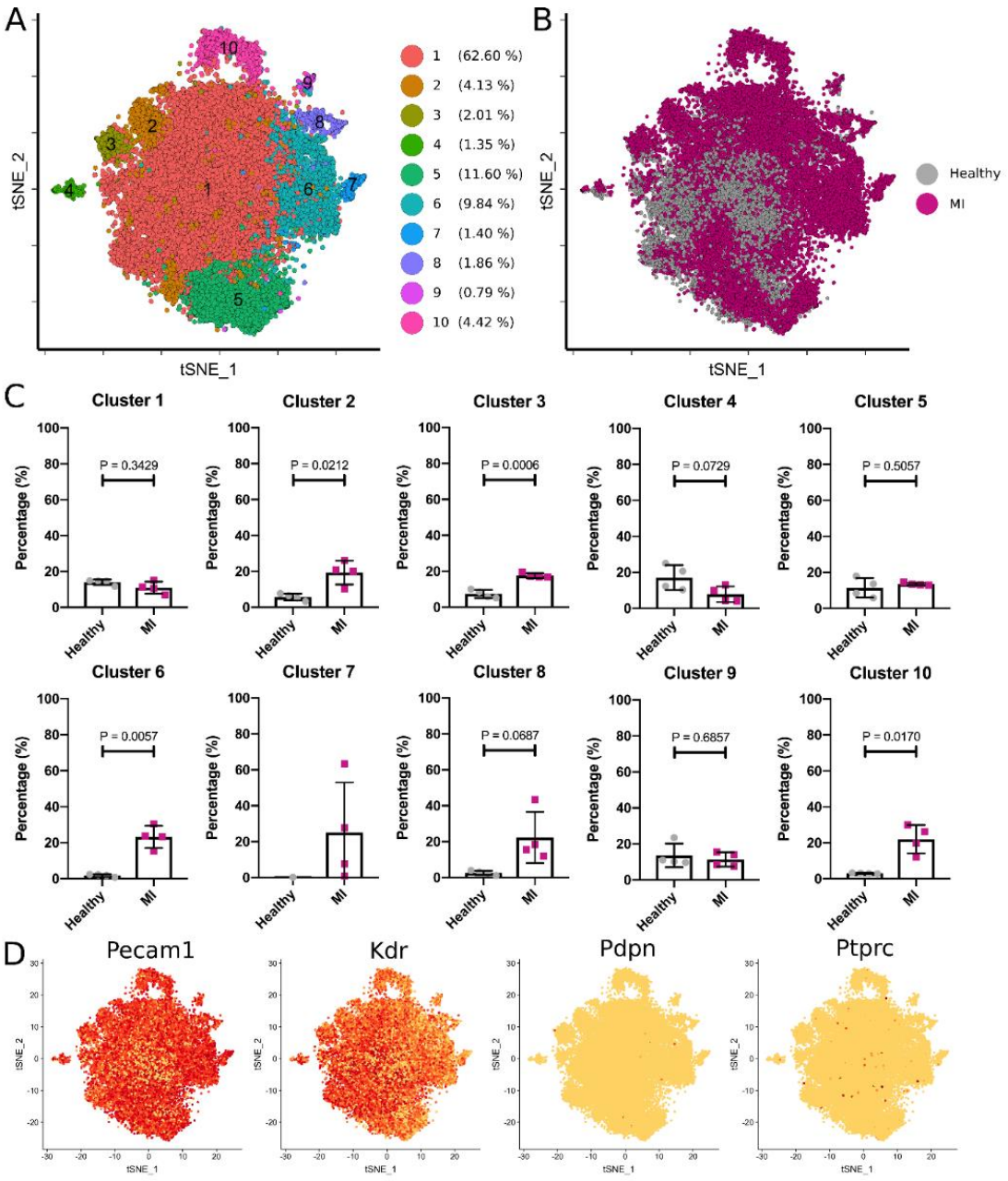

Figure 3.6 Single cell RNA sequencing of cardiac ECs reveals 10 heterogeneous transcriptional cell states in the post ischaemic adult mouse heart

(A) t-distributed stochastic neighbour embedding (t-SNE) map showing clustering of cardiac endothelial cells in 10 unique cell states according to their transcriptomic profile (B) t-SNE map of cardiac endothelial cells according to condition (healthy vs MI) (C) Percentage ratios of cardiac ECs from the healthy and MI groups was different according to each cluster (D) t-SNE plot of endothelial *Pecam1/Kdr*, lymphatic *Pdpn* and haematopoietic *Ptprc*. Mann-Whitney test. N=4/group.

Table 3.1 Top differentially expressed genes per cluster and gene ontology analysis

Gene ontology analysis in the top differentially expressed genes was performed in each of the clusters. Each cluster was composed from *Pdgfb* lineage endothelial cells from both MI and healthy datasets as per Figure 3.6.

Cluster	Top 10 differentially expressed genes	Gene Ontology term
1	Car4, Cyp4b1, Lpl, Gpihbp1, Rgcc, C1qtnf9, Timp4, Sgk1, Aqp1, Gm12002	Cellular homeostasis
2	Ifit3, Cxcl10, Ifit1, Rsad2, Ifit3b, Isg15, Ifit2, Usp18, Cmpk2, Cxcl9	Interferon signalling
3	Myl2, Mb, Myl3, Tnnt2, Tnni3, Actc1, Cox6a2, Fabp3, Tnnc1, Tpm1	Ventricular cardiac muscle remodelling
4	Klra9, Klra3, Klra10, Car4, Gm12002, Gm11808, Gm10076, Rps27rt, Gm10073, Rpl10-ps3	Killer cell lectin-like receptor signalling
5	Fbln5, Gja4, Stmn2, Clu, Glul, Nebl, Hey1, Vegfc, Alpl, Mgp	Endothelial cell regulation *via* Notch signalling
6	Plvap, Rbp1, Lrg1, Bgn, Vwf, Prss23, Col15a1, Eln, Fam167b, Igfbp3	Ventricular remodelling [via retinoic acid (RA) signalling]
7	Lrg1, Plvap, Ackr1, Clu, Tmem176a, Ehd4, Tmem176b, Tmem176b, Tmem252, Selp, Tagln	Stalk cell markers. Tip and stalk cell-mediated neovasculogenesis
8	Igfbp5, Cfh, Cpe, Cytl1, Tmem108, Dcn, Vwf, Mgp, Mgp, Pi16, Bgn	Endothelial ECM proteins, cardiac remodelling post-MI
9	Serpina1e, Serpina1d, Serpina1b, Igfbp5, Ptgs1, Cd9, AU021092, Pi16, Klk8, Emp3	Serine protease inhibitor alpha-1 antitrypsin (AAT) signalling
10	Hmgb2, Stmn1, Top2a, Cenpf, Cks2, Birc5, Cenpa, Ube2c, Cdc20, Prc1	Proliferation and cell cycle regulation

3.4.4 EndMT does not contribute to cardiac neovascularisation at 7 days post-MI

EndMT was recently hypothesized to play a role in neovascularisation in the ischaemic mouse heart.[392] Expression markers of EndMT were investigated in cardiac ECs from healthy and 7day post-MI hearts but the overall EndMT signature was unchanged in both groups (Figure 3.7, A) despite an increase in some EndMT markers after MI (*Icam1, Vcam1, Vim, Fn1 and Smtn,* Figure 3.7, B). Therefore, EndMT is unlikely to participate in cardiac neovascularisation in the presented MI model.

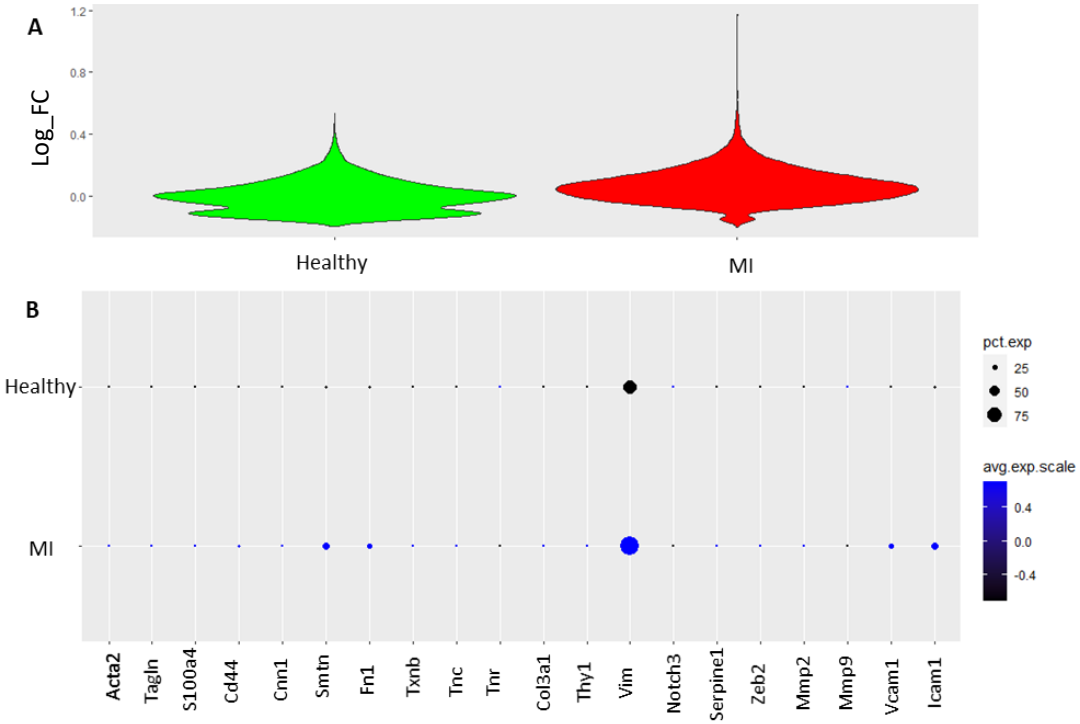

Figure 3.7 EndMT does not contribute to cardiac neovascularisation at 7 days post-MI

(A) Violin plot showing that the overall endothelial-to-mesenchymal transition (EndMT) marker signature in Log_FC (fold change) in cardiac *Pdgfb* lineage endothelial cells (ECs) from healthy and 7-day post-myocardial infarction (MI) hearts (B) Dotplot of EndMT marker expression from healthy and 7-day post MI *Pdgfb* lineage cardiac ECs showing percentage expression of EndMT markers (pct.exp) in *Pdgfb* lineage endothelial cells (ECs) and expression level (avg.exp.scale) (log2FC). Level of expression and percentage ECs expression was increased in some EndMT markers (*Icam1, Vcam1, Vim, Fn1 and Smtn)* but most remained unchanged. N=4/group. Mann-Whitney test.

3.5 Discussion

The aim of this chapter was to investigate the spatiotemporal dynamics and transcriptomic profile of ECs in the healthy and post-ischaemic heart. ECs play an essential role in the neovascularisation process that takes place in the border region of the ischaemic area of the heart[38,39,381,382], and is critical at stimulating regeneration post-MI.[154] Thus, therapies have aimed to enhance the neovascularisation process. However, most studies on this topic have been plagued by questions regarding efficacy and mechanism of action. [162] This could be explained, in part, by the lack of a more in depth understanding of the resident mechanisms that drive neovascularisation in the heart.

In the presented study, the hypothesis was that endogenous neovascularisation in the post-ischaemic adult mouse heart occurs through clonal expansion of resident adult ECs, i.e. the ability to produce clones of identical cells. This was tested using the *Pdgfb-iCreER^{T2}-R26R-Brainbow2.1* mouse model which permits lineage tracing specifically in *Pdgfb* lineage ECs. Firstly, it was shown that the heart undergoes clonal turnover of endothelial cells under physiological conditions, showing that a group of cardiac ECs produces identical ECs as a method of homeostatic cell turnover. This is aligned with recent existing literature demonstrating that the adult cardiac endothelium is not quiescent.[161,393] Bergmann *et al.* showed, through the use of carbon dating, that ECs have the highest turnover rate amongst the cardiac cell populations with the whole population being wholly exchanged every 6 years in human adulthood and approximately 9 times between 20 and 75 years of age.[161] Mesenchymal cells were exhibited both less turnover than ECs and an age-dependent decline in renewal. However, they still showed a 3.9% turnover rate per year in adult life. [161] Cardiomyocytes were shown to have a 0.8% turnover per year in individuals aged 20 years and a 0.3% turnover per year in individuals aged 75 years. [161] This information reinforces the idea that the cardiac cell populations are more dynamic than previously thought.

The process of clonal expansion of cardiac ECs was found to be significantly upregulated at 7 days following MI with large monochromatic clones of ECs contributing to the neovascularisation of the infarcted border area, suggesting that it is a key cellular mechanism in the response of the tissue to hypoxia and subsequent ischaemia.

Endothelial cell replication in the adult heart had been previously reported in the 1970s by Benditt *et al*.[169] At the time, however, it was not possible to study the clonal nature of the cardiac EC population at a single cell level. A conclusion could not be drawn on the ability of the endothelium to be maintained by clonal proliferation or whether it is a polyclonal tissue maintained by turnover of adjacent mature ECs. Findings in this chapter support existing studies showing that pre-existing cardiac ECs form new vessels after cardiac ischaemia.[133] Importantly, this chapter shows that the contribution of ECs to neovascularisation *via* clonal proliferation from the bone marrow is minimal, further increasing the claim that only locally-resident cardiac ECs are responsible for post-MI neovascularisation. The lack of bone marrow contribution could in part explain the disappointing results of clinical studies using autologous bone marrow-derived cells for therapeutic neovascularization in patients with ischaemic heart disease. [394,395] It should be noted, however, that contribution from a non-*Pdgfb* EC lineage to new vessels post-MI cannot be discounted.

The clonal characteristic of neovascularisation in heart ischaemia was recently reported by Manavski *et al.* who utilized a *Cdh5* driven Brainbow2.1 lineage tracing mouse model. [396] They showed that *Cdh5+* cells contribute to the generation of perfused and mature microvessels at 7 and 14 days post-MI, possibly driven by a VEGFR2 signalling mechanism. [396] Despite the similarity in showing clonal EC expansion in cardiac ischaemia, Manavski *et al.* used a *Cdh5* driven model which includes cells of haematopoietic origin and thus doesn't discount bone marrow cell contribution from bone marrow derived cells. [335,336] Migration of cells from the bone marrow and/or the circulation has been shown to occur during ischaemic injury.[397,398] Consequently, the cardiac *Pdfdb*+ and *Cdh5*+ EC cell populations are different despite having a potential overlap. It should be noted that the fact that clonal EC expansion

is observed in both *Cdh5*+ and *Pdgfb+* EC lineages is a testament to post-MI neovascularisation *via* clonal EC expansion being a robust process.

However, cell population differences are important to consider when drawing conclusions about transcriptomic signatures. For instance, in Manavski *et al*., bulk RNA sequencing in expanding Brainbow2.1 cells isolated by laser capture microscopy revealed an enrichment in genes involved in EndMT, when compared to non-clonally expanded cells of the same regions and ECs that were isolated from the remote zone of the myocardium.[396] However, results from this chapter show that the EndMT signature is unchanged in both healthy and post-MI *Pdgfb* lineage ECs. This discrepancy may be due to the transient nature of EndMT, as Manavski *et al*. did not clarify whether EndMT genes were enriched at 7 or 14-days post-MI. Moreover, this inconsistency could be attributed to the difference in *Cdh5* vs *Pdgfb* EC populations. A different study using single cell RNA sequencing of *Cdh5* lineage ECs supported the idea of endothelial-to-mesenchymal activation (EndMA) rather than transition.[399] The authors of this study showed that ECs undergo transient mesenchymal activation that is associated with metabolic changes.[399] *Cdh5* lineage ECs were found to transiently express transcripts that are typically linked to EndMT but levels of expression returned to physiological levels 10 days post-MI. [399] Moreover, the same study utilised a *Cdh5* driven lineage tracing system to detect potential cells that have fully transitioned to a mesenchymal cell type and thus lost EC marker expression, and showed that the number of traced cells expressing the endothelial marker *Cdh5* and mesenchymal markers, such as *Col1a1*, *Col3a1*, or *Serpine1*, increased transiently, with a maximum between days 3 and 7. It is thus likely, that the EndMA could not be detected in the presented study due to the 7-day post-MI timepoint.

In the presented model, most vessels formed were monoclonal but not all Brainbow2.1+ ECs resulted in polyclonal vessels. It is unclear whether this is due to a subset of adult cardiac ECs with progenitor-like characteristics or due to specific micro-environmental changes close to the infarct border that stimulate resident ECs to clonally proliferate. The possibility of a progenitor-like population is supported by

studies that show evidence of a highly clonogenic EPC population that may reside in a niche in the intimal layer of the adult human vessel wall. [176] The single cell RNA sequencing results that are presented here cannot differentiate between ECs that are part of large polychromatic clones due to lack of spatial information. More work will need to be conducted on the transcriptomic differences between Brainbow2.1+ cells that form larger *vs* smaller vs no clones (described in more detail in section 6.2). An interesting hypothesis is the existence of mature ECs (i.e. not progenitor-like) that are pro-proliferative via somatic cell adaptation. This event has been documented in chronic diseases such as cancer where environments such as hypoxia promote carcinogenic mutations or epigenetic changes.[400] However, this is less likely as the heart is a low turnover organ (despite the presence of EC turnover[161]). Moreover, MI is an acute event and does not allow for a significant length of time for adaptation which is required for the accumulation of mutations.[401]

Using single cell RNA-sequencing, this study defined endothelial heterogeneity in the healthy and injured mouse heart through characterisation of 10 EC states with distinct gene expression signatures. Moreover, the transcriptional changes arising in each subset following injury were mapped at the single cell level. Single cell RNA-sequencing was also recently applied to map cell populations in the healthy and injured mouse heart 3 days after ischaemia–reperfusion surgery.[402] This study identified two EC clusters, although detailed EC gene expression analysis was not included as this study focused on alterations of cardiomyocyte subpopulations.[402] A study by Tombor *et al.* [399] performed single cell RNA-sequencing of the non-cardiomyocyte fraction of mouse hearts at days 0, 1, 3, 5, 7, 14, and 28 post MI. Results revealed 4 clusters of ECs, characterized by *Cdh5* and *CD31* expression.[399] However, a significant limitation of this study was that only one biological replicate was included for each timepoint. [399] Recently, a study by Litviňuková *et al*. [403] utilized single cell RNA sequencing to characterize the cellulome of six anatomical adult human heart regions. Ten EC populations were characterised which included three capillary ECs (57.4% of all ECs), one capillary-like immune EC group related to antigen presentation and immune regulation, arterial ECs, venous ECs, atrial ECs, lymphatic

ECs and finally one group of ECs with fibroblast-like and one with cardiomyocyte-like features. These studies strengthen the claim that the human heart is home to different EC populations with unique expression profiles and that any attempt to manipulate their function to augment neovascularisation post-MI needs to be specific to the target group. One interesting question that is worth pursuing in the future is whether differences in EC profiles and function are solely due to the microenvironment they reside in *versus* the idea of an inherent difference. This is supported by *in vitro* studies that show that, following long-term culture of *in-vivo*-derived ECs, gene expression patterns and structural characteristics are severely altered.[404]

Attention should be drawn to limitations of this study. It was observed that in the fluorophore expression analysis there was a significant bias towards YFP expression. This did not affect subsequent results, however, since the *Pdgfb* EC clonal patch size was similar across all fluorophores. Interestingly, it has been reported that when using this model it is not uncommon to observe biases towards certain colours but the reasons for this are still unclear.[405] The possibility that some putative clones may derive from merger events where two independently marked cells or clones are associated by chance, was addressed using quantitative clonal analysis. Moreover, the single cell EC expression results presented here are generated from a single snap-shot in time, i.e. 7 days post-injury. In addition, with the data generated in this thesis it is not possible to comment whether the new blood vessels generated as a result of clonal proliferation of Pdgfb lineage ECs, despite perfusion as shown by IB4 staining, will go to develop more mature-like larger vessel (perivascular cell support) or will regress. A later MI timepoint such as 28 days post-MI can be used to assess this possibility.

In summary, the presented study shows the clonal nature of EC proliferation turnover under physiological conditions and the significant upregulation of this process in the peri-infarct border following MI. Moreover, this study provides a high-resolution single cell gene expression atlas of 10 transcriptionally distinct states of resident cardiac EC in physiological conditions and at 7 days post-MI. The heterogeneity

exhibited in the cardiac EC population signifies that when attempting to enhance the neovascularisation response post-MI in future studies, these differences have to be considered to guide novel therapeutic strategies aimed at enhancing myocardial repair and regeneration.

Chapter 4 Plasmalemma Vesicle Associated Protein (PLVAP) is a novel target with a potential role in neovascularisation in ischaemia

4.1 Chapter acknowledgments

I would like to thank Dr Richard Taylor for his help with the trajectory analysis. Moreover, I would like to give my thanks to Dr Cass Li for helping to design and perform the siRNA experiment with me. Furthermore, I would like to thank Dr Cass Li for performing the qPCR experiment investigating *Plvap* expression 4-weeks post-MI. I would like to also thank Dr Julie Rodor and Dr Helen Spencer for their guidance in designing the siRNA experiment. Finally, I would like to thank Dr Andrew Chapman, Dr Takeshi Fujisawa, and Professor Nicholas Mills for their help in acquiring the plasma-EDTA samples from type I MI and healthy patients and designing the relevant experiment.

4.2 Introduction

Data presented in Chapter 3 of this thesis show that single cell RNA-sequencing analysis of 7-day post-MI and healthy cardiac ECs revealed significant differences in gene signatures and transcriptional heterogeneity. Interestingly, when comparing the gene expression profile of healthy and injured ECs, clusters were identified that were predominantly or fully composed of ECs from the MI group. These potentially represent ECs that have responded to ischaemic injury through the activation of regenerative genes and pathways.

Plasmalemma Vesicle Associated Protein (*Plvap)* gene was selected for further study based on its increased expression in mouse cardiac ECs 7-day post-MI compared to healthy controls.

The gene coding for PLVAP is 25,893 bases located on chromosome 19 in humans. PLVAP is a dimer-forming type II integral membrane glycoprotein (60kDA)[406] that consists of three domains: a 27 amino acid intracellular tail, a transmembrane domain and a 358 amino acid extracellular C-terminal domain.[407] PLVAP is an endothelial specific marker and an antigen for two EC selective antibodies: mouse EC antigen MECA-32, and Pathologische Anatomie Leiden-endothelium (PAL-E) [408–410]. PLVAP is expressed in ECs in the lungs, kidneys, spleen, endocrine glands and the endocardial lining of the heart chambers.[406,411]

PLVAP is one of the major molecular components of fenestrae and is essential for fenestral diaphragms (FD) and stomatal diaphragms (SD) in ECs. [412,413] FDs and SDs are critical to maintain homeostasis of vascular permeability which is one of the fundamental roles of the endothelium. The main structures that govern EC permeability are caveolae, transendothelial channels (TECs) and fenestrae.[73,89] Caveolae are membrane proteins that contain SD [414,415] whereas fenestrae are transcellular pores made by FDs (60-80nm in size) [416] and TECs consist of two SDs.[416]

The essential role of *Plvap* in permeability has been demonstrated using PLVAP-null C57BL/6N mouse embryos which die *in utero* due to severe oedema, haemorrhage and weakness of the vascular wall; and more specifically, due to the absence of SDs

and FDs. [417] Deleting *Plvap* in mixed BALB/c-C57Bl/6J-129Sv/J background mice attenuated the lethality of *Plvap* deletion and increased survival until 3-4 months of age compared to a pure C57BL/6N background.[418] However, these animals also exhibited vascular defects, such as leaky capillaries due to disruption of FDs/SDs, leading to oedema in the kidney, pancreas and intestine.[418] This signifies the importance of *Plvap* in murine vascular development.

PLVAP also regulates leukocyte migration and angiogenesis.[419–423] For example, inhibition of *PLVAP* expression *via* siRNA in HUVECs resulted in a significant reduction in transmigration of peripheral blood mononuclear cells (PBMCs).[421] Interestingly, the rolling and adhesion functions were not altered, suggesting that PLVAP is not implicated in these functions. [421] PLVAP was also found to be present and synthesized in subcapsular sinus lymphatic ECs in the lymph nodes, regulating the entry of antigens and lymphocytes in the parenchyma. [424]

PLVAP has also been positively associated with angiogenesis, as *PLVAP* silencing resulted in attenuation of tubulogenesis of Human Dermal Microvascular Endothelial Cells (HMVECs), HUVECs and human primary brain EC lines. [423] In addition, PLVAP has been associated previously with tumour endothelium. [419] In ECs that originate from patients with glioblastoma, PLVAP was significantly upregulated when compared with controls.[419] PLVAP expression was also detected in secondary metastatic carcinomas. [419] Interestingly, downregulation of PLVAP using small hairpin RNA inhibited the formation of pancreatic adenocarcinoma in xenografts.[425] This suggests that PLVAP facilitates vascular growth in cancer.

In addition to its essential role in vascular development and homeostasis, PLVAP has also been associated with pathologies such as: cancer, ischaemic brain disease, ocular disease, spinal cord injury and glomerulopathy[412,419,422,425–429] However, its role in the heart, and more specifically in cardiac ischaemia and angiogenesis, has not been investigated.

4.3 Hypothesis and aims

The following hypothesis was proposed:

- *Plasmalemma Vesicle Associated Protein (PLVAP) is a novel target associated with an increase in neovascularisation in response to ischaemia.*

The hypothesis was addressed by the following aims:

- *Plvap* gene and protein expression will be investigated in mouse cardiac ECs in healthy and 7-day post MI adult hearts.
- The role of PLVAP in neovascularisation in human hearts tissues of patients with acute and chronic MI, will be explored *via* PLVAP expression quantification.
- The effects of siRNA induced gene knockdown of *PLVAP* in EC proliferation will be investigated *in vitro.*
- The potential role of PLVAP as a circulating biomarker of myocardial damage will be investigated in patients with type I MI.

4.4 Results

4.4.1 *Plvap* expression is increased in mouse cardiac ECs at 7 days post-MI

Single cell RNA-sequencing analysis of healthy and post-MI adult mouse cardiac ECs revealed 10 transcriptionally-different clusters, as introduced in Chapter 3. Clusters 6, 7 and 8 were predominantly composed of cells from the MI group, with cluster 7 being completely absent from the healthy dataset (Figure 4.1,A, B). Differential gene expression analysis showed that *Plvap* expression was significantly increased in ECs from the MI group (average gene expression in healthy: 0.08 ± 0.01 *vs* MI: 3.22 ± 1.07 log2FC, P=0.029; Figure 4.1, C) and that the percentage of ECs that expressed *Plvap* was also significantly increased (healthy: 0.99 ± 0.14 % *vs* MI: 33.76 ± 7.23 %, P=0.029; Figure 4.1, C). *Plvap* was also increased in a cluster-specific manner in cells from the MI group in clusters 6, 7 and 8 (cluster 6; healthy 1.66 ± 0.33 % vs MI 23.34 ± 1.71 %, P=0.0057 - cluster 7; healthy 0 ± 0 % vs MI 25.00 ± 14.03 %, cluster 8; healthy 2.68 ± 0.60 % vs MI 22.36 ± 7.11 %, P=0.0687; Figure 4.1). Immunostaining of Plvap in mouse heart tissues 7 days post-MI confirmed these results at the protein level and showed a significant increase in the percentage of PLVAP-expressing cells in MI (MI; 70.5 ± 19.9 % *vs* healthy; 38.7 ± 28.2 %, P = 0.02**,** Figure 4.2). In summary, due to MI and cluster specific elevation of expression of *Plvap* at 7 days post-MI, *Plvap* was chosen as a candidate for further analysis.

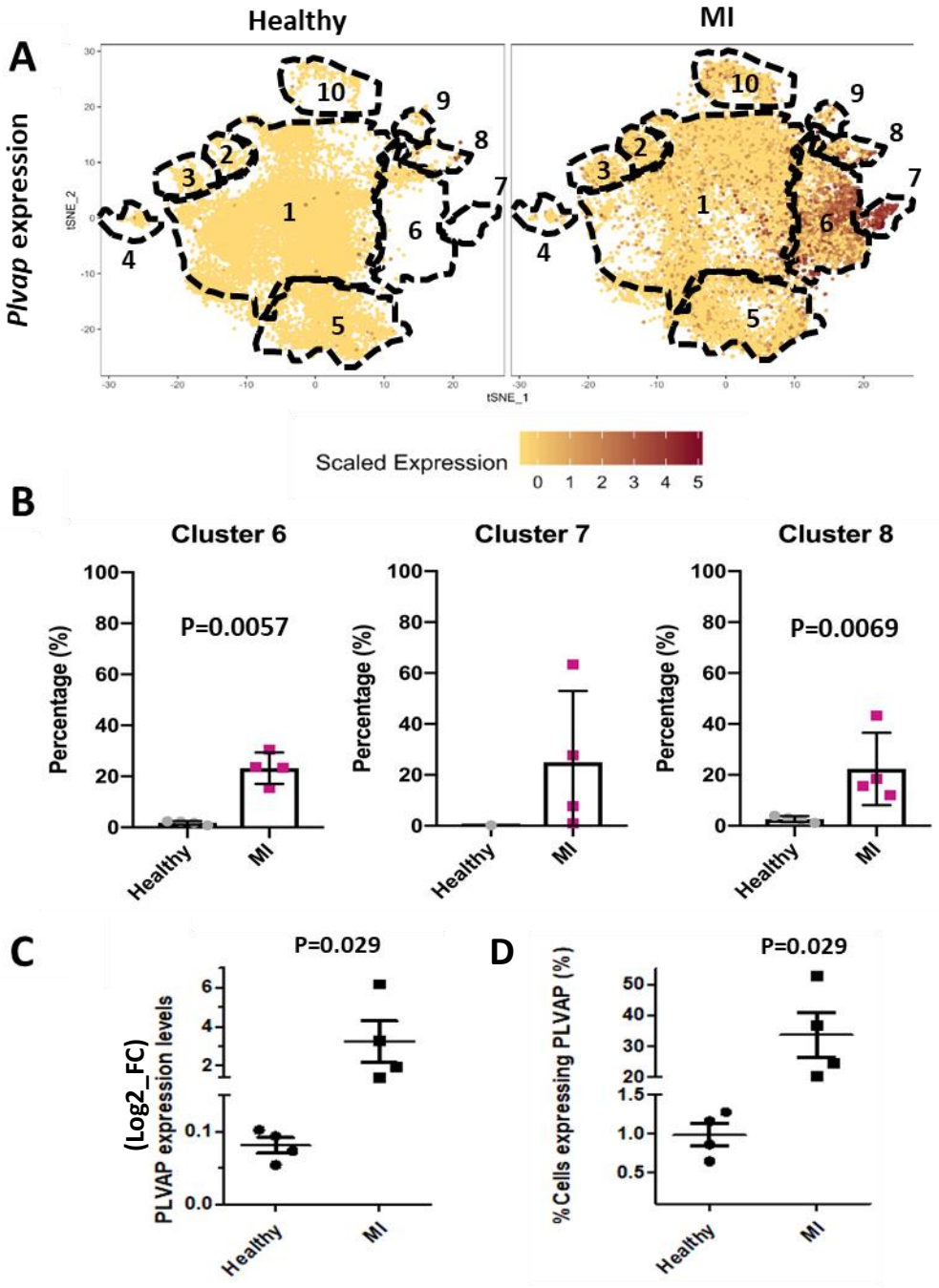

Figure 4.1 *Plvap* expression is increased in mouse cardiac endothelial cells in the adult mouse heart at 7 days post-MI compared to the healthy heart.

(A) Heat map showing the level of *Plvap* expression in the healthy and MI datasets. The expression of *Plvap* was increased in the MI group, in a cluster specific manner, in clusters 6, 7 and 8. (B) Clusters 6, 7 and 8 were predominantly composed from endothelial cells from the MI group, with cluster 7 being completely absent from the healthy dataset (cluster 6; healthy 1.66 ± 0.33 % vs MI 23.34 ± 1.71 %, P=0.0057 - cluster 7; healthy 0 ± 0 % vs MI 25.00± 14.03%, cluster 8; healthy 2.68 ± 0.60 vs MI 22.36 ± 7.11%, P=0.0-69). (C) *Plvap* expression

was significantly increased in endothelial cells from the MI dataset (healthy 0.08 ± 0.01 *vs* MI 3.22 ± 1.07 log2FC=Fold change). (D) The percentage of ECs expressing *Plvap* was significantly increased in EC from the MI dataset (Healthy % 0.99 ± 0.14 *vs* MI % 33.76 ±7.23). Mann-Whitney test. Data presented as Mean ± SEM. N=4/group.

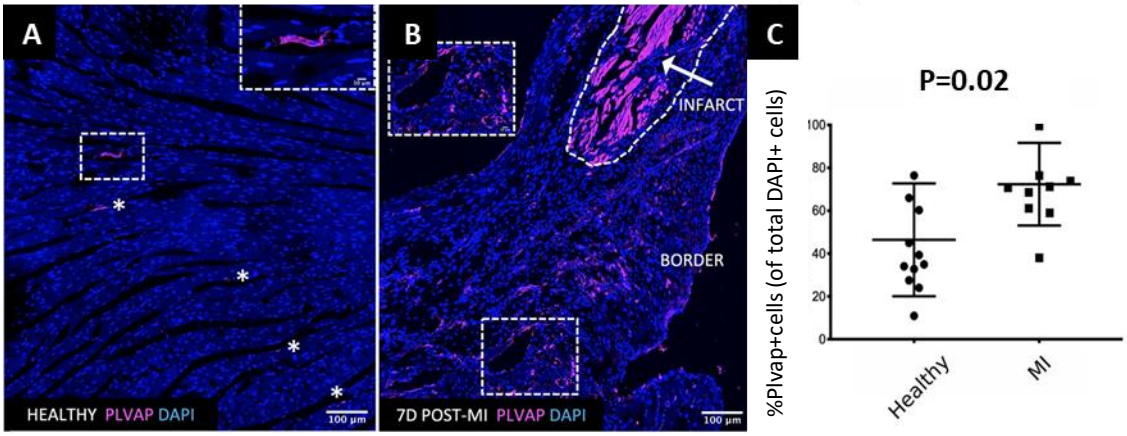

Figure 4.2 PLVAP expression is increased in mouse coronary endothelial cells at 7 days post-MI compared to the healthy heart.

(A) PLVAP immunostaining was performed in healthy and (B) 7 days post-myocardial infarction (MI) mouse heart sections. (C) PLVAP-expressing cells were found to be significantly increased at 7 days post-MI when compared to healthy control hearts specifically in the infarct border region of the left ventricle. (MI; 70.5 ± 19.9 % cells versus healthy; 38.7 ± 28.2 % cells, as percentages of total DAPI+ cells, P = 0.02). The cluster of purple stain assigned to PLVAP in the infarct region (arrow) was considered an artifact. N=11 for the healthy group, N=9 for MI group. Mann Whitney test. Results presented as Mean ± SEM.

4.4.2 *Plvap* expression is increased in mouse cardiac ECs 4 weeks post-MI

To address whether elevated *Plvap* expression was sustained in vascular ECs at later stages post-MI, and thereby may play a role in neovasculogenic responses, *Plvap* expression was studied in the *Pdgfb-iCreER^{T2}-R26R-Brainbow2.1* mouse heart vasculature at 4 weeks post MI. Cardiac CD31+ ECs were isolated using FACS from healthy and 4 weeks post-MI mouse hearts and analysis of *Plvap* expression showed a significant increase in the 4 week MI EC group when compared to the healthy heart EC (RQ; Healthy 1 vs 4W MI 2.5, P=0.0422, Figure 4.3).

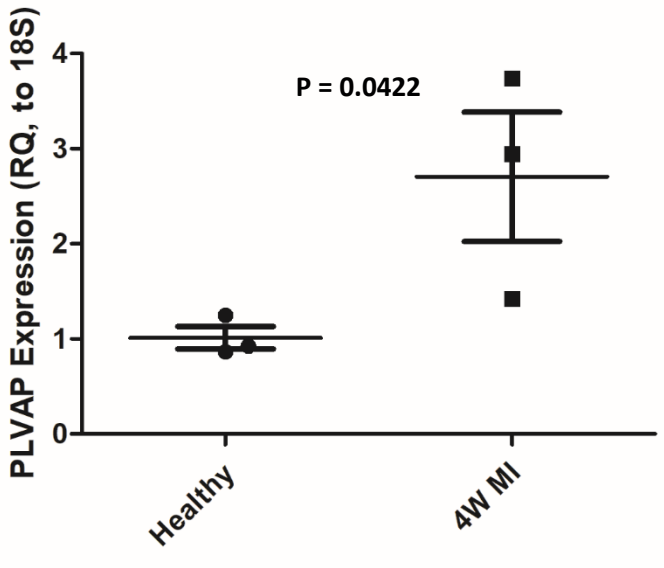

Figure 4.3 *Plvap* expression is increased is mouse cardiac ECs 4 weeks post-MI
Ischaemic damage was induced via permanent ligation of the LAD coronary artery in *Pdgfb-iCreER^{T2}-R26R-Brainbow2.1* mice. At 4 weeks post MI cardiac ECs were isolated using FACS based on CD31 expression. RNA was extracted and qPCR showed that *Plvap* expression levels were significantly increased in ECs from 4W MI group (RQ; Healthy 1 vs 4 weeks post-MI 2.5, P = 0.0422. Mann-Whitney test. N = 3 mice per group, with 3 technical replicates for qPCR**.** LAD = left anterior descending. MI = myocardial infarction.

4.4.3 Cardiac endothelial cells from cluster 6 appear to be an origin point for transition to clusters 7 and 8

As seen in previous sections, cardiac ECs from clusters 6, 7 and 8 contained a significant majority of EC specifically from the MI group and expressed Plvap. Using Monocle[378,379] to perform a trajectory analysis (as *per* 2.9) individual cell fate decisions were mapped in pseudotime as indicated by branching (Figure 4.4). ECs from clusters 6, 7 and 8 were connected by many intermediate cells located along these branching trajectories. The predicted pseudotime analysis indicated that cells in cluster 6 appeared to be primed to respond to ischaemic injury and undergo transcriptional differentiation towards clusters 7 and 8. (Figure 4.4).

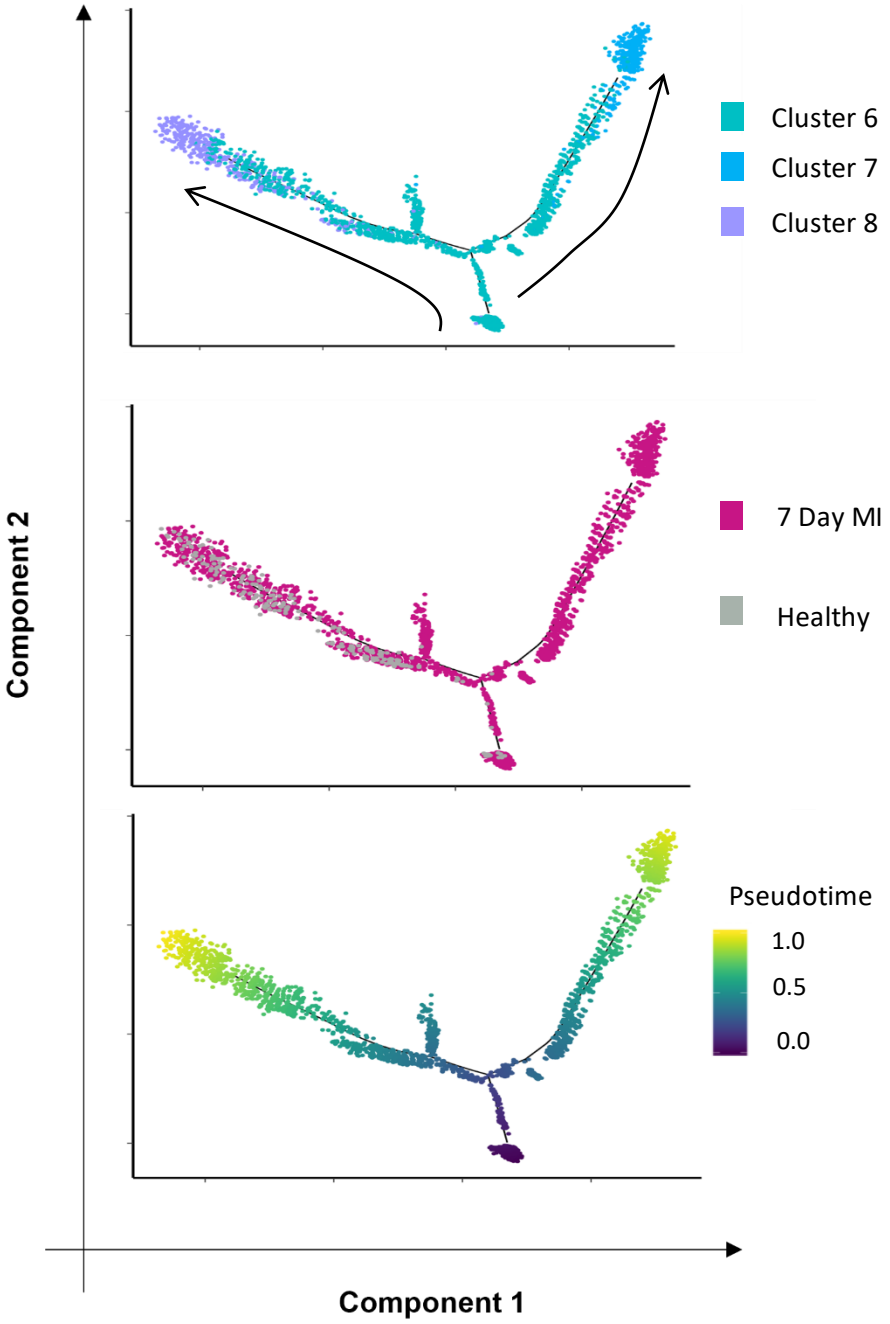

Figure 4.4 ECs from cluster 6 appear to be an origin point for transition to clusters 7 and 8. Cells in clusters 6, 7 and 8 were arranged in pseudotime using Monocle[378,379] to perform a trajectory analysis where individual cell fate decisions are indicated by branching. Direction is indicated by the arrows. Cells from clusters 6, 7 and 8 are connected with many intermediate cells located along branching trajectories. The predicted pseudotime analysis showed that cells in cluster 6 appear primed to undergo transcriptional differentiation towards clusters 7 and 8 in response to ischaemic injury.

4.4.4 Endothelial cells from cluster 7 have a stalk cell gene expression signature phenotype

Following the finding that cluster 7 is composed solely from cells from the MI group and that cluster 6 ECs transition to cluster 7 following ischaemic injury, the transcriptomic profile of these ECs was interrogated further. Differential expression analysis showed an endothelial 'stalk cell' signature in cluster 7 ECs with upregulation of known stalk cell markers including Ackr1, Tmem176a, Ehd4, Tmem176b, Tmem252, Selp, Csrp2, Lrg1 and Spint2[430] (Figure 4.5). Since these markers appeared largely specific to cluster 7, I then analysed whether ECs in this cluster co-expressed *Plvap*, as *Plvap* seemed to be dominantly expressed in cluster 7. This showed that a significant proportion of ECs that expressed the tested stalk cell markers also expressed *Plvap* (Figure 4.6).

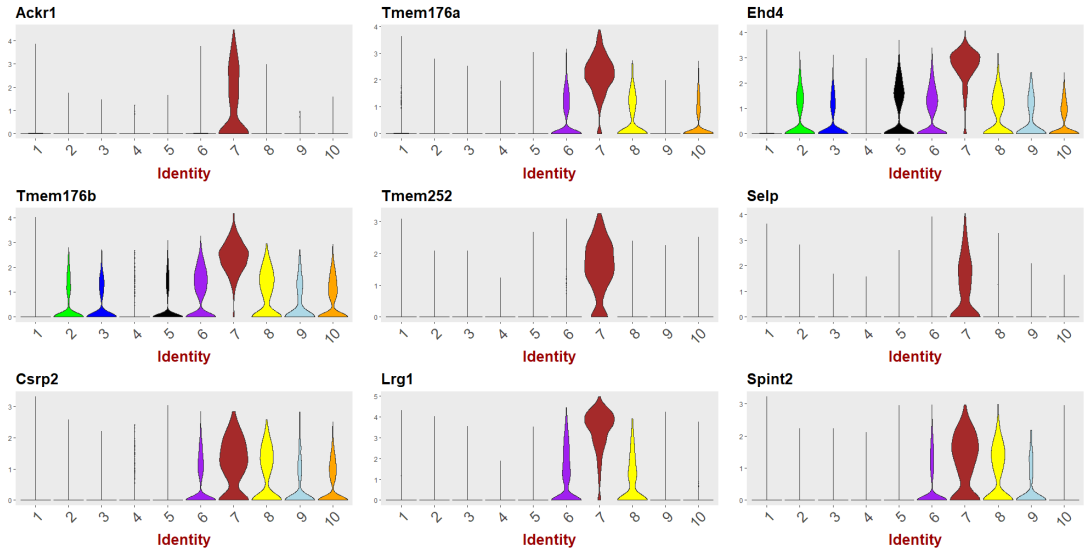

Figure 4.5 Endothelial cells from cluster 7 have a stalk cell signature phenotype

Violin plots showing known endothelial stalk cell markers in cardiac ECs in clusters 1 – 10. ECs from cluster 7 showed specific upregulation of known stalk cell markers such as Ackr1, Tmem176a, Ehd4, Tmem176b, Tmem252, Selp, Csrp2, Lrg1 and Spint2.[430]

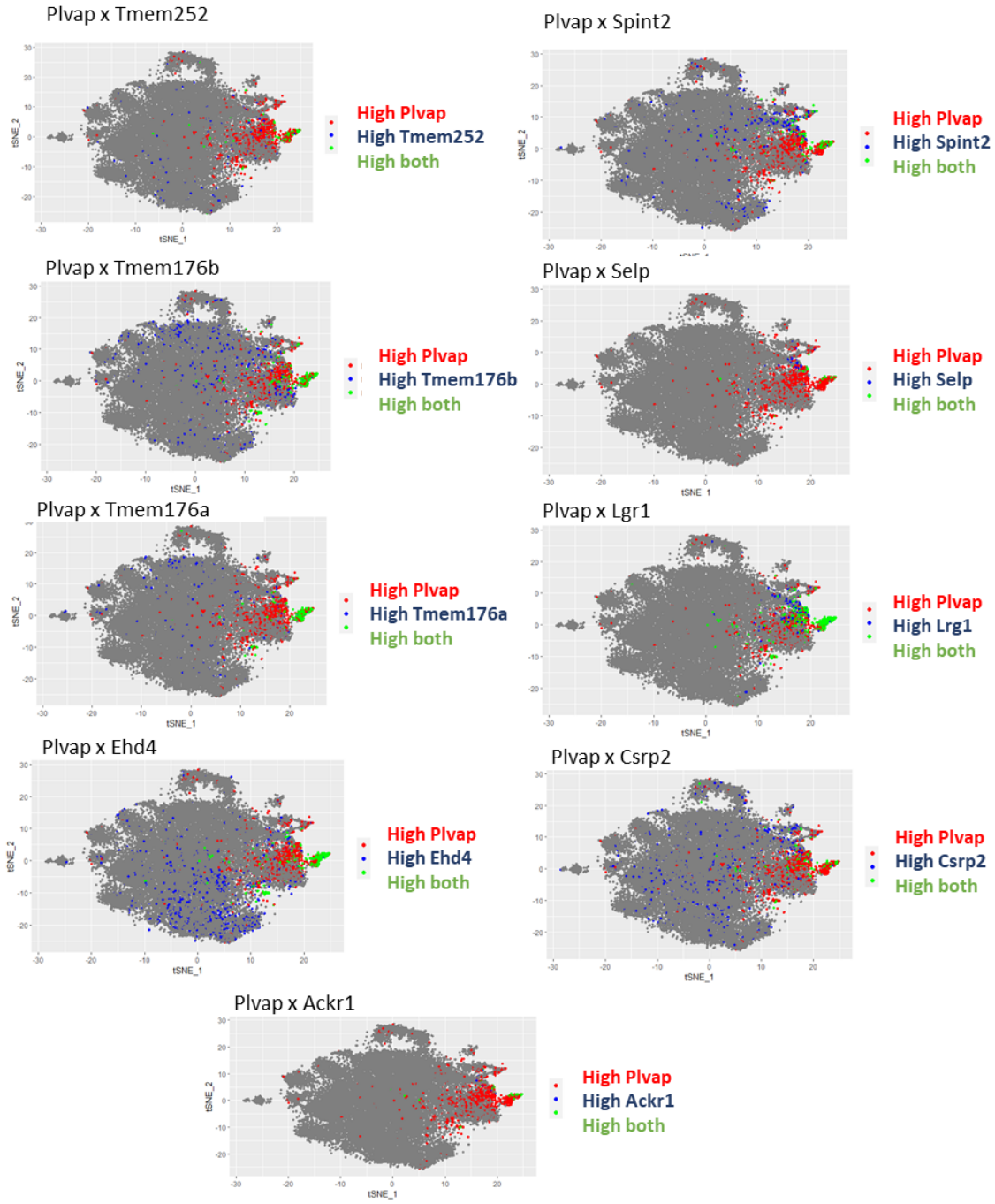

Figure 4.6 Endothelial cells from cluster 7 have a stalk cell signature phenotype and express Plvap.

T-distributed stochastic neighbour embedding (t-SNE) plots of stalk cell markers and *Plvap*. ECs from cluster 7 show co-expression of *Plvap* with known stalk cell markers including Ackr1, Tmem176a, Ehd4, Tmem176b, Tmem252, Selp, Csrp2, Lrg1 and Spint2[430].

4.4.5 PLVAP expression is increased in microvessels in cardiac tissues from patients with acute MI and chronic ischaemic heart disease.

Following the observation that *Plvap* expression was increased in mouse coronary ECs at 7-days and 4-weeks post-MI, the expression of PLVAP in cardiac tissues from patients with chronic and acute ischaemic heart disease was investigated.

4.4.5.1 Chronic ischaemic heart disease

PLVAP expressing (PLVAP+) vessels, as defined by CD31+ co-expression, were significantly increased in regions of myocardium adjacent to areas of fibrosis/scarring compared to vessels in control hearts from healthy subjects (% PLVAP expressing vessels; 36.9 ± 10.1 % vs. 11.1 ± 8.8 %, P = 0.0008, Figure 4.7). Subsequently, PLVAP expression was quantified according to vessel diameter. Vessels less than 30 µm in diameter were termed "small capillary-like vessels" and vessels larger than 30 µm in diameter were termed "larger vessels". [64 66]

Most PLVAP-expressing vessels in diseased myocardium were small capillary-like vessels (33.57 ± 9.17 vs 1.55 ± 0.25 vessels/ROI, P=0.006, Figure 4.8). Total vessel number was also quantified in each group, which revealed that both small capillary-like and larger vessels were significantly increased in tissues from patients with ischaemic heart disease (small capillaries; Control 40.63 ± 10.80 vs Disease 128.8 ± 21.65 vessels/region of interest (ROI), P=0.04; larger vessels; Control 0.5 ± 0.29 vs Disease 3.944 ± 1.46 vessels/ROI, P=0.01, Figure 4.8).

4.4.5.2 Acute ischaemic heart disease

PLVAP-expressing vessels were also increased in regions adjacent to areas of fibrosis in patients with acute MI (Control 10.09 ± 2.38 vessels/ROI vs Acute MI 46.77 ± 2.23 vessels/ROI, P=0.0238) (Figure 4.9, A). Further phenotyping of these vessels in disease according to size, showed that they were predominantly small capillaries (Small capillaries 11.83 ± 0.93 vessels/ROI vs larger vessels 1.17 ± 0.44 vessels/ROI, P=0.05) (Figure 4.9, B).

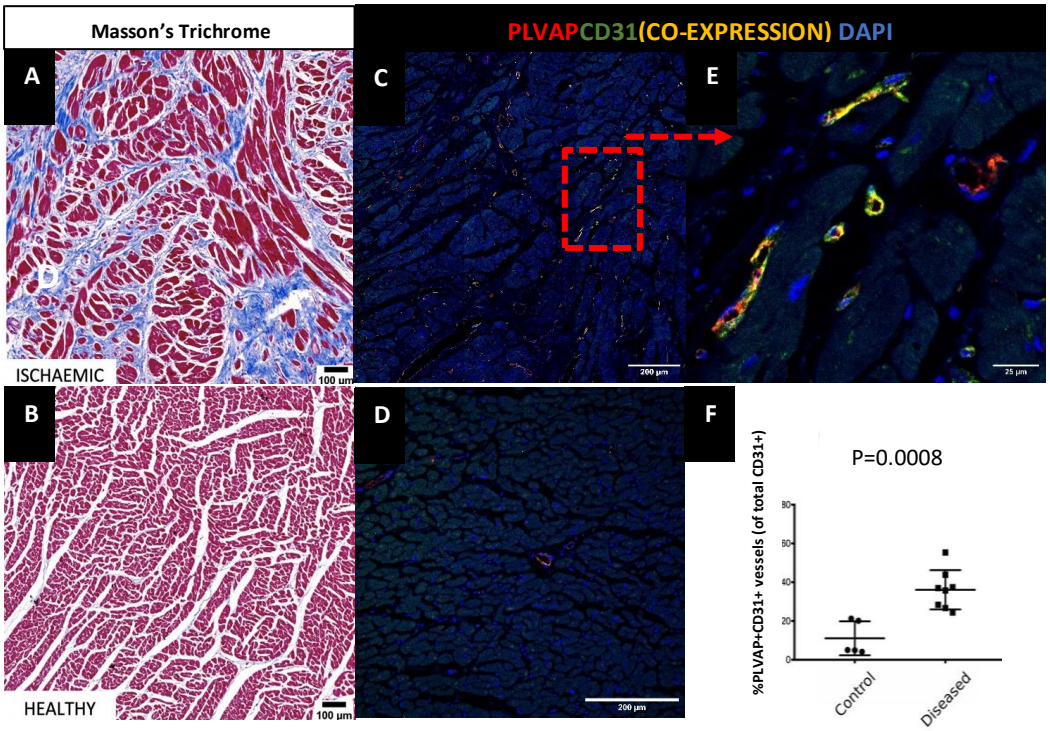

Figure 4.7 The number of PLVAP-expressing vessels was increased in the hearts of patients with chronic ischaemic heart disease.

(A), (B) Representative Masson's trichrome histology images of ischaemic and healthy human heart. Red stain indicates the healthy myocardium whereas the blue indicates collagen formation, indicative of fibrosis (C) PLVAP and CD31 immunostaining of ischaemic human myocardium specifically in regions of fibrosis and (D) healthy human myocardium (E) high power (dashed line red box) of vessels showing CD31 positivity and PLVAP+CD31 positivity in fibrotic areas (F) PLVAP-expressing vessels were increased in areas of fibrosis in hearts of human patients (11.1 ± 8.8 %, vs n=8 Acute MI 36.9 ± 10.1 %, P=0.0008, two-tailed Student's

t-test). N=5 for controls. N=8 for diseased. Mann Whitney test. Results presented as Mean ± SEM.

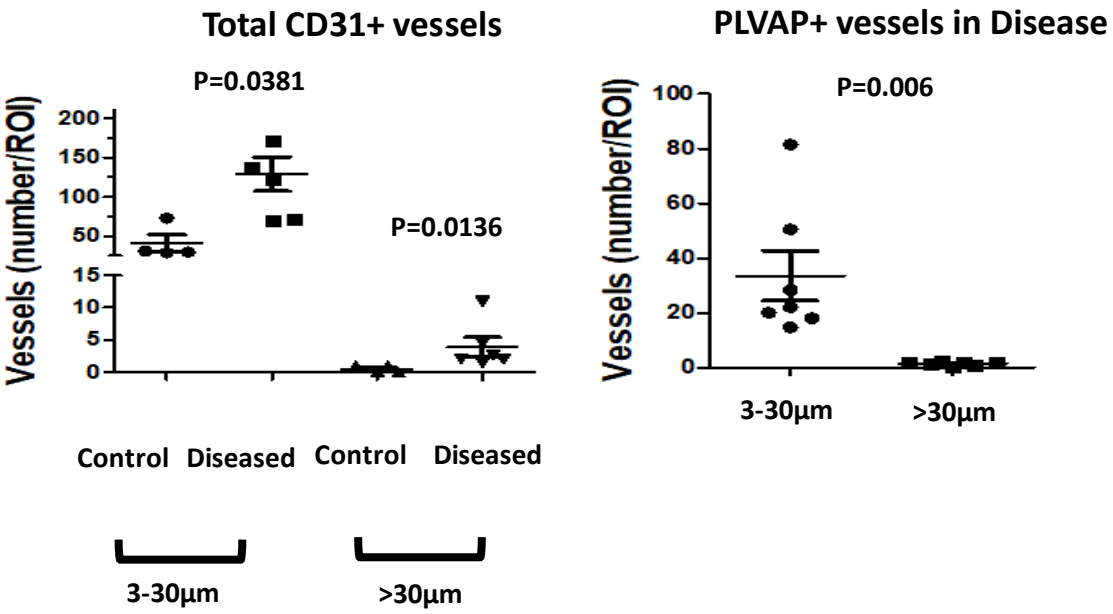

Figure 4.8 PLVAP-expressing vessels in the hearts of patients with chronic ischaemic heart disease are predominantly microvascular

An increase both in small capillaries and in larger vessels was observed in regions of fibrosis in hearts of chronic ischaemic heart disease patients compared to controls (Small Capillaries <30µm diameter; Control 40.63 ± 10.80 vessels/ROI vs Disease 128.8 ± 21.65 vessels/ROI, P=0.0381 – Larger Capillaries >30µm diameter; Control 0.50 ± 0.29 vs Disease 3.94 ± 1.46 vessels/ROI, P=0.0136). Phenotyping of PLVAP-expressing vessels according to diameter revealed that the majority of PLVAP-expressing vessels in diseased myocardium were capillary-like vessels of less than 30 µm diameter (Small capillaries, <30 µm diameter 33.57 ± 9.167 vessels/ROI vs larger vessels, >30µm diameter 1.55 ± 0.25 vessels/ROI, P=0.006). N=4 for controls. N=5 for patients. Mann Whitney test. Results presented as Mean ± SEM.

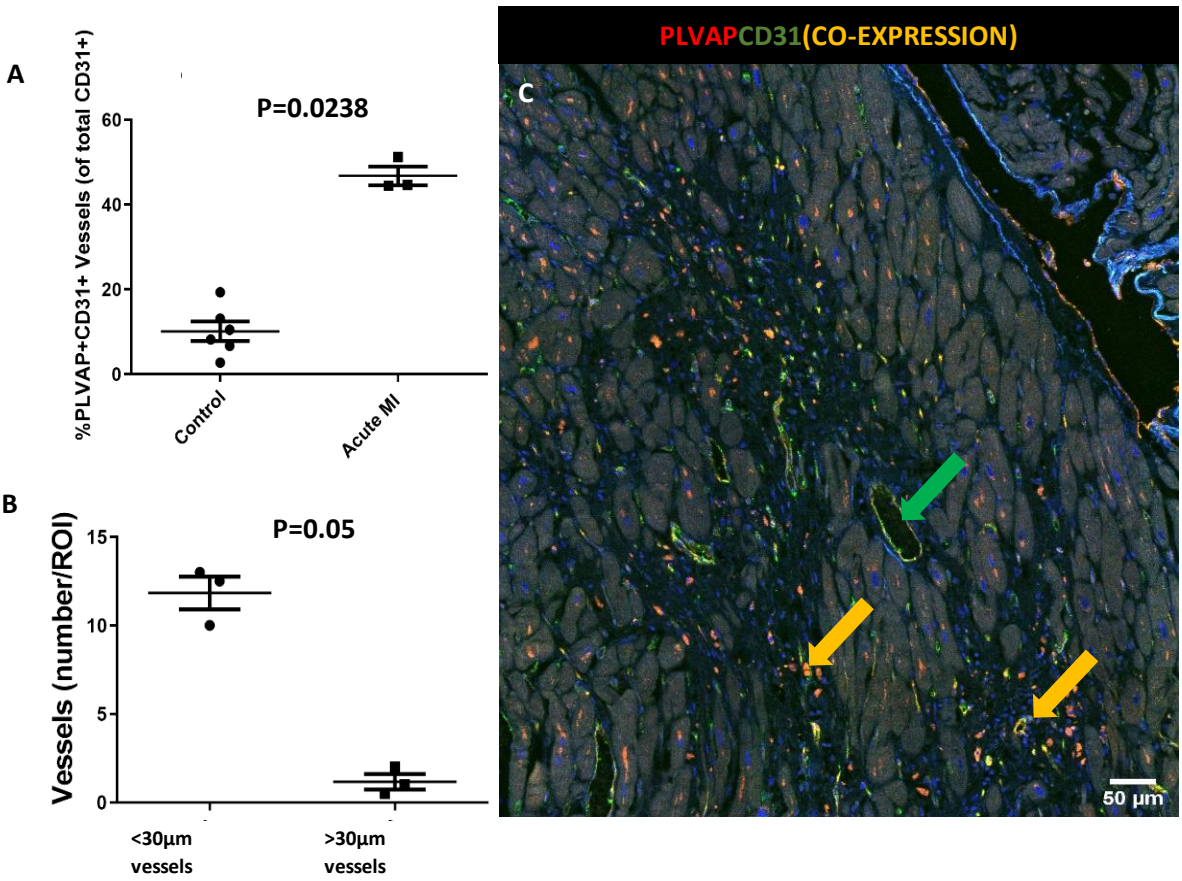

Figure 4.9 PLVAP expressing vessels were increased in hearts of patients with acute MI, and were predominantly microvascular

(A) The number of PLVAP+ vessels were increased in cardiac sections from human patients (Control 10.09 ± 2.38 vs Acute MI 46.77 ± 2.23, P=0.0238). (B) Further phenotyping of PLVAP-expressing vessels specifically in disease showed that they were predominantly microvasculature (<30µm vessel diameter) (Small capillaries 11.83 ± 0.93 vessels/ROI vs larger capillaries 1.17 ± 0.44, P=0.05 vessels/ROI). (C) Immunostaining of PLVAP and CD31 in human heart tissue. Orange arrows show PLVAP and CD31 co-expressed in the same vessel and green arrows show CD31 only expressing vessels. N=6 for controls. N=3 for acute MI. Mann Whitney test. Results presented as Mean ± SEM.

4.4.6 PLVAP is expressed and can be silenced in HUVECS

Gene silencing of *PLVAP via* siRNA technology was undertaken in HUVECs to study the role of PLVAP in EC proliferation (as *per 2.7.1.1* HUVEC proliferation assay). Successful knockdown was validated at the mRNA level (control siRNA RQ = 3.0 ± 0.9 vs *PLVAP* siRNA 0.2 ± 0.2, P = 0.003, Figure 4.10) as well as at the protein level via Western blotting (Figure 4.10)

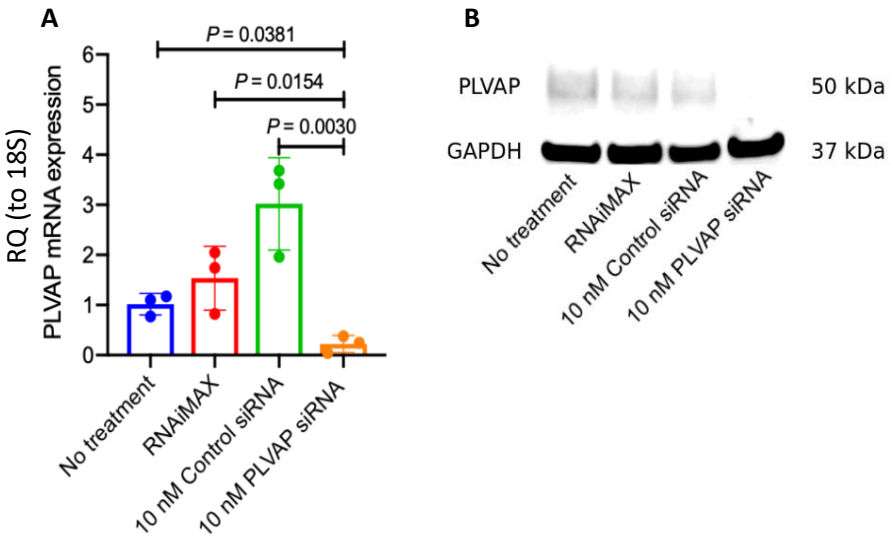

Figure 4.10 PLVAP is expressed and can be silenced in HUVECS

(A) *PLVAP* was silenced in human umbilical vein endothelial cells (HUVECs) *via* siRNA at the mRNA level (control siRNA RQ = 3.0 ± 0.9 vs PLVAP siRNA 0.2 ± 0.2, P = 0.003, relative to housekeeper 18S expression, one way ANOVA) (B) and was confirmed at the protein level by Western blot. Controls included no treatment control, vehicle RNAiMAX control and scramble control siRNA. N=3. Each N number was an independent HUVEC line pooled from multiple unknown donors. 3 technical replicates were performed for each line and group.

4.4.7 PLVAP silencing inhibits proliferation of HUVECS

EC proliferation is a fundamental function in angiogenesis.[99] An EdU incorporation assay was used to label actively proliferating HUVECS *in vitro*. Inhibition of *PLVAP* expression resulted in a significant reduction in EC proliferation (EdU+ ECs = 60.7 ± 3.9 % vs. 21.1 ± 11.0 %, P = 0.0038, Figure 4.11).

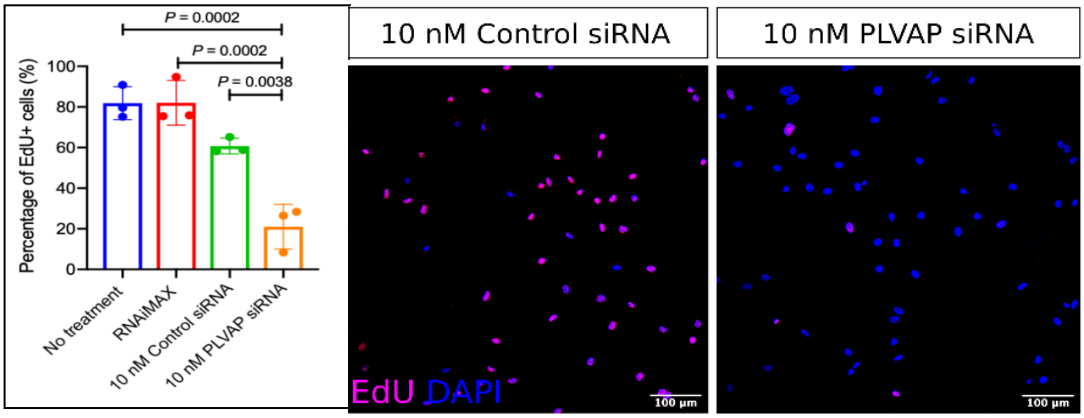

Figure 4.11 PLVAP silencing inhibits cell proliferation in HUVECS

The role of PLVAP in endothelial proliferation was investigated *via* an EdU incorporation assay. *PLVAP* inhibition significantly reduced EC proliferation compared to controls (EdU+ ECs = 60.7 ± 3.9 % vs. 21.1 ± 11.0 %, P = 0.0038). N=3/group. Mann-Whitney test. Each N number was an independent HUVECS line pooled from multiple unknown donors. 3 technical replicates were performed for each line and group.

4.4.8 PLVAP concentration in plasma-EDTA samples is not increased in patients with type I MI

Following the findings that i) *Plvap* is increased in mouse ECs following MI ii) PLVAP is increased in heart vasculature of patients with both chronic and acute MI, I postulated that PLVAP could be detected in the circulation of patients with acute MI, and thus may represent a potential clinical biomarker. An ELISA to detect PLVAP was performed on EDTA-plasma samples from 15 type I MI patients and controls. Type 1 MI is defined as myocardial ischaemia as the cause of myocardial injury due to acute atherothrombosis.[431] The concentration of PLVAP did not change between groups (Control 0.80 ± 0.18 ng/mL *vs* type I MI 0.48 ± 0.08 ng/mL, P= 0.17) (Figure 4.12). Moreover, the levels of troponin, a commonly used biomarker for myocardial injury, [432] were found to not be correlated with the levels of PLVAP in the same patient and control cohorts (Control; PLVAP concentration *vs* troponin, R^2=0.066, P=0.77) (MI; PLVAP concentration vs troponin, R^2=0.067, P=0.78) (Figure 4.13).

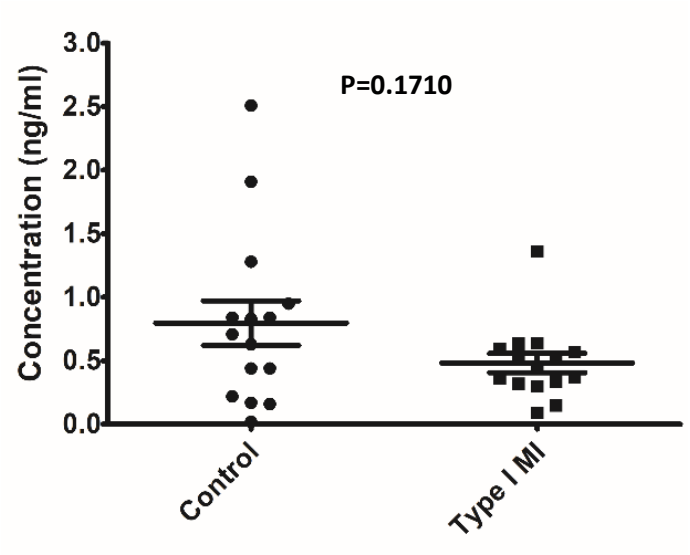

Figure 4.12 PLVAP concentration in EDTA-plasma is not increased in patients with type 1 MI

EDTA-plasma samples from patients with type 1 MI and controls (n=15/group) were processed without dilution for a PLVAP ELISA. The concentration of PLVAP was not different between the groups (Control 0.7967 ± 0.1754 ng/mL *vs* type 1 MI 0.4827 ± 0.0761 ng/mL, P= 0.1710>0.05, Mann Whitney test. Results presented as Mean ± SEM.

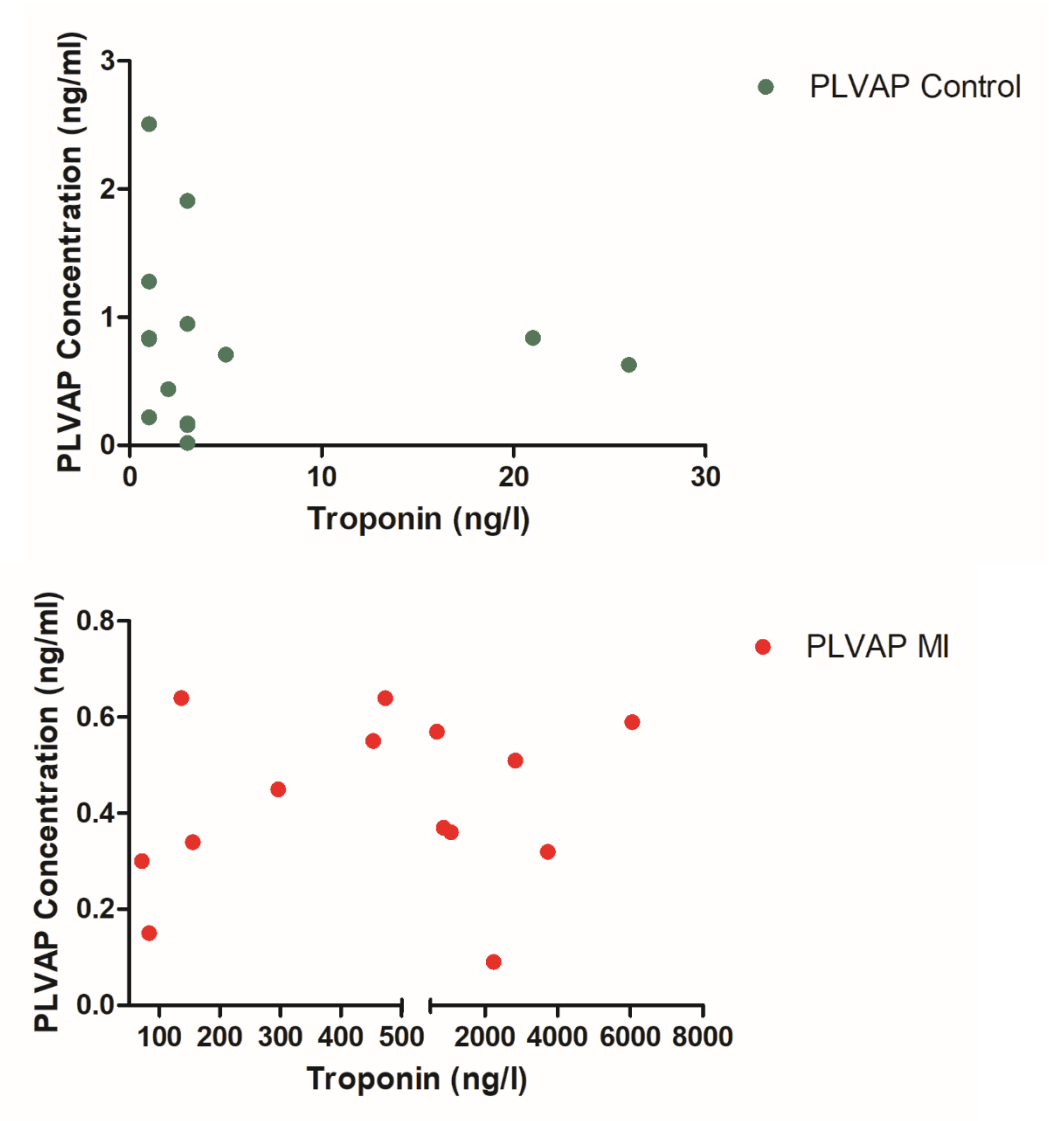

Figure 4.13 PLVAP concentration in EDTA-plasma is not correlated with troponin levels in patients with type 1 MI

Undiluted EDTA-plasma samples from patients of type 1 MI and controls (n=15/group) were processed for a PLVAP ELISA. Troponin levels in patients and controls were not correlated with levels of PLVAP in EDTA-plasma of the same patients (Control; PLVAP concentration *vs* troponin, R^2=0.06627, P=0.7730, Pearson correlation) (MI; PLVAP concentration vs troponin, R^2=0.06602, P=0.7825).

4.5 Discussion

In this chapter, PLVAP was shown to be a novel target with a potential role in neovascularisation in myocardial ischaemia. In the previous chapter, the transcriptional landscape of cardiac ECs 7 days post MI was explored using an established coronary artery ligation model in mice. Analysis of single cell RNA-sequencing data included investigation of heterogeneity of cardiac ECs post-MI, which clustered in 10 different 'states'. Clusters 6, 7, and 8 were of particular interest as they were predominantly composed of cells from the MI group. The transcriptional profile of the ECs that formed these clusters was now further investigated to potentially unravel genes that were significantly upregulated based on the postulation that they might underpin activated regenerative pathways. This identified *Plvap*, which was taken forward for further exploratory analysis in relation to endothelial cell function in the post-ischaemic heart.

The expression and function of PLVAP in response to cardiac injury has not been well characterised. In homeostasis, PLVAP has been shown to be expressed modestly in the heart including the endocardial lining of the heart chambers. [415] When MI injury was introduced in the present study, *Plvap* gene expression levels were significantly increased at 7 days post-MI and expression was localised specifically in ECs in the peri-infarct border zone. Moreover, the percentage of ECs expressing *Plvap* increased significantly. The expression of *Plvap* in mouse cardiac ECs was also increased 4 weeks post-MI which suggests that elevated *Plvap* expression is sustained following injury.

Previous studies have observed PLVAP expression in the capillaries of the heart [415 433] whereas other have not. [411] However, the latter studies[411] did not include a model of injury and could have failed to detect the low levels of expression of PLVAP in homeostasis. The expression pattern of PLVAP in injury was investigated in patients with chronic or acute ischaemic heart disease. Following analysis of the vasculature in areas of fibrosis in heart sections from these patients, the percentage of PLVAP expressing vessels was significantly increased both in acute and chronic MI. Moreover, the majority of these vessels were small capillaries which is aligned with

existing studies that claim that PLVAP is not expressed in ECs of large vessels. [406,411] The presence of PLVAP in many capillary-like vessels both in a mouse model of MI as well as in human patients of acute and chronic ischaemia, suggests that PLVAP is activated in injury and may, therefore, be associated with endogenous neovascularisation responses in areas of ischaemia and fibrosis.

The cellular mechanisms by which PLVAP might have an impact on neovascularisation in post ischaemic injury were investigated. Following silencing of PLVAP in HUVECS an inhibition in proliferative capacity was observed without affecting cell viability, a novel function for PLVAP. The importance of PLVAP in formation of vascular networks is further reinforced by existing studies that investigate the role of PLVAP in tubule formation.[423] When PLVAP was silenced in Human Dermal Microvascular Endothelial Cells (HMVEC) this significantly impaired the ability of those ECs to form cellular networks.[423] This was also the case in HUVECs as well as in other primary ECs.[423] Similar to results presented in this chapter, inhibition of PLVAP did not affect cell viability in those studies.[423] Other studies have also shown that PLVAP enhances angiogenesis; however, these studies have been mostly focused on tumorigenesis. More specifically, PLVAP has been shown to facilitate vascular growth in cancer as inhibition of PLVAP expression *via* small hairpin RNA prevented formation of pancreatic adenocarcinoma in xenografts.[425]

Regarding regulation of PLVAP, existing data have placed VEGF as the prime regulator of PLVAP.[434] VEGF has shown to regulate EC permeability.[435] It is therefore plausible that VEGF regulates PLVAP as PLVAP is an essential component of FDs and SDs which control EC permeability.[411] In fact, studies have demonstrated that treatment of HUVECs with VEGF increased the level of expression of PLVAP *via* a VEGFR2 mechanism.[434] This effect was reversed when using an anti-VEGF monoclonal antibody.[434] Moreover, addition of VEGF to ECs *in vitro* results in increased formation of caveolae and fenestrae. [436] This strengthens the idea that VEGF regulated the expression of PLVAP.

The mechanism of action of PLVAP activation *via* VEGF has been reported to be phosphatidylinositol 3-kinase (PI3K) and p38 mitogen-activated protein kinase(p38MAPK) pathways.[434] Use of the PI3K inhibitor LY294002 and the p38MAPK inhibitor SB203580 resulted in a reduction in the expression levels of PLVAP.[434]

In other studies, VEGF and PLVAP were both found to be upregulated in the retina of diabetic patients with retinal vascular leakage. However, this study did not provide a direct link between the two proteins.[437] Not all studies report a positive relationship between PLVAP and VEGF. Interestingly, the opposite effect was seen in an experiment, using caveolin-1 null mice, that reported that PLVAP in the lung was inversely correlated to higher VEGF.[438] However, this was not the case when using caveolin-2 null mice or wild type mice.[438] These results suggest that caveolin-1 might also have a role in the VEGF-mediated regulation of PLVAP. Moreover, due to the heterogeneity of the endothelium[397] it could be the case that the regulation of PLVAP in ECs varies in different vascular beds.

A different pathway that has been associated with PLVAP is the Wnt/β-catenin pathway. [439–442] This relationship appears to be inverse as downregulation of the Wnt/β-catenin pathway results in upregulation of PLVAP. [439–442] For example, low wnt/β-catenin signaling is associated with blood brain barrier disruption and higher PLVAP expression, a marker of blood brain barrier dysfunction.[441]

Furthermore, an upregulation in key stalk cell markers was observed in a cluster specific manner in cardiac ECs 7 days post-MI. Moreover, using pseudotime analysis, cardiac ECs of cluster 6 were shown to be primed to respond to injury and differentiate into a stalk cell phenotype (cluster 7). This suggests that at day 7 post cardiac injury, evidence of sprouting angiogenesis is present. During sprouting angiogenesis, ECs arrange into stalk and tip cells.[99] Tip cells lead the sprout following an angiogenic factor (such as VEGF) gradient and proliferate minimally.[99] In contrast, stalk cells form the main bulk of the sprout and have a substantially higher rate of proliferation.[99] Stalk cells form branches and form the main vascular lumen. Moreover, they establish junctions with adjacent cells and form the new basement

membrane.[99] The main *in vivo* tools that have helped us elucidate the mechanisms of sprouting angiogenesis focus primarily on the rabbit cornea, the developing mouse retina, and intersegmental vessel growth. [443] However, the level of information in the current literature on sprouting angiogenesis in the heart is limited. Sprouting ECs can be detected in the heart, as shown by Apelin-driven lineage tracing mouse models.[444] Apelin expression is normally low in the adult vasculature but is increased in response to hypoxia and is associated with sprouting angiogenesis.[445] However, the sprouting response is not enough to meet the regenerative demand, even when enhanced by VEGF gene therapy. [445] Moreover, the dynamics of sprouting angiogenesis in the heart are still poorly understood. Furthermore, in the majority, the ECs that adopt the stalk cell phenotype 7 days post MI, also express the gene of interest of this chapter, PLVAP.. PLVAP may be upregulated in stalk cells as they are in a more "immature" and leaky state. This is supported by the fact that PLVAP is found to be a marker of blood brain barrier damage[423] and tumour endothelium.[425] However, PLVAP itself was found to be important in proliferation of ECs in our study, as silencing of PLVAP in HUVECs resulted in attenuation of proliferation *in vitro*.

Following findings that PLVAP expression is increased in hearts of patients with cardiac ischaemia, the question was raised as to whether PLVAP can be detected in the circulation of patients with type I MI as a potential biomarker of ischaemic damage. To date, the concentration levels of PLVAP in the circulation of healthy donors and type I MI patients had not been characterised. In this chapter, PLVAP was reported to be detectable in plasma-EDTA samples at an average level of 0.7967 ng/mL. PLVAP levels however do not increase in patients with type 1 MI. Moreover, the levels of troponin, a marker commonly correlated with myocardial damage[432], were not found to be correlated with PLVAP in healthy controls and type 1 MI patients. This could be explained by the 1h early timepoint that these patient samples were taken post admission. As discussed previously, our data show elevated PLVAP expression in MI in mouse (7 days + 4 weeks post injury) as well as in human patients (acute and chronic MI). The case may be that increases in PLVAP expression is induced at a later timepoint.

Certain limitations of this chapter have to be addressed. Firstly, with regard to the MI specific signature of ECs from clusters 6,7 and 8 it is difficult to assess the area that these cells come from due to the lack of spatial information from tissue dissociation (e.g. area of injury *vs* a remote region). Future studies will assess the spatial characteristics of these cells in more detail (described in section 6.2 future directions). Moreover, the effect of PLVAP should be studied in other functions such as EC migration and *in vitro* angiogenesis (aortic ring model of angiogenesis[446]). As far as the pattern of Plvap protein expression in the heart post-MI, it was observed that the majority of Plvap+ cells were in the border region of the infarct. However, it is currently unclear what is the EC phenotype of these cells (e.g. venous vs arterial). This can be addressed *via* immunostaining of 7day post-MI mouse hearts to target Plvap and canonical vessel phenotype markers (e.g. EphrinB2 for arterial ECs, EphrinB4 for venous ECs). Moreover, mRNA expression results showed that elevated *Plvap expression* in cardiac ECs is sustained up to 4 weeks post-MI. However, due to the "snapshot" nature of the 4-week timepoint it is difficult to assess whether *Plvap expression* remains high following injury or undergoes more dynamic changes. In addition, immunostaining will need to be performed in future studies to ensure consistency in the transcriptomic *vs* proteomic signature of elevated *Plvap* expression at 28 days post-MI. Finally, as far as the levels of Plvap in the circulation of type I patients are concerned, it was observed that Plvap levels did not change in patients *vs* controls. These samples were collected 30 minutes post-admission for a MI event. As higher Plvap expression might be induced at a later timepoint, future studies using later timepoint samples may provide more information on the use of PLVAP as a clinical biomarker.

In summary, the results presented in this chapter show that PLVAP is a novel target potentially associated with neovascularisation in cardiac ischaemia both in acute and chronic mouse model of MI as well as in patients with acute and chronic ischaemic heart disease. Moreover, a novel functional role in regulating EC proliferation for PLVAP was established. Finally, ECs that express PLVAP in injury exhibit an EC stalk cell phenotype. These results provide insight into the potential mechanisms through

which PLVAP exerts its effects on ECs. However, further work is required to decipher the molecular and cellular mechanisms of PLVAP in cardiac ischaemia (described in *6.2 Future directions*).

Chapter 5 *Ex vivo* mouse myocardial slice culture to study the role of VEGF-C in cardiac neovascularisation

5.1 Chapter acknowledgements

I would like to give my thanks to Cardiovascular Science MScR student Bronwyn Berkeley whom I supervised during her rotation in the lab. Her help in performing the experiments and collecting data presented in this chapter was invaluable.

I would also like to thank Dr Jordan Crispin in providing statistical advice for analyses in this chapter.

5.2 Introduction

The development of high-throughput sequencing technologies has generated a wealth of information regarding changes in the transcriptome of cardiac cells in IHD and, more specific to this thesis, during MI. As discussed in previous chapters, such studies have revealed many molecular targets that deserve follow-up to elucidate their biological mechanisms and uncover their potential as therapeutic targets in ischaemic heart disease.

At present, development of new transgenic mouse models with associated disease models are the "gold standard" way to understand the underlying biological mechanisms of targets identified in RNA sequencing studies.[447] However, the development of these models is costly both in terms of funding and time, with transgenic mouse models taking up to a year to construct. As a result, it is not feasible to study all these novel targets in depth.

In vitro techniques in the form of 2D or 3D cultures have been used for decades as a method to study cellular functions.[448] These provide an effective and less costly avenue of investigating cell structure and function in narrowly defined conditions. Moreover, they are easy to genetically manipulate through methods such as RNA interference[449] as well as pharmacological methods such as use of small molecules.[450] These assays provide a high-throughput method for investigating different cellular functions. However, they lack the complexity of *in vivo* models; e.g. the absence of essential components such as extracellular matrix and a multicellular environment. In the realm of drug discovery, many promising pharmaceutical agents have failed to provide a beneficial effect when brought to a more complex *in vivo* model system.[451] Studies of a potentially interesting gene target shown to play an essential role in a biological function *in vitro* may lose these effects when progressed to an *in vivo* model. Such discrepancies can be attributed, in part, to the lack of physiological representation in existing *in vitro* models.

In the context of EC biology and angiogenesis, current *in vitro* methods can aid in the investigation of cellular functions such as migration, proliferation or network/tubule

formation of ECs.[452] However, when looking at the molecular processes of angiogenesis it is clear that these are multicellular in nature and occur in a complex 3-dimensional tissue environment.[99] Therefore, there is an increasing need for a higher complexity model while still maintaining the high throughput of previous models. This can in turn be used to investigate the biology of targets identified in RNA sequencing studies with the aim of guiding future translational studies.

One such model is the myocardial slice culture model.[453] These thin (100 - 400µm) sections of myocardium can be prepared from human or animal cardiac tissues.[453–455] They maintain contractility and electrophysiological function as well as a multicellular structure with extracellular matrix. [453–455] This allows for an *in vitro* model that more closely resembles *in vivo* myocardial properties and has pathophysiological relevance, compared to existing *in vitro* models. Importantly, myocardial slices can be prepared from human biopsies.[377,456] It is known that anatomic and genetic differences between animal models and humans result often in failure in translating findings into the clinic. Myocardial slices prepared from human biopsies can provide a clinically relevant *in vitro* model that is high throughput and offers mechanistic insight. Other human cardiac models that offer similar multicellular characteristics are whole heart preparation in the form of cardiac tissue wedges, trabeculae and Langendorff perfused hearts.[454] However, these cardiac models are very limited in throughput and come with many technical challenges in their maintenance. Thus, myocardial slices are the only human multicellular model that is high throughput, complex and has the capacity for chronic culture and *in vitro* manipulation. There have been a number of studies that have used the myocardial slice model for acute pharmacological testing and *in vitro* toxicology experiments[456–458] as it has a more representative electrophysiological signature compared with other cardiac models.[459]

Additionally, the use of myocardial slices serves the 3Rs: Replacement, Reduction and Refinement which aim to improve animal welfare in research, as multiple myocardial slices can be generated per animal.[450] Furthermore, in many cases, transgenic mouse models are generated for novel gene targets that originated from unreliable existing

in vitro methods. Due to their increased relevance to myocardial physiology, the use of myocardial slices can benefit the 3Rs by reducing the generation of new transgenic mouse models that do not produce expected results.

Mouse myocardial slice preparation and culture in this thesis was adapted from Watson *et al.*, 2017[377] and the detailed method has been described in *section 2.7.2 Myocardial slices*. In brief, the whole mouse heart was dissected followed by removal of the right atrium.[377] Subsequently, the left ventricle was flattened by cutting across the interventricular septum and then sectioned into slices using a high precision vibratome.[377]

Myocardial slices were initially described in 1946 to study metabolism of rat hearts in response to haemorrhagic shock.[460] In 1995, Parrish *et al*[461] showed that heart slices are not able to retain the contractility of cultured cardiomyocytes. However, this has seen substantial improved lately with labs reporting maintenance of a contractile phenotype for up to 3 months[462] in heart slices prepared from human biopsies. The culturing of myocardial slices has been used primarily for studying cardiomyocyte physiology, specifically to recreate a cardiac phenotype *in vitro* including sarcomeres, Ca^{+2} handling and t-tubule structures with the aim of introducing a new assay to test novel therapeutic agents in the context of electrophysiology of cardiac failure.[463]

In this chapter, I explored the use of the myocardial slice culture model to investigate EC biology and more specifically vascular network formation as a response to external stimuli of hypoxia and VEGF-C. The development of the coronary vasculature and the lymphatic system during embryogenesis are mediated by VEGF-C signalling through VEGFR3, which is expressed by blood and lymphatic ECs.[464,465] VEGF-C is typically associated with lymphangiogenesis in postnatal tissues. [466–468] This is due to VEGFR3 expression being thought to be specific to the lymphatic vasculature during the final stages of development [466–468], making VEGF-C a lymphatic EC-specific growth factor, with vascular angiogenesis occurring *via* independent mechanisms.[469,470] However, multiple studies have now shown that VEGFR3 expression is in fact present on adult

vascular ECs, suggesting that VEGF-C signalling may take part in postnatal vascular angiogenesis.[471–474] Furthermore, VEGF-C has been found to be a ligand that binds to several receptors (VEGFR-2, VEGFR-3, NRP-1, and NRP-2) all which have been shown to take part in angiogenesis.[475,476] Moreover, recent studies have shown enhanced lymphangiogenesis and improved cardiac function following injury in the adult mouse heart following treatment with VEGF-C_{156} which is a mutant form of VEGF-C that selectively targets VEGFR3.[477–479] However, the role of VEGF-C in the cardiac vasculature following MI has not been deduced. Interestingly, studies using a rat mesentery model have suggested that lymphangiogenesis is dependent on a preceding angiogenic response driven by VEGF-C.[480,481] Hence, the gap in knowledge of the angiogenic potential of VEGF-C specifically in the heart was the main rationale for the choice of follow up studies in this chapter.

5.3 Experimental design, hypothesis and aims

The following hypothesis was formed:

- *Exogenous VEGF-C and hypoxia can enhance the cardiac neovascularisation response via cardiac endothelial cell proliferation in the mouse myocardial slice culture model.*

The hypothesis will be addressed by the following aims:

1. The increase of VEGF-C expression in mouse cardiac ECs post-MI will be investigated *via* single cell RNA sequencing.
2. The mouse myocardial slice model will be developed using *Pdfdb-iCreER^{T2}-R26R-Brainbow2.1* mice to investigate the effect of hypoxia and VEGF-C in cardiac EC proliferation and angiogenesis (Figure 5.1)
3. Viability of myocardial slices will be assessed via TUNEL staining as a measure of cell apoptosis.[482]
4. Changes in vasculature will be assessed via CD31 immunostaining and analysis with IMARIS software.
5. Cell proliferation will be assessed via ki67 staining[483] and IMARIS analysis.

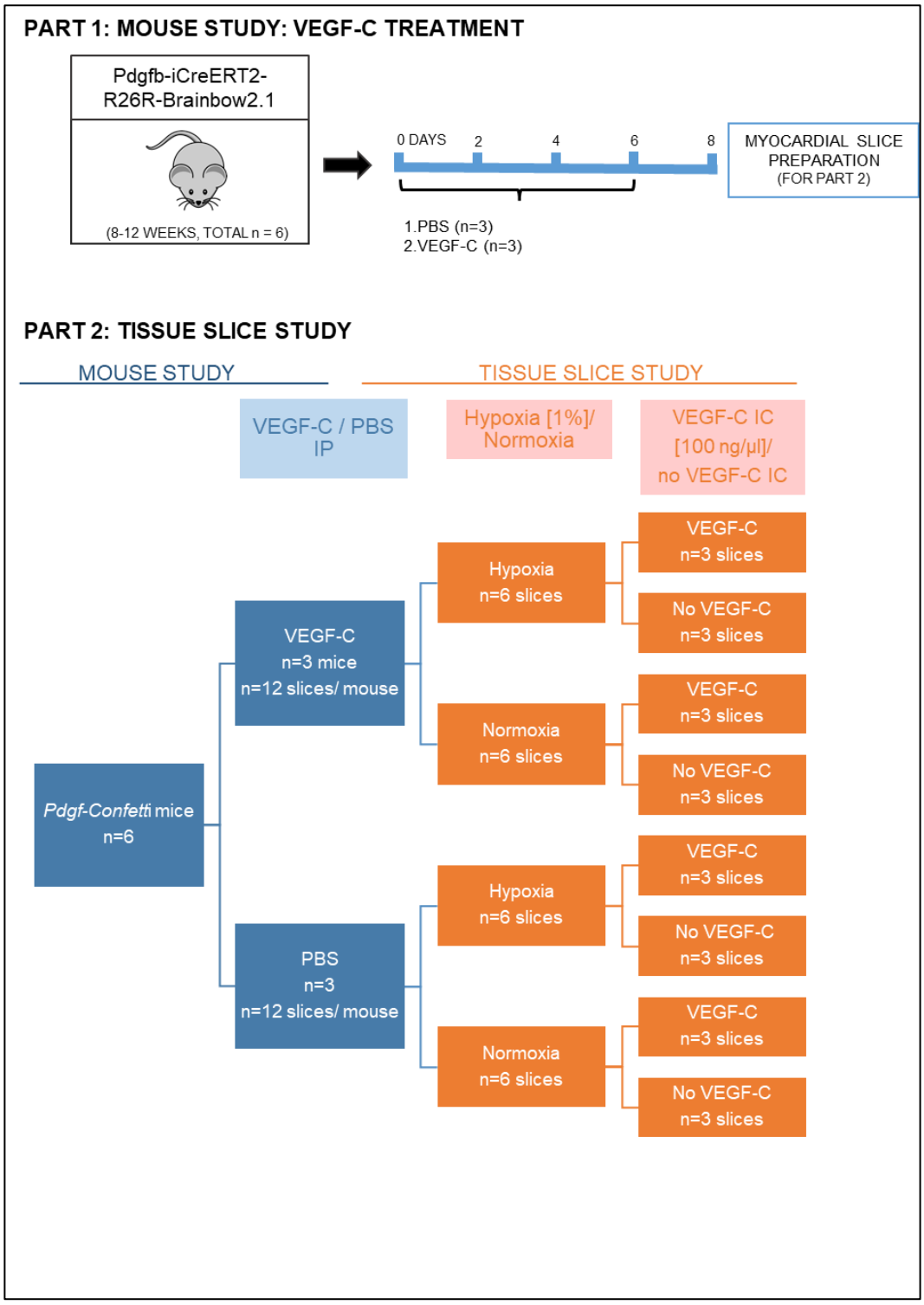

Figure 5.1 Experimental workflow for myocardial slice culture

Part1; *Pdgfb-iCreERT2-R26R-Brainbow2.*1 mice (8-12 weeks) were injected intraperitoneally with PBS (PBS IP, n=3) or human recombinant VEGF-C (0.1 µg/g,

n=3) (VEGF-C IP) at days -1, -3, -5 and -7 before culling and heart tissue collection. Hearts were dissected and myocardial slices prepared. An average of 12 myocardial slices were obtained per mouse. Part 2; Myocardial slices were cultured in 1% hypoxia or normoxia with or without 100 ng/µL human recombinant VEGF-C (VEGF-C IC) for 24 hours. Tissues were fixed in 4% PFA for imaging. IP= intraperitoneal injection, IC= in culture.

5.4 Results

5.4.1 Expression of members of the VEGF-C signalling pathway is increased in mouse cardiac *Pdgfb* lineage ECs at 7 days post-MI

Single cell RNA-sequencing analysis of adult mouse coronary vascular *Pdgfb* lineage ECs revealed differential expression of genes associated with VEGF-C signalling (*Vegfc, Vegfr3/Flt4, Nrp1, Nrp2)* in the healthy and injured heart at 7 days post-MI (Figure 5.2) i.e. during peak neovascularisation.[484,485]

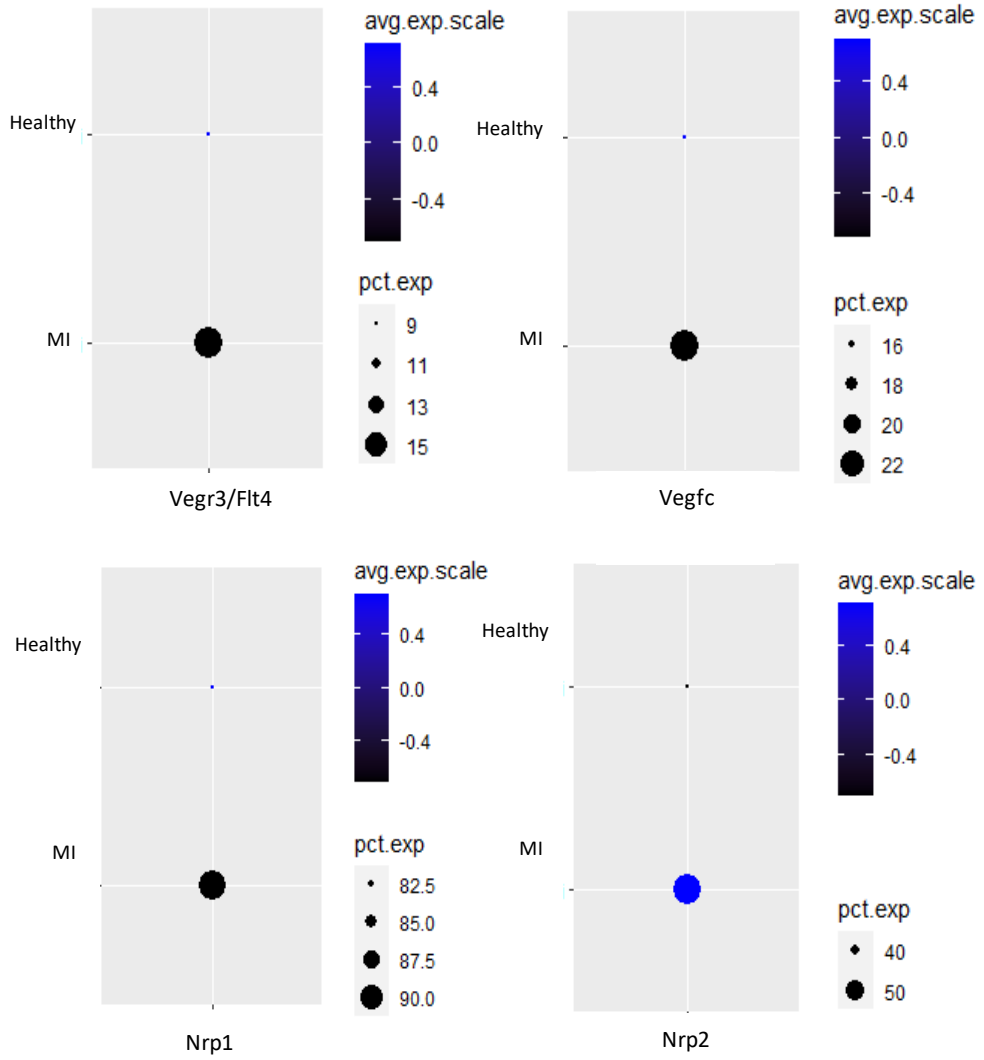

Figure 5.2 VEGF-C signalling related genes are differentially expressed in *Pdgfb* lineage cardiac endothelial cells at 7days post-MI

Dot plots displaying differential average and percentage expression of VEGF-C signalling genes (*Vegfc, Vegfr3/Flt4, Nrp1, Nrp2)* in healthy and 7days post-myocardial infarction (MI). N=4/ group. Mann-Whitney test.

5.4.2 Presence of VEGF-C in culture and hypoxia increases blood vessel network area in myocardial slices

Initially, vascular networks in the myocardial slices were identified by CD31 immunofluorescence staining (Figure 5.3). Subsequently, immunofluorescence was rendered using IMARIS to generate a 3D vascular network. The area of EC blood vessel networks in myocardial slices was determined using IMARIS 3D imaging software (according to section 2.13.2).

Exposure to hypoxia increased blood vessel area when compared to normoxic conditions (P=0.0405) (Figure 5.5). Exposure to VEGF-C in culture increased blood vessel area when compared to slices without VEGF-C in culture (P=0.0277) (Figure 5.5). Furthermore, assessment of blood vessel area via a 3-way ANOVA revealed a significant interaction between the effects of hypoxia and VEGF-C presence in culture (P=0.0385).

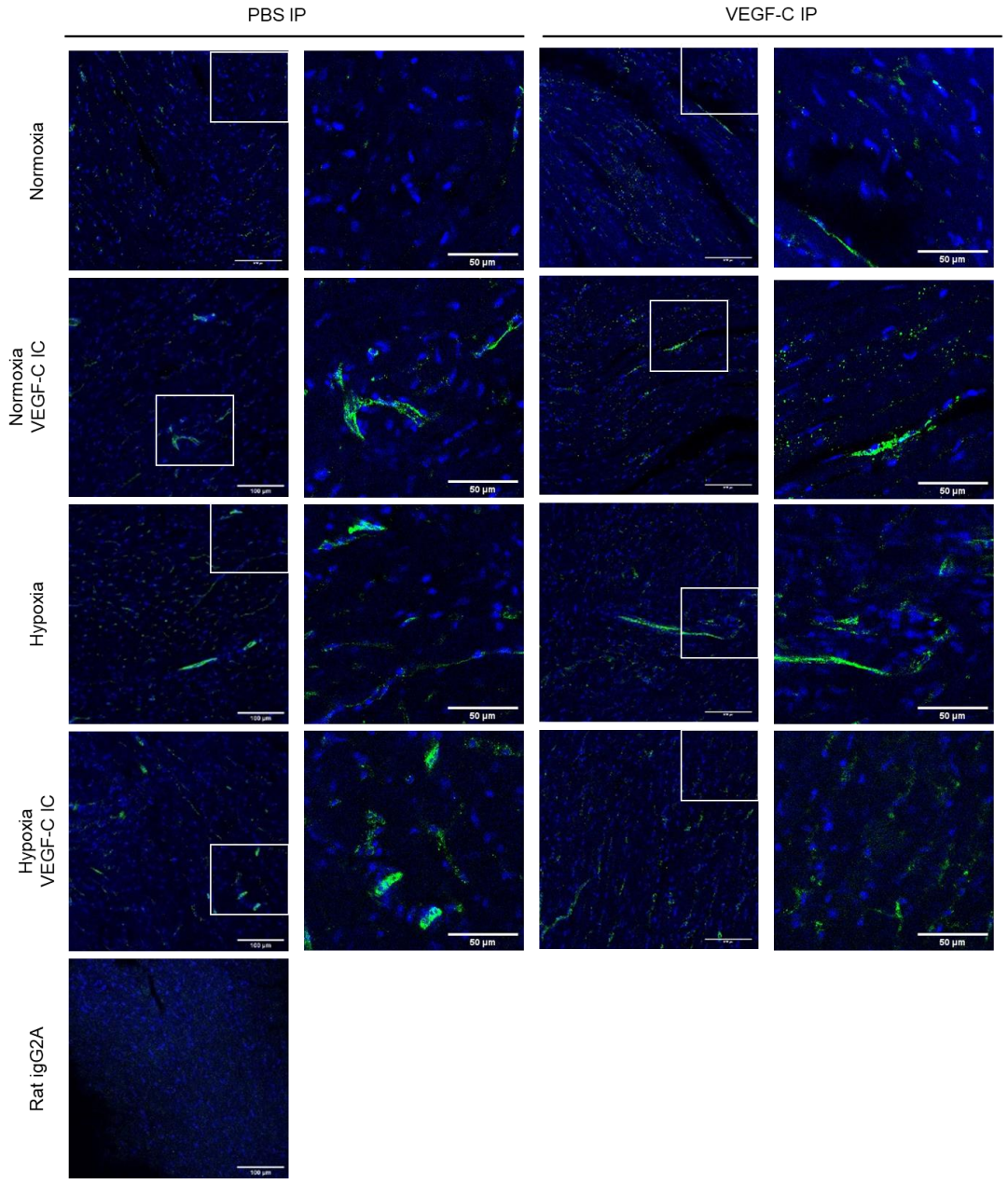

Figure 5.3 CD31 expression in myocardial slices

Mice were injected intraperitoneally (IP) with PBS or VEGF-C (n=3/group), myocardial slices were cultured in hypoxia/normoxia, with/without VEGF-C treatment in culture (IC). Representative images show immunofluorescence staining of CD31 (green) as a marker of ECs[73] with DAPI nuclear stain (blue) in myocardial slices. White boxes highlight magnified area (displayed adjacent to respective image). A rat igG2A isotype was used as a control. Scale bar sizes are =100µm and in magnified regions they are 50µm. IP= intraperitoneal injection, IC= in culture.

A

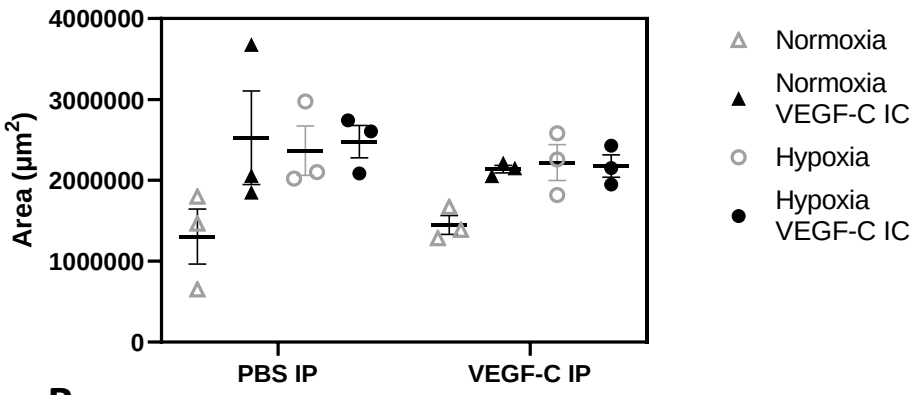

B

Group	Mean	SEM
PBS IP Normoxia	1305633.45	340875.18
PBS IP Normoxia+VEGF-C	2526791.09	577453.39
PBS IP Hypoxia	2366278.22	305069.95
PBS IP Hypoxia+VEGF-C	2477263.51	200472.37
VEGF-C IP Normoxia	1448360.86	116162.02
VEGF-C IP Normoxia+VEGF-C	2137277.24	47187.195
VEGF-C IP Hypoxia	2219147.77	221554.04
VEGF-C IP Hypoxia+VEGF-C	2176191.6	139208.62

C

Interaction	P value
VEGF-C IP vs PBS IP	0.4074
Normoxia vs Hypoxia	0.0405
VEGF-C vs no VEGF-C	0.0277
VEGF-C IP vs PBS IP x Normoxia vs Hypoxia	0.8084
VEGF-C IP vs PBS IP x VEGF-C vs no VEGF-C	0.4132
Normoxia vs Hypoxia x VEGF-C vs no VEGF-C	0.0385
VEGF-C IP vs PBS IP x Normoxia vs Hypoxia x VEGF-C vs no VEGF-C	0.6495

Figure 5.4 The area of blood vessel networks in myocardial slices was increased following culture in hypoxia and with exposure to VEGF-C

(A) Blood vessel area in myocardial slices from PBS or VEGF-C injected mice, cultured in hypoxia/normoxia and VEGF-C/no VEGF-C. Individual data points represent the average of 3 technical replicates (i.e. regions of interest where areas contained CD31 Immunofluorescence and were spaced evenly across the tissue) from each mouse. Each slice per group originated from independent biological replicates (B) Vessel area means and SEMs

for all groups (C) Three-way ANOVA analysing the effect VEGF-C IP, VEGF-C IC and hypoxia on blood vessel area. There were significant main level effects between Normoxia vs Hypoxia (P=0.0405, increase in blood vessel area in hypoxia) and VEGF-C vs no VEGF-C in culture (P=0.0277, increase in blood vessel area with VEGF-C in culture). There was a significant interaction effect between Normoxia vs Hypoxia x VEGF-C vs no VEGF-C in culture (P=0.0385). Data expressed as mean ± SEM. All groups, n=3 mice/group. IP= intraperitoneal injection, IC= in culture.

5.4.3 Presence of VEGF-C in culture and hypoxia increases blood vessel network volume in myocardial slices

The volume of vessel networks in myocardial slices was determined using IMARIS 3D imaging software, based on CD31 expression. Exposure to hypoxia increased blood vessel volume when compared to normoxic conditions (P=0.0234) (Figure 5.5). VEGF-C treatment in culture resulted in an increase in blood vessel volume (P=0.0325). Furthermore, the interaction between the effects of decreased oxygen concentration and VEGF-C IC on blood vessel volume was shown to be significant (P=0.0454) (Figure 5.5).

A

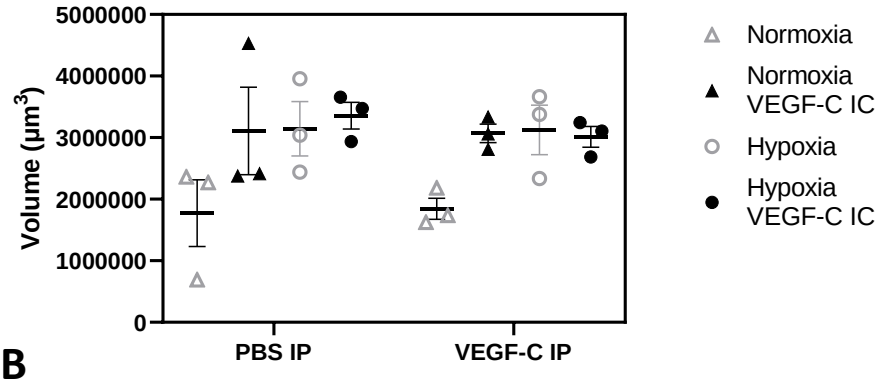

B

Group	Mean	SEM
PBS IP Normoxia	1772750.6	542676.58
PBS IP Normoxia+VEGF-C	3108012.18	711652.2
PBS IP Hypoxia	3144557.94	441769.61
PBS IP Hypoxia+VEGF-C	3355867.33	216344.01
VEGF-C IP Normoxia	1845243.66	170296.58
VEGF-C IP Normoxia+VEGF-C	3068344.29	151289.14
VEGF-C IP Hypoxia	3124930.35	404070.9
VEGF-C IP Hypoxia+VEGF-C	3011091.09	168204.98

C

Interaction	P value
VEGF-C IP vs PBS IP	0.7738
Normoxia vs Hypoxia	0.0234
VEGF-C vs no VEGF-C	0.0325
VEGF-C IP vs PBS IP x Normoxia vs Hypoxia	0.7307
VEGF-C IP vs PBS IP x VEGF-C vs no VEGF-C	0.7049
Normoxia vs Hypoxia x VEGF-C vs no VEGF-C	0.0454
VEGF-C IP vs PBS IP x Normoxia vs Hypoxia x VEGF-C vs no VEGF-C	0.8534

Figure 5.5 Volume of blood vessel networks in myocardial slices was increased following hypoxic culture and exposure to VEGF-C

(A) Blood vessel volume in myocardial slices from PBS or VEGF-C *in vivo* injected mice, cultured in hypoxia/normoxia and with media supplemented with/without VEGF-C. Individual data points represent the average of 3 technical replicates (i.e. regions of interest where areas contained CD31 Immunofluorescence and were spaced evenly across the tissue) from each mouse. Each slice per group originated from independent biological replicates. (B) Vessel volume means and SEMs for all groups. (C) Three-way ANOVA analysing the effect of VEGF-C IP, VEGF-C IC and hypoxia on blood vessel volume. There was a significant independent effect in normoxia vs hypoxia (P=0.2334, increase in hypoxia) and a significant

independent effect in VEGF-C vs no VEGF-C in culture (P=0.0325, increase in presence of VEGF-C in culture). There was a significant interaction effect in blood vessel volume between Normoxia vs Hypoxia x VEGF-C vs no VEGF-C in culture (P=0.0454). Data expressed as mean ± SEM. All groups, n=3 mice. IP= intraperitoneal injection, IC= in culture.

5.4.4 VEGF-C treatment *in vitro* interacts with hypoxia/normoxia to alter the number of blood vessel embedded nuclei in myocardial slices under normoxic conditions

The next aim was to clarify whether the observed increase in vessel area and volume in response to hypoxia and VEGF-C treatment *in vitro* was due to increased EC number. Total EC number within vessel networks was quantified for each group using IMARIS (according to section 2.13.2)

There were no changes in the percentage of ECs observed due to normoxia or hypoxia (P=0.1162), IP injection of VEGF-C prior to sacrifice (P=0.9875), or addition of VEGF-C in culture (P=0.3526), in an independent fashion. (Figure 5.6)**.** However, a significant interaction was detected between the effects of normoxia/hypoxia and VEGF-C presence in culture on the percentage of ECs following analysis using a three-way ANOVA (P=0.0472) (Figure 5.6).

A

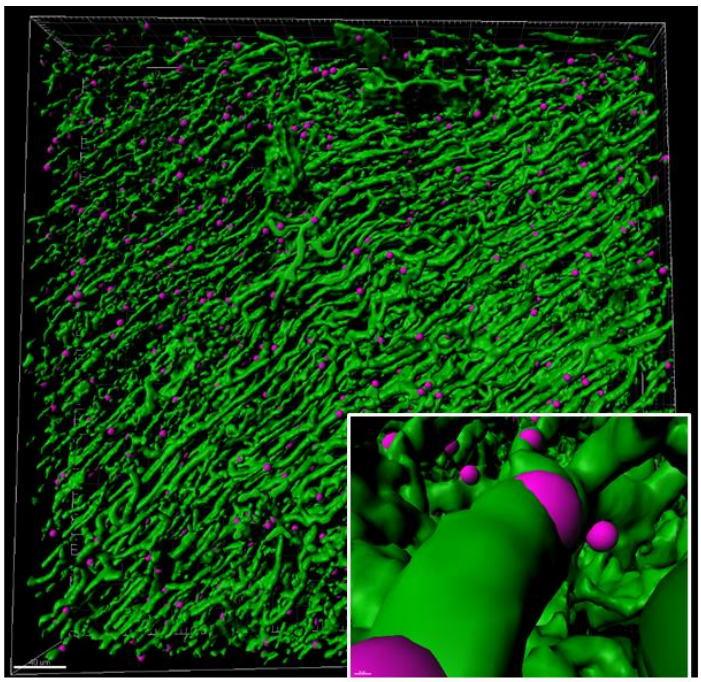

B

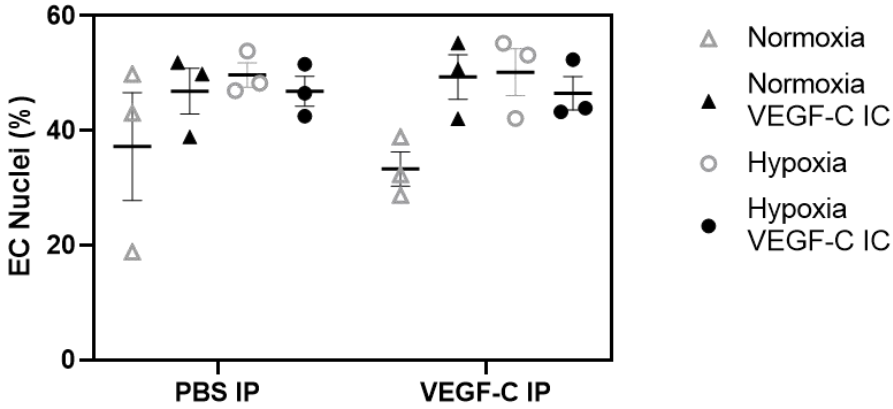

C

Group	Mean	SEM
PBS IP Normoxia	37.2217633	9.4086565
PBS IP Normoxia+VEGF-C	46.8849233	4.0142769
PBS IP Hypoxia	49.71088	2.1109033
PBS IP Hypoxia+VEGF-C	46.87682	2.6125366
VEGF-C IP Normoxia	33.3088667	2.964099
VEGF-C IP Normoxia+VEGF-C	49.3661733	3.8662224
VEGF-C IP Hypoxia	50.1825533	4.0715597
VEGF-C IP Hypoxia+VEGF-C	46.51758	2.9278902

D

Interaction	P value
VEGF-C IP vs PBS IP	0.9194
Normoxia vs Hypoxia	0.0555
VEGF-C vs no VEGF-C	0.1538
VEGF-C IP vs PBS IP x Normoxia vs Hypoxia	0.9058
VEGF-C IP vs PBS IP x VEGF-C vs no VEGF-C	0.6705
Normoxia vs Hypoxia x VEGF-C vs no VEGF-C	0.0232
VEGF-C IP vs PBS IP x Normoxia vs Hypoxia x VEGF-C vs no VEGF-C	0.5814

Figure 5.6 Endothelial cells are increased in number in myocardial slices following treatment with VEGF-C and culture in normoxic conditions

(A) IMARIS 3D rendering of CD31 and DAPI immunofluorescence. The distance from the centre of the nucleus (pink sphere) and vessel surface (green) was set to 1µm. Nuclei 0-1µm from a vessel surface were classed as ECs. (B) The percentage of ECs (from total DAPI+ nuclei) in myocardial slices was calculated in each group; PBS IP or VEGF-C IP, hypoxia/normoxia, and VEGF-C IC/ no VEGF-C IC. Individual data points represent the percentage of ECs from each slice. Each slice per group originated from independent biological replicate. (C) Means and SEMs of percentage ECs per group (D) Three-way ANOVA analysing the effect of VEGF-C IP, VEGF-C IC and hypoxia on the percentaeg of ECs. There were no significant independent effects observed. There was a significant interaction effect in the percentage of ECs observed between Normoxia vs Hypoxia x VEGF-C vs no VEGF-C in culture (P=0.0232). Data expressed as mean ± SEM. All groups, n=3 mice. IP= intraperitoneal injection, IC= in culture.

5.4.5 Cell proliferation in cultured mouse myocardial slices is not affected by hypoxia, exposure to VEGF-C *in vitro,* or IP administration of VEGF-C

Having shown that VEGF-C IC and hypoxia increased blood vessel area and volume, and that the percentage of blood vessel embedded nuclei increased when exposed to VEGF-C IC under normoxic conditions; the next aim was to evaluate the overall levels of cell proliferation. The total level of cell proliferation in myocardial slices in each group was assessed by performing Ki67 immunostaining. However, Ki67 expression was not significantly affected by hypoxia, VEGF-C IC and VEGF-C IP (Figure 5.8).

A

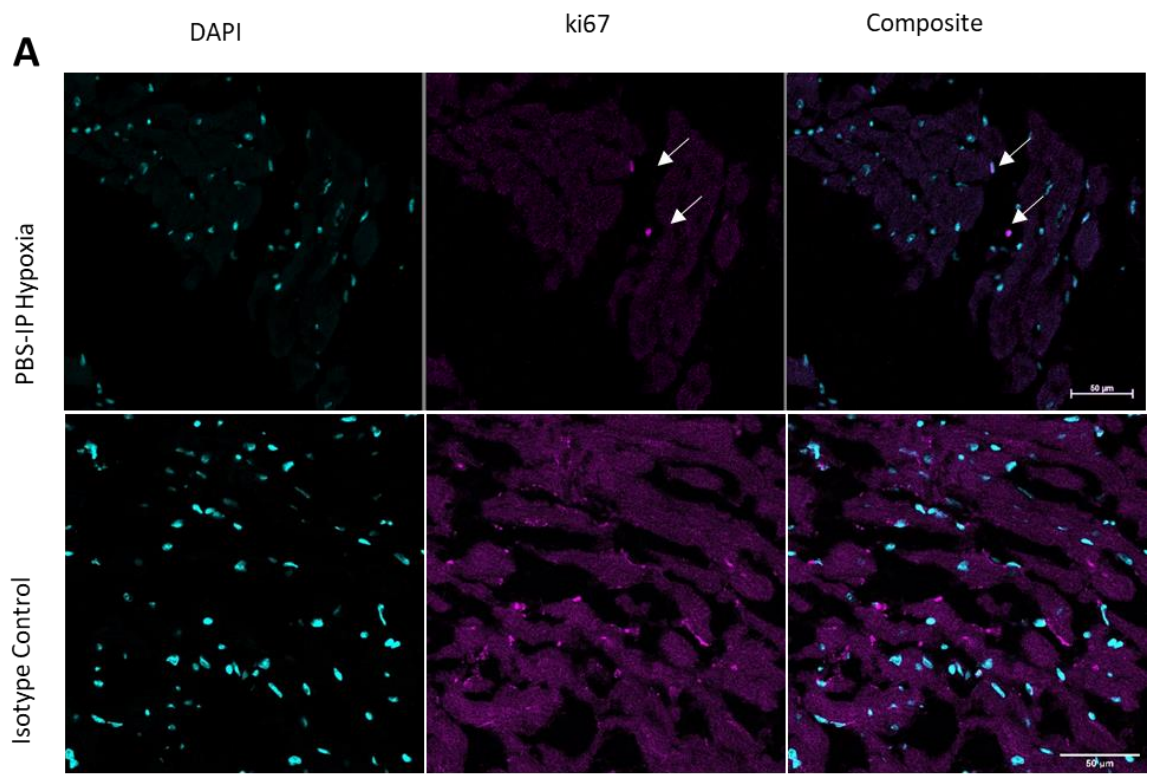

B

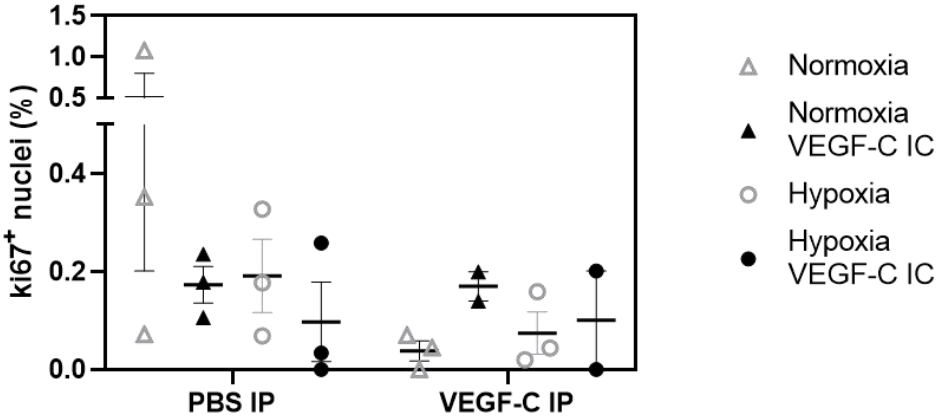

C

Group	Mean	SEM
PBS IP Normoxia	0.50033333	0.2994486
PBS IP Normoxia+VEGF-C	0.173	0.0373229
PBS IP Hypoxia	0.191	0.0748064
PBS IP Hypoxia+VEGF-C	0.09733333	0.0809307
VEGF-C IP Normoxia	0.03833333	0.0204803
VEGF-C IP Normoxia+VEGF-C	0.1695	0.0295
VEGF-C IP Hypoxia	0.07433333	0.0428965
VEGF-C IP Hypoxia+VEGF-C	0.1005	0.1005

D

Interaction	P value
VEGF-C IP vs PBS IP	0.9643
Normoxia vs Hypoxia	0.5932
VEGF-C vs no VEGF-C	0.8932
VEGF-C IP vs PBS IP x Normoxia vs Hypoxia	0.6086
VEGF-C IP vs PBS IP x VEGF-C vs no VEGF-C	0.4135
Normoxia vs Hypoxia x VEGF-C vs no VEGF-C	0.5196
VEGF-C IP vs PBS IP x Normoxia vs Hypoxia x VEGF-C vs no VEGF-C	0.6241

Figure 5.7 *In vivo* VEGF-C injection, hypoxia and VEGF-C treatment *in vitro* does not affect cell proliferation

(A) Representative images of DAPI and ki67 immunofluorescence in cryosections of myocardial slices. ki67 positive cells indicated with white arrows. Isotype control was rat igG2A. Scale bar = 50µm. Isotype expression did not colocalize with nuclear DAPI signal in the nucleus. (B) Percentage of ki67 positive cells in myocardial slices from PBS or VEGF-C injected mice, cultured in hypoxia/normoxia and VEGF-C/no VEGF-C (n=3 slices per group, n=2 slices VEGF-C IP/ Normoxia/ VEGFC-IC & VEGF-C IP/ Hypoxia/ VEGF-C IC. Individual data points represent the average of 3 technical replicates (i.e. regions of interest where areas contained CD31 Immunofluorescence and were spaced evenly across the tissue) from each mouse. Each slice per group originated from independent biological replicate. (C) Means and SEMs of % ki67 positive cells detected in myocardial slices (D) Three-way ANOVA of the effect of *in vivo* VEGF-C injection, hypoxia and VEGF-C treatment *in vitro* on the percentage of ki67 positive cells. There was no overall difference observed. Results are expressed as mean ± SEM. IP= intraperitoneal injection, IC= in culture.

5.4.6 The rate of cardiac cell apoptosis in cultured myocardial slices is not influenced by hypoxia, presence of VEGF-C in culture or VEGF-C injections

A TUNEL assay[482] was used to determine whether the myocardial slice culture process and conditions had an influence on cell integrity (Figure 5.8). 46.23 ± 3.16% of cells were apoptotic in the myocardial slices following 24 hours in culture (n=22, from all groups) (A, Figure 5.9). When comparing between the groups, intraperitoneal injection of VEGF-C, oxygen concentration (normoxia/hypoxia) or *in vitro* culture in VEGF-C did not significantly affect the percentage of apoptotic cells. (B, C, D Figure 5.9).

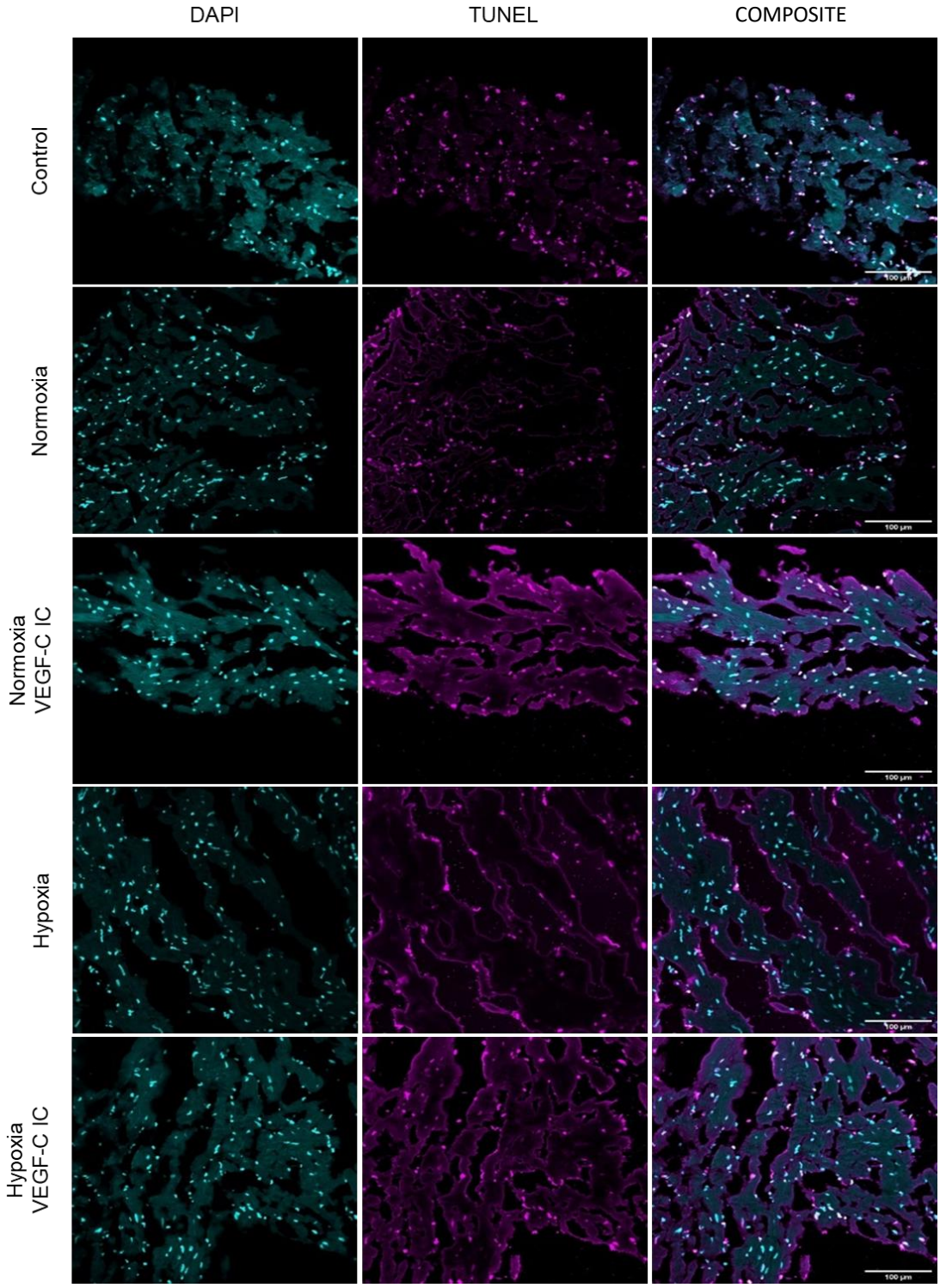

Figure 5.8 *In vivo* VEGF-C injection, hypoxia and VEGF-C treatment *in vitro* does not influence apoptosis in cultured myocardial slices.

TUNEL assay was performed on sections of myocardial slices (5µm) as a measure of apoptosis. Effect of VEGF-C injection, oxygen concentration and VEGF-C in culture on apoptosis assessed by TUNEL staining. Control = TUNEL positive control. Scale bar = 100µm.

A

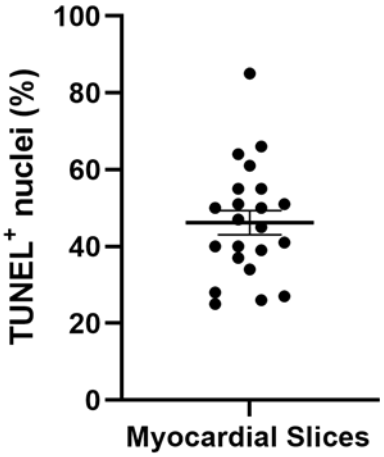

B

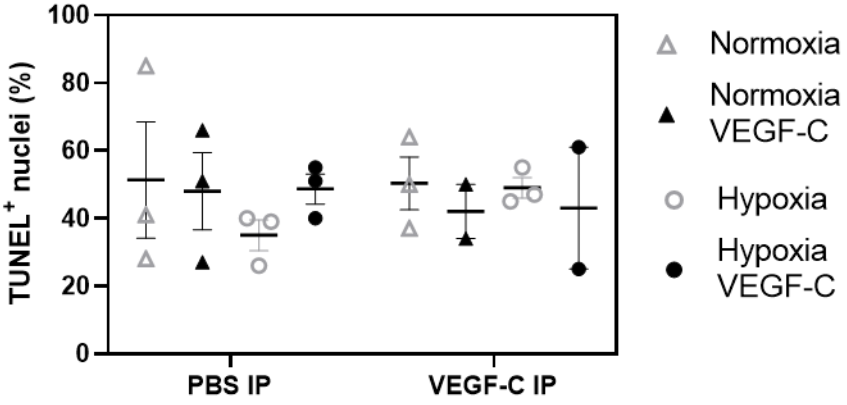

C

Group	Mean	SEM
PBS IP Normoxia	51.33	17.25
PBS IP Normoxia+VEGF-C	48.00	11.36
PBS IP Hypoxia	35.00	4.51
PBS IP Hypoxia+VEGF-C	48.67	4.48
VEGF-C IP Normoxia	50.33	7.80
VEGF-C IP Normoxia+VEGF-C	42.00	8.00
VEGF-C IP Hypoxia	49.00	3.06
VEGF-C IP Hypoxia+VEGF-C	43.00	18.00

D

Interaction	P value
VEGF-C IP vs PBS IP	0.9643
Normoxia vs Hypoxia	0.5932
VEGF-C vs no VEGF-C	0.8932
VEGF-C IP vs PBS IP x Normoxia vs Hypoxia	0.6086
VEGF-C IP vs PBS IP x VEGF-C vs no VEGF-C	0.4135
Normoxia vs Hypoxia x VEGF-C vs no VEGF-C	0.5196
VEGF-C IP vs PBS IP x Normoxia vs Hypoxia x VEGF-C vs no VEGF-C	0.6241

Figure 5.9 *In vivo* VEGF-C injection, hypoxia and VEGF-C treatment *in vitro* does not affect apoptosis in cultured myocardial slices (cont.)

TUNEL assay was performed on sections of myocardial slices (5µm) as a measure of apoptosis. (A) Overall apoptosis levels across all slices, 46.23 ± 3.16, n=22 slices. (B) TUNEL-positive cells (%) across the different groups (n=3 slices per group, n=2 for VEGF-C IP/ Normoxia/ VEGFC-IC & VEGF-C IP Hypoxia VEGF-C IC. Individual data points represent the average of 3 regions of interest (technical replicates) selected randomly within each slice, avoiding the edge of the tissue. (C) TUNEL-positive percentage means and SEMs for all groups. Each slice per group originated from independent biological replicates. (D) Three-way ANOVA analysing the effect of VEGF-C IP, VEGF-C IC and hypoxia on the percentage of TUNEL-positive cells. There was no overall difference in apoptosis. Data expressed as mean ± SEM. IP= intraperitoneal injection, IC= in culture.

5.5 Discussion

The aim of this chapter was to develop a model of *ex vivo* myocardial slice culture to study neovascularisation in the heart in an *in vitro* manner while still maintaining the complexity of the heart's cellular architecture. Existing cell culture methods studying EC contribution in neovascularisation have limitations as they do not provide the complexity of *in vivo* models. This is especially the case when investigating multicellular processes such as angiogenesis.[486] Hence, a model with more complexity that has increased translational potential is required. Furthermore, this model would need to be amenable to external stimulation and manipulation in the form of application of small drug molecules or genetically via gene therapy in order to study mechanisms in depth. Here, exogenous VEGF-C was successfully used to initiate a change in cardiac vasculature. Existing published studies that have used the myocardial slice culture model have focused primarily on cardiac electrophysiology[487] and *in vitro* drug safety screening.[488] No studies to date that have used this model to investigate cardiac EC dynamics in the context of cardiac angiogenesis/neovascularisation.

A point that is worthy of discussion is the rate of cell apoptosis that was observed in this study and its potential effects on the rest of the results. The proportion of apoptotic cells in the myocardial slice model could be considered high (46.23 ± 3.16%). Watson and colleagues[377] reported that 59.94 ± 4.35% of cells were alive on the surface of rat myocardial slices and 47.42 ± 4.59% of cells were alive on the surface of human HF slices. However, they reported that below the slide surface almost all cardiomyocytes were alive. A more recent study by the same group reported that the proportion of viable cells on the slide surface after 1 day in culture was 75% on average but ranged from 40% to 85%.[489] The rate of apoptosis in the presented study due to slicing damage or the culturing process cannot be excluded. However, there is one explanation that is worth considering. The rate of apoptosis in this study was investigated via TUNEL staining of thin (5µm) cryosections sections that were prepared from 200µm thick sectioned myocardial slices. As seen from the studies referenced above there is a discrepancy between the levels of cell death in

the surfaces of the myocardial slices and the inner layers of the tissue.[377] For this reason, the inner layer of slices were chosen for TUNEL staining to identify the rate of apoptosis. Following sectioning with the vibratome, these slices were embedded and frozen in Optimal Cutting Temperature (OCT) media for 5 µm sectioning and TUNEL staining. The perfect horizontal orientation of the 200µm in embedded OCT is technically challenging. As a result, upon sectioning, the sections obtained could contain cells that were part of the surface thus increasing the percentage of apoptotic cells detected. In the future, TUNEL staining of whole myocardial slices can be performed to address this issue. Moreover, in this study the identity of the cardiac apoptotic cells was not investigated. In the future, co-staining of TUNEL with cell specific markers (TNNT2 for cardiomyocytes, CD31 for ECs, RGS5 for pericytes, DCN for fibroblasts) can be used to identify if there is a particular cardiac cell type susceptible to apoptosis during culture or is in fact a mixture.

Another explanation for the high rate of apoptosis that was observed is the encasing of the heart into agarose prior to slicing, resulting in damage due to hypoxia. Agarose embedding for organotypic tissue slice culture has been used successfully before [490] but more recent studies advocate against it due to potential hypoxic damage.[377,453–455] In this study, the agarose casing was chosen out of necessity, due to the available equipment. The vibratome that was available for this project requires lateral mounting of the specimen. If used without agarose, then the tissue would only be held via tissue glue on the specimen holder, thus making it unstable and prone to falling. In the published studies where agarose is not used, the vibratome that is used requires horizontal mounting of the sample which is glued to the specimen holder via tissue glue.[377] However, although the use of agarose in myocardial slice preparation is not ideal, sample apoptosis due to agarose-induced hypoxia is unlikely as the addition of a 4^{o}C Tyrode's solution supplemented with 30mM 2,3-Butanedione Monoxime during slicing, reduces the energetic demands of the myocardium and minimizes the possibility for ischaemia.[453]

Another consideration is the choice of media for culture. The media chosen for this study were also used in the original myocardial slice preparation protocol.[377] That

study only showed substantial cell death on the surface of the myocardial slices. Thus, there is no reason to suggest that the choice of media contributed to apoptosis. Interestingly, more recent studies suggest that the culture medium used (Medium 199) is not sufficient to support the high energy demands of the cardiac tissue; and thus opted for 10% FBS, VEGF and FGF supplementation and made the case that they are essential.[491] The same study suggested that the liquid-air interface culture that is used in this study but also many others [489,492,493] contributes to cell death. Hence, they developed a submerged culture methodology that showed good myocardial slice viability for up to 6 days.[491] It is worth mentioning that different studies claim that nutrient demands in myocardial slice culture are fulfilled by serum free media.[462] Evidently, more work needs to be conducted to deduce the optimal culture media conditions for maximum myocardial slice viability but also similarity to the *in vivo* environment.

The mouse myocardial slice model is not used frequently, even by the most experienced groups in using the model. Recent reviews state that using mouse tissue for myocardial slice preparation comes with many technical hurdles as the heart is too small resulting in pronounced curved geometry and difficultly in handling, potentially resulting in reduced viability. [454] For this reason, myocardial slice preparation has shifted more to using slices prepared from rats, rabbits and human biopsies.[454]

A limitation that needs to be acknowledged is the lack of electro-mechanical stimulation in our model of myocardial slice culture. Recently, studies have suggested that, for the adult cardiomyocyte phenotype to be maintained in culture, there needs to be a physiological mechanical force applied as well as electrical stimulation.[492] When this is not the case, the transcriptomic profile of cardiomyocytes as well as their structure and function is prone to de-differentiation. Hence, results generated in this chapter should be validated using a myocardial slice model that includes mechanical force and electrical stimulation.

The gold standard method of culturing myocardial slices was initially described by Brandenburger and colleagues[494] and involved culturing in a liquid-air interface using a semi-porous tissue culture insert. This allows for cell survival up to 28 days. However, cardiomyocytes can undergo substantial dedifferentiation due to lack of flow, electrical stimulation and mechanical loading.[489] Moreover, there is proliferation of stromal cells and loss of usual ultrastructure myocyte phenotype.[489] Experiments using myocardial slices by Brandenburger and colleagues[494] showed good viability, β-adrenergic response and maintenance of electrophysiological properties for 28 days. However, loss of structural and functional integrity after 24 hours in culture as evident by loss in contractility and reduction in mRNA levels of α-actin. [494] Interestingly, static mechanical loading using A-frame stretches greatly reduced the rate of proliferation of cardiac fibroblasts on cultured myocardial slices at 3 and 7 days.[489] In general, slices have been shown to remain viable in culture for up to 3 months but this comes at a severe de-differentiation cost and change in transcriptomic and proteomic profile.[494]

In 2019, efforts were made to improve the similarities of myocardial slices to the *in vivo* environment. This includes electrical stimulation, mechanical loading (preload and afterload) as well as improved oxygenation and nutrient support. [462,493,495,496] More specifically, Qiao and colleagues[496] developed an automated heart-on-a-chip culture system using myocardial slices and enhanced culture conditions with continuous O_2/CO_2 control, an orbital shaker, media circulation , static mechanical loading and electrical stimulation.[496] Moreover, Watson and colleagues[493] aimed to improve the myocardial slice culture model via application of simultaneous electrical stimulation and preload on rat, rabbit and failing human heart slices.[493] Myocardial slices were progressively loaded to different sarcomeric lengths and achieved sub-micrometer resolution. Their results suggest that electromechanical stimulation while in culture is critical at preventing dedifferentiation. This was the case up to 5 days when using rabbit myocardial slices. Interestingly, hypertrophic genes and calcium transient amplitude were found to be upregulated after 24 hours in culture in comparison to fresh heart slices. However, cardiomyocyte size did not vary even

with these changes. This suggests that even though these improvements bring the myocardial slice model closer to the *in vivo* environment, they are still not totally representative. A different study that aimed to investigate the effect of mechanical stimulation to resident cells in the myocardial slices showed that mechanical loading attenuated cardiac fibroblast proliferation. [489] Moreover, cardiac fibroblasts in slices kept their structure longer than those singly cultured. In culture, cardiac fibroblasts started expressing αSMA within a few days whereas in slices that was not the case until day 7. [489]

Furthermore, Ou and colleagues[491,495] showed that despite proprietary culture media, frequent oxygenation, and electrical stimulation, myocardial slices showed dedifferentiation by day 10 in the form of loss of contractility and disruption of expression of more than 500 genes. This suggests that myocardial slices can be used over the span of a few days for testing, but techniques for long-term culture need improvement. In the future, new developments of the myocardial slice model, namely electromechanical stimulation, will be added to increase viability and similarity to the *in vivo* cardiac environment to study EC dynamics in the context of cardiac angiogenesis/neovascularisation.

Another limitation of the myocardial slice model is the lack of capillary flow dynamics, as all nutrient exchange is achieved through passive diffusion. Despite the myocardial slice model being improved constantly, the introduction of capillary flow will be something that will be difficult to achieve, considering the most recent iterations of the model.[453] Moreover, in order to accurately simulate the *in vivo* heart environment in culture there would be a need for hormonal and adrenergic stimulation, which is absent from most myocardial slice model iterations.[453] In addition, in spite of the myocardial slice model being shown to be beneficial in drug testing and discovery, especially in the realms of toxicology,[456–458] a limitation of the system is the lack of accurate *in vivo* pharmacokinetics as the majority of drug metabolism occurs in the liver.[497]

Sampling awareness in myocardial slice preparation is crucial. From the latest single cell RNA sequencing studies, it is clear there are anatomical differences between similar cell types in the heart.[498] Current studies utilizing myocardial slices tend to use tissue prepared from the left ventricle, as described in this thesis chapter. However, depending on pathology, different regions might be more appropriate; for example using the right ventricle to investigate right ventricular hypertrophy. Moreover, an important point is the acknowledgement of the difference in properties across the layers of the cardiac wall i.e. endocardium, myocardium, epicardium. For instance, the epicardium is known to harbour cell populations that are currently being investigated for their regenerative properties.[499]

In this study, the target of choice was VEGF-C, a member of the VEGF ligand family and a critical regulator of angiogenesis and lymphangiogenesis. [104] VEGF-C has been previously shown to also play an essential role in the lymphangiogenic responses in the heart post-MI.[500] Moreover, treatment with VEGF-C in mouse models of MI resulted in improved cardiac function.[500] However, its role in blood vessel angiogenesis in the heart is not well understood. The *in vivo* administration of VEGF-C prior to myocardial slice culture was found to not affect vascular network area, volume or EC proliferation. However, this could be due to the lack of sufficient stimulation like *in vivo* ischaemia. Ischaemia may prime the vascular environment and could perhaps be a pre-requisite for repair[501] and endogenous vascular activation by VEGF-C. On the other hand, exogenous VEGF-C added in culture was found to contribute to changes in vasculature in an independent manner but also in conjunction with hypoxia. An explanation for this may be that the myocardial slice culture process is a form of stress following slicing and culture which activates the VEGF-C induced changes in vasculature**.** Regarding the mechanism involved, VEGF-C primarily binds to VEGFR3 but also VEGFR2, albeit at a reduced affinity.[502] VEGF-C has been found to regulate angiogenesis when binding with VEGFR2. [502] Moreover, intramyocardial injection of VEGF-C can induce the establishment of collateral circulation in ischaemic myocardium, thus strengthening the claim of the potency of VEGF-C in the cardiac vasculature. [503] In the context of the myocardial slice model,

future work investigating the expression of members of the VEGF-C signalling pathway will be useful at elucidating similarities and differences with the aforementioned mechanistic studies about VEGF-C.

Hypoxia in culture also stimulated a pro-angiogenic response. Angiogenesis was indicated by an increase in the area and volume of the vascular network. An increased number of ECs confirmed that EC proliferation was the likely mechanism of vascular network activation following VEGF-C administration *in vitro*. Hypoxia inducible factors (HIFs) are a family of transcription factors that respond to hypoxia and regulate several processes required for angiogenesis. VEGF-C is a specific target for hypoxia inducible factor 2α (HIF2α).[504] This indicates the potential for hypoxia priming for EC repair at the transcriptional level. Mice that were pre-conditioned with VEGF-C prior to myocardial slice preparation, with further exposure to a hypoxic environment in culture, did not demonstrate enhanced vasculature activation. This indicates that there may be a physiological limit to the level of angiogenic stimulation achievable in myocardial slice culture. Similarly, it could indicate that they may be acting on the same pathway. Furthermore, hypoxia may have induced HIF2α and enhanced endogenous VEGF-C expression.

As far as proliferation levels are concerned, while there was no overall difference in total cell proliferation based on ki67 immunostaining, EC proliferation was increased following VEGF-C treatment, based on data showing increased blood vessel embedded nuclei in myocardial slices cultured in normoxia and VEGF-C. Ki67 is expressed during G1, S, G2 and mitotic phases of the cell cycle, but not G0.[483] Ki-67 is a late marker of cell-cycle entry and Ki-67 mRNA levels are highest in G2 while protein levels increase throughout the cell cycle, peaking in mitosis.[505] Cells may have already entered the cell cycle in response to VEGF-C and hypoxia, and then quiesced in G0. Thus, staining for ki67 may not be an informative method of assessing proliferation. It would be beneficial to examine EC proliferation specifically, and to introduce a timecourse of analysis. Ki67+/CD31+ cells could be quantified to specifically determine the effect of VEGF-C injection, oxygen concentration or culture in VEGF-C on EC proliferation.

A complex model such as the myocardial slice culture model is closer to the *in vivo* tissue environment and is thus better suited for translational research. However, it is worth mentioning that the complex nature of the model can hamper the identification of cause-effect relationships due to the multicellular and complex structural nature of the myocardial slice model. At the same time, less complex and reductionist models can aid in understanding cause-effect relationship in an easier way but at cost of harder translation ability. This fine balance is core to experimental model choice and should be always hypothesis-dependent in order to choose the best model depending on experiment question and design. In the context of this study, the enhancing effect of exogenous VEGF-C to the cardiac vasculature in the myocardial slice model is described and opens many opportunities for improvements in the culture model itself but also in the manner of specific target manipulation with the aim of enhancing the endogenous cardiac neovascularisation response. However, the level of cardiac cell apoptosis will need to be addressed in a more accurate way in the future to assess impact on results.

Chapter 6 Discussion & future work

6.1 Key findings

6.1.1 The healthy adult mouse heart undergoes endothelial cell turnover *via* clonal proliferation

The adult endothelium was originally thought to be in a state of quiescence, which was defined as a state in which ECs are not stimulated but are instead waiting to be activated by incoming signals.[73] The paradigm has now shifted to the idea that the endothelium is instead in a state of "active quiescence" that retains its incredibly dynamic functions. This involves a multitude of simultaneous dynamic molecular mechanisms, including signalling by FGF, VEGF, Wnt, Angiopoietin, BMP and TGFβ, that maintain the homeostatic functions of the endothelium according to the needs of each vascular bed.[506]

Using the *Pdgfb-iCreER^{T2}-R26R-Brainbow2.1* lineage tracing mouse model, this thesis showed that ECs with a *Pdgfb* lineage undergo turnover *via* clonal proliferation in the healthy adult mouse heart. This information adds to recent evidence that the EC population of the heart is dynamic under physiological conditions and is in fact the population with the highest turnover in the human heart in homeostasis.[161] More specifically, the whole EC population is fully exchanged every 6 years in human adulthood at a rate of 16.7% per year in adult life.[161] Importantly, results from this thesis show that the cellular mechanism behind this turnover is local clonal expansion of cardiac resident ECs. However, it is not currently clear if there are other turnover cellular mechanisms at play in the adult mammalian heart. Possible scenarios include differentiation from vascular wall-resident stem and progenitor cells (VW-SC) that reside in the adventitia of the vessel wall.[68] Older studies in the 1970s have shown that vessel wall ECs retained the capacity to undergo self-replication, possibly through clonal expansion. [168,169] However, this thesis investigated *Pdgfb* lineage ECs only. Different EC lineages in the heart could exhibit different homeostatic cellular mechanisms of turnover. In summary, this thesis increases current evidence of the dynamic nature of EC turnover in the adult mammalian heart and shows that the cellular mechanism is that of clonal proliferation.

6.1.2 Clonal proliferation of cardiac endothelial cells is a key mechanism of neovascularisation following myocardial infarction, with minimal contribution from the bone marrow

A key finding from this thesis is that clonal expansion of resident cardiac ECs is a cellular mechanism that underpins neovascularisation in the post-MI heart. Tracing cardiac ECs using a *Pdgfb-iCreER^{T2}-R26R-Brainbow2.1* adult mouse model showed large monochromatic clones of ECs contributing to the neovascularisation of the infarcted area at 7 days post-MI. These results expand on existing studies showing that pre-existing cardiac ECs form new vessels after cardiac ischaemia.[133] Moreover, this finding is consistent with recent findings by Manavski *et al.* that showed *Cdh5+* cells contributing to the generation of perfused and mature microvessels at 7 and 14 days post-MI *via* clonal proliferation.[396] The phenotype of the ECs that form these clones is still unclear. Ideas range from the existence of a subset of adult cardiac ECs with progenitor-like characteristics to micro-environmental changes that stimulate ECs to clonally proliferate but further work is required to decipher this.

The additional piece of evidence of clonal expansion of cardiac ECs post-MI that this study provides adds to the complicated literature of EC contribution to new vessels that are formed following myocardial injury. [146] Other studies have suggested that contributions from non-EC lineages, such as cardiac fibroblasts, is likely.[146] However, the most up to date lineage tracing mouse model has shown that the contribution of non-EC sources to the newly formed vasculature is minimal.[133] [134] Studies investigating the EC contribution to the post-MI vasculature have shown that ECs can also be derived from the endocardium[134], epicardium[144] and from migration of cells from the bone marrow and/or the circulation during ischaemic injury .[397,398] This topic gets more complicated when pro-angiogenic paracrine mechanisms from different cell populations are considered. For instance, epicardium-derived cells have been suggested to promote neovascularisation in the infarct region by secreting paracrine factors such as VEGFA, FGF2, Wnt family member 1 and thymosin beta 4 that stimulate EC proliferation and angiogenesis.[142]

Importantly, this thesis demonstrated that the *Pdgfb* lineage ECs that participate in neovascularisation in the peri-infarct border in the post-MI adult mouse heart via clonal proliferation do not derive from the bone marrow. This could explain in part the disappointing results of clinical studies using autologous bone marrow-derived cells for therapeutic angiogenesis in patients with ischaemic heart disease. [394,395]

As far as the molecular mechanisms behind clonal expansion of ECs in the post-MI heart are concerned, single cell RNA sequencing conducted in this thesis showed an upregulation of stalk cell markers indicating that tip/stalk cell angiogenesis is taking place. This is in line with existing literature that has implemented genetic targeting of sprouting angiogenesis using an *Apln-CreER* lineage tracing mouse model.[445] Apelin expression is low in the adult vasculature but increases in response to hypoxia and is associated with sprouting angiogenesis.[445 507] Moreover, *Apln-CreER* labels vascular ECs specifically, but not endocardial or lymphatic ECs, nor smooth muscle cells, thus aiding in the deduction of EC origin in cardiac neovascularisation. [445] Interestingly, *Pdgfb* expression has also been shown to be absent from the endocardium, suggesting an overlap between the two EC populations.[135] Liu *et al.* showed, through the use *Apln-CreER*, that apelin specifically labels angiogenic vessels after ischaemic heart injury.[445] However, other studies have suggested arteriogenesis as the main mechanism for collateral growth in the mouse heart post-MI where large and small coronary arteries in the infarcted myocardium and border region are derived not from capillaries, but from pre-existing arteries.[508] In summary, it is likely that the mammalian heart employs many different mechanisms in an attempt to revascularize the ischaemic heart regions, including the aforementioned mechanisms. However, a hierarchy of importance as far as perfusion establishment from each of the mechanisms has not been reached to date. This will be an important step forward as it would provide us with a guide of the most promising candidate of therapeutic neovascularisation to ameliorate ischaemic heart injury. This thesis shows that clonal proliferation by resident cardiac ECs is a key cellular mechanism of neovascularisation post-MI and can be potentially augmented to promote new vessel growth in IHD patients.

6.1.3 The cardiac endothelial cell population is heterogenous in homeostasis and the EC transcriptome significantly changes following myocardial injury

The endothelium is characterized by an extraordinary level of heterogeneity.[73,89] This characteristic is influenced by physiological function, environmental conditions and of course, pathological alterations. Homeostatic EC functions can range from oxygen/nutrient delivery, vasomotor regulation, haemostasis, angiogenesis, barrier role, and immune cell trafficking.[79] EC heterogeneity is problematic when considering therapeutic interventions as targeting different EC subtypes is challenging. However, through the increments of technical advancement, our understanding of EC biology has gained increasing depth. From initial histological observations of different vascular beds and differentiation between veins and arteries to current complex transcriptomics, our knowledge of the endothelium has expanded considerably. For instance, lineage tracing mouse models have been essential to reveal the diversity of EC types and plasticity in physiological and pathological conditions. Lineage tracing experiments were instrumental in demonstrating the ability of ECs to shift between an arterial and venous phenotype. [509–513] This was shown from increased expression of Notch and VEGF that showed specificity for arterial ECs whereas COUP-TF2 was associated with venous ECs.[509–513] The transcriptomics era has brought forward an additional level of depth to our understanding of endothelial cell heterogeneity. Bulk transcriptomics studies, which involve analysis of pooled cell populations, tissue sections or biopsies, have shown that ECs from different tissues have unique transcriptomic signatures.[514]

Single cell RNA-sequencing has been instrumental for defining EC heterogeneity. For instance, the endocardium has been shown to have a high expression of Npr3.[515] As a result, Nrp3 has been used through the use of *Npr3-CreER* lineage tracing mouse models to label the endocardium but not the remaining coronary ECs in the adult mouse heart.[134] However, Npr3 has now been shown to be expressed in capillaries

and arteries of the heart through single cell RNA sequencing.[516,517] Hence, it can no longer be utilized as an endocardial marker.

Single cell RNA sequencing studies can reveal novel EC subtypes only when EC enrichment is employed *via* the use of an EC specific surface marker. Recent studies that have investigated the transcriptome of ECs from different organ systems have shown that ECs from tissues such as skeletal muscle and the heart, clustered together, demonstrating similarities in transcriptomic signature.[518] This potentially correlates with similarities in biological processes. This was also the case with ECs from the brain and testis which resembled each other transcriptomically; possibly because these organs share a tight blood–tissue barrier.[518] Moreover, the similarities in the transcriptome of ECs from different vascular bodies that have similar functions is also supported by similarities in transcriptomic profile by ECs of arteries, capillaries, veins and lymphatics across different vascular beds.[518] Arterial, venous, and lymphatic ECs share multiple common markers across tissues with few tissue-specific markers. [518] This is not the case when it comes to capillaries which express few common markers between them but are characterised by tissue-specific markers. [518] This is possibly due to the differences in metabolic and physiological needs of each organ system. Similar findings have been reported from the Tabula Muris consortium, which conducted single cell transcriptomics from 20 different murine organs and tissues.[519,520] In summary, single cell RNA sequencing has offered us a new tool with which we can investigate in depth the transcriptome of ECs from different vascular beds, with the aim of harnessing these similarities and/or differences to improve patient outcomes.

The work presented in this thesis defined endothelial heterogeneity in the healthy and injured mouse heart through characterization of 10 EC states, with a *Pdgfb* lineage and distinct gene expression signatures. This high-resolution single cell gene expression atlas of resident cardiac EC both in physiological conditions and at 7 days post-MI adds to the existing single cell RNA sequencing studies investigating the cardiac endothelium. Tombor *et al.* [399] show 4 clusters of ECs, characterized by *Cdh5*

and *CD31* expression following single-cell RNA sequencing of the non-cardiomyocyte fraction of mouse hearts at day 0 and at days 1, 3, 5, 7, 14, or 28 post MI. Litviňuková *et al*. [403] reported 10 EC populations in the adult human heart which included three capillary ECs, one capillary-like immune EC group related to antigen presentation and immune regulation, arterial ECs, venous ECs, atrial ECs, lymphatic ECs and finally one group of ECs with fibroblast-like, and one with cardiomyocyte-like, features. Kalucka *et al.*[517] added further concrete evidence of cardiac EC heterogeneity in the healthy adult mouse heart by demonstrating the existence of 8 different EC states namely: arterial, capillary arterial, capillary, capillary venous, large vein, interferon, angiogenic, lymphatic, and unexpected EC phenotypes of IFN-activated ECs and angiogenic ECs characterized by *Aplnr*, *Adm*, *Apln*, *Col15a1*, *Col4a1*, *Col4a2*, *Trp53i11*. Independent studies have confirmed the existence of angiogenic ECs after ischaemic injury through the use of *Apln-CreER* lineage tracing mouse models.[445] Interestingly, IFN-activated ECs have been observed in the brain, muscle, heart and spleen.[518] This is in agreement with results presented in this chapter where a cardiac EC population associated with the interferon signalling was observed in homeostasis and was increased post-MI. This raises the question as to whether these ECs might be involved in immune surveillance. This is a logical argument as ECs constitute the first line of defence to pathogens present in the circulation. The argument is supported by studies demonstrating that inflamed lung, heart, and brain ECs, induced by lipopolysaccharide (LPS), activate a set of genes in these ECs involved in leukocyte/immune cell trafficking.[521] It is worth mentioning, however, that the studies by Litviňuková *et al*.[403] and Kalucka *et al.*[517] included ECs from healthy organs only and not from pathological states. As evident by the results presented in this thesis, ischaemia is capable of drastically altering the cardiac EC transcriptome, further complicating EC characterisation especially when transition is present where cells are in a dynamic state of fluctuating phenotype. [93] This is problematic as it can make targeting specific EC subtypes in cardiac ischaemia difficult. Future work should aim to establish a timeline of these transcriptomic changes from the onset of injury until the resolution of inflammation.

In summary, single cell RNA sequencing results described in this thesis expand our understanding of EC heterogeneity in general but also specifically in the adult mammalian heart. It should be noted that extra layers of complexity of EC characterization besides the transcriptome exist such as metabolomics[522], proteomics[523], epigenetics[524], and the secretome.[525] A multiomics approach will be required to further characterize the phenotype and molecular mechanisms of ECs that drive neovascularisation in the post-MI heart. The main question that will need to be addressed is what the changes are in ECs following ischaemia across all facets (transcriptome, proteomics etc) as well as dimensions (space and time). This approach will be crucial for making therapeutic angiogenesis a reality.

6.1.4 PLVAP is a novel target with a potential role in cardiac neovascularisation following ischaemia

Single cell RNA sequencing of *Pdgfb* lineage ECs from healthy and 7-day post-MI adult mouse hearts identified EC states that were predominantly composed from ECs from the MI groups (such as clusters 6, 7, 8, 10). This signifies the remarkable plasticity that is exhibited by the cardiac endothelium following cardiac ischaemia and adds to existing evidence on the impact of pathogenesis to EC heterogeneity.[349] Furthermore, a main aim of this thesis was to investigate the molecular pathways behind the activation of neovascularisation post-MI. There is concrete evidence suggesting that neovascularisation takes places in the post-ischaemic heart as a natural response to hypoxia.[38] However, the molecular mechanisms driving this response in the adult mammalian heart are largely unknown.

In this thesis, it was observed that a subset of cardiac ECs (cluster 6) appears to be primed to respond to injury and differentiate into a stalk cell phenotype (cluster 7) and ECs associated with cardiac remodelling (cluster 8). This suggests that sprouting angiogenesis is present at 7 days post-MI, something that has been observed in the

ischaemic heart before, as shown by Apelin driven lineage tracing mouse models.[444] Interestingly, ECs that adopt the stalk cell phenotype 7 days post MI, also expressed *Plvap*, an EC specific marker and a major component of fenestrae, essential for FDs and SDs in ECs. [412,413] *Plvap* expression was found to be significantly increased in ECs at 7 days post-MI in a cluster-specific manner in clusters 6, 7, 8. However, *Plvap* cannot serve as a marker of a stalk cell phenotype as there are *Plvap+* ECs that do not express stalk cell markers. Moreover, this thesis showed that PLVAP was found to have a role in EC proliferation but its direct vs indirect effect is still unclear. The fact that that PLVAP is involved with EC proliferation is aligned with the observed stalk cell phenotype, as stalk cells form the backbone of the angiogenic sprout and have a high rate of proliferation.[99] PLVAP has been implicated in angiogenesis before, in the realm of tumorigenesis. For instance, PLVAP has been found to promote angiogenesis in cholangiocarcinoma via the DKK1/CKAP4/PI3K signalling pathway.[526] Since PLVAP is upregulated in ECs from the MI group the question could be asked whether PLVAP should be a target for overexpression or inhibition. However, it is still unclear whether PLVAP is directly involved in the formation of new blood vessels in the peri-infarct border following MI. Further work will need to be conducted on the necessity of PLVAP in post-MI neovascularisation response post-MI (described in *6.2 Future work*)

Importantly, results in this thesis show that the increase of mouse *Plvap* in MI is mirrored in regions of fibrosis in hearts of patients with acute and chronic ischaemia, when compared to healthy controls. This suggests that human PLVAP is activated in injury and may be associated with endogenous neovascularisation responses in areas of ischaemia and fibrosis. Interestingly, the majority of the PLVAP+ vessels were small capillaries which is in agreement with existing studies that show that PLVAP is not expressed in ECs of large vessels.[406,411]. Existing studies have associated PLVAP with VEGF as its prime regulator [434] which is increased *via* HIF1α[435] while other studies place PLVAP in the Wnt/β-catenin pathway.[439–442] The molecular mechanisms that

govern the increase of PLVAP expression in the ischaemic heart are still unclear and future work will be essential at deciphering these.

6.1.5 The *ex vivo* myocardial slice culture model can be used to study cardiac neovascularisation

The development of an *ex vivo* myocardial slice culture model was described in this thesis. The purpose of developing this model was to use it investigate molecular targets identified in single cell RNA sequencing to clarify their potential role in therapeutic angiogenesis in ischaemic heart disease. The myocardial slice model has been used before, mostly for cardiac electrophysiology[487] and *in vitro* drug safety screening.[488] The myocardial slice model provides an *in vitro* model that more closely resembles *in vivo* myocardial properties and has pathophysiological relevance, compared to existing *in vitro* models. Existing *in vitro* models investigating EC biology provide a high-throughput method of investigating different cellular functions such as migration, proliferation or network/tubule formation of ECs.[452] However, they lack the complexity of *in vivo* models which is problematic when studying multicellular processes such as neovascularisation that take place in a complex 3-dimensional tissue environment.[99]

More specifically, exogenous VEGF-C and hypoxia were successfully used to initiate a change in cardiac vasculature. VEGF-C and the associated VEGFR3 were identified as upregulated gene targets *via* single cell RNA sequencing in ECs 7 days post-MI. Existing studies have shown increased lymphangiogenesis and improved cardiac function following injury in the adult mouse heart following treatment with VEGF-C_{156} that selectively targets VEGFR3.[477–479] However, the role of VEGF-C in the cardiac blood vasculature and specifically in neovascularisation following MI is still unclear. Interestingly however, VEGF-C has been found to be a ligand that bind to receptors VEGFR-2, VEGFR-3, NRP-1, and NRP-2, all which have been shown to play a role in angiogenesis.[475,476] Despite showing a positive effect of VEGF-C and hypoxia on the cardiac vasculature in the myocardial slice model, however, further optimisation is

required to reduce levels of cellular apoptosis and biomimetic characteristics of the myocardial slice model.

6.2 Future directions

6.2.1 Determining the transcriptomic profile of large pro-angiogenic clones at the infarct border with spatial transcriptomics

Using the *Pdgfb-iCreERT2-Brainbow2.1* lineage tracing model, clonal expansion of cardiac ECs was observed to significantly contribute to neovascularisation post-MI. However, not all labelled Brainbow2.1 ECs resulted in monochromatic clonal blood vessels. Some ECs formed large clones whereas others did not.

What is the driver of the formation of these large clonal vessels? Characterisation of the EC transcriptome showed that cardiac ischaemic injury results in the presence of injury-specific cardiac EC states. This showed the upregulation of different markers for processes such as proliferation, cardiac remodelling or tip/stalk cell angiogenesis. These observations hint that there are pathways in cardiac ECs that are specifically activated in cardiac ischaemia and may hint at the regenerative pathways that can be manipulated for therapeutic angiogenesis.

However, it is not possible to directly correlate these MI-specific transcriptomic profiles to the ECs that form these large clonal vessels in the peri-infarct border. Single cell RNA sequencing is a powerful tool but results in loss of spatial resolution due to the need for tissue dissociation. To address the signature of these large EC clones, these transcriptomic changes in MI will need to be linked to spatial information. An existing method to tackle this problem is laser capture microdissection which allows isolation of the desired tissue/cells under direct microscopic visualization.[527] These cells can then be interrogated for their transcriptome. However, this method is labour intensive and results in small numbers of cells captured. Importantly, this method relies on known markers that characterise

the cell of interest. This is of course problematic as it is established that even robust EC markers are often unreliable in states of pathology where cell transition is common.[528]

Spatial transcriptomics (ST) [529] is a new method that allows for unbiased investigation of the transcriptome of the tissue while retaining spatial information. Existing ST methods do not tag individual cells but rather rely on tagging areas of the tissue on a slide. These areas are coated with oligonucleotides that contain spatial barcodes and in turn capture RNA (Figure 6.1). Subsequently, *in situ* cDNA library preparation takes place followed by standard sequencing.

I propose the use of spatial transcriptomics to investigate the transcriptome of large monochromatic Brainbow clones formed in the peri-infarct border of *Pdgfb-iCreERT2-Brainbow2.1 mice* post-MI and to compare them with Brainbow2.1+ ECs that do not form large clones. It is unclear whether the differences between the two groups are the result of a subset of adult cardiac ECs with progenitor-like characteristics, from micro-environmental changes, or from neighbouring cellular interactions that stimulate resident ECs to clonally proliferate. ST will allow for correlation of environmental adaptations to the formation of large, monochromatic EC clones in the peri-infarct border. A key limitation of existing grid-based ST methods is the lack of single-cell resolution, as ST combines multiple cells.[530,531] To combat this, spatial transcriptomics data can be integrated with single cell RNA sequencing to resolve cell types that can be mapped onto the tissue.[532] ST transcriptomics will be crucial to decipher the transcriptomics differences between large and monochromatic Brainbow clones. This approach was originally going to be included in this thesis but complications such as the COVID-19 pandemic made it beyond the scope of this project.

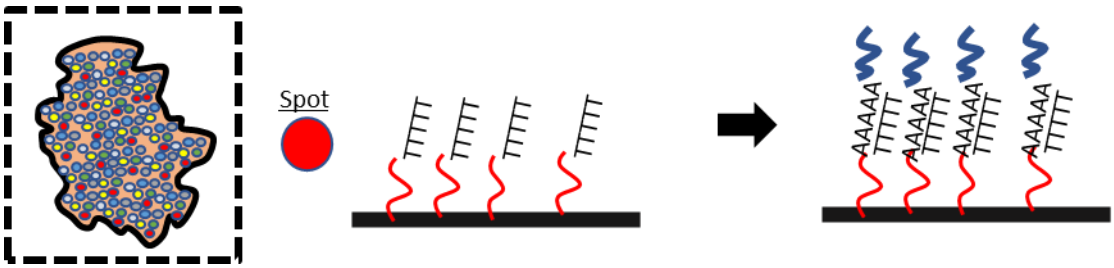

Figure 6.1 Example of Grid-based spatial transcriptomics that captures poly-A RNA transcripts

Existing grid-based spatial transcriptomics (ST) methods rely on tissue placement on slides that are coated withs "spots" containing barcoded oligonucleotides. These barcode oligonucleotides subsequently bind to RNA transcripts followed by *in situ* cDNA library preparation.

6.2.2 Investigating the effect of PLVAP deletion in blood vessel regeneration following myocardial infarction

The role of PLVAP in the heart, and specifically in MI, is largely unknown. Work described in this thesis demonstrated that *Plvap* was upregulated in mouse cardiac ECs with a *Pdgfb* lineage at 7 days post-MI: and specifically in ECs associated with markers of stalk cells. Moreover, PLVAP silencing attenuated proliferation of HUVECs indicating that it plays an essential role in EC proliferation. Finally, PLVAP was upregulated in areas of cardiac fibrosis in patients with acute or chronic MI. However, the role of PLVAP in the formation of new blood vessels in the peri-infarct border is still unclear.

I propose the use of a *Pdgfb*-driven, tamoxifen-inducible, *Plvap* knock-out mouse model to investigate the effects of *Plvap* deletion in recovery post-MI and more specifically in neovascularisation post-MI (Figure 6.2). I hypothesise that the mice that undergo deletion of PLVAP prior to injury will have a worse recovery rate following MI due to disruption in neovascularisation in the peri-infarct border *via* clonal proliferation. Endpoints will include the effect of PLVAP deletion on survival and cardiac recovery (LV ejection fraction) following MI. Moreover, quantification of

monochromatic clones and single cell RNA sequencing of CD31+Brainbow2.1+Podo- will be conducted to interrogate changes in clonal proliferation and transcriptome of ECs. Importantly, characterisation of the vasculature of tissues where Plvap has been shown to be of importance will take place (e.g. kidney, brain, liver).

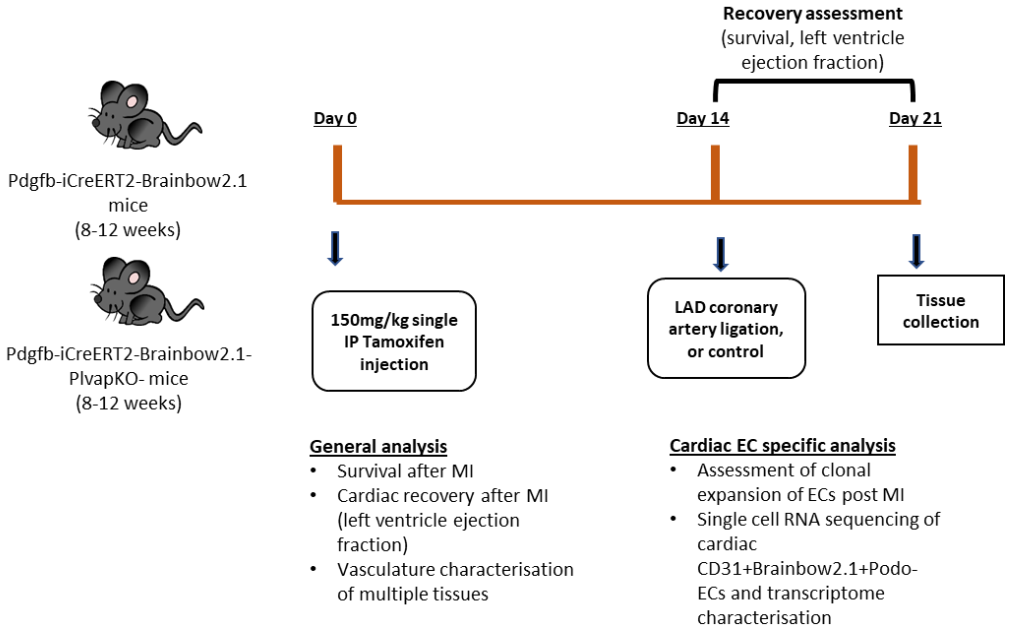

Figure 6.2 Using a Plvap inducible knockout model to investigate the role of Plvap in clonal expansion of cardiac ECs post-MI

6.2.3 Determining the molecular mechanisms and regulation of PLVAP in endothelial cells

Current studies point to the VEGF/hypoxia pathway[434] and Wnt/β-catenin pathway [439–442] as the main regulators of PLVAP. However, there has not been much work on the place of PLVAP in these pathways. Here, I propose an *in vitro* study to investigate the effect of PLVAP inhibition on VEGF and Wnt pathways during hypoxia (Figure 6.3). The *in vitro* setting will allow for good experimental control while trying to decipher the role of PLVAP in the VEGF/hypoxia and Wnt/β-catenin pathways.

HUVECs will be cultured in normal conditions. Subsequently, PLVAP will be silenced using siRNA and cells will be transferred to 1% hypoxia (Figure 6.4). Following a 24 hour incubation cells will be collected for RNA analysis and investigation of VEGF[533] and Wnt/β-catenin[534] related genes.

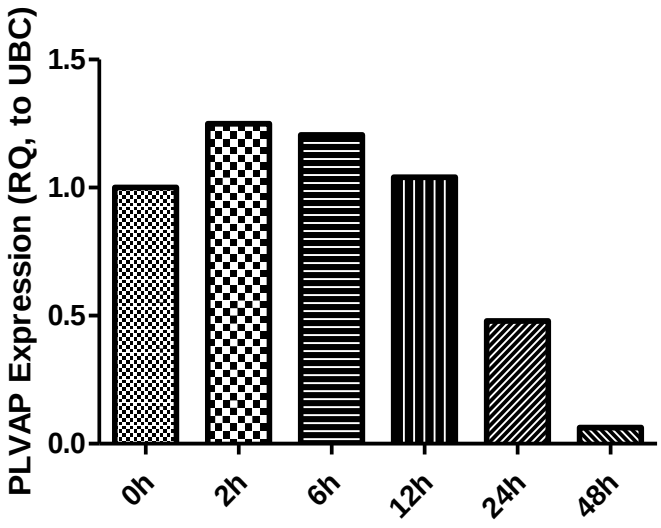

Figure 6.3 Pilot experiment investigating the effect of 1% hypoxia on PLVAP expression in HUVECS

HUVECs were cultured in 1% hypoxic conditions for 0h to 48h. PLVAP expression was measured via q-PCR and normalised to UBC. Hypoxia appeared to reduce mRNA levels of PLVAP when compared to normoxia (0h) with a trend towards an increase in the first few hours of hypoxia (RQ values, 0h; 1 *vs* 2h; 1.25 *vs* 6h; 1.21 vs 12h;1.04) and then a drop-off in 24h and 48h (RQ values, 0h;1 *vs* 24h; 0.48 *vs* 48h;0.06). N=1, 3 technical replicates.

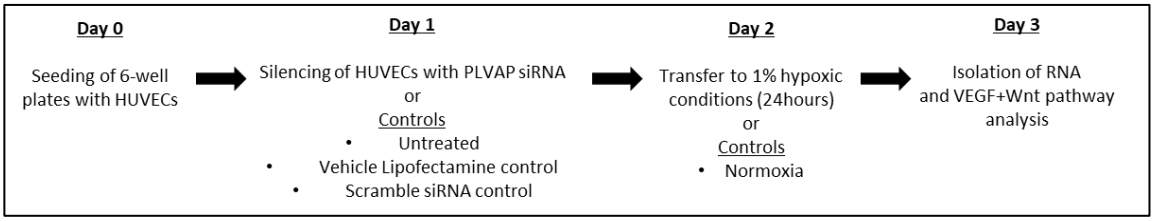

Figure 6.4 Experimental design of *in vivo* PLVAP knockdown study

6.2.4 Improving the biomimetic characteristics of the myocardial slice culture model

The biomimetic characteristic of the *ex vivo* myocardial slice model developed in this thesis can be further optimized. This can be achieved with the use of electrical stimulation and mechanical loading. Cardiomyocytes can undergo substantial differentiation due to lack of flow, electrical stimulation and mechanical loading.[489]

More recent studies have shown that including electrical stimulation and mechanical loading resulted in reduced de-differentiation, possibly due to similarities to the *in vivo* environment.[462,493,495,496] It should be mentioned, however, that even with the inclusion of biomimicry through frequent oxygenation, electrical stimulation and mechanical loading, dedifferentiation can still be observed *via* loss of structural integrity and disruption of gene expression.[491,495] This suggests that myocardial slices can be used over a few days for testing, but techniques of long-term culture need improvement. In the future, the new developments of the myocardial slice model, namely electromechanical stimulation, will be added to the model to increase viability and similarity to the *in vivo* cardiac environment to study EC dynamics in the context of cardiac angiogenesis/neovascularisation.

6.2.5 Visualization of clonal dynamics of cardiac endothelial cells *via* live imaging

An exciting opportunity of the myocardial slice culture model is to perform live imaging of cardiac ECs using the *Pdgfb-iCreERT2-R26R-Brainbow2.*1 lineage tracing mouse model. As shown in the third chapter of this thesis, clonal proliferation is a mechanism by which resident cardiac ECs proliferate in response to cardiac ischaemic injury. However, the data obtained (day 7 post-injury) provide only a snapshot of this proliferative response. Performing live-imaging of this clonal proliferation response using the myocardial slice culture model will be crucial to understand the cardiac EC proliferation dynamics in response to injury. Moreover, an "injury-like" stimulation (such as hypoxia, a known stimulant of neovascularisation[101]) can be introduced into the system. Other approaches that have not been studied in the literature but were briefly explored in the span of this project were laser injury[535] or cryoinjury.[536] These

were inspired by existing methods of inducing cardiac injury in models of heart regeneration in zebrafish[151] and are worthy of further exploration as current data from this thesis show that hypoxia alone is insufficient for inducing cell proliferation in the myocardial slice model.

In vivo imaging of transgenic labelling in mice has been achieved for other organs (such as the liver[537]) but the heart is particularly difficult to image due to its continuous and unpredictable motion. A recent study by Taylor and colleagues[538] utilized light sheet microscopy in addition to a new algorithm capable of maintaining day-long phase-lock, permitting routine acquisition of synchronised 3D and time video time-lapse data of the beating embryonic zebrafish heart. This allows for a detailed observation of developmental and cellular processes in the beating zebrafish heart. However, there are many technical limitations to consider as Taylor and colleagues used an embryonic zebrafish heart which is orders of magnitude smaller than an adult mammalian heart. Moreover, a live imaging experiment with an adult mouse model would require a complex imaging and surgical set up. These technical difficulties can be surpassed if the live-imaging experiment is performed *in vitro* using the myocardial slice model. This would allow for greater experimental control while still maintaining the complex cardiac architecture. Moreover, it will allow manipulation *via* pharmacological or gene therapy approaches. Naturally, the *in vitro* myocardial tissue slice environment would not be wholly representative of the *in vivo* environment. Live imaging of myocardial slices has recently been described by Honkoop and colleagues[490] using myocardial slices prepared from adult zebrafish with the aim of gaining insight of the cellular dynamics of cardiomyocyte proliferation within the native tissue. Zebrafish retain the ability to regenerate heart tissue even in adulthood, as opposed to mammals.[151] Honkoop *et al.* cultured slices from healthy hearts as well as cryoinjured hearts, an experimental model of cardiac zebrafish injury.[536] Moreover, they showed that cardiomyocytes from injured hearts retain their proliferative signature in culture and managed to image cardiomyocyte proliferative events in culture.[490]

Finally, visualization of clonal proliferation of cardiac ECs using the the *Pdgfb-iCreERT2-R26R-Brainbow2* lineage tracing mouse model and the myocardial slice model will help elucidate on which myocardial layer proliferative ECs reside (endocardium, myocardium, epicardium). Despite the current convincing evidence that preexisting cardiac ECs are responsible for new blood vessels following MI[133] it is still unclear from which myocardial layer they originate. Previous studies have suggested both the endocardium[141] and the epicardium [144] as origins of ECs that contribute to new vessels. Interestingly, the epicardium has been suggested to be a hub of cells with progenitor-like characteristics with the potential to enhance neovascularisation.[122] Thus, live-imaging of EC clonal proliferation will increase our understanding of myocardial layer EC contribution to new cardiac blood vessels.

6.2.6 Gene therapy using the myocardial slice culture model

An interesting approach for future work is the addition of a gene therapy strategy in the myocardial slice culture model. This is a not a well investigated approach in the current literature. One recent strategy[539] utilized an adeno-associated virus (AAV) gene therapy approach to investigate gene transfer efficiency, expression, kinetics, penetration depth, cell type tropism and cytotoxicity. AAVs are an attractive vector for gene therapy as they naturally infect humans, produce a mild immune response and have no disease phenotype.[540] Results from the same study suggest that AAV6 had the best transfection efficiency and penetration (300µm) from the strains used.[539] AAV6 was found to predominantly infect cardiomyocytes rather than cardiac fibroblasts. ECs and smooth muscle cell infection efficiency was not investigated. This approach can be used in the myocardial slice model to manipulate expression of targets such as PLVAP and VEGF-C, *via* overexpression or downregulation, that have been shown to drive neovascularisation. This will allow a high throughput, intermediate complexity method to study the roles of these targets, relative to *in vivo* models, while maintaining good experimental control and serving the 3Rs:

Replacement, Reduction and Refinement by reducing the number of transgenic mouse models that are generated for novel gene targets.[450]

6.3 Final conclusions

This thesis set out to determine the clonal dynamics, origin and transcriptomic profile of ECs that participate in neovascularisation post-MI. This was achieved *via* lineage tracing using a multispectral transgenic mouse model (*Pdgfb-iCreERT2-Brainbow2.1*) followed by single cell RNA sequencing of clonal ECs. Here, I reported that clonal proliferation of cardiac ECs is a key cellular mechanism by which new vessels form in the ischaemic infarct border following myocardial injury, with minimal contribution of the bone marrow. This information adds to an exciting field and strengthens the idea that future research should shift to investigating ways of enhancing the regenerative capacity of endogenous resident cardiac endothelial to promote therapeutic neovasculogenesis in the injured heart.

A comprehensive and single cell resolution atlas of gene expression of cardiac ECs in healthy and injured hearts was reported. The transcriptomic profile of cardiac ECs was found to be heterogenous and significantly altered following myocardial injury, clustering in 10 different cell states with certain EC clusters being unique to the injured hearts, revealing potential neovascularisation pathways and targets. Bioinformatics analyses revealed PLVAP, as a marker with a potential role in cardiac neovascularisation and associated with EC stalk cell markers. Moreover, I report a novel role for PLVAP in EC proliferation, but further work is needed to fully unravel the molecular mechanisms involved in this process. Furthermore, a model of mouse myocardial slice culture is established to study the effect of VEGF-C in cardiac neovascularisation *in vitro*. However, more work is needed to improve the biomimetic characteristics of this model and thus fully take advantage of its potential in interrogating potential therapeutic pro-angiogenic targets.

In summary, the results presented in this thesis add to our understanding of EC dynamics following myocardial injury and increase our knowledge on the molecular

targets with a potential in promoting neovascularization by endogenous cardiac ECs. These may guide novel therapeutic strategies aimed at enhancing myocardial repair and regeneration, and ultimately improve patient outcomes.

References

1. Dai, H., Much, A. A., Maor, E., Asher, E., Younis, A., Xu, Y., Lu, Y., Liu, X., Shu, J. & Bragazzi, N. L. Global, regional, and national burden of ischaemic heart disease and its attributable risk factors, 1990–2017: results from the Global Burden of Disease Study 2017. *Eur. Hear. J. - Qual. Care Clin. Outcomes* **8**, 50–60 (2020).

2. BHF. UK Factsheet March 2021. *Br. Hear. Found.* 1–21 (2019).

3. Braunwald, E. Heart failure. *JACC Hear. Fail.* **1**, 1–20 (2013).

4. Thygesen, K., Alpert, J. S., Jaffe, A. S., Chaitman, B. R., Bax, J. J., Morrow, D. A., White, H. D., Mickley, H., Crea, F., Van De Werf, F., Bucciarelli-Ducci, C., Katus, H. A., Pinto, F. J., Antman, E. M., Hamm, C. W., De Caterina, R., Januzzi, J. L., Apple, F. S., Garcia, M. A. A., *et al.* Fourth universal definition of myocardial infarction (2018). *Eur. Heart J.* **40**, 237–269 (2019).

5. Ponikowski, P., Voors, A. A., Anker, S. D., Bueno, H., Cleland, J. G. F., Coats, A. J. S., Falk, V., González-Juanatey, J. R., Harjola, V. P., Jankowska, E. A., Jessup, M., Linde, C., Nihoyannopoulos, P., Parissis, J. T., Pieske, B., Riley, J. P., Rosano, G. M. C., Ruilope, L. M., Ruschitzka, F., *et al.* 2016 ESC Guidelines for the diagnosis and treatment of acute and chronic heart failure. *Eur. Heart J.* **37**, 2129-2200m (2016).

6. Libby, P., Ridker, P. M. & Hansson, G. K. Inflammation in Atherosclerosis. From Pathophysiology to Practice. *J. Am. Coll. Cardiol.* **54**, 2129–2138 (2009).

7. Lu, H. & Daugherty, A. Atherosclerosis. *Arterioscler. Thromb. Vasc. Biol.* **35**, 485–491 (2015).

8. Brown, R. A., Shantsila, E., Varma, C. & Lip, G. Y. H. Current Understanding of Atherogenesis. *Am. J. Med.* **130**, 268–282 (2017).

9. Thygesen, K., Alpert, J. S., Jaffe, A. S., Chaitman, B. R., Bax, J. J., Morrow, D. A. & White, H. D. Fourth Universal Definition of Myocardial Infarction (2018). *J. Am. Coll. Cardiol.* **72**, 2231–2264 (2018).

10. Kalogeris, T., Baines, C. P., Krenz, M. & Korthuis, R. J. Cell Biology of Ischemia/Reperfusion Injury. *Int. Rev. Cell Mol. Biol.* **298**, 229–317 (2012).

11. Frangogiannis, N. G. Pathophysiology of myocardial infarction. *Compr. Physiol.* **5**,

1841–1875 (2015).

12. Jennings, R. B. Historical perspective on the pathology of myocardial ischemia/reperfusion injury. *Circ. Res.* **113**, 428–438 (2013).

13. Vargas, S. O., Sampson, B. A. & Schoen, F. J. Pathologic detection of early myocardial infarction: A critical review of the evolution and usefulness of modern techniques. *Mod. Pathol.* **12**, 635–645 (1999).

14. Burke, A. P. & Virmani, R. Pathophysiology of Acute Myocardial Infarction. *Med. Clin. North Am.* **91**, 553–572 (2007).

15. Stanley, W. C. Cardiac energetics during ischaemia and the rationale for metabolic interventions. *Coron. Artery Dis.* **12**, Suppl 1:S3-7 (2001).

16. Ladilov, Y. V., Siegmund, B. & Piper, H. M. Protection of reoxygenated cardiomyocytes against hypercontracture by inhibition of Na+/H+ exchange. *Am. J. Physiol. - Hear. Circ. Physiol.* **268**, (1995).

17. Coulombe, A., Coraboeuf, E. & Deroubaix, E. Computer simulation of acidosis-induced abnormal repolarization and repetitive activity in dog Purkinje fibers. *J Physiol* **76**, 107–112 (1980).

18. Kleber, A. G. Resting membrane potential, extracellular potassium activity, and intracellular sodium activity during acute global ischemia in isolated perfused guinea pig hearts. *Circ. Res.* **52**, 442–450 (1983).

19. Weiss, J. & Shine, K. I. Extracellular K+ accumulation during myocardial ischemia in isolated rabbit heart. *Am. J. Physiol. - Hear. Circ. Physiol.* **11**, (1982).

20. Lazar, E. J., Goldberger, J., Peled, H., Sherman, M. & Frishman, W. H. Atrial infarction: diagnosis and management. *Am. Heart J.* **116**, 1058–1063 (1988).

21. Albulushi, A., Giannopoulos, A., Kafkas, N., Dragasis, S., Pavlides, G. & Chatzizisis, Y. S. Acute right ventricular myocardial infarction. *Expert Rev. Cardiovasc. Ther.* **16**, 455–464 (2018).

22. St John Sutton, M. G. & Sharpe, N. Left Ventricular Remodeling After Myocardial Infarction Pathophysiology and Therapy Clinical Cardiology: New Frontiers. *Circulation* **101**, 2981–2988 (2000).

23. Erlebacher, J. A., Weiss, J. L., Weisfeldt, M. L. & Bulkley, B. H. Early dilation of the infarcted segment in acute transmural myocardial infarction: role of infarct expansion in acute left ventricular enlargement. *J. Am. Coll. Cardiol.* **4**, 201–208 (1984).

24. Reimer, K. A. & Jennings, R. B. The 'wavefront phenomenon' of myocardial ischemic cell death. II. Transmural progression of necrosis within the framework of ischemic bed size (myocardium at risk) and collateral flow. *Lab. Investig.* **40**, 633–644 (1979).

25. Frangogiannis, N. G. Chemokines in the ischemic myocardium: From inflammation to fibrosis. *Inflamm. Res.* **53**, 585–595 (2004).

26. Cowan, M. J., Reichenbach, D., Turner, P. & Thostenson, C. Cellular response of the evolving myocardial infarction after therapeutic coronary artery reperfusion. *Hum. Pathol.* **22**, 154–163 (1991).

27. Hartzler, G. O., Rumerford, B. D., McConahay, D. R., Johnson, W. L., McCallister, B. D., Gura, G. M., Conn, R. C. & Crockett, J. E. Percutaneous transluminal coronary angioplasty with and without thrombolytic therapy for treatment of acute myocardial infarction. *Am. Heart J.* **106**, 965–973 (1983).

28. Eefting, F., Rensing, B., Wigman, J., Pannekoek, W. J., Liu, W. M., Cramer, M. J., Lips, D. J. & Doevendans, P. A. Role of apoptosis in reperfusion injury. *Cardiovasc. Res.* **61**, 414–426 (2004).

29. Sam, F., Sawyer, D. B., Chang, D. L. F., Eberli, F. R., Ngoy, S., Jain, M., Amin, J., Apstein, C. S. & Colucci, W. S. Progressive left ventricular remodeling and apoptosis late after myocardial infarction in mouse heart. *Am. J. Physiol. - Hear. Circ. Physiol.* **279**, (2000).

30. Konstantinidis, K., Whelan, R. S. & Kitsis, R. N. Mechanisms of cell death in heart disease. *Arterioscler. Thromb. Vasc. Biol.* **32**, 1552–1562 (2012).

31. Knaapen, M. W. M., Davies, M. J., De Bie, M., Haven, A. J., Martinet, W. & Kockx, M. M. Apoptotic versus autophagic cell death in heart failure. *Cardiovasc. Res.* **51**, 304–312 (2001).

32. Elsässer, A., Vogt, A. M., Nef, H., Kostin, S., Möllmann, H., Skwara, W., Bode, C., Hamm, C. & Schaper, J. Human hibernating myocardium is jeopardized by apoptotic

and autophagic cell death. *J. Am. Coll. Cardiol.* **43**, 2191–2199 (2004).

33. Tannous, P., Zhu, H., Nemchenko, A., Berry, J. M., Johnstone, J. L., Shelton, J. M., Miller, F. J., Rothermel, B. A. & Hill, J. A. Intracellular protein aggregation is a proximal trigger of cardiomyocyte autophagy. *Circulation* **117**, 3070–3078 (2008).

34. Przyklenk, K., Undyala, V. V. R., Wider, J., Sala-Mercado, J. A., Gottlieb, R. A. & Mentzer, R. M. Acute induction of autophagy as a novel strategy for cardioprotection: Getting to the heart of the matter. *Autophagy* **7**, 432 (2011).

35. Dong, Y., Undyala, V. V., Gottlieb, R. A., Mentzer, R. M. & Przyklenk, K. Autophagy: definition, molecular machinery, and potential role in myocardial ischemia-reperfusion injury. *J. Cardiovasc. Pharmacol. Ther.* **15**, 220–230 (2010).

36. Litviňuková, M., Talavera-López, C., Maatz, H., Reichart, D., Worth, C. L., Lindberg, E. L., Kanda, M., Polanski, K., Heinig, M., Lee, M., Nadelmann, E. R., Roberts, K., Tuck, L., Fasouli, E. S., DeLaughter, D. M., McDonough, B., Wakimoto, H., Gorham, J. M., Samari, S., *et al.* Cells of the adult human heart. *Nature* **588**, 466–472 (2020).

37. Pinto, A. R., Ilinykh, A., Ivey, M. J., Kuwabara, J. T., D'antoni, M. L., Debuque, R., Chandran, A., Wang, L., Arora, K., Rosenthal, N. A. & Tallquist, M. D. Revisiting cardiac cellular composition. *Circ. Res.* **118**, 400–409 (2016).

38. Cochain, C., Channon, K. M. & Silvestre, J. S. Angiogenesis in the infarcted myocardium. *Antioxidants Redox Signal.* **18**, 1100–1113 (2013).

39. Wu, X., Reboll, M. R., Korf-Klingebiel, M. & Wollert, K. C. Angiogenesis after acute myocardial infarction. *Cardiovasc. Res.* **117**, 1257–1273 (2021).

40. G, R., LH, M., ML, E. & NG, F. Morphological characteristics of the microvasculature in healing myocardial infarcts. *J. Histochem. Cytochem.* **50**, 71–79 (2002).

41. Stergiopoulos, K., Boden, W. E., Hartigan, P., Möbius-Winkler, S., Hambrecht, R., Hueb, W., Hardison, R. M., Abbott, J. D. & Brown, D. L. Percutaneous coronary intervention outcomes in patients with stable obstructive coronary artery disease and myocardial ischemia : A collaborativemeta-analysis of contemporary randomized clinical trials. *JAMA Intern. Med.* **174**, 232–240 (2014).

42. Alexander, J. H. & Smith, P. K. Coronary-Artery Bypass Grafting. *N. Engl. J. Med.* **374**,

1954–1964 (2016).

43. Grines, C. L. & DeMaria, A. N. Optimal utilization of thrombolytic therapy for acute myocardial infarction: Concepts and controversies. *J. Am. Coll. Cardiol.* **16**, 223–231 (1990).

44. Grech, E. D. Percutaneous coronary intervention. I: History and development. *Bmj* **326**, 1080–1082 (2003).

45. Jhund, P. S. & McMurray, J. J. V. Heart failure after acute myocardial infarction a lost battle in the war on heart failure? *Circulation* **118**, 2019–2021 (2008).

46. Heusch, G., Libby, P., Gersh, B., Yellon, D., Böhm, M., Lopaschuk, G. & Opie, L. Cardiovascular remodelling in coronary artery disease and heart failure. *Lancet* **383**, 1933–1943 (2014).

47. Hochman, J. S. & Bulkley, B. H. Expansion of acute myocardial infarction: An experimental study. *Circulation* **65**, 1446–1450 (1982).

48. Mill, J. G., Gomes, A. P. V., Carrara, A. B., Gomes, M. G. S. & Vassallo, D. V. Influence of chronic captopril therapy on the mechanical performance of the infarcted rat heart. *Pharmacol. Res.* **29**, 77–88 (1994).

49. Heusch, G. Postconditioning: Old wine in a new bottle? *J. Am. Coll. Cardiol.* **44**, 1111–1112 (2004).

50. Yellon, D. M. & Hausenloy, D. J. Myocardial Reperfusion Injury. *N. Engl. J. Med.* **357**, 1121–1135 (2007).

51. Heusch, G. & Gersh, B. J. The pathophysiology of acute myocardial infarction and strategies of protection beyond reperfusion: A continual challenge. *Eur. Heart J.* **38**, 774–784 (2017).

52. Schömig, A., Mehilli, J., Antoniucci, D., Ndrepepa, G., Markwardt, C., Di Pede, F., Nekolla, S. G., Schlotterbeck, K., Schühlen, H., Pache, J., Seyfarth, M., Martinoff, S., Benzer, W., Schmitt, C., Dirschinger, J., Schwaiger, M. & Kastrati, A. Mechanical reperfusion in patients with acute myocardial infarction presenting more than 12 hours from symptom onset: A randomized controlled trial. *J. Am. Med. Assoc.* **293**, 2865–2872 (2005).

53. Burgoyne, T., Morris, E. P. & Luther, P. K. Three-Dimensional Structure of Vertebrate Muscle Z-Band: The Small-Square Lattice Z-Band in Rat Cardiac Muscle. *J. Mol. Biol.* **427**, 3527 (2015).

54. Jaffe, R., Charron, T., Puley, G., Dick, A. & Strauss, B. H. Microvascular obstruction and the no-reflow phenomenon after percutaneous coronary intervention. *Circulation* **117**, 3152–3156 (2008).

55. Kim, M. C., Cho, J. Y., Jeong, H. C., Lee, K. H., Park, K. H., Sim, D. S., Yoon, N. S., Youn, H. J., Kim, K. H., Hong, Y. J., Park, H. W., Kim, J. H., Jeong, M. H., Cho, J. G., Park, J. C., Seung, K. B., Chang, K. & Ahn, Y. Long-term clinical outcomes of transient and persistent no reflow phenomena following percutaneous coronary intervention in patients with acute myocardial infarction. *Korean Circ. J.* **46**, 490–498 (2016).

56. Morishima, I., Sone, T., Okumura, K., Tsuboi, H., Kondo, J., Mukawa, H., Matsui, H., Toki, Y., Ito, T. & Hayakawa, T. Angiographic no-reflow phenomenon as a predictor of adverse long-term outcome in patients treated with percutaneous transluminal coronary angioplasty for first acute myocardial infarction. *J. Am. Coll. Cardiol.* **36**, 1202–1209 (2000).

57. Jaffe, R., Charron, T., Puley, G., Dick, A. & Strauss, B. H. Microvascular obstruction and the no-reflow phenomenon after percutaneous coronary intervention. *Circulation* **117**, 3152–3156 (2008).

58. Bouleti, C., Mewton, N. & Germain, S. The no-reflow phenomenon: State of the art. *Arch. Cardiovasc. Dis.* **108**, 661–674 (2015).

59. de Villiers, C. & Riley, P. R. Mouse models of myocardial infarction: Comparing permanent ligation and ischaemia-reperfusion. *DMM Dis. Model. Mech.* **13**, (2020).

60. Bayat, H., Swaney, J. S., Ander, A. N., Dalton, N., Kennedy, B. P., Hammond, H. K. & Roth, D. M. Progressive heart failure after myocardial infarction in mice. *Basic Res. Cardiol.* **97**, 206–213 (2002).

61. De Celle, T., Cleutjens, J. P., Blankesteijn, W. M., Debets, J. J., Smits, J. F. & Janssen, B. J. Long-term structural and functional consequences of cardiac ischaemia-reperfusion injury in vivo in mice. *Exp. Physiol.* **89**, 605–615 (2004).

62. Tang, Y.-P., Liu, Y., Fan, Y.-J., Zhao, Y.-Y., Feng, J.-Q. & Liu, Y. To develop a novel

animal model of myocardial infarction: A research imperative. *Anim. Model. Exp. Med.* **1**, 36–39 (2018).

63. Hall, J. E. *Medical Physiology*. *Neurology* vol. 12 (1962).

64. Gao, Y. Architecture of the Blood Vessels. *Biol. Vasc. Smooth Muscle Vasoconstriction Dilatation* 3–12 (2017) doi:10.1007/978-981-10-4810-4_1.

65. Oliver, G., Kipnis, J., Randolph, G. J. & Harvey, N. L. The Lymphatic Vasculature in the 21st Century: Novel Functional Roles in Homeostasis and Disease. *Cell* **182**, 270–296 (2020).

66. Bunce, D. F. M. *Atlas of Arterial Histology*. (W.H. Green, 1974).

67. Buja, L. M. & Butany, J. *Cardiovascular Pathology: Fourth Edition*. *Cardiovascular Pathology: Fourth Edition* (Elsevier Inc., 2015). doi:10.1016/C2013-0-12761-4.

68. Wörsdörfer, P., Mekala, S. R., Bauer, J., Edenhofer, F., Kuerten, S. & Ergün, S. The vascular adventitia: An endogenous, omnipresent source of stem cells in the body. *Pharmacol. Ther.* **171**, 13–29 (2017).

69. Taylor, A. M. & Bordoni, B. *Histology, Blood Vascular System*. *StatPearls* (StatPearls Publishing, 2020).

70. Marieb, E. & Hoehn, K. *Human Anatomy & Physiology, Global Edition. Human Anatomy & Physiology* (Pearson Education Limited, 2015).

71. Rhodin, J. A. G. Architecture of the Vessel Wall. *Compr. Physiol.* 1–31 (1980) doi:10.1002/CPHY.CP020201.

72. BURTON, A. C. Relation of structure to function of the tissues of the wall of blood vessels. *Physiol. Rev.* **34**, 619–642 (1954).

73. Aird, W. C. Phenotypic heterogeneity of the endothelium: I. Structure, function, and mechanisms. *Circ. Res.* **100**, 158–173 (2007).

74. Pillinger, N. L. & Kam, P. C. A. Endothelial glycocalyx: Basic science and clinical implications. *Anaesth. Intensive Care* **45**, 295–307 (2017).

75. Makarov, V., Zueva, L., Sanabria, P., Wessinger, W. D., Golubeva, T., Khmelinskii, I. & Inyushin, M. On the Role of the Blood Vessel Endothelial Microvilli in the Blood Flow

in Small Capillaries. *J. Biophys.* **2015**, (2015).

76. Carman, C. V., Jun, C.-D., Salas, A. & Springer, T. A. Endothelial Cells Proactively Form Microvilli-Like Membrane Projections upon Intercellular Adhesion Molecule 1 Engagement of Leukocyte LFA-1. *J. Immunol.* **171**, 6135–6144 (2003).

77. Lenting, P. J., Christophe, O. D. & Denis, C. V. von Willebrand factor biosynthesis, secretion, and clearance: connecting the far ends. *Blood* **125**, 2019–2028 (2015).

78. Palmer, R. M. J., Ashton, D. S. & Moncada, S. Vascular endothelial cells synthesize nitric oxide from L-arginine. *Nature* **333**, 664–666 (1988).

79. Furchgott, R. F. & Zawadzki, J. V. The obligatory role of endothelial cells in the relaxation of arterial smooth muscle by acetylcholine. *Nature* **288**, 373–376 (1980).

80. Furchgott, R. F., Cherry, P. D., Zawadzki, J. V. & Jothianandan, D. Endothelial cells as mediators of vasodilation of arteries. *J. Cardiovasc. Pharmacol.* **6**, S336–S343 (1984).

81. Van De Voorde, J. & Leusen, I. Role of the endothelium in the vasodilator response of rat thoracic aorta to histamine. *Eur. J. Pharmacol.* **87**, 113–120 (1983).

82. Hutchinson, P. J. A., Palmer, R. M. J. & Moncada, S. Comparative pharmacology of EDRF and nitric oxide on vascular strips. *Eur. J. Pharmacol.* **141**, 445–451 (1987).

83. Furchgott, R. F. Endothelium-derived relaxing factor: Discovery, early studies, and identification as nitric oxide. *Biosci. Rep.* **19**, 235–251 (1999).

84. Deanfield, J. E., Halcox, J. P. & Rabelink, T. J. Endothelial function and dysfunction: Testing and clinical relevance. *Circulation* **115**, 1285–1295 (2007).

85. Davignon, J. & Ganz, P. Role of endothelial dysfunction in atherosclerosis. *Circulation* **109**, (2004).

86. Drexler, H. Factors involved in the maintenance of endothelial function. *Am. J. Cardiol.* **82**, (1998).

87. Hadi, H. A. R., Carr, C. S. & Al Suwaidi, J. Endothelial dysfunction: cardiovascular risk factors, therapy, and outcome. *Vasc. Health Risk Manag.* **1**, 183–198 (2005).

88. Lee, L. L. & Chintalgattu, V. Pericytes in the heart. *Adv. Exp. Med. Biol.* **1122**, 187–210 (2019).

89. Aird, W. C. Phenotypic heterogeneity of the endothelium: II. Representative vascular beds. *Circ. Res.* **100**, 174–190 (2007).

90. Othman-Hassan, K., Patel, K., Papoutsi, M., Rodriguez-Niedenführ, M., Christ, B. & Wilting, J. Arterial identity of endothelial cells is controlled by local cues. *Dev. Biol.* **237**, 398–409 (2001).

91. Gosling, M., Golledge, J., Turner, R. J. & Powell, J. T. Arterial flow conditions downregulate thrombomodulin on saphenous vein endothelium. *Circulation* **99**, 1047–1053 (1999).

92. Woodfin, A., Voisin, M. B. & Nourshargh, S. PECAM-1: A multi-functional molecule in inflammation and vascular biology. *Arterioscler. Thromb. Vasc. Biol.* **27**, 2514–2523 (2007).

93. Margadant, C. Endothelial heterogeneity and plasticity. *Angiogenesis* **24**, 197–198 (2021).

94. Cai, Y., Zhang, J., Wu, J. & Li, Z. Y. Oxygen transport in a three-dimensional microvascular network incorporated with early tumour growth and preexisting vessel cooption: Numerical simulation study. *Biomed Res. Int.* **2015**, (2015).

95. Conway, E. M., Collen, D. & Carmeliet, P. Molecular mechanisms of blood vessel growth. *Cardiovasc. Res.* **49**, 507–521 (2001).

96. Risau, W. & Flamme, I. Vasculogenesis. *Annu. Rev. Cell Dev. Biol.* **11**, 73–91 (1995).

97. Fina, L., Molgaard, H. V., Robertson, D., Bradley, N. J., Monaghan, P., Delia, D., Sutherland, D. R., Baker, M. A. & Greaves, M. F. Expression of the CD34 gene in vascular endothelial cells. *Blood* **75**, 2417–2426 (1990).

98. Asahara, T., Takahashi, T., Masuda, H., Kalka, C., Chen, D., Iwaguro, H., Inai, Y., Silver, M. & Isner, J. M. VEGF contributes to postnatal neovascularization by mobilizing bone marrow-derived endothelial progenitor cells. *EMBO J.* **18**, 3964–3972 (1999).

99. Carmeliet, P. & Jain, R. K. Molecular Mechanisms and and clinical applications of angiogenesis. *Nature* **473**, 298–307 (2011).

100. Bikfalvi, A. History and conceptual developments in vascular biology and angiogenesis research: a personal view. *Angiogenesis* **20**, 463–478 (2017).

101. Ratcliffe, P. J., Maxwell, P. H., Wiesener, M. S., Chang, G.-W., Clifford, S. C., Vaux, E. C., Cockman, M. E., Wykoff, C. C., Pugh, C. W. & Maher, E. R. The tumour suppressor protein VHL targets hypoxia-inducible factors foroxygen-dependent proteolysis. *Nature* **399**, 271–275 (1999).

102. Ferrara, N. VEGF-A: A critical regulator of blood vessel growth. *Eur. Cytokine Netw.* **20**, 158–163 (2009).

103. Neufeld, G. & Kessler, O. The semaphorins: Versatile regulators of tumour progression and tumour angiogenesis. *Nat. Rev. Cancer* **8**, 632–645 (2008).

104. Kukk, E., Lymboussakl, A., Taira, S., Kaipainen, A., Jeltsch, M., Joukov, V. & Alitalo, K. VEGF-C receptor binding and pattern of expression with VEGFR-3 suggests a role in lymphatic vascular development. *Development* **122**, 3829–3837 (1996).

105. Arroyo, A. G. & Iruela-Arispe, M. L. Extracellular matrix, inflammation, and the angiogenic response. *Cardiovasc. Res.* **86**, 226 (2010).

106. Potente, M., Gerhardt, H. & Carmeliet, P. Basic and Therapeutic Aspects of Angiogenesis. *Cell* **146**, 873–887 (2011).

107. Hellström, M., Phng, L. K., Hofmann, J. J., Wallgard, E., Coultas, L., Lindblom, P., Alva, J., Nilsson, A. K., Karlsson, L., Gaiano, N., Yoon, K., Rossant, J., Iruela-Arispe, M. L., Kalén, M., Gerhardt, H. & Betsholtz, C. Dll4 signalling through Notch1 regulates formation of tip cells during angiogenesis. *Nature* **445**, 776–780 (2007).

108. Del Toro, R., Prahst, C., Mathivet, T., Siegfried, G., Kaminker, J. S., Larrivee, B., Breant, C., Duarte, A., Takakura, N., Fukamizu, A., Penninger, J. & Eichmann, A. Identification and functional analysis of endothelial tip cell–enriched genes. *Blood* **116**, 4025–4033 (2010).

109. Isogai, S., Lawson, N. D., Torrealday, S., Horiguchi, M. & Weinstein, B. M. Angiogenic network formation in the developing vertebrate trunk. *Development* **130**, 5281–5290 (2003).

110. Thurston, G. & Kitajewski, J. VEGF and Delta-Notch: interacting signalling pathways in tumour angiogenesis. *Br. J. Cancer 2008 998* **99**, 1204–1209 (2008).

111. Bentley, K., Gerhardt, H. & Bates, P. A. Agent-based simulation of notch-mediated

tip cell selection in angiogenic sprout initialisation. *J. Theor. Biol.* **250**, 25–36 (2008).

112. Eelen, G., Treps, L., Li, X. & Carmeliet, P. Basic and Therapeutic Aspects of Angiogenesis Updated. *Circ. Res.* **127**, 310–329 (2020).

113. De Spiegelaere, W., Casteleyn, C., Van Den Broeck, W., Plendl, J., Bahramsoltani, M., Simoens, P., Djonov, V. & Cornillie, P. Intussusceptive Angiogenesis: A Biologically Relevant Form of Angiogenesis. *J. Vasc. Res.* **49**, 390–404 (2012).

114. Makanya, A. N., Hlushchuk, R. & Djonov, V. G. Intussusceptive angiogenesis and its role in vascular morphogenesis, patterning, and remodeling. *Angiogenesis* **12**, 113–123 (2009).

115. Heil, M., Eitenmüller, I., Schmitz-Rixen, T. & Schaper, W. Arteriogenesis versus angiogenesis: Similarities and differences. *J. Cell. Mol. Med.* **10**, 45–55 (2006).

116. Scholz, D., Ito, W., Fleming, I., Deindl, E., Sauer, A., Wiesnet, M., Busse, R., Schaper, J. & Schaper, W. Ultrastructure and molecular histology of rabbit hind-limb collateral artery growth (arteriogenesis). *Virchows Arch.* **436**, 257–270 (2000).

117. Cai, W. J., Kocsis, E., Wu, X., Rodríguez, M., Luo, X., Schaper, W. & Schaper, J. Remodeling of the vascular tunica media is essential for development of collateral vessels in the canine heart. *Mol. Cell. Biochem.* **264**, 201–210 (2004).

118. Cai, W. J., Koltai, S., Kocsis, E., Scholz, D., Kostin, S., Luo, X., Schaper, W. & Schaper, J. Remodeling of the adventitia during coronary arteriogenesis. *Am. J. Physiol. - Hear. Circ. Physiol.* **284**, 31–40 (2003).

119. Grundmann, S., Piek, J. J., Pasterkamp, G. & Hoefer, I. E. Arteriogenesis: basic mechanisms and therapeutic stimulation. *Eur. J. Clin. Invest.* **37**, 755–766 (2007).

120. Reese, D. E., Mikawa, T. & Bader, D. M. Development of the coronary vessel system. *Circ. Res.* **91**, 761–768 (2002).

121. Tian, X., Hu, T., He, L., Zhang, H., Huang, X., Poelmann, R. E., Liu, W., Yang, Z., Yan, Y., Pu, W. T. & Zhou, B. Peritruncal coronary endothelial cells contribute to proximal coronary artery stems and their aortic orifices in the mouse heart. *PLoS One* **8**, e80857 (2013).

122. Smart, N. & Riley, P. R. The epicardium as a candidate for heart regeneration. *Future*

Cardiol. **8**, 53–69 (2012).

123. Lupu, I. E., De Val, S. & Smart, N. Coronary vessel formation in development and disease: mechanisms and insights for therapy. *Nat. Rev. Cardiol.* **17**, 790–806 (2020).

124. Gittenberger-De Groot, A. C., Vrancken Peeters, M. P. F. M., Bergwerff, M., Mentink, M. M. T. & Poelmann, R. E. Epicardial outgrowth inhibition leads to compensatory mesothelial outflow tract collar and abnormal cardiac septation and coronary formation. *Circ. Res.* **87**, 969–971 (2000).

125. Acharya, A., Baek, S. T., Banfi, S., Eskiocak, B. & Tallquist, M. D. Efficient inducible Cre-mediated recombination in Tcf21cell lineages in the heart and kidney. *Genesis* **49**, 870–877 (2011).

126. Cai, C. L., Martin, J. C., Sun, Y., Cui, L., Wang, L., Ouyang, K., Yang, L., Bu, L., Liang, X., Zhang, X., Stallcup, W. B., Denton, C. P., McCulloch, A., Chen, J. & Evans, S. M. A myocardial lineage derives from Tbx18 epicardial cells. *Nature* **454**, 104–108 (2008).

127. Red-Horse, K., Ueno, H., Weissman, I. L. & Krasnow, M. A. Coronary arteries form by developmental reprogramming of venous cells. *Nature* **464**, 549–553 (2010).

128. Zhang, H., Pu, W., Li, G., Huang, X., He, L., Tian, X., Liu, Q., Zhang, L., Wu, S. M., Sucov, H. M. & Zhou, B. Endocardium Minimally Contributes to Coronary Endothelium in the Embryonic Ventricular Free Walls. *Circ. Res.* **118**, 1880–1893 (2016).

129. Tian, X., Hu, T., Zhang, H., He, L., Huang, X., Liu, Q., Yu, W., He, L., Yang, Z., Yan, Y., Yang, X., Zhong, T. P., Pu, W. T. & Zhou, B. De novo formation of a distinct coronary vascular population in neonatal heart. *Science (80-.).* **345**, 90–94 (2014).

130. Prabhu, S. D. & Frangogiannis, N. G. The biological basis for cardiac repair after myocardial infarction. *Circ. Res.* **119**, 91–112 (2016).

131. Kobayashi, K., Maeda, K., Takefuji, M., Kikuchi, R., Morishita, Y., Hirashima, M. & Murohara, T. Dynamics of angiogenesis in ischemic areas of the infarcted heart. *Sci. Rep.* **7**, 1–13 (2017).

132. Kenneth Mallory, G., White, P. D. & Salcedo-Salgar, J. The speed of healing of myocardial infarction. A study of the pathologic anatomy in seventy-two cases. *Am.*

Heart J. **18**, 647–671 (1939).

133. He, L., Huang, X., Kanisicak, O., Li, Y. Y., Wang, Y., Li, Y. Y., Pu, W., Liu, Q., Zhang, H., Tian, X., Zhao, H., Liu, X., Zhang, S., Nie, Y., Hu, S., Miao, X., Wang, Q. D., Wang, F., Chen, T., *et al.* Preexisting endothelial cells mediate cardiac neovascularization after injury. *J. Clin. Invest.* **127**, 2968–2981 (2017).

134. Tang, J., Zhang, H., He, L., Huang, X., Li, Y., Pu, W., Yu, W., Zhang, L., Cai, D., Lui, K. O. & Zhou, B. Genetic Fate Mapping Defines the Vascular Potential of Endocardial Cells in the Adult Heart. *Circ. Res.* **122**, 984–993 (2018).

135. Dubé, K. N., Thomas, T. M., Munshaw, S., Rohling, M., Riley, P. R. & Smart, N. Recapitulation of developmental mechanisms to revascularize the ischemic heart. *JCI insight* **2**, (2017).

136. Zhou, B., Honor, L. B., He, H., Qing, M., Oh, J. H., Butterfield, C., Lin, R. Z., Melero-Martin, J. M., Dolmatova, E., Duffy, H. S., Von Gise, A., Zhou, P., Hu, Y. W., Wang, G., Zhang, B., Wang, L., Hall, J. L., Moses, M. A., McGowan, F. X., *et al.* Adult mouse epicardium modulates myocardial injury by secreting paracrine factors. *J. Clin. Invest.* **121**, 1894–1904 (2011).

137. van Wijk, B., Gunst, Q. D., Moorman, A. F. M. & van den Hoff, M. J. B. Cardiac Regeneration from Activated Epicardium. *PLoS One* **7**, (2012).

138. Gittenberger-de Groot, A. C., Winter, E. M., Bartelings, M. M., Jose Goumans, M., DeRuiter, M. C. & Poelmann, R. E. The arterial and cardiac epicardium in development, disease and repair. *Differentiation* **84**, 41–53 (2012).

139. Zhang, H., Lui, K. O. & Zhou, B. Endocardial cell plasticity in cardiac development, diseases and regeneration. *Circ. Res.* **122**, 774–789 (2018).

140. Tian, X., Pu, W. T. & Zhou, B. Cellular origin and developmental program of coronary angiogenesis. *Circ. Res.* **116**, 515–530 (2015).

141. Miquerol, L., Thireau, J., Bideaux, P., Sturny, R., Richard, S. & Kelly, R. G. Endothelial plasticity drives arterial remodeling within The endocardium after myocardial infarction. *Circ. Res.* **116**, 1765–1771 (2015).

142. Zhou, B., Honor, L. B., He, H., Qing, M., Oh, J. H., Butterfield, C., Lin, R. Z., Melero-

Martin, J. M., Dolmatova, E., Duffy, H. S., Von Gise, A., Zhou, P., Hu, Y. W., Wang, G., Zhang, B., Wang, L., Hall, J. L., Moses, M. A., McGowan, F. X., *et al.* Adult mouse epicardium modulates myocardial injury by secreting paracrine factors. *J. Clin. Invest.* **121**, 1894–1904 (2011).

143. Limana, F., Zacheo, A., Mocini, D., Mangoni, A., Borsellino, G., Diamantini, A., De Mori, R., Battistini, L., Vigna, E., Santini, M., Loiaconi, V., Pompilio, G., Germani, A. & Capogrossi, M. C. Identification of myocardial and vascular precursor cells in human and mouse epicardium. *Circ. Res.* **101**, 1255–1265 (2007).

144. Sultana, N., Zhang, L., Yan, J., Chen, J., Cai, W., Razzaque, S., Jeong, D., Sheng, W., Bu, L., Xu, M., Huang, G. Y., Hajjar, R. J., Zhou, B., Moon, A. & Cai, C. L. Resident c-kit+ cells in the heart are not cardiac stem cells. *Nat. Commun.* **6**, (2015).

145. Ubil, E., Duan, J., Pillai, I. C. L., Rosa-Garrido, M., Wu, Y., Bargiacchi, F., Lu, Y., Stanbouly, S., Huang, J., Rojas, M., Vondriska, T. M., Stefani, E. & Deb, A. Mesenchymal-endothelial transition contributes to cardiac neovascularization. *Nature* **514**, 585–590 (2014).

146. Ubil, E., Duan, J., Pillai, I. C. L., Rosa-Garrido, M., Wu, Y., Bargiacchi, F., Lu, Y., Stanbouly, S., Huang, J., Rojas, M., Vondriska, T. M., Stefani, E. & Deb, A. Mesenchymal-endothelial-transition contributes to cardiac neovascularization. *Nature* **514**, 585 (2014).

147. Potente, M. & Mäkinen, T. Vascular heterogeneity and specialization in development and disease. *Nat. Rev. Mol. Cell Biol. 2017 188* **18**, 477–494 (2017).

148. Sheehan, F. H., Doerr, R., Schmidt, W. G., Bolson, E. L., Uebis, R., von Essen, R., Effert, S. & Dodge, H. T. Early recovery of left ventricular function after thrombolytic therapy for acute myocardial infarction: An important determinant of survival. *J. Am. Coll. Cardiol.* **12**, 289–300 (1988).

149. Jugdutt, B. I., Menon, V., Kumar, D. & Idikio, H. Vascular remodeling during healing after myocardial infarction in the dog model: Effects of reperfusion, amlodipine and enalapril. *J. Am. Coll. Cardiol.* **39**, 1538–1545 (2002).

150. Liebson, P. R. Stem-cell angiogenesis and regeneration of the heart: Review of a saga of 2 decades. *Clin. Cardiol.* **38**, 309–316 (2015).

151. Ross Stewart, K. M., Walker, S. L., Baker, A. H., Riley, P. R. & Brittan, M. Hooked on heart regeneration: the zebrafish guide to recovery. *Cardiovasc. Res.* **0**, 1–13 (2021).

152. Poss, K. D., Wilson, L. G. & Keating, M. T. Heart regeneration in zebrafish. *Science (80-.).* **298**, 2188–2190 (2002).

153. Jopling, C., Sleep, E., Raya, M., Martí, M., Raya, A. & Belmonte, J. C. I. I. Zebrafish heart regeneration occurs by cardiomyocyte dedifferentiation and proliferation. *Nature* **464**, 606–609 (2010).

154. Marín-Juez, R., Marass, M., Gauvrit, S., Rossi, A., Lai, S. L., Materna, S. C., Black, B. L. & Stainier, D. Y. R. Fast revascularization of the injured area is essential to support zebrafish heart regeneration. *Proc. Natl. Acad. Sci. U. S. A.* **113**, 11237–11242 (2016).

155. Porrello, E. R., Mahmoud, A. I., Simpson, E., Hill, J. A., Richardson, J. A., Olson, E. N. & Sadek, H. A. Transient regenerative potential of the neonatal mouse heart. *Science (80-.).* **331**, 1078–1080 (2011).

156. Jopling, C., Sleep, E., Raya, M., Martí, M., Raya, A. & Belmonte, J. C. I. Zebrafish heart regeneration occurs by cardiomyocyte dedifferentiation and proliferation. *Nat. 2010 4647288* **464**, 606–609 (2010).

157. Ingason, A. B., Goldstone, A. B., Paulsen, M. J., Thakore, A. D., Truong, V. N., Edwards, B. B., Eskandari, A., Bollig, T., Steele, A. N. & Woo, Y. J. Angiogenesis precedes cardiomyocyte migration in regenerating mammalian hearts. *J. Thorac. Cardiovasc. Surg.* **155**, 1118-1127.e1 (2018).

158. Lam, N. T. & Sadek, H. A. Neonatal heart regeneration comprehensive literature review. *Circulation* **138**, 421–423 (2018).

159. Huddleston, C. B., Balzer, D. T. & Mendeloff, E. N. Repair of anomalous left main coronary artery arising from the pulmonary artery in infants: long-term impact on the mitral valve. *Ann. Thorac. Surg.* **71**, 1985–1988 (2001).

160. Ling, Y., Bhushan, S., Fan, Q. & Tang, M. Midterm outcome after surgical correction of anomalous left coronary artery from the pulmonary artery. *J. Cardiothorac. Surg.* **11**, 1–5 (2016).

161. Bergmann, O., Zdunek, S., Felker, A., Salehpour, M., Alkass, K., Bernard, S., Sjostrom,

S. L., Szewczykowska, M., Jackowska, T., Dos Remedios, C., Malm, T., Andrä, M., Jashari, R., Nyengaard, J. R., Possnert, G., Jovinge, S., Druid, H. & Frisén, J. Dynamics of Cell Generation and Turnover in the Human Heart. *Cell* **161**, 1566–1575 (2015).

162. Cambria, E., Pasqualini, F. S., Wolint, P., Günter, J., Steiger, J., Bopp, A., Hoerstrup, S. P. & Emmert, M. Y. Translational cardiac stem cell therapy: advancing from first-generation to next-generation cell types. *NPJ Regen. Med.* **2**, 17 (2017).

163. Fernández-Avilés, F., Sanz-Ruiz, R., Climent, A. M., Badimon, L., Bolli, R., Charron, D., Fuster, V., Janssens, S., Kastrup, J., Kim, H. S., Lüscher, T. F., Martin, J. F., Menasche, P., Simari, R. D., Stone, G. W., Terzic, A., Willerson, J. T., Wu, J. C., Joseph, C. W., *et al.* Global position paper on cardiovascular regenerative medicine. *Eur. Heart J.* **38**, 2532–2546 (2017).

164. Orlic, D., Kajstura, J., Chimenti, S., Jakoniuk, I., Anderson, S. M., Li, B., Pickel, J., McKay, R., Nadal-Ginard, B., Bodine, D. M., Leri, A. & Anversa, P. Bone marrow cells regenerate infarcted myocardium. *Nature* **410**, 701–705 (2001).

165. Kudo, M., Wang, Y., Wani, M. A., Xu, M., Ayub, A. & Ashraf, M. Implantation of bone marrow stem cells reduces the infarction and fibrosis in ischemic mouse heart. *J. Mol. Cell. Cardiol.* **35**, 1113–1119 (2003).

166. Murry, C. E., Soonpaa, M. H., Reinecke, H., Nakajima, H., Nakajima, H. O., Rubart, M., Pasumarthi, K. B. S., Virag, J. I., Bartelmez, S. H., Poppa, V., Bradford, G., Dowell, J. D., Williams, D. A. & Field, L. J. Haematopoietic stem cells do not transdifferentiate into cardiac myocytes in myocardial infarcts. *Nature* **428**, 664–668 (2004).

167. Zhang, S., Ge, J., Zhao, L., Qian, J., Huang, Z., Shen, L., Sun, A., Wang, K. & Zou, Y. Host Vascular Niche Contributes to Myocardial Repair Induced by Intracoronary Transplantation of Bone Marrow CD34+ Progenitor Cells in Infarcted Swine Heart. *Stem Cells* **25**, 1195–1203 (2007).

168. Schwartz, S. M. & Benditt, E. P. Clustering of replicating cells in aortic endothelium. *Proc. Natl. Acad. Sci. U. S. A.* **73**, 651–3 (1976).

169. Schwartz, S. M. & Benditt, E. P. Aortic endothelial cell replication. I. Effects of age and hypertension in the rat. *Circ. Res.* **41**, 248–55 (1977).

170. Psaltis, P. J. & Simari, R. D. Vascular Wall Progenitor Cells in Health and Disease. *Circ.*

Res. **116**, (2015).

171. Asahara, T., Murohara, T., Sullivan, A., Silver, M., van der Zee, R., Li, T., Witzenbichler, B., Schatteman, G. & Isner, J. M. Isolation of Putative Progenitor Endothelial Cells for Angiogenesis. *Science (80-.).* **275**, 964–967 (1997).

172. Urbich, C. & Dimmeler, S. Endothelial Progenitor Cells. *Circ. Res.* **95**, 343–353 (2004).

173. King, T. F. J. & McDermott, J. H. Endothelial progenitor cells and cardiovascular disease. *J. Stem Cells* **9**, 93–106 (2014).

174. Kleinman, M. E., Blei, F. & Gurtner, G. C. Circulating endothelial progenitor cells and vascular anomalies. *Lymphat. Res. Biol.* **3**, 234–239 (2005).

175. Fujisawa, T., Tura-Ceide, O., Hunter, A., Mitchell, A., Vesey, A., Medine, C., Gallogly, S., Hadoke, P. W. F., Keith, C., Sproul, A., Roddie, H., McQuaker, G., Wilmut, I., Mills, N. L. & Brittan, M. Endothelial Progenitor Cells Do Not Originate From the Bone Marrow. *Circulation* **140**, 1524–1526 (2019).

176. Ingram, D. A., Mead, L. E., Tanaka, H., Meade, V., Fenoglio, A., Mortell, K., Pollok, K., Ferkowicz, M. J., Gilley, D. & Yoder, M. C. Identification of a novel hierarchy of endothelial progenitor cells using human peripheral and umbilical cord blood. *Blood* **104**, 2752–2760 (2004).

177. Payling Wright, H. Mitosis patterns in aortic endothelium. *Atherosclerosis* **15**, 93–100 (1972).

178. Schwartz, S. M. & Benditt, E. P. Clustering of replicating cells in aortic endothelium. *Proc. Natl. Acad. Sci. U. S. A.* **73**, 651–653 (1976).

179. Choudry, F., Hamshere, S., Saunders, N., Veerapen, J., Bavnbek, K., Knight, C., Pellerin, D., Locca, D., Westwood, M., Rakhit, R., Crake, T., Kastrup, J., Parmar, M., Agrawal, S., Jones, D., Martin, J. & Mathur, A. A randomized double-blind control study of early intra-coronary autologous bone marrow cell infusion in acute myocardial infarction: the REGENERATE-AMI clinical trial†. *Eur. Heart J.* **37**, 256–263 (2016).

180. Yousef, M., Schannwell, C. M., Köstering, M., Zeus, T., Brehm, M. & Strauer, B. E. The BALANCE Study: clinical benefit and long-term outcome after intracoronary

autologous bone marrow cell transplantation in patients with acute myocardial infarction. *J. Am. Coll. Cardiol.* **53**, 2262–2269 (2009).

181. Dohmann, H. F. R., Silva, S. A., Sousa, A. L. S., Braga, A. M. S., Branco, R. V. C., Haddad, A. F., Oliveira, M. A., Moreira, R. C., Tuche, F. A. A., Peixoto, C. M., Tura, B. R., Borojevic, R., Ribeiro, J. P., Nicolau, J. C., Nóbrega, A. C. & Carvalho, A. C. C. Multicenter double blind trial of autologous bone marrow mononuclear cell transplantation through intracoronary injection post acute myocardium infarction - MiHeart/AMI study. *Trials* **9**, 1–8 (2008).

182. Bartunek, J., Vanderheyden, M., Vandekerckhove, B., Mansour, S., De Bruyne, B., De Bondt, P., Van Haute, I., Lootens, N., Heyndrickx, G. & Wijns, W. Intracoronary injection of CD133-positive enriched bone marrow progenitor cells promotes cardiac recovery after recent myocardial infarction: feasibility and safety. *Circulation* **112**, (2005).

183. Huikuri, H. V., Kervinen, K., Niemelä, M., Ylitalo, K., Säily, M., Koistinen, P., Savolainen, E. R., Ukkonen, H., Pietilä, M., Airaksinen, J. K. E., Knuuti, J. & Mäkikallio, T. H. Effects of intracoronary injection of mononuclear bone marrow cells on left ventricular function, arrhythmia risk profile, and restenosis after thrombolytic therapy of acute myocardial infarction. *Eur. Heart J.* **29**, 2723–2732 (2008).

184. Assmus, B., Honold, J., Schächinger, V., Britten, M. B., Fischer-Rasokat, U., Lehmann, R., Teupe, C., Pistorius, K., Martin, H., Abolmaali, N. D., Tonn, T., Dimmeler, S. & Zeiher, A. M. Transcoronary Transplantation of Progenitor Cells after Myocardial Infarction. *N. Engl. J. Med.* **355**, 1222–1232 (2006).

185. Assmus, B., Schächinger, V., Teupe, C., Britten, M., Lehmann, R., Döbert, N., Grünwald, F., Aicher, A., Urbich, C., Martin, H., Hoelzer, D., Dimmeler, S. & Zeiher, A. M. Transplantation of Progenitor Cells and Regeneration Enhancement in Acute Myocardial Infarction (TOPCARE-AMI). *Circulation* **106**, 3009–3017 (2002).

186. Tendera, M., Wojakowski, W., Ruyłło, W., Chojnowska, L., Kpka, C., Tracz, W., Musiałek, P., Piwowarska, W., Nessler, J., Buszman, P., Grajek, S., Brborowicz, P., Majka, M. & Ratajczak, M. Z. Intracoronary infusion of bone marrow-derived selected CD34+CXCR4+ cells and non-selected mononuclear cells in patients with acute STEMI and reduced left ventricular ejection fraction: results of randomized,

multicentre Myocardial Regeneration by Intracoronary Infusion of Selected Population of Stem Cells in Acute Myocardial Infarction (REGENT) Trial. *Eur. Heart J.* **30**, 1313–1321 (2009).

187. Nasseri, B. A., Ebell, W., Dandel, M., Kukucka, M., Gebker, R., Doltra, A., Knosalla, C., Choi, Y. H., Hetzer, R. & Stamm, C. Autologous CD133+ bone marrow cells and bypass grafting for regeneration of ischaemic myocardium: the Cardio133 trial. *Eur. Heart J.* **35**, 1263–1274 (2014).

188. Perin, E. C., Willerson, J. T., Pepine, C. J., Henry, T. D., Ellis, S. G., Zhao, D. X. M., Silva, G. V., Lai, D., Thomas, J. D., Kronenberg, M. W., Martin, A. D., Anderson, R. D., Traverse, J. H., Penn, M. S., Anwaruddin, S., Hatzopoulos, A. K., Gee, A. P., Taylor, D. A., Cogle, C. R., *et al.* Effect of transendocardial delivery of autologous bone marrow mononuclear cells on functional capacity, left ventricular function, and perfusion in chronic heart failure: the FOCUS-CCTRN trial. *JAMA* **307**, 1717–1726 (2012).

189. Hirsch, A., Nijveldt, R., Van Der Vleuten, P. A., Tijssen, J. G. P., Van Der Giessen, W. J., Tio, R. A., Waltenberger, J., Ten Berg, J. M., Doevendans, P. A., Aengevaeren, W. R. M., Zwaginga, J. J., Biemond, B. J., Van Rossum, A. C., Piek, J. J. & Zijlstra, F. Intracoronary infusion of mononuclear cells from bone marrow or peripheral blood compared with standard therapy in patients after acute myocardial infarction treated by primary percutaneous coronary intervention: results of the randomized controlled HEBE trial. *Eur. Heart J.* **32**, 1736–1747 (2011).

190. Assmus, B., Rolf, A., Erbs, S., Elsässer, A., Haberbosch, W., Hambrecht, R., Tillmanns, H., Yu, J., Corti, R., Mathey, D. G., Hamm, C. W., Süselbeck, T., Tonn, T., Dimmeler, S., Dill, T., Zeiher, A. M. & Schächinger, V. Clinical outcome 2 years after intracoronary administration of bone marrow-derived progenitor cells in acute myocardial infarction. *Circ. Heart Fail.* **3**, 89–96 (2010).

191. Schächinger, V., Erbs, S., Elsässer, A., Haberbosch, W., Hambrecht, R., Hölschermann, H., Yu, J., Corti, R., Mathey, D. G., Hamm, C. W., Süselbeck, T., Werner, N., Haase, J., Neuzner, J., Germing, A., Mark, B., Assmus, B., Tonn, T., Dimmeler, S., *et al.* Improved clinical outcome after intracoronary administration of bone-marrow-derived progenitor cells in acute myocardial infarction: final 1-year results of the REPAIR-AMI trial. *Eur. Heart J.* **27**, 2775–2783 (2006).

192. Schächinger, V., Erbs, S., Elsässer, A., Haberbosch, W., Hambrecht, R., Hölschermann, H., Yu, J., Corti, R., Mathey, D. G., Hamm, C. W., Süselbeck, T., Assmus, B., Tonn, T., Dimmeler, S. & Zeiher, A. M. Intracoronary bone marrow-derived progenitor cells in acute myocardial infarction. *N. Engl. J. Med.* **355**, 1210–1221 (2006).

193. Meyer, G. P., Wollert, K. C., Lotz, J., Steffens, J., Lippolt, P., Fichtner, S., Hecker, H., Schaefer, A., Arseniev, L., Hertenstein, B., Ganser, A. & Drexler, H. Intracoronary bone marrow cell transfer after myocardial infarction: eighteen months' follow-up data from the randomized, controlled BOOST (BOne marrOw transfer to enhance ST-elevation infarct regeneration) trial. *Circulation* **113**, 1287–1294 (2006).

194. Wollert, K. C., Meyer, G. P., Lotz, J., Ringes-Lichtenberg, S., Lippolt, P., Breidenbach, C., Fichtner, S., Korte, T., Hornig, B., Messinger, D., Arseniev, L., Hertenstein, B., Ganser, A. & Drexler, H. Intracoronary autologous bone-marrow cell transfer after myocardial infarction: the BOOST randomised controlled clinical trial. *Lancet (London, England)* **364**, 141–148 (2004).

195. Lunde, K., Solheim, S., Aakhus, S., Arnesen, H., Abdelnoor, M., Egeland, T., Endresen, K., Ilebekk, A., Mangschau, A., Fjeld, J. G., Smith, H. J., Taraldsrud, E., Grøgaard, H. K., Bjørnerheim, R., Brekke, M., Müller, C., Hopp, E., Ragnarsson, A., Brinchmann, J. E., *et al.* Intracoronary injection of mononuclear bone marrow cells in acute myocardial infarction. *N. Engl. J. Med.* **355**, 1199–1209 (2006).

196. Roncalli, J., Mouquet, F., Piot, C., Trochu, J. N., Le Corvoisier, P., Neuder, Y., Le Tourneau, T., Agostini, D., Gaxotte, V., Sportouch, C., Galinier, M., Crochet, D., Teiger, E., Richard, M. J., Polge, A. S., Beregi, J. P., Manrique, A., Carrie, D., Susen, S., *et al.* Intracoronary autologous mononucleated bone marrow cell infusion for acute myocardial infarction: results of the randomized multicenter BONAMI trial. *Eur. Heart J.* **32**, 1748–1757 (2011).

197. Janssens, S., Dubois, C., Bogaert, J., Theunissen, K., Deroose, C., Desmet, W., Kalantzi, M., Herbots, L., Sinnaeve, P., Dens, J., Maertens, J., Rademakers, F., Dymarkowski, S., Gheysens, O., Van Cleemput, J., Bormans, G., Nuyts, J., Belmans, A., Mortelmans, L., *et al.* Autologous bone marrow-derived stem-cell transfer in patients with ST-segment elevation myocardial infarction: double-blind, randomised

controlled trial. *Lancet (London, England)* **367**, 113–121 (2006).

198. Hirsch, A., Nijveldt, R., Van Der Vleuten, P. A., Tijssen, J. G. P., Van Der Giessen, W. J., Tio, R. A., Waltenberger, J., Ten Berg, J. M., Doevendans, P. A., Aengevaeren, W. R. M., Zwaginga, J. J., Biemond, B. J., Van Rossum, A. C., Piek, J. J. & Zijlstra, F. Intracoronary infusion of mononuclear cells from bone marrow or peripheral blood compared with standard therapy in patients after acute myocardial infarction treated by primary percutaneous coronary intervention: Results of the randomized controlled HEBE . *Eur. Heart J.* **32**, 1736–1747 (2011).

199. Delewi, R., Van Der Laan, A. M., Robbers, L. F. H. J., Hirsch, A., Nijveldt, R., Van Der Vleuten, P. A., Tijssen, J. G. P., Tio, R. A., Waltenberger, J., Ten Berg, J. M., Doevendans, P. A., Gehlmann, H. R., Van Rossum, A. C., Piek, J. J. & Zijlstra, F. Long term outcome after mononuclear bone marrow or peripheral blood cells infusion after myocardial infarction. *Heart* **101**, 363–368 (2015).

200. Sürder, D., Schwitter, J., Moccetti, T., Astori, G., Rufibach, K., Plein, S., Cicero, V. Lo, Soncin, S., Windecker, S., Moschovitis, A., Wahl, A., Erne, P., Jamshidi, P., Auf Der Maur, C., Manka, R., Soldati, G., Bühler, I., Wyss, C., Landmesser, U., *et al.* Cell-based therapy for myocardial repair in patients with acute myocardial infarction: rationale and study design of the SWiss multicenter Intracoronary Stem cells Study in Acute Myocardial Infarction (SWISS-AMI). *Am. Heart J.* **160**, 58–64 (2010).

201. Traverse, J. H., Henry, T. D., Vaughn, D. E., Ellis, S. G., Pepine, C. J., Willerson, J. T., Zhao, D. X. M., Piller, L. B., Penn, M. S., Byrne, B. J., Perin, E. C., Gee, A. P., Hatzopoulos, A. K., McKenna, D. H., Forder, J. R., Taylor, D. A., Cogle, C. R., Olson, R. E., Jorgenson, B. C., *et al.* Rationale and design for TIME: A phase II, randomized, double-blind, placebo-controlled pilot trial evaluating the safety and effect of timing of administration of bone marrow mononuclear cells after acute myocardial infarction. *Am. Heart J.* **158**, 356–363 (2009).

202. Traverse, J. H., Henry, T. D., Vaughan, D. E., Ellis, S. G., Pepine, C. J., Willerson, J. T., Zhao, D. X. M., Simpson, L. M., Penn, M. S., Byrne, B. J., Perin, E. C., Gee, A. P., Hatzopoulos, A. K., Mckenna, D. H., Forder, J. R., Taylor, D. A., Cogle, C. R., Baraniuk, S., Olson, R. E., *et al.* LateTIME: A Phase-II, randomized, double-blinded, placebo-controlled, pilot trial evaluating the safety and effect of administration of bone

marrow mononuclear cells 2 to 3 weeks after acute myocardial infarction. *Texas Hear. Inst. J.* **37**, 412–420 (2010).

203. Lee, S. H., Hong, J. H., Cho, K. H., Noh, J. W. & Cho, H. J. Discrepancy between short-term and long-term effects of bone marrow-derived cell therapy in acute myocardial infarction: A systematic review and meta-analysis. *Stem Cell Res. Ther.* **7**, 153 (2016).

204. Kang, W. J., Kang, H.-J., Kim, H.-S., Chung, J.-K., Lee, M. C. & Lee, D. S. Tissue distribution of 18F-FDG-labeled peripheral hematopoietic stem cells after intracoronary administration in patients with myocardial infarction. *J. Nucl. Med.* **47**, 1295–1301 (2006).

205. Li, Z., Solomonidis, E. G., Meloni, M., Taylor, R. S., Duffin, R., Dobie, R., Magalhaes, M. S., Henderson, B. E. P., Louwe, P. A., D'Amico, G., Hodivala-Dilke, K. M., Shah, A. M., Mills, N. L., Simons, B. D., Gray, G. A., Henderson, N. C., Baker, A. H. & Brittan, M. Single-cell transcriptome analyses reveal novel targets modulating cardiac neovascularization by resident endothelial cells following myocardial infarction. *Eur. Heart J.* **40**, 2507–2520 (2019).

206. Mathur, A., Arnold, R., Assmus, B., Bartunek, J., Belmans, A., Bönig, H., Crea, F., Dimmeler, S., Dowlut, S., Fernández-Avilés, F., Galiñanes, M., Garcia-Dorado, D., Hartikainen, J., Hill, J., Hogardt-Noll, A., Homsy, C., Janssens, S., Kala, P., Kastrup, J., *et al.* The effect of intracoronary infusion of bone marrow-derived mononuclear cells on all-cause mortality in acute myocardial infarction: Rationale and design of the BAMI trial. *Eur. J. Heart Fail.* **19**, 545–550 (2017).

207. Kim, H., Kim, S.-W., Nam, D., Kim, S. & Yoon, Y.-S. Cell Therapy with Bone Marrow Cells for Myocardial Regeneration. *Antioxid. Redox Signal* **11**, 1897–1911 (2009).

208. Kocher, A. A., Schuster, M. D., Szabolcs, M. J., Takuma, S., Burkhoff, D., Wang, J., Homma, S., Edwards, N. M. & Itescu, S. Neovascularization of ischemic myocardium by human bone-marrow-derived angioblasts prevents cardiomyocyte apoptosis, reduces remodeling and improves cardiac function. *Nat. Med.* **7**, 430–436 (2001).

209. Caplan, A. I. & Dennis, J. E. Mesenchymal stem cells as trophic mediators. *J. Cell. Biochem.* **98**, 1076–1084 (2006).

210. Asli, N. S., Xaymardan, M. & Harvey, R. P. Epicardial origin of resident mesenchymal

stem cells in the adult mammalian heart. *J. Dev. Biol.* **2**, 117–137 (2014).

211. Chong, J. J. H., Chandrakanthan, V., Xaymardan, M., Asli, N. S., Li, J., Ahmed, I., Heffernan, C., Menon, M. K., Scarlett, C. J., Rashidianfar, A., Biben, C., Zoellner, H., Colvin, E. K., Pimanda, J. E., Biankin, A. V., Zhou, B., Pu, W. T., Prall, O. W. J. & Harvey, R. P. Adult cardiac-resident MSC-like stem cells with a proepicardial origin. *Cell Stem Cell* **9**, 527–540 (2011).

212. Williams, A. R. & Hare, J. M. Mesenchymal stem cells: biology, pathophysiology, translational findings, and therapeutic implications for cardiac disease. *Circ. Res.* **109**, 923–940 (2011).

213. Shi, W., Xin, Q., Yuan, R., Yuan, Y., Cong, W. & Chen, K. Neovascularization: The Main Mechanism of MSCs in Ischemic Heart Disease Therapy. *Front. Cardiovasc. Med.* **8**, 10 (2021).

214. Silva, G. V., Litovsky, S., Assad, J. A. R., Sousa, A. L. S., Martin, B. J., Vela, D., Coulter, S. C., Lin, J., Ober, J., Vaughn, W. K., Branco, R. V. C., Oliveira, E. M., He, R., Geng, Y. J., Willerson, J. T. & Perin, E. C. Mesenchymal stem cells differentiate into an endothelial phenotype, enhance vascular density, and improve heart function in a canine chronic ischemia model. *Circulation* **111**, 150–156 (2005).

215. Wang, H. H., Cui, Y. L., Zaorsky, N. G., Lan, J., Deng, L., Zeng, X. L., Wu, Z. Q., Tao, Z., Guo, W. H., Wang, Q. X., Zhao, L. J., Yuan, Z. Y., Lu, Y., Wang, P. & Meng, M. Bin. Mesenchymal stem cells generate pericytes to promote tumor recurrence via vasculogenesis after stereotactic body radiation therapy. *Cancer Lett.* **375**, 349–359 (2016).

216. Jeon, E. S., Park, W. S., Lee, M. J., Kim, Y. M., Han, J. & Kim, J. H. A rho kinase/myocardin-related transcription factor-a-dependent mechanism underlies the sphingosylphosphorylcholine-induced differentiation of mesenchymal stem cells into contractile smooth muscle cells. *Circ. Res.* **103**, 635–642 (2008).

217. Gu, W., Hong, X., Le Bras, A., Nowak, W. N., Bhaloo, S. I., Deng, J., Xie, Y., Hu, Y., Ruan, X. Z. & Xu, Q. Smooth muscle cells differentiated from mesenchymal stem cells are regulated by microRNAs and suitable for vascular tissue grafts. *J. Biol. Chem.* **293**, 8089 (2018).

218. Oswald, J., Boxberger, S., Joergensen, B., Bornhaeuser, M., Ehninger, G. & Werner, C. Mesenchymal stem cells can be differentiated into endothelial cells in vitro. *Stem Cells* **22**, 506 (2004).

219. Beitnes, J. O., Øie, E., Shahdadfar, A., Karlsen, T., Müller, R. M. B., Aakhus, S., Reinholt, F. P. & Brinchmann, J. E. Intramyocardial injections of human mesenchymal stem cells following acute myocardial infarction modulate scar formation and improve left ventricular function. *Cell Transplant.* **21**, 1697–1709 (2012).

220. Zeng, L., Hu, Q., Wang, X., Mansoor, A., Lee, J., Feygin, J., Zhang, G., Suntharalingam, P., Boozer, S., Mhashilkar, A., Panetta, C. J., Swingen, C., Deans, R., From, A. H. L., Bache, R. J., Verfaillie, C. M. & Zhang, J. Bioenergetic and functional consequences of bone marrow-derived multipotent progenitor cell transplantation in hearts with postinfarction left ventricular remodeling. *Circulation* **115**, 1866–1875 (2007).

221. Hatzistergos, K. E., Quevedo, H., Oskouei, B. N., Hu, Q., Feigenbaum, G. S., Margitich, I. S., Mazhari, R., Boyle, A. J., Zambrano, J. P., Rodriguez, J. E., Dulce, R., Pattany, P. M., Valdes, D., Revilla, C., Heldman, A. W., McNiece, I. & Hare, J. M. Bone marrow mesenchymal stem cells stimulate cardiac stem cell proliferation and differentiation. *Circ. Res.* **107**, 913–922 (2010).

222. Williams, A. R., Suncion, V. Y., McCall, F., Guerra, D., Mather, J., Zambrano, J. P., Heldman, A. W. & Hare, J. M. Durable Scar Size Reduction Due to Allogeneic Mesenchymal Stem Cell Therapy Regulates Whole-Chamber Remodeling. *J Am Hear. Assoc* **2**, (2013).

223. Quevedo, H. C., Hatzistergos, K. E., Oskouei, B. N., Feigenbaum, G. S., Rodriguez, J. E., Valdes, D., Pattany, P. M., Zambrano, J. P., Hu, Q., McNiece, I., Heldman, A. W. & Hare, J. M. Allogeneic mesenchymal stem cells restore cardiac function in chronic ischemic cardiomyopathy via trilineage differentiating capacity. *Proc. Natl. Acad. Sci. U. S. A.* **106**, 14022–14027 (2009).

224. Schuleri, K. H., Feigenbaum, G. S., Centola, M., Weiss, E. S., Zimmet, J. M., Turney, J., Kellner, J., Zviman, M. M., Hatzistergos, K. E., Detrick, B., Conte, J. V., McNiece, I., Steenbergen, C., Lardo, A. C. & Hare, J. M. Autologous mesenchymal stem cells produce reverse remodelling in chronic ischaemic cardiomyopathy. *Eur. Heart J.* **30**,

2722–2732 (2009).

225. Suncion, V. Y., Ghersin, E., Fishman, J. E., Zambrano, J. P., Karantalis, V., Mandel, N., Nelson, K. H., Gerstenblith, G., Difede Velazquez, D. L., Breton, E., Sitammagari, K., Schulman, I. H., Taldone, S. N., Williams, A. R., Sanina, C., Johnston, P. V., Brinker, J., Altman, P., Mushtaq, M., *et al.* Does transendocardial injection of mesenchymal stem cells improve myocardial function locally or globally?: An analysis from the Percutaneous Stem Cell Injection Delivery Effects on Neomyogenesis (POSEIDON) randomized trial. *Circ. Res.* **114**, 1292–1301 (2014).

226. Hare, J. M., Fishman, J. E., Gerstenblith, G., DiFede Velazquez, D. L., Zambrano, J. P., Suncion, V. Y., Tracy, M., Ghersin, E., Johnston, P. V., Brinker, J. A., Breton, E., Davis-Sproul, J., Schulman, I. H., Byrnes, J., Mendizabal, A. M., Lowery, M. H., Rouy, D., Altman, P., Wong Po Foo, C., *et al.* Comparison of allogeneic vs autologous bone marrow–derived mesenchymal stem cells delivered by transendocardial injection in patients with ischemic cardiomyopathy: the POSEIDON randomized trial. *JAMA* **308**, 2369–2379 (2012).

227. Kinnaird, T., Stabile, E., Burnett, M. S., Lee, C. W., Barr, S., Fuchs, S. & Epstein, S. E. Marrow-Derived Stromal Cells Express Genes Encoding a Broad Spectrum of Arteriogenic Cytokines and Promote In Vitro and In Vivo Arteriogenesis Through Paracrine Mechanisms. *Circ. Res.* **94**, 678–685 (2004).

228. Gnecchi, M., He, H., Noiseux, N., Liang, O. D., Zhang, L., Morello, F., Mu, H., Melo, L. G., Pratt, R. E., Ingwall, J. S. & Dzau, V. J. Evidence supporting paracrine hypothesis for Akt-modified mesenchymal stem cell-mediated cardiac protection and functional improvement. *FASEB J.* **20**, 661–669 (2006).

229. Terzic, A. & Behfar, A. Stem cell therapy for heart failure: Ensuring regenerative proficiency. *Trends Cardiovasc. Med.* **26**, 395–404 (2016).

230. Behfar, A., Yamada, S., Crespo-Diaz, R., Nesbitt, J. J., Rowe, L. A., Perez-Terzic, C., Gaussin, V., Homsy, C., Bartunek, J. & Terzic, A. Guided cardiopoiesis enhances therapeutic benefit of bone marrow human mesenchymal stem cells in chronic myocardial infarction. *J. Am. Coll. Cardiol.* **56**, 721–734 (2010).

231. Bartunek, J., Behfar, A., Dolatabadi, D., Vanderheyden, M., Ostojic, M., Dens, J., El

Nakadi, B., Banovic, M., Beleslin, B., Vrolix, M., Legrand, V., Vrints, C., Vanoverschelde, J. L., Crespo-Diaz, R., Homsy, C., Tendera, M., Waldman, S., Wijns, W. & Terzic, A. Cardiopoietic stem cell therapy in heart failure: the C-CURE (Cardiopoietic stem Cell therapy in heart failURE) multicenter randomized trial with lineage-specified biologics. *J. Am. Coll. Cardiol.* **61**, 2329–2338 (2013).

232. Bartunek, J., Terzic, A., Davison, B. A., Filippatos, G. S., Radovanovic, S., Beleslin, B., Merkely, B., Musialek, P., Wojakowski, W., Andreka, P., Horvath, I. G., Katz, A., Dolatabadi, D., El Nakadi, B., Arandjelovic, A., Edes, I., Seferovic, P. M., Obradovic, S., Vanderheyden, M., *et al.* Cardiopoietic cell therapy for advanced ischaemic heart failure: results at 39 weeks of the prospective, randomized, double blind, sham-controlled CHART-1 clinical trial. *Eur. Heart J.* **38**, 648–660 (2017).

233. Jopling, C., Sleep, E., Raya, M., Martí, M., Raya, A. & Belmonte, J. C. I. Zebrafish heart regeneration occurs by cardiomyocyte dedifferentiation and proliferation. *Nature* **464**, 606 (2010).

234. Beltrami, A. P., Barlucchi, L., Torella, D., Baker, M., Limana, F., Chimenti, S., Kasahara, H., Rota, M., Musso, E., Urbanek, K., Leri, A., Kajstura, J., Nadal-Ginard, B. & Anversa, P. Adult cardiac stem cells are multipotent and support myocardial regeneration. *Cell* **114**, 763–776 (2003).

235. Dawn, B., Stein, A. B., Urbanek, K., Rota, M., Whang, B., Rastaldo, R., Torella, D., Tang, X. L., Rezazadeh, A., Kajstura, J., Leri, A., Hunt, G., Varma, J., Prabhu, S. D., Anversa, P. & Bolli, R. Cardiac stem cells delivered intravascularly traverse the vessel barrier, regenerate infarcted myocardium, and improve cardiac function. *Proc. Natl. Acad. Sci. U. S. A.* **102**, 3766–3771 (2005).

236. Zaruba, M. M., Soonpaa, M., Reuter, S. & Field, L. J. Cardiomyogenic potential of C-kit(+)-expressing cells derived from neonatal and adult mouse hearts. *Circulation* **121**, 1992–2000 (2010).

237. Koninckx, R., Hensen, K., Rummens, J. L. & Hendrikx, M. Cardiac stem cells in the real world. *J. Thorac. Cardiovasc. Surg.* **136**, 797–798 (2008).

238. Vicinanza, C., Aquila, I., Cianflone, E., Scalise, M., Marino, F., Mancuso, T., Fumagalli, F., Giovannone, E. D., Cristiano, F., Iaccino, E., Marotta, P., Torella, A., Latini, R.,

Agosti, V., Veltri, P., Urbanek, K., Isidori, A. M., Saur, Di., Indolfi, C., *et al.* Kit cre knock-in mice fail to fate-map cardiac stem cells. *Nature* **555**, E1–E17 (2018).

239. Sultana, N., Zhang, L., Yan, J., Chen, J., Cai, W., Razzaque, S., Jeong, D., Sheng, W., Bu, L., Xu, M., Huang, G. Y., Hajjar, R. J., Zhou, B., Moon, A. & Cai, C. L. Resident c-kit(+) cells in the heart are not cardiac stem cells. *Nat. Commun.* **6**, (2015).

240. Liu, Q., Yang, R., Huang, X., Zhang, H., He, L., Zhang, L., Tian, X., Nie, Y., Hu, S., Yan, Y., Zhang, L., Qiao, Z., Wang, Q. D., Lui, K. O. & Zhou, B. Genetic lineage tracing identifies in situ Kit-expressing cardiomyocytes. *Cell Res. 2016 261* **26**, 119–130 (2015).

241. Chugh, A. R., Beache, G. M., Loughran, J. H., Mewton, N., Elmore, J. B., Kajstura, J., Pappas, P., Tatooles, A., Stoddard, M. F., Lima, J. A. C., Slaughter, M. S., Anversa, P. & Bolli, R. Administration of cardiac stem cells in patients with ischemic cardiomyopathy: the SCIPIO trial: surgical aspects and interim analysis of myocardial function and viability by magnetic resonance. *Circulation* **126**, (2012).

242. Editors, T. L. Expression of concern: the SCIPIO trial. *Lancet* **383**, 1279 (2014).

243. Oh, H., Bradfute, S. B., Gallardo, T. D., Nakamura, T., Gaussin, V., Mishina, Y., Pocius, J., Michael, L. H., Behringer, R. R., Garry, D. J., Entman, M. L. & Schneider, M. D. Cardiac progenitor cells from adult myocardium: homing, differentiation, and fusion after infarction. *Proc. Natl. Acad. Sci. U. S. A.* **100**, 12313–12318 (2003).

244. Matsuura, K., Nagai, T., Nishigaki, N., Oyama, T., Nishi, J., Wada, H., Sano, M., Toko, H., Akazawa, H., Sato, T., Nakaya, H., Kasanuki, H. & Komuro, I. Adult cardiac Sca-1-positive cells differentiate into beating cardiomyocytes. *J. Biol. Chem.* **279**, 11384–11391 (2004).

245. Clayton, E. & Forbes, S. J. The isolation and in vitro expansion of hepatic Sca-1 progenitor cells. *Biochem. Biophys. Res. Commun.* **381**, 549–553 (2009).

246. McQualter, J. L., Brouard, N., Williams, B., Baird, B. N., Sims-Lucas, S., Yuen, K., Nilsson, S. K., Simmons, P. J. & Bertoncello, I. Endogenous Fibroblastic Progenitor Cells in the Adult Mouse Lung Are Highly Enriched in the Sca-1 Positive Cell Fraction. *Stem Cells* **27**, 623–633 (2009).

247. Xin, L., Lawson, D. A. & Witte, O. N. The Sca-1 cell surface marker enriches for a

prostate-regenerating cell subpopulation that can initiate prostate tumorigenesis. *Proc. Natl. Acad. Sci.* **102**, 6942–6947 (2005).

248. Welm, B. E., Tepera, S. B., Venezia, T., Graubert, T. A., Rosen, J. M. & Goodell, M. A. Sca-1pos Cells in the Mouse Mammary Gland Represent an Enriched Progenitor Cell Population. *Dev. Biol.* **245**, 42–56 (2002).

249. Matsuura, K., Honda, A., Nagai, T., Fukushima, N., Iwanaga, K., Tokunaga, M., Shimizu, T., Okano, T., Kasanuki, H., Hagiwara, N. & Komuro, I. Transplantation of cardiac progenitor cells ameliorates cardiac dysfunction after myocardial infarction in mice. *J. Clin. Invest.* **119**, 2204–2217 (2009).

250. Uchida, S., De Gaspari, P., Kostin, S., Jenniches, K., Kilic, A., Izumiya, Y., Shiojima, I., Grosse Kreymborg, K., Renz, H., Walsh, K. & Braun, T. Sca1-derived cells are a source of myocardial renewal in the murine adult heart. *Stem Cell Reports* **1**, 397–410 (2013).

251. Takamiya, M., Haider, K. H. & Ashraf, M. Identification and Characterization of a Novel Multipotent Sub-Population of Sca-1+ Cardiac Progenitor Cells for Myocardial Regeneration. *PLoS One* **6**, e25265 (2011).

252. Soonpaa, M. H., Lafontant, P. J., Reuter, S., Scherschel, J. A., Srour, E. F., Zaruba, M. M., Rubart-Von Der Lohe, M. & Field, L. J. Research letter: Absence of cardiomyocyte differentiation following transplantation of adult cardiac-resident Sca-1+ cells into infarcted mouse hearts. *Circulation* **138**, 2963–2966 (2018).

253. Tang, J., Li, Y., Huang, X., He, L., Zhang, L., Wang, H., Yu, W., Pu, W., Tian, X., Nie, Y., Hu, S., Wang, Q. D., Lui, K. O. & Zhou, B. Fate mapping of Sca1+ cardiac progenitor cells in the adult mouse heart. *Circulation* **138**, 2967–2969 (2018).

254. Neidig, L. E., Weinberger, F., Palpant, N. J., Mignone, J., Martinson, A. M., Sorensen, D. W., Bender, I., Nemoto, N., Reinecke, H., Pabon, L., Molkentin, J. D., Murry, C. E. & Van Berlo, J. H. Evidence for Minimal Cardiogenic Potential of Stem Cell Antigen 1–Positive Cells in the Adult Mouse Heart. *Circulation* **138**, 2960 (2018).

255. Zhang, L., Sultana, N., Yan, J., Yang, F., Chen, F., Chepurko, E., Yang, F. C., Du, Q., Zangi, L., Xu, M., Bu, L. & Cai, C. L. Cardiac Sca-1+ cells are not intrinsic stem cells for myocardial development, renewal, and repair. *Circulation* **138**, 2919–2930 (2018).

256. Vagnozzi, R. J., Sargent, M. A., Lin, S. C. J., Palpant, N. J., Murry, C. E. & Molkentin, J. D. Genetic lineage tracing of Sca-1+ cells reveals endothelial but not myogenic contribution to the murine heart. *Circulation* **138**, 2931–2939 (2018).

257. Martin, C. M., Meeson, A. P., Robertson, S. M., Hawke, T. J., Richardson, J. A., Bates, S., Goetsch, S. C., Gallardo, T. D. & Garry, D. J. Persistent expression of the ATP-binding cassette transporter, Abcg2, identifies cardiac SP cells in the developing and adult heart. *Dev. Biol.* **265**, 262–275 (2004).

258. Oyama, T., Nagai, T., Wada, H., Naito, A. T., Matsuura, K., Iwanaga, K., Takahashi, T., Goto, M., Mikami, Y., Yasuda, N., Akazawa, H., Uezumi, A., Takeda, S. & Komuro, I. Cardiac side population cells have a potential to migrate and differentiate into cardiomyocytes in vitro and in vivo. *J. Cell Biol.* **176**, 329 (2007).

259. Doyle, M. J., Maher, T. J., Li, Q., Garry, M. G., Sorrentino, B. P. & Martin, C. M. Abcg2-Labeled Cells Contribute to Different Cell Populations in the Embryonic and Adult Heart. *Stem Cells Dev.* **25**, 277–284 (2016).

260. Maher, T. J., Ren, Y., Li, Q., Braunlin, E., Garry, M. G., Sorrentino, B. P. & Martin, C. M. ATP-binding cassette transporter Abcg2 lineage contributes to the cardiac vasculature after oxidative stress. *Am. J. Physiol. Heart Circ. Physiol.* **306**, (2014).

261. Yellamilli, A., Ren, Y., McElmurry, R. T., Lambert, J. P., Gross, P., Mohsin, S., Houser, S. R., Elrod, J. W., Tolar, J., Garry, D. J. & van Berlo, J. H. Abcg2-expressing side population cells contribute to cardiomyocyte renewal through fusion. *FASEB J.* **34**, 5642–5657 (2020).

262. Valiente-Alandi, I., Albo-Castellanos, C., Herrero, D., Sanchez, I. & Bernad, A. Bmi1 + cardiac progenitor cells contribute to myocardial repair following acute injury. *Stem Cell Res. Ther.* **7**, 100 (2016).

263. Valiente-Alandi, I., Albo-Castellanos, C., Herrero, D., Arza, E., Garcia-Gomez, M., Segovia, J. C., Capecchi, M. & Bernad, A. Cardiac Bmi1+ cells contribute to myocardial renewal in the murine adult heart. *Stem Cell Res. Ther.* **6**, 1–16 (2015).

264. Eschenhagen, T., Bolli, R., Braun, T., Field, L. J., Fleischmann, B. K., Frisén, J., Giacca, M., Hare, J. M., Houser, S., Lee, R. T., Marbán, E., Martin, J. F., Molkentin, J. D., Murry, C. E., Riley, P. R., Ruiz-Lozano, P., Sadek, H. A., Sussman, M. A. & Hill, J. A.

Cardiomyocyte Regeneration: A Consensus Statement. *Circulation* **136**, 680–686 (2017).

265. Vagnozzi, R. J., Molkentin, J. D. & Houser, S. R. New Myocyte Formation in the Adult Heart. *Circ. Res.* **123**, 159–176 (2018).

266. Cai, C. L. & Molkentin, J. D. The Elusive Progenitor Cell in Cardiac Regeneration: Slip-Slidin' Away. *Circ. Res.* **120**, 400 (2017).

267. Barile, L., Gherghiceanu, M., Popescu, L. M., Moccetti, T. & Vassalli, G. Human cardiospheres as a source of multipotent stem and progenitor cells. *Stem Cells Int.* **2013**, (2013).

268. Messina, E., De Angelis, L., Frati, G., Morrone, S., Chimenti, S., Fiordaliso, F., Salio, M., Battaglia, M., Latronico, M. V. G., Coletta, M., Vivarelli, E., Frati, L., Cossu, G. & Giacomello, A. Isolation and expansion of adult cardiac stem cells from human and murine heart. *Circ. Res.* **95**, 911–921 (2004).

269. Grigorian-Shamagian, L., Liu, W., Fereydooni, S., Middleton, R. C., Valle, J., Cho, J. H. & Marbán, E. Cardiac and systemic rejuvenation after cardiosphere-derived cell therapy in senescent rats. *Eur. Heart J.* **38**, 2957–2967 (2017).

270. Malliaras, K., Smith, R. R., Kanazawa, H., Yee, K., Seinfeld, J., Tseliou, E., Dawkins, J. F., Kreke, M., Cheng, K., Luthringer, D., Ho, C. S., Blusztajn, A., Valle, I., Chowdhury, S., Makkar, R. R., Dharmakumar, R., Li, D., Marbán, L. & Marbán, E. Validation of contrast-enhanced magnetic resonance imaging to monitor regenerative efficacy after cell therapy in a porcine model of convalescent myocardial infarction. *Circulation* **128**, 2764–2775 (2013).

271. Tseliou, E., Pollan, S., Malliaras, K., Terrovitis, J., Sun, B., Galang, G., Marbán, L., Luthringer, D. & Marbán, E. Allogeneic cardiospheres safely boost cardiac function and attenuate adverse remodeling after myocardial infarction in immunologically mismatched rat strains. *J. Am. Coll. Cardiol.* **61**, 1108–1119 (2013).

272. Malliaras, K., Li, T. S., Luthringer, D., Terrovitis, J., Cheng, K., Chakravarty, T., Galang, G., Zhang, Y., Schoenhoff, F., Van Eyk, J., Marbán, L. & Marbán, E. Safety and efficacy of allogeneic cell therapy in infarcted rats transplanted with mismatched cardiosphere-derived cells. *Circulation* **125**, 100–112 (2012).

273. Smith, R. R., Barile, L., Cho, H. C., Leppo, M. K., Hare, J. M., Messina, E., Giacomello, A., Abraham, M. R. & Marbán, E. Regenerative potential of cardiosphere-derived cells expanded from percutaneous endomyocardial biopsy specimens. *Circulation* **115**, 896–908 (2007).

274. Williams, A. R., Hatzistergos, K. E., Addicott, B., McCall, F., Carvalho, D., Suncion, V., Morales, A. R., Da Silva, J., Sussman, M. A., Heldman, A. W. & Hare, J. M. Enhanced effect of combining human cardiac stem cells and bone marrow mesenchymal stem cells to reduce infarct size and to restore cardiac function after myocardial infarction. *Circulation* **127**, 213–223 (2013).

275. Chimenti, I., Smith, R. R., Li, T. S., Gerstenblith, G., Messina, E., Giacomello, A. & Marbán, E. Relative roles of direct regeneration versus paracrine effects of human cardiosphere-derived cells transplanted into infarcted mice. *Circ. Res.* **106**, 971–980 (2010).

276. Malliaras, K., Makkar, R. R., Smith, R. R., Cheng, K., Wu, E., Bonow, R. O., Marbán, L., Mendizabal, A., Cingolani, E., Johnston, P. V., Gerstenblith, G., Schuleri, K. H., Lardo, A. C. & Marbán, E. Intracoronary cardiosphere-derived cells after myocardial infarction: evidence of therapeutic regeneration in the final 1-year results of the CADUCEUS trial (CArdiosphere-Derived aUtologous stem CElls to reverse ventricUlar dySfunction). *J. Am. Coll. Cardiol.* **63**, 110–122 (2014).

277. Chong, J. J. H., Yang, X., Don, C. W., Minami, E., Liu, Y. W., Weyers, J. J., Mahoney, W. M., Van Biber, B., Cook, S. M., Palpant, N. J., Gantz, J. A., Fugate, J. A., Muskheli, V., Gough, G. M., Vogel, K. W., Astley, C. A., Hotchkiss, C. E., Baldessari, A., Pabon, L., *et al.* Human embryonic-stem-cell-derived cardiomyocytes regenerate non-human primate hearts. *Nature* **510**, 273–277 (2014).

278. Lo, B. & Parham, L. Ethical issues in stem cell research. *Endocr. Rev.* **30**, 204–213 (2009).

279. Takahashi, K. & Yamanaka, S. Induction of pluripotent stem cells from mouse embryonic and adult fibroblast cultures by defined factors. *Cell* **126**, 663–676 (2006).

280. Menasché, P., Vanneaux, V., Hagège, A., Bel, A., Cholley, B., Cacciapuoti, I., Parouchev, A., Benhamouda, N., Tachdjian, G., Tosca, L., Trouvin, J. H., Fabreguettes,

J. R., Bellamy, V., Guillemain, R., Suberbielle Boissel, C., Tartour, E., Desnos, M. & Larghero, J. Human embryonic stem cell-derived cardiac progenitors for severe heart failure treatment: first clinical case report. *Eur. Heart J.* **36**, 2011–2017 (2015).

281. Hirschi, K. K., Li, S. & Roy, K. Induced Pluripotent Stem Cells for Regenerative Medicine. *Annu. Rev. Biomed. Eng.* **16**, 277 (2014).

282. Yamashita, J., Itoh, H., Hirashima, M., Ogawa, M., Nishikawa, S., Yurugi, T., Naito, M., Nakao, K. & Nishikawa, S. I. Flk1-positive cells derived from embryonic stem cells serve as vascular progenitors. *Nature* **408**, 92–96 (2000).

283. White, M. P., Rufaihah, A. J., Liu, L., Ghebremariam, Y. T., Ivey, K. N., Cooke, J. P. & Srivastava, D. Limited gene expression variation in human embryonic stem cell and induced pluripotent stem cell-derived endothelial cells. *Stem Cells* **31**, 92–103 (2013).

284. Rufaihah, A. J., Huang, N. F., Jamé, S., Lee, J. C., Nguyen, H. N., Byers, B., De, A., Okogbaa, J., Rollins, M., Reijo-Pera, R., Gambhir, S. S. & Cooke, J. P. Endothelial cells derived from human iPSCS increase capillary density and improve perfusion in a mouse model of peripheral arterial disease. *Arterioscler. Thromb. Vasc. Biol.* **31**, (2011).

285. Lian, X., Bao, X., Al-Ahmad, A., Liu, J., Wu, Y., Dong, W., Dunn, K. K., Shusta, E. V. & Palecek, S. P. Efficient differentiation of human pluripotent stem cells to endothelial progenitors via small-molecule activation of WNT signaling. *Stem cell reports* **3**, 804–816 (2014).

286. Li, Z., Wu, J. C., Sheikh, A. Y., Kraft, D., Cao, F., Xie, X., Patel, M., Gambhir, S. S., Robbins, R. C., Cooke, J. P. & Wu, J. C. Differentiation, survival, and function of embryonic stem cell derived endothelial cells for ischemic heart disease. *Circulation* **116**, (2007).

287. Gu, M., Nguyen, P. K., Lee, A. S., Xu, D., Hu, S., Plews, J. R., Han, L., Huber, B. C., Lee, W. H., Gong, Y., De Almeida, P. E., Lyons, J., Ikeno, F., Pacharinsak, C., Connolly, A. J., Gambhir, S. S., Robbins, R. C., Longaker, M. T. & Wu, J. C. Microfluidic single-cell analysis shows that porcine induced pluripotent stem cell-derived endothelial cells improve myocardial function by paracrine activation. *Circ. Res.* **111**, 882–893 (2012).

288. Johnson, T., Zhao, L., Manuel, G., Taylor, H. & Liu, D. Approaches to therapeutic angiogenesis for ischemic heart disease. *J. Mol. Med.* **97**, 141–151 (2019).

289. Lötvall, J., Hill, A. F., Hochberg, F., Buzás, E. I., Vizio, D. Di, Gardiner, C., Gho, Y. S., Kurochkin, I. V., Mathivanan, S., Quesenberry, P., Sahoo, S., Tahara, H., Wauben, M. H., Witwer, K. W. & Théry, C. Minimal experimental requirements for definition of extracellular vesicles and their functions: a position statement from the International Society for Extracellular Vesicles. *J. Extracell. Vesicles* **3**, (2014).

290. Harp, D., Driss, A., Mehrabi, S., Chowdhury, I., Xu, W., Liu, D., Garcia-Barrio, M., Taylor, R. N., Gold, B., Jefferson, S., Sidell, N. & Thompson, W. Exosomes derived from endometriotic stromal cells have enhanced angiogenic effects in vitro. *Cell Tissue Res.* **365**, 187–196 (2016).

291. Zhu, H. & Fan, G.-C. Extracellular/circulating microRNAs and their potential role in cardiovascular disease. *Am. J. Cardiovasc. Dis.* **1**, 138–149 (2011).

292. Camussi, G., Deregibus, M. C., Bruno, S., Cantaluppi, V. & Biancone, L. Exosomes/microvesicles as a mechanism of cell-to-cell communication. *Kidney Int.* **78**, 838–848 (2010).

293. Vagnozzi, R. J., Maillet, M., Sargent, M. A., Khalil, H., Johansen, A. K. Z., Schwanekamp, J. A., York, A. J., Huang, V., Nahrendorf, M., Sadayappan, S. & Molkentin, J. D. An acute immune response underlies the benefit of cardiac stem cell therapy. *Nature* **577**, 405 (2020).

294. Eppler, S. M., Combs, D. L., Henry, T. D., Lopez, J. J., Ellis, S. G., Yi, J. H., Annex, B. H., McCluskey, E. R. & Zioncheck, T. F. A target-mediated model to describe the pharmacokinetics and hemodynamic effects of recombinant human vascular endothelial growth factor in humans. *Clin. Pharmacol. Ther.* **72**, 20–32 (2002).

295. Giacca, M. & Zacchigna, S. VEGF gene therapy: Therapeutic angiogenesis in the clinic and beyond. *Gene Ther.* **19**, 622–629 (2012).

296. Kastrup, J., Jørgensen, E., Rück, A., Tägil, K., Glogar, D., Ruzyllo, W., Bøtker, H. E., Dudek, D., Drvota, V., Hesse, B., Thuesen, L., Blomberg, P., Gyöngyösi, M. & Sylvén, C. Direct intramyocardial plasmid vascular endothelial growth factor-A 165 gene therapy in patients with stable severe angina pectoris: A randomized double-blind

placebo-controlled study: The Euroinject One trial. *J. Am. Coll. Cardiol.* **45**, 982–988 (2005).

297. Stewart, D. J., Kutryk, M. J. B., Fitchett, D., Freeman, M., Camack, N., Su, Y., Siega, A. Della, Bilodeau, L., Burton, J. R., Proulx, G. & Radhakrishnan, S. VEGF gene therapy fails to improve perfusion of ischemic myocardium in patients with advanced coronary disease: Results of the NORTHERN trial. *Mol. Ther.* **17**, 1109–1115 (2009).

298. Hedman, M., Hartikainen, J., Syvänne, M., Stjernvall, J., Hedman, A., Kivelä, A., Vanninen, E., Mussalo, H., Kauppila, E., Simula, S., Närvänen, O., Rantala, A., Peuhkurinen, K., Nieminen, M. S., Laakso, M. & Ylä-Herttuala, S. Safety and feasibility of catheter-based local intracoronary vascular endothelial growth factor gene transfer in the prevention of postangioplasty and in-stent restenosis and in the treatment of chronic myocardial ischemia: Phase II results of the Kuopio . *Circulation* **107**, 2677–2683 (2003).

299. Kukuła, K., Chojnowska, L., Dąbrowski, M., Witkowski, A., Chmielak, Z., Skwarek, M., Kądziela, J., Teresińska, A., Małecki, M., Janik, P., Lewandowski, Z., Kłopotowski, M., Wnuk, J. & Ruzyłło, W. Intramyocardial plasmid-encoding human vascular endothelial growth factor A165/basic fibroblast growth factor therapy using percutaneous transcatheter approach in patients with refractory coronary artery disease (VIF-CAD). *Am. Heart J.* **161**, 581–589 (2011).

300. Ripa, R. S., Wang, Y., Jørgensen, E., Johnsen, H. E., Hesse, B. & Kastrup, J. Intramyocardial injection of vascular endothelial growth factor-A 165 plasmid followed by granulocyte-colony stimulating factor to induce angiogenesis in patients with severe chronic ischaemic heart disease. *Eur. Heart J.* **27**, 1785–1792 (2006).

301. Kastrup, J., Jørgensen, E., Fuchs, S., Nikol, S., Bøtker, H. E., Gyöngyösi, M., Glogar, D. & Kornowski, R. A randomised, double-blind, placebo-controlled, multicentre study of the safety and efficacy of BIOBYPASS (AdGVVEGF121.10NH) gene therapy in patients with refractory advanced coronary artery disease: The NOVA trial. *EuroIntervention* **6**, 813–818 (2011).

302. Stewart, D. J., Hilton, J. D., Arnold, J. M. O., Gregoire, J., Rivard, A., Archer, S. L., Charbonneau, F., Cohen, E., Curtis, M., Buller, C. E., Mendelsohn, F. O., Dib, N., Page, P., Ducas, J., Plante, S., Sullivan, J., Macko, J., Rasmussen, C., Kessler, P. D., *et al.*

Angiogenic gene therapy in patients with nonrevascularizable ischemic heart disease: A phase 2 randomized, controlled trial of AdVEGF121 (AdVEGF121) versus maximum medical treatment. *Gene Ther.* **13**, 1503–1511 (2006).

303. Grines, C. L. The AGENT clinical trials programme. *Eur. Hear. Journal, Suppl.* **6**, (2004).

304. Kaski, J. C. & Consuegra-Sanchez, L. Evaluation of ASPIRE trial: A Phase III pivotal registration trial, using intracoronary administration of Generx (Ad5FGF4) to treat patients with recurrent angina pectoris. *Expert Opin. Biol. Ther.* **13**, 1749–1753 (2013).

305. Gupta, R., Tongers, J. & Losordo, D. W. Human studies of angiogenic gene therapy. *Circ. Res.* **105**, 724–736 (2009).

306. Rutanen, J., Rissanen, T. T., Markkanen, J. E., Gruchala, M., Silvennoinen, P., Kivelä, A., Hedman, A., Hedman, M., Heikura, T., Ordén, M. R., Stacker, S. A., Achen, M. G., Hartikainen, J. & Ylä-Herttuala, S. Adenoviral Catheter-Mediated Intramyocardial Gene Transfer Using the Mature Form of Vascular Endothelial Growth Factor-D Induces Transmural Angiogenesis in Porcine Heart. *Circulation* **109**, 1029–1035 (2004).

307. Hartikainen, J., Hassinen, I., Hedman, A., Kivelä, A., Saraste, A., Knuuti, J., Husso, M., Mussalo, H., Hedman, M., Rissanen, T. T., Toivanen, P., Heikura, T., Witztum, J. L., Tsimikas, S. & Ylä-Herttuala, S. Adenoviral intramyocardial VEGF-DDNDC gene transfer increasesmyocardial perfusion reserve in refractory angina patients: A phase I/IIa study with 1-year follow-up. *Eur. Heart J.* **38**, 2547–2555 (2017).

308. Kaminsky, S. M., Quach, L., Chen, S., Pierre-Destine, L., Van de Graaf, B., Monette, S., Rosenberg, J. B., De, B. P., Sondhi, D., Hackett, N. R., Mezey, J. G., Rosengart, T. K. & Crystal, R. G. Safety of direct cardiac administration of AdVEGF-All6A+, a replication-deficient adenovirus vector cDNA/genomic hybrid expressing all three major isoforms of human vascular endothelial growth factor, to the ischemic myocardium of rats. *Hum. Gene Ther. Clin. Dev.* **24**, 38–46 (2013).

309. Fox, D.T., Morris, L.X., Nystul, T., and Spradling, A. C. Lineage analysis of stem cells. in *StemBook* (Harvard Stem Cell Institute, 2009). doi:10.3824/stembook.1.33.1.

310. Kretzschmar, K., Watt, F. M., Su, H. H., Muzumdar, M. D., Luo, L., Achouri, Y., Sotiropoulou, P. A., Blanpain, C., Olson, S., Grompe, M. & Kopan, R. Lineage tracing. *Cell* **148**, 33–45 (2012).

311. Turan, S., Galla, M., Ernst, E., Qiao, J., Voelkel, C., Schiedlmeier, B., Zehe, C. & Bode, J. Recombinase-mediated cassette exchange (RMCE): Traditional concepts and current challenges. *J. Mol. Biol.* **407**, 193–221 (2011).

312. Mao, X., Fujiwara, Y., Chapdelaine, A., Yang, H. & Orkin, S. H. Activation of EGFP expression by Cre-mediated excision in a new ROSA26 reporter mouse strain. *Blood* **97**, 324–326 (2001).

313. Muzumdar, M. D., Tasic, B., Miyamichi, K., Li, N. & Luo, L. A global double-fluorescent Cre reporter mouse. *genesis* **45**, 593–605 (2007).

314. Schwenk, F., Kühn, R., Angrand, P. O., Rajewsky, K. & Stewart, A. F. Temporally and spatially regulated somatic mutagenesis in mice. *Nucleic Acids Res.* **26**, 1427–1432 (1998).

315. Livet, J., Weissman, T. A., Kang, H., Draft, R. W., Lu, J., Bennis, R. A., Sanes, J. R. & Lichtman, J. W. Transgenic strategies for combinatorial expression of fluorescent proteins in the nervous system. *Nature* **450**, 56–62 (2007).

316. Hadjantonakis, A. K., MacMaster, S. & Nagy, A. Embryonic stem cells and mice expressing different GFP variants for multiple non-invasive reporter usage within a single animal. *BMC Biotechnol.* **2**, 11 (2002).

317. Branda, C. S. & Dymecki, S. M. Talking about a revolution: The impact of site-specific recombinases on genetic analyses in mice. *Dev. Cell* **6**, 7–28 (2004).

318. Kim, H., Kim, M., Im, S.-K. & Fang, S. Mouse Cre-LoxP system: general principles to determine tissue-specific roles of target genes. *Lab. Anim. Res.* **34**, 147 (2018).

319. Mondor, I., Jorquera, A., Sene, C., Adriouch, S., Adams, R. H., Zhou, B., Wienert, S., Klauschen, F. & Bajénoff, M. Clonal Proliferation and Stochastic Pruning Orchestrate Lymph Node Vasculature Remodeling. *Immunity* **45**, 877–888 (2016).

320. Ganuza, M., Hall, T., Finkelstein, D., Chabot, A., Kang, G. & McKinney-Freeman, S. Lifelong haematopoiesis is established by hundreds of precursors throughout

mammalian ontogeny. *Nat. Cell Biol.* **19**, 1153–1163 (2017).

321. Lamprecht, S., Schmidt, E. M., Blaj, C., Hermeking, H., Jung, A., Kirchner, T. & Horst, D. Multicolor lineage tracing reveals clonal architecture and dynamics in colon cancer. *Nat. Commun.* **8**, 1406 (2017).

322. Payne, S., Val, S. De & Neal, A. Endothelial-specific cre mouse models is your cre CREdibile? *Arterioscler. Thromb. Vasc. Biol.* **38**, 2550–2561 (2018).

323. Dumont, D. J., Yamaguchi, T. P., Conlon, R. A., Rossant, J. & Breitman, M. L. tek, a novel tyrosine kinase gene located on mouse chromosome 4, is expressed in endothelial cells and their presumptive precursors. *Oncogene* **7**, 1471–1480 (1992).

324. Dumont, D. J., Gradwohl, G. J., Fong, G. H., Auerbach, R. & Breitman, M. L. The endothelial-specific receptor tyrosine kinase, tek, is a member of a new subfamily of receptors. *Oncogene* **8**, 1293–1301 (1993).

325. Dumont, D. J., Gradwohl, G., Fong, G. H., Puri, M. C., Gertsenstein, M., Auerbach, A. & Breitman, M. L. Dominant-negative and targeted null mutations in the endothelial receptor tyrosine kinase, tek, reveal a critical role in vasculogenesis of the embryo. *Genes Dev.* **8**, 1897–1909 (1994).

326. Tang, Y., Harrington, A., Yang, X., Friesel, R. E. & Liaw, L. The contribution of the Tie2+ lineage to primitive and definitive hematopoietic cells. *Genesis* **48**, 563 (2010).

327. Theis, M., De Wit, C., Schlaeger, T. M., Eckardt, D., Krger, O., Dring, B., Risau, W., Deutsch, U., Pohl, U. & Willecke, K. Endothelium-specific replacement of the connexin43 coding region by a lacZ reporter gene. *Genesis* **29**, 1–13 (2001).

328. Heffner, C. S., Herbert Pratt, C., Babiuk, R. P., Sharma, Y., Rockwood, S. F., Donahue, L. R., Eppig, J. T. & Murray, S. A. Supporting conditional mouse mutagenesis with a comprehensive cre characterization resource. *Nat. Commun.* **3**, (2012).

329. Vestweber, D. VE-cadherin: the major endothelial adhesion molecule controlling cellular junctions and blood vessel formation. *Arterioscler. Thromb. Vasc. Biol.* **28**, 223–232 (2008).

330. Chen, M. J., Yokomizo, T., Zeigler, B. M., Dzierzak, E. & Speck, N. A. Runx1 is required for the endothelial to haematopoietic cell transition but not thereafter. *Nature* **457**,

887–891 (2009).

331. Olsson, A. K., Dimberg, A., Kreuger, J. & Claesson-Welsh, L. VEGF receptor signalling - in control of vascular function. *Nat. Rev. Mol. Cell Biol.* **7**, 359–371 (2006).

332. Ehling, M., Adams, S., Benedito, R. & Adams, R. H. Notch controls retinal blood vessel maturation and quiescence. *Development* **140**, 3051–3061 (2013).

333. Liao, W. P., Uetzmann, L., Burtscher, I. & Lickert, H. Generation of a mouse line expressing Sox17-driven Cre recombinase with specific activity in arteries. *Genesis* **47**, 476–483 (2009).

334. Kocher, A. A., Schuster, M. D., Szabolcs, M. J., Takuma, S., Burkhoff, D., Wang, J., Homma, S., Edwards, N. M. & Itescu, S. Neovascularization of ischemic myocardium by human bone-marrow-derived angioblasts prevents cardiomyocyte apoptosis, reduces remodeling and improves cardiac function. *Nat. Med.* **7**, 430–436 (2001).

335. Kanisicak, O., Khalil, H., Ivey, M. J., Karch, J., Maliken, B. D., Correll, R. N., Brody, M. J., J. Lin, S.-C., Aronow, B. J., Tallquist, M. D., Molkentin, J. D., Lin, S. C. J., Aronow, B. J., Tallquist, M. D. & Molkentin, J. D. Genetic lineage tracing defines myofibroblast origin and function in the injured heart. *Nat. Commun.* **7**, 12260 (2016).

336. Tang, Y., Harrington, A., Yang, X., Friesel, R. E. & Liaw, L. The contribution of the Tie2+ lineage to primitive and definitive hematopoietic cells. *Genesis* **48**, 563–7 (2010).

337. Claxton, S., Kostourou, V., Jadeja, S., Chambon, P., Hodivala-Dilke, K. & Fruttiger, M. Efficient, inducible cre-recombinase activation in vascular endothelium. *Genesis* **46**, 74–80 (2008).

338. Shimshek, D. R., Kim, J., Hübner, M. R., Spergel, D. J., Buchholz, F., Casanova, E., Stewart, A. F., Seeburg, P. H. & Sprengel, R. Codon-improved Cre recombinase (iCre) expression in the mouse. *genesis* **32**, 19–26 (2002).

339. Feil, R., Wagner, J., Metzger, D. & Chambon, P. Regulation of Cre recombinase activity by mutated estrogen receptor ligand-binding domains. *Biochem. Biophys. Res. Commun.* **237**, 752–757 (1997).

340. Soriano, P. Generalized lacZ expression with the ROSA26 Cre reporter strain. *Nat.*

Genet. 1999 211 **21**, 70–71 (1999).

341. Beer, H. D., Longaker, M. T. & Werner, S. Reduced Expression of PDGF and PDGF Receptors During Impaired Wound Healing. *J. Invest. Dermatol.* **109**, 132–138 (1997).

342. Kaminski, W. E., Lindahl, P., Lin, N. L., Broudy, V. C., Crosby, J. R., Hellström, M., Swolin, B., Bowen-Pope, D. F., Martin, P. J., Ross, R., Betsholtz, C. & Raines, E. W. Basis of hematopoietic defects in platelet-derived growth factor (PDGF)-B and PDGF beta-receptor null mice. *Blood* **97**, 1990–1998 (2001).

343. Abdellah, Z., Ahmadi, A., Ahmed, S., Aimable, M., Ainscough, R., Almeida, J., Almond, C., Ambler, A., Ambrose, K., Ambrose, K., Andrew, R., Andrews, D., Andrews, N., Andrews, D., Apweiler, E., Arbery, H., Archer, B., Ash, G., Ashcroft, K., *et al.* Finishing the euchromatic sequence of the human genome. *Nature* **431**, 931–945 (2004).

344. Robinson, E. L., Baker, A. H., Brittan, M., McCracken, I., Condorelli, G., Emanueli, C., Srivastava, P. K., Gaetano, C., Thum, T., Vanhaverbeke, M., Angione, C., Heymans, S., Devaux, Y., Pedrazzini, T. & Martelli, F. Dissecting the transcriptome in cardiovascular disease. *Cardiovasc. Res.* **118**, 1004–1019 (2022).

345. Sanger, F., Nicklen, S. & Coulson, A. R. DNA sequencing with chain-terminating inhibitors. *Proc. Natl. Acad. Sci. U. S. A.* **74**, 5463–5467 (1977).

346. Maxam, A. M. & Gilbert, W. [57] Sequencing End-Labeled DNA with Base-Specific Chemical Cleavages. *Methods Enzymol.* **65**, 499–560 (1980).

347. Espina, V., Wulfkuhle, J. D., Calvert, V. S., VanMeter, A., Zhou, W., Coukos, G., Geho, D. H., Petricoin, E. F. & Liotta, L. A. Laser-capture microdissection. *Nat. Protoc. 2006 12* **1**, 586–603 (2006).

348. Tang, F., Barbacioru, C., Wang, Y., Nordman, E., Lee, C., Xu, N., Wang, X., Bodeau, J., Tuch, B. B., Siddiqui, A., Lao, K. & Surani, M. A. mRNA-Seq whole-transcriptome analysis of a single cell. *Nat. Methods* **6**, 377–382 (2009).

349. Dejana, E., Hirschi, K. K. & Simons, M. The molecular basis of endothelial cell plasticity. *Nat. Commun.* **8**, 1–11 (2017).

350. Allahverdian, S., Chaabane, C., Boukais, K., Francis, G. A. & Bochaton-Piallat, M. L.

Smooth muscle cell fate and plasticity in atherosclerosis. *Cardiovasc. Res.* **114**, 540–550 (2018).

351. Chaffer, C. L., San Juan, B. P., Lim, E. & Weinberg, R. A. EMT, cell plasticity and metastasis. *Cancer Metastasis Rev.* **35**, 645–654 (2016).

352. Wong, A., Hamidzada, H. & Epelman, S. A cardioimmunologist's toolkit: genetic tools to dissect immune cells in cardiac disease. *Nat Rev Cardiol* **19**, 395–413 (2022).

353. Stubbington, M. J. T., Lönnberg, T., Proserpio, V., Clare, S., Speak, A. O., Dougan, G. & Teichmann, S. A. T cell fate and clonality inference from single-cell transcriptomes. *Nat. Methods* **13**, 329–332 (2016).

354. Zeisel, A., M͡oz-Manchado, A. B., Codeluppi, S., Lönnerberg, P., Manno, G. La, Juréus, A., Marques, S., Munguba, H., He, L., Betsholtz, C., Rolny, C., Castelo-Branco, G., Hjerling-Leffler, J. & Linnarsson, S. Brain structure. Cell types in the mouse cortex and hippocampus revealed by single-cell RNA-seq. *Science* **347**, 1138–1142 (2015).

355. Blakeley P, Fogarty NM, del Valle I, Wamaitha SE, Hu TX, Elder K, Snell P, Christie L, Robson P, N. K. Defining the three cell lineages of the human blastocyst by single-cell RNA-seq. *Development* **142**, 3613 (2015).

356. Shalek, A. K., Satija, R., Adiconis, X., Gertner, R. S., Gaublomme, J. T., Raychowdhury, R., Schwartz, S., Yosef, N., Malboeuf, C., Lu, D., Trombetta, J. J., Gennert, D., Gnirke, A., Goren, A., Hacohen, N., Levin, J. Z., Park, H. & Regev, A. Single-cell transcriptomics reveals bimodality in expression and splicing in immunecells. *Nature* **498**, 236 (2013).

357. La Manno, G., Soldatov, R., Zeisel, A., Braun, E., Hochgerner, H., Petukhov, V., Lidschreiber, K., Kastriti, M. E., Lönnerberg, P., Furlan, A., Fan, J., Borm, L. E., Liu, Z., van Bruggen, D., Guo, J., He, X., Barker, R., Sundström, E., Castelo-Branco, G., *et al.* RNA velocity of single cells. *Nature* **560**, 494 (2018).

358. Head, S. R., Kiyomi Komori, H., LaMere, S. A., Whisenant, T., Van Nieuwerburgh, F., Salomon, D. R. & Ordoukhanian, P. Library construction for next-generation sequencing: Overviews and challenges. *Biotechniques* **56**, 61–77 (2014).

359. Slatko, B. E., Gardner, A. F. & Ausubel, F. M. Overview of Next Generation Sequencing Technologies. *Curr. Protoc. Mol. Biol.* **122**, e59 (2018).

360. Brüning, R. S., Tombor, L., Schulz, M. H., Dimmeler, S. & John, D. Comparative analysis of common alignment tools for single-cell RNA sequencing. *Gigascience* **11**, 1–12 (2022).

361. Stuart, T. & Satija, R. Integrative single-cell analysis. *Nat. Rev. Genet. 2019 205* **20**, 257–272 (2019).

362. Chen, G., Ning, B. & Shi, T. Single-cell RNA-seq technologies and related computational data analysis. *Front. Genet.* **10**, 317 (2019).

363. Poirion, O. B., Zhu, X., Ching, T. & Garmire, L. Single-Cell Transcriptomics Bioinformatics and Computational Challenges. *Front. Genet.* **7**, (2016).

364. Snippert, H. J., van der Flier, L. G., Sato, T., van Es, J. H., van den Born, M., Kroon-Veenboer, C., Barker, N., Klein, A. M., van Rheenen, J., Simons, B. D. & Clevers, H. Intestinal crypt homeostasis results from neutral competition between symmetrically dividing Lgr5 stem cells. *Cell* **143**, 134–44 (2010).

365. Kobayashi, T., Kato-Itoh, M., Yamaguchi, T., Tamura, C., Sanbo, M., Hirabayashi, M. & Nakauchi, H. Identification of rat Rosa26 locus enables generation of knock-in rat lines ubiquitously expressing tdTomato. *Stem Cells Dev.* **21**, 2981–2986 (2012).

366. Gray, G. A., White, C. I., Thomson, A., Kozak, A., Moran, C. & Jansen, M. A. Imaging the healing murine myocardial infarct in vivo: ultrasound, magnetic resonance imaging and fluorescence molecular tomography. *Exp. Physiol.* **98**, 606–13 (2013).

367. IHC protocol for paraffin, frozen and free floating sections. https://www.abcam.com/protocols/immunostaining-paraffin-frozen-free-floating-protocol#Paraffin and frozen (2017).

368. TaqMan Assays QPCR Guarantee | Thermo Fisher Scientific - EC. https://www.thermofisher.com/ec/en/home/life-science/pcr/real-time-pcr/real-time-pcr-assays/why-choose-taqman-assays/taqman-guarantee.html.

369. Monteiro, J. P., Rodor, J., Caudrillier, A., Scanlon, J. P., Spiroski, A. M., Dudnakova, T., Pflüger-Müller, B., Shmakova, A., Von Kriegsheim, A., Deng, L., Taylor, R. S., Wilson-Kanamori, J. R., Chen, S. H., Stewart, K., Thomson, A., Mitić, T., McClure, J. D., Iynikkel, J., Hadoke, P. W. F., *et al.* MIR503HG Loss Promotes Endothelial-to-Mesenchymal Transition in Vascular Disease. *Circ. Res.* **128**, 1173 (2021).

370. Goidin, D., Mamessier, A., Staquet, M. J., Schmitt, D. & Berthier-Vergnes, O. Ribosomal 18S RNA prevails over glyceraldehyde-3-phosphate dehydrogenase and beta-actin genes as internal standard for quantitative comparison of mRNA levels in invasive and noninvasive human melanoma cell subpopulations. *Anal. Biochem.* **295**, 17–21 (2001).

371. Monteiro, J. P., Rodor, J., Caudrillier, A., Scanlon, J. P., Spiroski, A. M., Dudnakova, T., Pflüger-Müller, B., Shmakova, A., Von Kriegsheim, A., Deng, L., Taylor, R. S., Wilson-Kanamori, J. R., Chen, S. H., Stewart, K., Thomson, A., Mitić, T., McClure, J. D., Iynikkel, J., Hadoke, P. W. F., *et al.* MIR503HG Loss Promotes Endothelial-to-Mesenchymal Transition in Vascular Disease. *Circ. Res.* **128**, 1173 (2021).

372. Spencer, H. L., Sanders, R., Boulberdaa, M., Meloni, M., Cochrane, A., Spiroski, A. M., Mountford, J., Emanueli, C., Caporali, A., Brittan, M., Rodor, J. & Baker, A. H. The LINC00961 transcript and its encoded micropeptide, small regulatory polypeptide of amino acid response, regulate endothelial cell function. *Cardiovasc. Res.* **116**, 1981–1994 (2020).

373. Park, K., Chen, Y., Hu, Y., Mayo, A. S., Kompella, U. B., Longeras, R. & Ma, J. X. Nanoparticle-Mediated Expression of an Angiogenic Inhibitor Ameliorates Ischemia-Induced Retinal Neovascularization and Diabetes-Induced Retinal Vascular Leakage. *Diabetes* **58**, 1902 (2009).

374. De Souza, A. I., Felkin, L. E., McCormack, A. M., Holder, A., Barton, P. J. R., Banner, N. R. & Rose, M. L. Sequential expression of three known protective genes in cardiac biopsies after transplantation. *Transplantation* **79**, 584–590 (2005).

375. Tricarico, C., Pinzani, P., Bianchi, S., Paglierani, M., Distante, V., Pazzagli, M., Bustin, S. A. & Orlando, C. Quantitative real-time reverse transcription polymerase chain reaction: Normalization to rRNA or single housekeeping genes is inappropriate for human tissue biopsies. *Anal. Biochem.* **309**, 293–300 (2002).

376. Meissner, K., Heydrich, B., Jedlitschky, G., Meyer Zu Schwabedissen, H., Mosyagin, I., Dazert, P., Eckel, L., Vogelgesang, S., Warzok, R. W., Böhm, M., Lehmann, C., Wendt, M., Cascorbi, I. & Kroemer, H. K. The ATP-binding cassette transporter ABCG2 (BCRP), a marker for side population stem cells, is expressed in human heart. *J. Histochem. Cytochem.* **54**, 215–221 (2006).

377. Watson, S. A., Scigliano, M., Bardi, I., Ascione, R., Terracciano, C. M. & Perbellini, F. Preparation of viable adult ventricular myocardial slices from large and small mammals. *Nat. Protoc.* **12**, 2623–2639 (2017).

378. Qiu, X., Hill, A., Packer, J., Lin, D., Ma, Y. A. & Trapnell, C. Single-cell mRNA quantification and differential analysis with Census. *Nat. Methods* **14**, 309–315 (2017).

379. Trapnell, C., Cacchiarelli, D., Grimsby, J., Pokharel, P., Li, S., Morse, M., Lennon, N. J., Livak, K. J., Mikkelsen, T. S. & Rinn, J. L. The dynamics and regulators of cell fate decisions are revealed by pseudotemporal ordering of single cells. *Nat. Biotechnol.* **32**, 381–386 (2014).

380. Rulands, S., Lescroart, F., Chabab, S., Hindley, C. J., Prior, N., Sznurkowska, M. K., Huch, M., Philpott, A., Blanpain, C. & Simons, B. D. Universality of clone dynamics during tissuedevelopment. *Nat. Phys.* **14**, 469 (2018).

381. Tabibiazar, R. & Rockson, S. G. Angiogenesis and the ischaemic heart. *Eur. Heart J.* **22**, 903–918 (2001).

382. Kutryk, M. J. B. & Stewart, D. J. Angiogenesis of the heart. *Microsc. Res. Tech.* **60**, 138–158 (2003).

383. Jaitin, D. A., Kenigsberg, E., Keren-Shaul, H., Elefant, N., Paul, F., Zaretsky, I., Mildner, A., Cohen, N., Jung, S., Tanay, A. & Amit, I. Massively parallel single-cell RNA-seq for marker-free decomposition of tissues into cell types. *Science (80-.).* **343**, 776–779 (2014).

384. Yan, L., Yang, M., Guo, H., Yang, L., Wu, J., Li, R. R., Liu, P., Lian, Y., Zheng, X., Yan, J., Huang, J., Li, M., Wu, X., Wen, L., Lao, K., Li, R. R., Qiao, J. & Tang, F. Single-cell RNA-Seq profiling of human preimplantation embryos and embryonic stem cells. *Nat. Struct. Mol. Biol.* **20**, 1131–1139 (2013).

385. Stifter, S. A. & Greter, M. STOP floxing around: Specificity and leakiness of inducible Cre/loxP systems. *Eur. J. Immunol.* **50**, 338–341 (2020).

386. Scott, R. E., Ghule, P. N., Stein, J. L. & Stein, G. S. Cell cycle gene expression networks discovered using systems biology: Significance in carcinogenesis. *J. Cell. Physiol.* **230**, 2533–2542 (2015).

387. Van Den Borne, P., Quax, P. H. A., Hoefer, I. E. & Pasterkamp, G. The multifaceted functions of CXCL10 in cardiovascular disease. *Biomed Res. Int.* **2014**, (2014).

388. Gomez, D. & Reich, N. C. Stimulation of primary human endothelial cell proliferation by IFN. *J. Immunol.* **170**, 5373–5381 (2003).

389. MacK, J. J. & Luisa Iruela-Arispe, M. NOTCH regulation of the endothelial cell phenotype. *Curr. Opin. Hematol.* **25**, 212–218 (2018).

390. Moya, I. M., Umans, L., Maas, E., Pereira, P. N. G., Beets, K., Francis, A., Sents, W., Robertson, E. J., Mummery, C. L., Huylebroeck, D. & Zwijsen, A. Stalk cell phenotype depends on integration of Notch and Smad1/5 signaling cascades. *Dev. Cell* **22**, 501–514 (2012).

391. Hellström, M., Phng, L. K., Hofmann, J. J., Wallgard, E., Coultas, L., Lindblom, P., Alva, J., Nilsson, A. K., Karlsson, L., Gaiano, N., Yoon, K., Rossant, J., Iruela-Arispe, M. L., Kalén, M., Gerhardt, H. & Betsholtz, C. Dll4 signalling through Notch1 regulates formation of tip cells during angiogenesis. *Nature* **445**, 776–780 (2007).

392. Manavski, Y., Lucas, T., Belz, C., Boon, R. & Dimmeler, S. Revascularization After Ischemia is Mediated by Clonally Expanding Endothelial Cells and is Impaired by Aging. *Circulation* **134**, 75231 (2016).

393. Bergmann, O., Bhardwaj, R. D., Bernard, S., Zdunek, S., Barnabé-Heide, F., Walsh, S., Zupicich, J., Alkass, K., Buchholz, B. A., Druid, H., Jovinge, S. & Frisén, J. Evidence for cardiomyocyte renewal in humans. *Science (80-.).* **324**, 98–102 (2009).

394. Henry, T. D., Moyé, L. & Traverse, J. H. Consistently Inconsistent-Bone Marrow Mononuclear Stem Cell Therapy Following Acute Myocardial Infarction: A Decade Later. *Circ. Res.* **119**, 404–406 (2016).

395. Boudoulas, K. D. & Hatzopoulos, A. K. Cardiac repair and regeneration: the Rubik's cube of cell therapy for heart disease. *Dis. Model. Mech.* **2**, 344–358 (2009).

396. Manavski, Y., Lucas, T., Glaser, S. F., Dorsheimer, L., Günther, S., Braun, T., Rieger, M. A., Zeiher, A. M., Boon, R. A. & Dimmeler, S. Clonal expansion of endothelial cells contributes to ischemia-induced neovascularization. *Circ. Res.* **122**, 670–677 (2018).

397. Aird, W. C. Endothelial cell heterogeneity. *Cold Spring Harb. Perspect. Med.* **2**,

a006429 (2012).

398. Kieda, C. Heterogeneity of endothelial cells--role in vessel specialization and cooperation in vasculogenic mimicry. *Postepy Biochem.* **59**, 372–8 (2013).

399. Tombor, L., John, D., Glaser, S. ., Luxan, G., Forte, E., Furtado, M., Rosenthal, N., Manavski, Y., Fischer, A., Muhly-Reinholz, M., Looso, M., Acker, T., Harvey, R., Abplanalp, A. & Dimmeler, S. Single cell sequencing reveals endothelial plasticity with transient mesenchymal activation after myocardial infarction. *Eur. Heart J.* **41**, (2020).

400. Gatenby, R. A., Smallbone, K., Maini, P. K., Rose, F., Averill, J., Nagle, R. B., Worrall, L. & Gillies, R. J. Cellular adaptations to hypoxia and acidosis during somatic evolution of breast cancer. *Br. J. Cancer 2007 975* **97**, 646–653 (2007).

401. Gao, Y., Park, H. J., Traulsen, A. & Pichugin, Y. Evolution of irreversible somatic differentiation. *Elife* **10**, (2021).

402. Paik, D. T., Cho, S., Tian, L., Chang, H. Y. & Wu, J. C. Single-cell RNA sequencing in cardiovascular development, disease and medicine. *Nat. Rev. Cardiol. 2020 178* **17**, 457–473 (2020).

403. Litviňuková, M., Talavera-López, C., Maatz, H., Reichart, D., Worth, C. L., Lindberg, E. L., Kanda, M., Polanski, K., Heinig, M., Lee, M., Nadelmann, E. R., Roberts, K., Tuck, L., Fasouli, E. S., DeLaughter, D. M., McDonough, B., Wakimoto, H., Gorham, J. M., Samari, S., *et al.* Cells of the adult human heart. *Nature* **588**, 466–472 (2020).

404. DeLeve, L. D., Wang, X., Hu, L., McCuskey, M. K. & McCuskey, R. S. Rat liver sinusoidal endothelial cell phenotype is maintained by paracrine and autocrine regulation. *Am. J. Physiol. - Gastrointest. Liver Physiol.* **287**, (2004).

405. Amitai-Lange, A., Berkowitz, E., Altshuler, A., Dbayat, N., Nasser, W., Suss-Toby, E., Tiosano, B. & Shalom-Feuerstein, R. A Method for Lineage Tracing of Corneal Cells Using Multi-color Fluorescent Reporter Mice. *J. Vis. Exp* **53370**, (2015).

406. Hnasko, R., McFarland, M. & Ben-Jonathan, N. Distribution and characterization of plasmalemma vesicle protein-1 in rat endocrine glands. *J. Endocrinol.* **175**, 649–661 (2002).

407. Stan, R. V., Arden, K. C. & Palade, G. E. cDNA and protein sequence, genomic organization, and analysis of cis regulatory elements of mouse and human PLVAP genes. *Genomics* **72**, 304–313 (2001).

408. Stan, R. V. Endothelial stomatal and fenestral diaphragms in normal vessels and angiogenesis. *J. Cell. Mol. Med.* **11**, 621–643 (2007).

409. Hallmann, R., Mayer, D. N., Berg, E. L., Broermann, R. & Butcher, E. C. Novel mouse endothelial cell surface marker is suppressed during differentiation of the blood brain barrier. *Dev. Dyn.* **202**, 325–332 (1995).

410. Niemelä, H., Elima, K., Henttinen, T., Irjala, H., Salmi, M. & Jalkanen, S. Molecular identification of PAL-E, a widely used endothelial-cell marker. *Blood* **106**, 3405–3409 (2005).

411. Stan, R. V., Kubitza, M. & Palade, G. E. PV-1 is a component of the fenestral and stomatal diaphragms in fenestrated endothelia. *Proc. Natl. Acad. Sci. U. S. A.* **96**, 13203–13207 (1999).

412. Ioannidou, S., Deinhardt, K., Miotla, J., Bradley, J., Cheung, E., Samuelsson, S., Ng, Y.-S. S. & Shima, D. T. An in vitro assay reveals a role for the diaphragm protein PV-1 in endothelial fenestra morphogenesis. *Proc Natl Acad Sci U S A* **103**, 16770–16775 (2006).

413. Stan, R. V., Tkachenko, E. & Niesman, I. R. PV1 is a key structural component for the formation of the stomatal and fenestral diaphragms. *Mol. Biol. Cell* **15**, 3615–3630 (2004).

414. Stan, R. V., Ghitescu, L., Jacobson, B. S. & Palade, G. E. Isolation, cloning, and localization of rat PV-1, a novel endothelial caveolar protein. *J. Cell Biol.* **145**, 1189–1198 (1999).

415. Stan, R. V. Structure of caveolae. *Biochim. Biophys. Acta - Mol. Cell Res.* **1746**, 334–348 (2005).

416. Bearer, E. L., Orci, L. & Sors, P. Endothelial fenestral diaphragms: A quick-freeze, deep-etch study. *J. Cell Biol.* **100**, 418–428 (1985).

417. Herrnberger, L., Seitz, R., Kuespert, S., Bösl, M. R., Fuchshofer, R. & Tamm, E. R. Lack

of endothelial diaphragms in fenestrae and caveolae of mutant Plvap-deficient mice. *Histochem. Cell Biol.* **138**, 709–724 (2012).

418. Stan, R. V., Tse, D., Deharvengt, S. J., Smits, N. C., Xu, Y., Luciano, M. R., McGarry, C. L., Buitendijk, M., Nemani, K. V., Elgueta, R., Kobayashi, T., Shipman, S. L., Moodie, K. L., Daghlian, C. P., Ernst, P. A., Lee, H. K., Suriawinata, A. A., Schned, A. R., Longnecker, D. S., *et al.* The Diaphragms of Fenestrated Endothelia: Gatekeepers of Vascular Permeability and Blood Composition. *Dev. Cell* **23**, 1203–1218 (2012).

419. Madden, S. L., Cook, B. P., Nacht, M., Weber, W. D., Callahan, M. R., Jiang, Y., Dufault, M. R., Zhang, X., Zhang, W., Walter-Yohrling, J., Rouleau, C., Akmaev, V. R., Wang, C. J., Cao, X., St. Martin, T. B., Roberts, B. L., Teicher, B. A., Klinger, K. W., Stan, R. V., *et al.* Vascular gene expression in nonneoplastic and malignant brain. *Am. J. Pathol.* **165**, 601–608 (2004).

420. Minshall, R. D. & Malik, A. B. Transport across the endothelium: Regulation of endothelial permeability. *Handb. Exp. Pharmacol.* **176**, 107–144 (2006).

421. Keuschnigg, J., Henttinen, T., Auvinen, K., Karikoski, M., Salmi, M. & Jalkanen, S. The prototype endothelial marker PAL-E is a leukocyte trafficking molecule. *Blood* **114**, 478–484 (2009).

422. Liu, Y., Carson-Walter, E. B., Cooper, A., Winans, B. N., Johnson, M. D. & Walter, K. A. Vascular gene expression patterns are conserved in primary and metastatic brain tumors. *J. Neurooncol.* **99**, 13–24 (2010).

423. Carson-Walter, E. B., Hampton, J., Shue, E., Geynisman, D. M., Pillai, P. K., Sathanoori, R., Madden, S. L., Hamilton, R. L. & Walter, K. A. Plasmalemmal vesicle associated protein-1 is a novel marker implicated in brain tumor angiogenesis. *Clin. Cancer Res.* **11**, 7643–7650 (2005).

424. Rantakari, P., Auvinen, K., Jäppinen, N., Kapraali, M., Valtonen, J., Karikoski, M., Gerke, H., Iftakhar-E-Khuda, I., Keuschnigg, J., Umemoto, E., Tohya, K., Miyasaka, M., Elima, K., Jalkanen, S. & Salmi, M. The endothelial protein PLVAP in lymphatics controls the entry of lymphocytes and antigens into lymph nodes. *Nat. Immunol.* **16**, 386–396 (2015).

425. Deharvengt, S. J., Tse, D., Sideleva, O., McGarry, C., Gunn, J. R., Longnecker, D. S.,

Carriere, C. & Stan, R. V. PV1 down-regulation via shRNA inhibits the growth of pancreatic adenocarcinoma xenografts. *J. Cell. Mol. Med.* **16**, 2690–2700 (2012).

426. Yamamoto, I., Horita, S., Takahashi, T., Tanabe, K., Fuchinoue, S., Teraoka, S., Hattori, M. & Yamaguchi, Y. Glomerular expression of plasmalemmal vesicle-associated protein-1 in patients with transplant glomerulopathy. *Am. J. Transplant.* **7**, 1954–1960 (2007).

427. Shue, E. H., Carson-Walter, E. B., Liu, Y., Winans, B. N., Ali, Z. S., Chen, J. & Walter, K. A. Plasmalemmal vesicle associated protein-1 (PV-1) is a marker of blood-brain barrier disruption in rodent models. *BMC Neurosci.* **9**, (2008).

428. Van Der Wijk, A. E., Wisniewska-Kruk, J., Vogels, I. M. C., Van Veen, H. A., Ip, W. F., Van Der Wel, N. N., Van Noorden, C. J. F., Schlingemann, R. O. & Klaassen, I. Expression patterns of endothelial permeability pathways in the development of the blood-retinal barrier in mice. *FASEB J.* **33**, 5320–5333 (2019).

429. Bosma, E. K., Van Noorden, C. J. F., Schlingemann, R. O. & Klaassen, I. The role of plasmalemma vesicle-associated protein in pathological breakdown of blood-brain and blood-retinal barriers: Potential novel therapeutic target for cerebral edema and diabetic macular edema. *Fluids Barriers CNS* **15**, 24 (2018).

430. Chen, W., Xia, P., Wang, H., Tu, J., Liang, X., Zhang, X. & Li, L. The endothelial tip-stalk cell selection and shuffling during angiogenesis. *J. Cell Commun. Signal.* **13**, 291–301 (2019).

431. DeFilippis, A. P., Chapman, A. R., Mills, N. L., De Lemos, J. A., Arbab-Zadeh, A., Newby, L. K. & Morrow, D. A. Assessment and treatment of patients with type 2 myocardial infarction and acute nonischemic myocardial injury. *Circulation* **140**, 1661–1678 (2019).

432. Taggart, C., Wereski, R., Mills, N. L. & Chapman, A. R. Diagnosis, Investigation and Management of Patients with Acute and Chronic Myocardial Injury. *J. Clin. Med.* **10**, 2331 (2021).

433. Stan, R. V., Ghitescu, L., Jacobson, B. S. & Palade, G. E. Isolation, cloning, and localization of rat PV-1, a novel endothelial caveolar protein. *J. Cell Biol.* **145**, 1189–1198 (1999).

434. Strickland, L. A., Jubb, A. M., Hongo, J. A., Zhong, F., Burwick, J., Fu, L., Frantz, G. D. & Koeppen, H. Plasmalemmal vesicle-associated protein (PLVAP) is expressed by tumour endothelium and is upregulated by vascular endothelial growth factor-A (VEGF). *J. Pathol.* **206**, 466–475 (2005).

435. Carmeliet, P. Mechanisms of angiogenesis and arteriogenesis. *Nat. Med.* **6**, 389–395 (2000).

436. Esser, S., Wolburg, K., Wolburg, H., Breier, G., Kurzchalia, T. & Risau, W. Vascular endothelial growth factor induces endothelial fenestrations in vitro. *J. Cell Biol.* **140**, 947–959 (1998).

437. Hofman, P., Blaauwgeers, H. G. T., Vrensen, G. F. J. M. & Schlingemann, R. O. Role of VEGF-A in endothelial phenotypic shift in human diabetic retinopathy and VEGF-A-induced retinopathy in monkeys. *Ophthalmic Res.* **33**, 156–162 (2001).

438. Hnasko, R., Frank, P. G., Ben-Jonathan, N. & Lisanti, M. P. PV-1 is negatively regulated by VEGF in the lung of caveolin-1, but not caveolin-2, null mice. *Cell Cycle* **5**, 2012–2020 (2006).

439. Benz, F., Wichitnaowarat, V., Lehmann, M., Germano, R. F., Mihova, D., Macas, J., Adams, R. H., Mark Taketo, M., Plate, K. H., Guérit, S., Vanhollebeke, B. & Liebner, S. Low wnt/β-catenin signaling determines leaky vessels in the subfornical organ and affects water homeostasis in mice. *Elife* **8**, (2019).

440. Paes, K. T., Wang, E., Henze, K., Vogel, P., Read, R., Suwanichkul, A., Kirkpatrick, L. L., Potter, D., Newhouse, M. M. & Rice, D. S. Frizzled 4 is required for retinal angiogenesis and maintenance of the blood-retina barrier. *Investig. Ophthalmol. Vis. Sci.* **52**, 6452–6461 (2011).

441. Laksitorini, M. D., Yathindranath, V., Xiong, W., Parkinson, F. E., Thliveris, J. A. & Miller, D. W. Impact of Wnt/β-catenin signaling on ethanol-induced changes in brain endothelial cell permeability. *J. Neurochem.* **157**, 1118–1137 (2021).

442. Laksitorini, M. D., Yathindranath, V., Xiong, W., Hombach-Klonisch, S. & Miller, D. W. Modulation of Wnt/β-catenin signaling promotes blood-brain barrier phenotype in cultured brain endothelial cells. *Sci. Rep.* **9**, (2019).

443. Ribatti, D. & Crivellato, E. 'Sprouting angiogenesis', a reappraisal. *Dev. Biol.* **372**,

157–165 (2012).

444. Kocijan, T., Rehman, M., Colliva, A., Groppa, E., Leban, M., Vodret, S., Volf, N., Zucca, G., Cappelletto, A., Piperno, G. M., Zentilin, L., Giacca, M., Benvenuti, F., Zhou, B., Adams, R. H. & Zacchigna, S. Genetic lineage tracing reveals poor angiogenic potential of cardiac endothelial cells. *Cardiovasc. Res.* **117**, 256–270 (2021).

445. Liu, Q., Hu, T., He, L., Huang, X., Tian, X., Zhang, H., He, L., Pu, W., Zhang, L., Sun, H., Fang, J., Yu, Y., Duan, S., Hu, C., Hui, L., Zhang, H., Quertermous, T., Xu, Q., Red-Horse, K., *et al.* Genetic targeting of sprouting angiogenesis using Apln-CreER. *Nat. Commun.* **6**, (2015).

446. Baker, M., Robinson, S. D., Lechertier, T., Barber, P. R., Tavora, B., D'Amico, G., Jones, D. T., Vojnovic, B., Hodivala-Dilke, K. & Baker, M. Use of the mouse aortic ring assay to study angiogenesis. *Nat. Protoc.* **7**, 89–104 (2011).

447. Gurumurthy, C. B. & Kent Lloyd, K. C. Generating mouse models for biomedical research: Technological advances. *DMM Dis. Model. Mech.* **12**, (2019).

448. Zuppinger, C. 3D Cardiac Cell Culture: A Critical Review of Current Technologies and Applications. *Front. Cardiovasc. Med.* **6**, 87 (2019).

449. Wilson, R. C. & Doudna, J. A. Molecular mechanisms of RNA interference. *Annu. Rev. Biophys.* **42**, 217–239 (2013).

450. Zhang, L., Yin, J. C., Yeh, H., Ma, N. X., Lee, G., Chen, X. A., Wang, Y., Lin, L., Chen, L., Jin, P., Wu, G. Y. & Chen, G. Small Molecules Efficiently Reprogram Human Astroglial Cells into Functional Neurons. *Cell Stem Cell* **17**, 735–747 (2015).

451. Mead, B. E. & Karp, J. M. All models are wrong, but some organoids may be useful. *Genome Biol.* **20**, 1–3 (2019).

452. Staton, C. A., Reed, M. W. R. & Brown, N. J. A critical analysis of current in vitro and in vivo angiogenesis assays. *Int. J. Exp. Pathol.* **90**, 195–221 (2009).

453. Pitoulis, F. G., Watson, S. A., Perbellini, F. & Terracciano, C. M. Myocardial slices come to age: An intermediate complexity in vitro cardiac model for translational research. *Cardiovasc. Res.* **116**, 1275–1287 (2020).

454. Watson, S. A., Terracciano, C. M. & Perbellini, F. Myocardial Slices: an Intermediate

Complexity Platform for Translational Cardiovascular Research. *Cardiovasc. Drugs Ther.* **33**, 239–244 (2019).

455. Perbellini, F. & Thum, T. Living myocardial slices: A novel multicellular model for cardiac translational research. *Eur. Heart J.* **41**, 2405–2408 (2020).

456. Camelliti, P., Al-Saud, S. A., Smolenski, R. T., Al-Ayoubi, S., Bussek, A., Wettwer, E., Banner, N. R., Bowles, C. T., Yacoub, M. H. & Terracciano, C. M. Adult human heart slices are a multicellular system suitable for electrophysiological and pharmacological studies. *J. Mol. Cell. Cardiol.* **51**, 390–398 (2011).

457. Hattori, H., Takeshita, D., Takeuchi, A., Kim, B., Shibata, M., Matsuoka, S., Obata, K., Mitsuyama, S., Zhang, G. X. & Takaki, M. NHE-1 blockade reversed changes in calcium transient in myocardial slices from isoproterenol-induced hypertrophied rat left ventricle. *Biochem. Biophys. Res. Commun.* **419**, 431–435 (2012).

458. Bussek, A., Schmidt, M., Bauriedl, J., Ravens, U., Wettwer, E. & Lohmann, H. Cardiac tissue slices with prolonged survival for in vitro drug safety screening. *J. Pharmacol. Toxicol. Methods* **66**, 145–151 (2012).

459. Himmel, H. M., Bussek, A., Hoffmann, M., Beckmann, R., Lohmann, H., Schmidt, M. & Wettwer, E. Field and action potential recordings in heart slices: correlation with established in vitro and in vivo models. *Br. J. Pharmacol.* **166**, 276 (2012).

460. Burdette, W. J. & Wilhelmi, A. E. Respiration of heart muscle slices from rats in the terminal stage of hemorrhagic shock. *Proc. Soc. Exp. Biol. Med.* **61**, 411–413 (1946).

461. Parrish, A. R., Gandolfi, A. J. & Brendel, K. Precision-cut tissue slices: applications in pharmacology and toxicology. *Life Sci.* **57**, 1887–1901 (1995).

462. Fischer, C., Milting, H., Fein, E., Reiser, E., Lu, K., Seidel, T., Schinner, C., Schwarzmayr, T., Schramm, R., Tomasi, R., Husse, B., Cao-Ehlker, X., Pohl, U. & Dendorfer, A. Long-term functional and structural preservation of precision-cut human myocardium under continuous electromechanical stimulation in vitro. *Nat. Commun. 2019 101* **10**, 1–12 (2019).

463. Watson, S. A., Duff, J., Bardi, I., Zabielska, M., Atanur, S. S., Jabbour, R. J., Simon, A., Tomas, A., Smolenski, R. T., Harding, S. E., Perbellini, F. & Terracciano, C. M. Biomimetic electromechanical stimulation to maintain adult myocardial slices in

vitro. *Nat. Commun.* **10**, (2019).

464. Chen, H. I., Poduri, A., Numi, H., Kivela, R., Saharinen, P., McKay, A. S., Raftrey, B., Churko, J., Tian, X., Zhou, B., Wu, J. C., Alitalo, K. & Red-Horse, K. VEGF-C and aortic cardiomyocytes guide coronary artery stem development. *J. Clin. Invest.* **124**, 4899–4914 (2014).

465. Chen, H. I., Sharma, B., Akerberg, B. N., Numi, H. J., Kivelä, R., Saharinen, P., Aghajanian, H., McKay, A. S., Bogard, P. E., Chang, A. H., Jacobs, A. H., Epstein, J. A., Stankunas, K., Alitalo, K. & Red-Horse, K. The sinus venosus contributes to coronary vasculature through VEGFC-stimulated angiogenesis. *Development* **141**, 4500–4512 (2014).

466. Aspelund, A., Robciuc, M. R., Karaman, S., Makinen, T. & Alitalo, K. Lymphatic System in Cardiovascular Medicine. *Circ. Res.* **118**, 515–530 (2016).

467. Kukk, E., Lymboussakl, A., Taira, S., Kaipainen, A., Jeltsch, M., Joukov, V. & Alitalo, K. VEGF-C receptor binding and pattern of expression with VEGFR-3 suggests a role in lymphatic vascular development. *Development* **122**, 3829–3837 (1996).

468. Kaipainen, A., Korhonen, J., Mustonen, T., Van Hinsbergh, V. W. M., Fang, G. H., Dumont, D., Breitman, M. & Alitalo, K. Expression of the fms-like tyrosine kinase 4 gene becomes restricted to lymphatic endothelium during development. *Proc. Natl. Acad. Sci. U. S. A.* **92**, 3566–3570 (1995).

469. Jeltsch, M., Kaipainen, A., Joukov, V., Meng, X., Lakso, M., Rauvala, H., Swartz, M., Fukumura, D., Jain, R. K. & Alitalo, K. Hyperplasia of lymphatic vessels in VEGF-C transgenic mice. *Science (80-.).* **276**, 1423–1425 (1997).

470. Oh, S. J., Jeltsch, M. M., Birkenhäger, R., McCarthy, J. E. G., Weich, H. A., Christ, B., Alitalo, K. & Wilting, J. VEGF and VEGF-C: specific induction of angiogenesis and lymphangiogenesis in the differentiated avian chorioallantoic membrane. *Dev. Biol.* **188**, 96–109 (1997).

471. Tammela, T., Zarkada, G., Wallgard, E., Murtomäki, A., Suchting, S., Wirzenius, M., Waltari, M., Hellström, M., Schomber, T., Peltonen, R., Freitas, C., Duarte, A., Isoniemi, H., Laakkonen, P., Christofori, G., Ylä-Herttuala, S., Shibuya, M., Pytowski, B., Eichmann, A., *et al.* Blocking VEGFR-3 suppresses angiogenic sprouting and

vascular network formation. *Nature* **454**, 656–660 (2008).

472. Podgrabinska, S., Braun, P., Velasco, P., Kloos, B., Pepper, M. S., Jackson, D. G. & Skobe, M. Molecular characterization of lymphatic endothelial cells. *Proc. Natl. Acad. Sci. U. S. A.* **99**, 16069–16074 (2002).

473. Chien, M. H., Ku, C. C., Johansson, G., Chen, M. W., Hsiao, M., Su, J. L., Inoue, H., Hua, K. T., Wei, L. H. & Kuo, M. L. Vascular endothelial growth factor-C (VEGF-C) promotes angiogenesis by induction of COX-2 in leukemic cells via the VEGF-R3/JNK/AP-1 pathway. *Carcinogenesis* **30**, 2005–2013 (2009).

474. Witmer, A. N., Dai, J., Weich, H. A., Vrensen, G. F. J. M. & Schlingemann, R. O. Expression of vascular endothelial growth factor receptors 1, 2, and 3 in quiescent endothelia. *J. Histochem. Cytochem.* **50**, 767–777 (2002).

475. Simons, M., Gordon, E. & Claesson-Welsh, L. Mechanisms and regulation of endothelial VEGF receptor signalling. *Nat. Rev. Mol. Cell Biol. 2016 1710* **17**, 611–625 (2016).

476. Apte, R. S., Chen, D. S. & Ferrara, N. VEGF in Signaling and Disease: Beyond Discovery and Development. *Cell* **176**, 1248–1264 (2019).

477. Houssari, M., Dumesnil, A., Tardif, V., Kivelä, R., Pizzinat, N., Boukhalfa, I., Godefroy, D., Schapman, D., Hemanthakumar, K. A., Bizou, M., Henry, J. P., Renet, S., Riou, G., Rondeaux, J., Anouar, Y., Adriouch, S., Fraineau, S., Alitalo, K., Richard, V., *et al.* Lymphatic and Immune Cell Cross-Talk Regulates Cardiac Recovery After Experimental Myocardial Infarction. *Arterioscler. Thromb. Vasc. Biol.* **40**, 1722–1737 (2020).

478. Shimizu, Y., Polavarapu, R., Eskla, K. L., Pantner, Y., Nicholson, C. K., Ishii, M., Brunnhoelzl, D., Mauria, R., Husain, A., Naqvi, N., Murohara, T. & Calvert, J. W. Impact of Lymphangiogenesis on Cardiac Remodeling After Ischemia and Reperfusion Injury. *J. Am. Heart Assoc.* **7**, (2018).

479. Klotz, L., Norman, S., Vieira, J. M., Masters, M., Rohling, M., Dubé, K. N., Bollini, S., Matsuzaki, F., Carr, C. A. & Riley, P. R. Cardiac lymphatics are heterogeneous in origin and respond to injury. *Nat. 2015 5227554* **522**, 62–67 (2015).

480. Sweat, R. S., Sloas, D. C. & Murfee, W. L. VEGF-C Induces Lymphangiogenesis and

Angiogenesis in the Rat Mesentery Culture Model. *Microcirculation* **21**, 532 (2014).

481. Benest, A. V., Harper, S. J., Herttuala, S. Y., Alitalo, K. & Bates, D. O. VEGF-C induced angiogenesis preferentially occurs at a distance from lymphangiogenesis. *Cardiovasc. Res.* **78**, 315–323 (2008).

482. Loo, D. T. In situ detection of apoptosis by the TUNEL assay: an overview of techniques. *Methods Mol. Biol.* **682**, 3–13 (2011).

483. Gerdes, J., Lemke, H., Baisch, H., Wacker, H. H., Schwab, U. & Stein, H. Cell cycle analysis of a cell proliferation-associated human nuclear antigen defined by the monoclonal antibody Ki-67. *J. Immunol.* **133**, 1710–5 (1984).

484. Protti, A., Mongue-Din, H., Mylonas, K. J., Sirker, A., Sag, C. M., Swim, M. M., Maier, L., Sawyer, G., Dong, X., Botnar, R., Salisbury, J., Gray, G. A. & Shah, A. M. Bone marrow transplantation modulates tissue macrophage phenotype and enhances cardiac recovery after subsequent acute myocardial infarction. *J. Mol. Cell. Cardiol.* **90**, 120–128 (2016).

485. White, C. I., Jansen, M. A., McGregor, K., Mylonas, K. J., Richardson, R. V., Thomson, A., Moran, C. M., Seckl, J. R., Walker, B. R., Chapman, K. E. & Gray, G. A. Cardiomyocyte and Vascular Smooth Muscle-Independent 11β-Hydroxysteroid Dehydrogenase 1 Amplifies Infarct Expansion, Hypertrophy, and the Development of Heart Failure After Myocardial Infarction in Male Mice. *Endocrinology* **157**, 346–357 (2016).

486. Carmeliet, P. & Jain, R. K. Molecular mechanisms and clinical applications of angiogenesis. *Nature* **473**, 298–307 (2011).

487. Wang, K., Lee, P., Mirams, G. R., Sarathchandra, P., Borg, T. K., Gavaghan, D. J., Kohl, P. & Bollensdorff, C. Cardiac tissue slices: preparation, handling, and successful optical mapping. *Am. J. Physiol. Heart Circ. Physiol.* **308**, H1112–H1125 (2015).

488. Bussek, A., Schmidt, M., Bauriedl, J., Ravens, U., Wettwer, E. & Lohmann, H. Cardiac tissue slices with prolonged survival for in vitro drug safety screening. *J. Pharmacol. Toxicol. Methods* **66**, 145–151 (2012).

489. Perbellini, F., Watson, S. A., Scigliano, M., Alayoubi, S., Tkach, S., Bardi, I., Quaife, N., Kane, C., Dufton, N. P., Simon, A., Sikkel, M. B., Faggian, G., Randi, A. M., Gorelik, J.,

Harding, S. E. & Terracciano, C. M. Investigation of cardiac fibroblasts using myocardial slices. *Cardiovasc. Res.* **114**, 77–89 (2018).

490. Honkoop, H., Nguyen, P. D., van der Velden, V. E. M., Sonnen, K. F. & Bakkers, J. Live imaging of adult zebrafish cardiomyocyte proliferation ex vivo. *Dev.* **148**, 1–15 (2021).

491. Ou, Q., Abouleisa, R. R. E., Tang, X. L., Juhardeen, H. R., Meki, M. H., Miller, J. M., Giridharan, G., El-Baz, A., Bolli, R. & Mohamed, T. M. A. Slicing and culturing pig hearts under physiological conditions. *J. Vis. Exp.* **2020**, (2020).

492. Pitoulis, F. G., Nunez-Toldra, R., Xiao, K., Kit-Anan, W., Mitzka, S., Jabbour, R. J., Harding, S. E., Perbellini, F., Thum, T., De Tombe, P. P. & Terracciano, C. M. Remodelling of adult cardiac tissue subjected to physiological and pathological mechanical load in vitro. *Cardiovasc. Res.* **118**, 814–827 (2022).

493. Watson, S. A., Duff, J., Bardi, I., Zabielska, M., Atanur, S. S., Jabbour, R. J., Simon, A., Tomas, A., Smolenski, R. T., Harding, S. E., Perbellini, F. & Terracciano, C. M. Biomimetic electromechanical stimulation to maintain adult myocardial slices in vitro. *Nat. Commun.* **10**, (2019).

494. Brandenburger, M., Wenzel, J., Bogdan, R., Richardt, D., Nguemo, F., Reppel, M., Hescheler, J., Terlau, H. & Dendorfer, A. Organotypic slice culture from human adult ventricular myocardium. *Cardiovasc. Res.* **93**, 50–59 (2012).

495. Ou, Q., Jacobson, Z., Abouleisa, R. R. E., Tang, X. L., Hindi, S. M., Kumar, A., Ivey, K. N., Giridharan, G., El-Baz, A., Brittian, K., Rood, B., Lin, Y. H., Watson, S. A., Perbellini, F., McKinsey, T. A., Hill, B. G., Jones, S. P., Terracciano, C. M., Bolli, R., *et al.* Physiological Biomimetic Culture System for Pig and Human Heart Slices. *Circ. Res.* **125**, 628–642 (2020).

496. Qiao, Y., Dong, Q., Li, B., Obaid, S., Miccile, C., Yin, R. T., Talapatra, T., Lin, Z., Li, S., Li, Z. & Efimov, I. R. Multiparametric slice culture platform for the investigation of human cardiac tissue physiology. *Prog. Biophys. Mol. Biol.* **144**, 139–150 (2019).

497. Rodighiero, V. Effects of liver disease on pharmacokinetics. An update. *Clin. Pharmacokinet.* **37**, 399–431 (1999).

498. Litviňuková, M., Talavera-López, C., Maatz, H., Reichart, D., Worth, C. L., Lindberg, E.

L., Kanda, M., Polanski, K., Heinig, M., Lee, M., Nadelmann, E. R., Roberts, K., Tuck, L., Fasouli, E. S., DeLaughter, D. M., McDonough, B., Wakimoto, H., Gorham, J. M., Samari, S., *et al.* Cells of the adult human heart. *Nat. 2020 5887838* **588**, 466–472 (2020).

499. Cao, J. & Poss, K. D. The epicardium as a hub for heart regeneration. *Nat. Rev. Cardiol. 2018 1510* **15**, 631–647 (2018).

500. Klotz, L., Norman, S., Vieira, J. M., Masters, M., Rohling, M., Dubé, K. N., Bollini, S., Matsuzaki, F., Carr, C. A. & Riley, P. R. Cardiac lymphatics are heterogeneous in origin and respond to injury. *Nature* **522**, 62–67 (2015).

501. Ho, S. S., Hung, B. P., Heyrani, N., Lee, M. A. & Leach, J. K. Hypoxic Preconditioning of Mesenchymal Stem Cells with Subsequent Spheroid Formation Accelerates Repair of Segmental Bone Defects. *Stem Cells* **36**, 1393–1403 (2018).

502. Zhou, Y., Zhu, X., Cui, H., Shi, J., Yuan, G., Shi, S. & Hu, Y. The Role of the VEGF Family in Coronary Heart Disease. *Front. Cardiovasc. Med.* **8**, (2021).

503. Pätilä, T., Ikonen, T., Rutanen, J., Ahonen, A., Lommi, J., Lappalainen, K., Krogerus, L., Ihlberg, L., Partanen, T. A., Lähteenoja, L., Virtanen, K., Alitalo, K., Ylä-Herttuala, S. & Harjula, A. Vascular Endothelial Growth Factor C–induced Collateral Formation in a Model of Myocardial Ischemia. *J. Hear. Lung Transplant.* **25**, 206–213 (2006).

504. Downes, N. L., Laham-Karam, N., Kaikkonen, M. U. & Ylä-Herttuala, S. Differential but Complementary HIF1α and HIF2α Transcriptional Regulation. *Mol. Ther.* **26**, 1735–1745 (2018).

505. Sobecki, M., Mrouj, K., Colinge, J., Gerbe, F., Jay, P., Krasinska, L., Dulic, V. & Fisher, D. Cell-Cycle Regulation Accounts for Variability in Ki-67 Expression Levels. *Cancer Res.* **77**, 2722–2734 (2017).

506. Ricard, N., Bailly, S., Guignabert, C. & Simons, M. The quiescent endothelium: signalling pathways regulating organ-specific endothelial normalcy. *Nat. Rev. Cardiol.* **18**, 565–580 (2021).

507. Tempel, D., De Boer, M., Van Deel, E. D., Haasdijk, R. A., Duncker, D. J., Cheng, C., Schulte-Merker, S. & Duckers, H. J. Apelin enhances cardiac neovascularization after myocardial infarction by recruiting aplnr+ circulating cells. *Circ. Res.* **111**, 585–598

(2012).

508. He, L., Liu, Q., Hu, T., Huang, X., Zhang, H., Tian, X., Yan, Y., Wang, L., Huang, Y., Miquerol, L., Wythe, J. D. & Zhou, B. Genetic lineage tracing discloses arteriogenesis as the main mechanism for collateral growth in the mouse heart. *Cardiovasc. Res.* **109**, 419–430 (2016).

509. Luo, W., Garcia-Gonzalez, I., Fernández-Chacón, M., Casquero-Garcia, V., Sanchez-Muñoz, M. S., Mühleder, S., Garcia-Ortega, L., Andrade, J., Potente, M. & Benedito, R. Arterialization requires the timely suppression of cell growth. *Nature* **589**, 437–441 (2021).

510. Nicenboim, J., Malkinson, G., Lupo, T., Asaf, L., Sela, Y., Mayseless, O., Gibbs-Bar, L., Senderovich, N., Hashimshony, T., Shin, M., Jerafi-Vider, A., Avraham-Davidi, I., Krupalnik, V., Hofi, R., Almog, G., Astin, J. W., Golani, O., Ben-Dor, S., Crosier, P. S., *et al.* Lymphatic vessels arise from specialized angioblasts within a venous niche. *Nature* **522**, 56–61 (2015).

511. Red-Horse, K., Ueno, H., Weissman, I. L. & Krasnow, M. A. Coronary arteries form by developmental reprogramming of venous cells. *Nature* **464**, 549–553 (2010).

512. MacK, J. J. & Luisa Iruela-Arispe, M. NOTCH regulation of the endothelial cell phenotype. *Curr. Opin. Hematol.* **25**, 212–218 (2018).

513. You, L. R., Lin, F. J., Lee, C. T., DeMayo, F. J., Tsai, M. J. & Tsai, S. Y. Suppression of Notch signalling by the COUP-TFII transcription factor regulates vein identity. *Nature* **435**, 98–104 (2005).

514. Nolan, D. J., Ginsberg, M., Israely, E., Palikuqi, B., Poulos, M. G., James, D., Ding, B. Sen, Schachterle, W., Liu, Y., Rosenwaks, Z., Butler, J. M., Xiang, J., Rafii, A., Shido, K., Rabbany, S. Y., Elemento, O. & Rafii, S. Molecular Signatures of Tissue-Specific Microvascular Endothelial Cell Heterogeneity in Organ Maintenance and Regeneration. *Dev. Cell* **26**, 204–219 (2013).

515. Feng, W., Chen, L., Nguyen, P. K., Wu, S. M. & Li, G. Single Cell Analysis of Endothelial Cells Identified Organ-Specific Molecular Signatures and Heart-Specific Cell Populations and Molecular Features. *Front. Cardiovasc. Med.* **6**, 165 (2019).

516. Hu, P., Liu, J., Zhao, J., Wilkins, B. J., Lupino, K., Wu, H. & Pei, L. Single-nucleus

transcriptomic survey of cell diversity and functional maturation in postnatal mammalian hearts. *Genes Dev.* **32**, 1344–1357 (2018).

517. Kalucka, J., de Rooij, L. P. M. H., Goveia, J., Rohlenova, K., Dumas, S. J., Meta, E., Conchinha, N. V., Taverna, F., Teuwen, L. A., Veys, K., García-Caballero, M., Khan, S., Geldhof, V., Sokol, L., Chen, R., Treps, L., Borri, M., de Zeeuw, P., Dubois, C., *et al.* Single-Cell Transcriptome Atlas of Murine Endothelial Cells. *Cell* **180**, 764-779.e20 (2020).

518. Kalucka, J., de Rooij, L. P. M. H., Goveia, J., Rohlenova, K., Dumas, S. J., Meta, E., Conchinha, N. V., Taverna, F., Teuwen, L. A., Veys, K., García-Caballero, M., Khan, S., Geldhof, V., Sokol, L., Chen, R., Treps, L., Borri, M., de Zeeuw, P., Dubois, C., *et al.* Single-Cell Transcriptome Atlas of Murine Endothelial Cells. *Cell* **180**, 764-779.e20 (2020).

519. Schaum, N., Karkanias, J., Neff, N. F., May, A. P., Quake, S. R., Wyss-Coray, T., Darmanis, S., Batson, J., Botvinnik, O., Chen, M. B., Chen, S., Green, F., Jones, R. C., Maynard, A., Penland, L., Pisco, A. O., Sit, R. V, Stanley, G. M., Webber, J. T., *et al.* Single-cell transcriptomics of 20 mouse organs creates a Tabula Muris. *Nature* **562**, 367–372 (2018).

520. Paik, D. T., Tian, L., Williams, I. M., Rhee, S., Zhang, H., Liu, C., Mishra, R., Wu, S. M., Red-Horse, K. & Wu, J. C. Single-Cell RNA Sequencing Unveils Unique Transcriptomic Signatures of Organ-Specific Endothelial Cells. *Circulation* **142**, 1848–1862 (2020).

521. Jambusaria, A., Hong, Z., Zhang, L., Srivastava, S., Jana, A., Toth, P. T., Dai, Y., Malik, A. B. & Rehman, J. Endothelial heterogeneity across distinct vascular beds during homeostasis and inflammation. *Elife* **9**, (2020).

522. Rohlenova, K., Veys, K., Miranda-Santos, I., De Bock, K. & Carmeliet, P. Endothelial Cell Metabolism in Health and Disease. *Trends Cell Biol.* **28**, 224–236 (2018).

523. González-Cabrero, J., Pozo, M., Durán, M. C., De Nicolás, R., Egido, J. & Vivanco, F. The proteome of endothelial cells. *Methods Mol. Biol.* **357**, 181–198 (2007).

524. Yan, M. S. & Marsden, P. A. Epigenetics in the Vascular Endothelium: Looking from a Different Perspective in the Epigenomics Era. *Arterioscler. Thromb. Vasc. Biol.* **35**, 2297–2306 (2015).

525. Fromer, M. W., Chang, S., Hagaman, A. L. R., Koko, K. R., Nolan, R. S., Zhang, P., Brown, S. A., Carpenter, J. P. & Caputo, F. J. The endothelial cell secretome as a novel treatment to prime adipose-derived stem cells for improved wound healing in diabetes. *J. Vasc. Surg.* **68**, 234–244 (2018).

526. Wang, Y., Yu, H., Xie, X., Deng, T., Ye, L., Wu, L., Ding, X., Yang, Z., Zhu, Q., Li, J., Zheng, Y., Yu, Z. & Chen, G. Plasmalemma vesicle-associated protein promotes angiogenesis in cholangiocarcinoma via the DKK1/CKAP4/PI3K signaling pathway. *Oncogene* **40**, 4324–4337 (2021).

527. Roux, B., Rodde, N., Moreau, S., Jardinaud, M. F. & Gamas, P. Laser capture micro-dissection coupled to RNA sequencing: A powerful approach applied to the model legume Medicago truncatula in interaction with Sinorhizobium meliloti. *Methods Mol. Biol.* **1830**, 191–224 (2018).

528. Pasut, A., Becker, L. M., Cuypers, A. & Carmeliet, P. Endothelial cell plasticity at the single-cell level. *Angiogenes. 2021 242* **24**, 311–326 (2021).

529. Method of the Year 2020: spatially resolved transcriptomics. *Nat. Methods* **18**, 1 (2021).

530. Junker, J. P., Noël, E. S., Guryev, V., Peterson, K. A., Shah, G., Huisken, J., McMahon, A. P., Berezikov, E., Bakkers, J. & Van Oudenaarden, A. Genome-wide RNA Tomography in the Zebrafish Embryo. *Cell* **159**, 662–675 (2014).

531. Ståhl, P. L., Salmén, F., Vickovic, S., Lundmark, A., Navarro, J. F., Magnusson, J., Giacomello, S., Asp, M., Westholm, J. O., Huss, M., Mollbrink, A., Linnarsson, S., Codeluppi, S., Borg, Å., Pontén, F., Costea, P. I., Sahlén, P., Mulder, J., Bergmann, O., *et al.* Visualization and analysis of gene expression in tissue sections by spatial transcriptomics. *Science (80-.).* **353**, 78–82 (2016).

532. Kleshchevnikov, V., Shmatko, A., Dann, E., Aivazidis, A., King, H. W., Li, T., Elmentaite, R., Lomakin, A., Kedlian, V., Gayoso, A., Jain, M. S., Park, J. S., Ramona, L., Tuck, E., Arutyunyan, A., Vento-Tormo, R., Gerstung, M., James, L., Stegle, O., *et al.* Cell2location maps fine-grained cell types in spatial transcriptomics. *Nat. Biotechnol. 2022* **40**, 1–11 (2022).

533. TaqMan™ Array Human VEGF Pathway.

https://www.thermofisher.com/order/catalog/product/4414199.

534. TaqMan™ Array Human WNT Pathway. https://www.thermofisher.com/order/catalog/product/4414100.

535. Matrone, G., Taylor, J. M., Wilson, K. S., Baily, J., Love, G. D., Girkin, J. M., Mullins, J. J., Tucker, C. S. & Denvir, M. A. Laser-targeted ablation of the zebrafish embryonic ventricle: a novel model of cardiac injury and repair. *Int. J. Cardiol.* **168**, 3913–3919 (2013).

536. Chablais, F., Veit, J., Rainer, G. & Jawiska, A. The zebrafish heart regenerates after cryoinjury-induced myocardial infarction. *BMC Dev. Biol.* **11**, 1–13 (2011).

537. Delhove, J. M. K. M., Buckley, S. M. K., Perocheau, D. P., Karda, R., Arbuthnot, P., Henderson, N. C., Waddington, S. N. & McKay, T. R. Longitudinal in vivo bioimaging of hepatocyte transcription factor activity following cholestatic liver injury in mice. *Sci. Reports 2017 71* **7**, 1–12 (2017).

538. Taylor, J. M., Nelson, C. J., Bruton, F. A., Baghbadrani, A. K., Buckley, C., Tucker, C. S., Rossi, A. G., Mullins, J. J. & Denvir, M. A. Adaptive prospective optical gating enables day-long 3D time-lapse imaging of the beating embryonic zebrafish heart. *Nat. Commun. 2019 101* **10**, 1–15 (2019).

539. Liu, Z., Klose, K., Neuber, S., Jiang, M., Gossen, M. & Stamm, C. Comparative analysis of adeno-associated virus serotypes for gene transfer in organotypic heart slices. *J. Transl. Med.* **18**, (2020).

540. Wang, D., Tai, P. W. L. & Gao, G. Adeno-associated virus vector as a platform for gene therapy delivery. *Nat. Rev. Drug Discov. 2019 185* **18**, 358–378 (2019).